Modelling prion-induced neurodegeneration in PrP transgenic *Drosophila*

Alzbeta Cardova
Wolfson College, Cambridge

September 2018

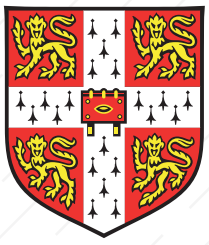

A dissertation submitted for the degree of Doctor of Philosophy

Department of Veterinary Medicine
University of Cambridge

Declaration

I hereby declare that my dissertation entitled
Modelling prion-induced neurodegeneration in PrP transgenic *Drosophila*:

- Is the result of my own work and includes nothing which is the outcome of work done in collaboration except as declared in the Preface and specified in the text
- Is not substantially the same as any that I have submitted, or, is being concurrently submitted for a degree or diploma or other qualification at the University of Cambridge or any other University or similar institution except as declared in the Preface and specified in the text. I further state that no substantial part of my dissertation has already been submitted, or, is being concurrently submitted for any such degree, diploma or other qualification at the University of Cambridge or any other University of similar institution except as declared in the Preface and specified in the text
- Does not exceed the prescribed word limit

I have also:

- Resided in Cambridge for at least three terms
- Undertaken the minimum requirement of research terms
- Submitted this thesis by my submission date or requested leave to defer it
- Formally applied for examiners to be appointed

I will also keep my contact details up to date using my self-service pages throughout the examination process.

DATE: . . . . . . **SIGNATURE:** . . . .

Acknowledgements

I would like to thank my supervisor **Dr Raymond Bujdoso** for his guidance and helpfulness during the research that preceded my thesis and then for his valuable comments and advice with regards to the writing process and successful generation of my dissertation. It has been a long and sometimes painful process and I am really grateful for the continuous support and great advice that has been provided to me.

I would also like to acknowledge my PhD advisor **Dr Alana Thackray** who has been a great role model for me and was a huge help every time I needed to perform a new method, verify some steps in a protocol or required some of her reagents or transgenic flies. Alana has always been a great source of advice and encouragement during my PhD.

Thank you both for the numerous scientific and non-scientific chats and overall support.

Also, I would like to express the eternal gratitude to my partner, Ondrej Hauser, who has always been there for me and helped me to get through the uneasy bits with his unconditional support and inappropriate jokes. Thanks so, so much.

The same thanks go to my whole family and friends who patiently asked me about the thesis advancements and who really tried to understand whatever I study here.

Last but not least, I wish to thank BBSRC DTP programme for providing me with the financial support and therefore this amazing opportunity to study in Cambridge.

List of abbreviations

245	Purified anti-PrP capture antibody (CD-ELISA)
51D	Non-PrP transgenic *Drosophila* (control)
AD	Alzheimer's disease
AEBSF	4-(2-Aminoethyl) benzensulfonyl fluoride
Amp	Ampicillin
AMPA	α-amino-3-hydroxy-5-methyl-4-isoxazolepropionic acid receptor
APS	Ammonium persulphate
ARQ	Ovine PrP genotype ($A^{136}R^{154}Q^{171}$)
ASA	Amyloid seeding assay
BCA	Bicinchoninic acid assay
BSA	Bovine serum albumin
BSE	Bovine spongiform encephalopathy
C57BL/6	Transgenic mouse genotype (control for ME7 prion strain)
CD1	Transgenic mouse genotype (control for RML prion strain)
CD-ELISA	Capture-detector enzyme-linked immunosorbent assay
CJD	Creutzfeldt-Jakob disease
CNS	Central nervous system
CPD	Camel prion disease
CWD	Chronic wasting disease
D178N	Fatal familial insomnia-associated polymorphism
DA1	Dorsal acute muscle 1
E200K	Creutzfeldt-Jakob disease-associated polymorphism
ECL	Enhanced chemiluminescence
EDTA	Ethylenediaminetetraacetic acid
ELISA	Enzyme-linked immunosorbent assay
ER	Endoplasmic reticulum
EUE	Exotic ungulate encephalopathy
DH5α	E. coli competent strain used for cloning

fCJD	Familial (genetic) Creutzfeldt-Jakob disease
FDC	Follicular dendritic cells
FFI	Fatal familial insomnia
FSE	Feline spongiform encephalopathy
gCJD	Genetic (familial) Creutzfeldt-Jakob disease
GFP	Green fluorescent protein
GPI	Glycosyl phosphatidyl inositol
GSS	Gertschmann-Straussler-Scheinker syndrome
HD	Huntington's disease
HRP	Horseradish peroxidase (detection on WB)
iCJD	Iatrogenic Creutzfeldt-Jakob disease
LB	Laura Bertani (broth)
M129V	Polymorphism influencing susceptibility to prion disease
MBM	Meat-and-bone meal
ME7	Mouse-adapted ovine scrapie prion strain
NaPTA	Sodium phosphotungstic acid
NCJDRSU	National CJD Research & Surveillance Unit in Edinburgh
NHP	Non-human primates' transmissible encephalopathy
NMJ	Neuromuscular junction
Nor98	Atypical scrapie
OD	Optical density
PAGE	Polyacrylamide gel electrophoresis
PBS	Phosphate buffered saline
PBS-T	Phosphate buffered saline-Tween 80
PCR	Polymerase chain reaction
PD	Parkinson's disease
PIPLC	Phosphoinositide phospholipase C
PK	Proteinase-K
PMCA	Protein misfolding cyclic amplification
PRNP	Human PrP gene

Prnp	Murine PrP gene
Prnp$^{-/-}$	PrP-knockout mouse
PrP	Prion protein
PrP^{C}	Cellular form of prion protein
PrP^{Sc}	Scrapie-associated prion protein
RML	Rocky Mountain Laboratory mouse-adapted ovine scrapie prion strain
RT-QuIC	Real-time quaking-induced conversion assay
SAF32	Secondary anti- PrP antibody (CD-ELISA)
sCJD	Sporadic Creutzfeldt-Jakob disease
SD	Standard deviation
SDS	Sodium dodecyl sulphate
sFI	Sporadic fatal insomnia
Sha31	Anti-PrP monoclonal antibody (WB)
TAE	Tris base, acetic acid and EDTA buffer
TBS-T	Tris buffered saline-0.5% Tween 20
tdTom	Tomato red fluorescent protein
ThT	Thioflavin-T
TME	Transmissible mink encephalopathy
TSE	Transmissible spongiform encephalopathy
vCJD	Variant Creutzfeldt-Jakob disease
VPSPr	Variably protease-sensitive prionopathy
VRQ	Ovine PrP genotype ($V^{136}R^{154}Q^{171}$)
VRQ(cyt)	Cytosolic form of ovine VRQ PrP
VRQ(GPI)	Membrane bound form of ovine VRQ PrP
VRQ(ΔGPI)	Secreted form of ovine VRQ PrP
WB	Western blot

Table of contents

Summary

The aim of my thesis was to develop and characterise PrP transgenic *Drosophila melanogaster* of various genotypes to study the process of prion-induced neurodegeneration in this model. Prion diseases are caused by the occurrence of an abnormally-folded form of PrP (PrP^{Sc}) protein that arises either from the environment as an acquired disease, from mutation in the PrP-coding gene as a genetic disease or sporadically from causes unknown. The PrP^{Sc} then recruits PrP^{C}, the normal form of PrP, that is ubiquitously present in the mammalian CNS and triggers neurotoxicity and neurodegeneration that is transmissible between individuals of the same or even different species. All prion diseases are currently incurable, fatal and the mechanism of prion-induced neurodegeneration remains to be discovered.

In this thesis, *Drosophila* transgenic for ovine (chromosome 3 and dual PrP transgenic flies), hamster, humanised murine, human and cervid PrP were characterised for expression and biochemical properties. The ultimate goal of my thesis was investigation of cell-to-cell spread of misfolded PrP in *Drosophila* CNS. To achieve this, a mutant form of PrP that is thought to misfold was co-expressed with the normal form PrP^{C} that served as a substrate in the same dual PrP-transgenic fly. The process was modelled using hamster, humanised murine or ovine PrP transgenes that carry human mutations associated with the spontaneous onset of transmissible neurodegeneration in the natural host. Various approaches towards independent spatial expression of PrP in *Drosophila* were exploited here in both single and dual PrP expressing flies. Moreover, the ability to initiate misfolding and the impact of this on the fly phenotype was investigated. Both apparent misfolding and phenotypic changes were seen in different fly models suggesting the models were successful. To this extent, PrP transgenic *Drosophila* were developed to allow for relatively rapid modelling of mammalian prion disease in this invertebrate organism.

1 Introduction

1.1 Prion diseases

Prion diseases or transmissible spongiform encephalopathies (TSEs) are progressive neurodegenerative disorders that affect many animal species. The neurodegeneration associated with prion disease is caused by aggregation of a pathological form of prion protein, PrP^{Sc}. This infectious protein arises through misfolding of a cellular form of PrP^{C} ubiquitously present in mammalian brains (Prusiner, 1982, Prusiner, 1998). The PrP^{Sc} of a pathological conformation is deposited into aggregates in prion infected brain and the associated pathology generally comprises spongiform degeneration of grey matter, neuronal loss and astrocytic gliosis (Aguzzi et al., 2008). In TSEs, there is a distinct lack of immune response (Harman and Silva, 2009). Prion diseases show prolonged incubation time, are uniformly fatal and so far, irreversible. Increasingly, neurodegenerative disease research has uncovered links between prion disease and other neurodegenerative disease, such as Alzheimer's or Parkinson's, as all these conditions arise through misfolding of a disease-specific protein (Collinge and Clarke, 2007, Brundin et al., 2010, Lloyd et al., 2013).

Prion diseases can occur in three aetiologies – acquired, inherited and sporadic (Prusiner and DeArmond, 1994, Aguzzi et al., 2008). Acquired prion disease arises by exposure to prion-contaminated material; inherited disease is associated with mutations in the PrP-encoding gene and sporadic disease arises from spontaneous conversion of PrP^{C} into PrP^{Sc} or by a somatic mutation. Prion diseases affect a variety of vertebrate species (Imran and Mahmood, 2011a, Imran and Mahmood, 2011b). The first identified prion disorder in animals was scrapie. This neurological disease affects sheep and goats and was reported in 1700s in the UK (Poser, 2002). In later years, bovine spongiform encephalopathy (BSE) was observed in cattle (Wells and Wilesmith, 1995), followed by transmissible mink encephalopathy (TME) (Marsh and Hadlow, 1992), chronic wasting disease (CWD) in deer (Williams and Young, 1992) and camel prion disease in dromedary camels (CPD) (Babelhadj et al., 2018). The identified human prion diseases are Creutzfeldt-Jakob disease (CJD), Gerstmann–Sträussler–Scheinker syndrome (GSS), fatal familial insomnia (FFI) and kuru which is an endemic disease of Fore people in Papua New Guinea believed to be associated with cannibalism (Poser, 2002, Gajdusek and Zigas, 1957). An important human prion disease is variant CJD (vCJD) that is believed to originate from BSE (Bruce et al., 1997, Collinge, 1999). A list of animal and human prion diseases known to date can

be seen in the following table (Overview of animal and human prion disease and their aetiologies).

ANIMAL PRION DISEASE

Disease	Host	Origin	Year
Scrapie	Sheep, goats	Unknown	1732
TME	Mink	Sheep or cattle	1947
CWD	Cervids	Unknown	1967
BSE	Cattle	Unknown	1986
Exotic ungulate encephalopathy (EUE)	Nyala, Kudu	BSE	1986
Feline spongiform encephalopathy (FSE)	Cats	BSE	1990
TSE in non-human primates (NHP)	Lemurs	BSE	1996
Prion disease in dromedary camels (CPD)	Dromedaries	Unknown	2018

HUMAN PRION DISEASE

Disease	Origin	Year
Kuru	Cannibalism	1900s
Sporadic CJD (sCJD)	Spontaneous conversion/somatic mutation	1920
Familial (genetic) CJD (fCJD, gCJD)	Mutations in *PRNP* (gene)	1924
GSS	Mutations in *PRNP* (gene)	1936
Iatrogenic CJD (iCJD)	Transmission by cadaveric grafts or hGH	1974
FFI	Mutations in *PRNP*	1986
vCJD	BSE	1996
Sporadic fatal insomnia (sFI)	Spontaneous conversion/somatic mutation	1999
Variably protease-sensitive prionopathy (VPSPr)	Spontaneous conversion/somatic mutation	2008

Overview of animal and human prion diseases and their aetiologies. *Adapted from (Imran and Mahmood, 2011a, Imran and Mahmood, 2011b) + (Babelhadj et al., 2018)*

1.2 History of prion research

The transmissibility of prion diseases was first confirmed by intraocular scrapie transmission of spinal cord tissue from scrapie affected sheep (Cuillé, 1936). Subsequently, the inter species transmissibility was demonstrated when scrapie was successfully transmitted from sheep to goats (Cuillé, 1939). In 1950s, the neuropathological features of scrapie were compared to those that arise in Kuru, a neurological disease that affected the Fore tribe in Papua New Guinea. The resemblance of the neuropathology between these diseases was striking (Hadlow, 1959, Gajdusek and Zigas, 1957). The first successful experimental inoculation of kuru to chimpanzees demonstrated its transmissibility (Gajdusek et al., 1966). The experimental transmission of CJD to chimpanzees followed and confirmed this neurodegenerative disease was also transmissible (Gibbs et al., 1968). An important step was demonstrated by the successful transmission of scrapie to rodents; this has served as a basis for contemporary prion research (Chandler and Turfrey, 1972, Kimberlin and Walker, 1977). The use of rodent models allowed experiments to be performed in shorter time lines than in natural hosts of these conditions. The introduction of PrP transgenesis has further significantly advanced rodent models as the standard animal model for prion disease research. The portfolio of animal models used for prion protein research is now even broader as there has been research successfully carried out in multiple animal models such as zebra fish *Danio rerio* or the invertebrate *Drosophila melanogaster* (Cotto et al., 2005, Thackray et al., 2012b, Gavin et al., 2006).

1.3 Molecular nature of prions

Initially, the pathological agent causing prion diseases was considered to be a “slow virus” (Sigurdsson, 1954). The limitations of this idea were suggested after experiments were carried out to identify the infectious moiety. The scrapie agent showed resistance to treatments that modify nucleic acids as well as virus decontamination methods (Pattison, 1965, Alper et al., 1967, Adams et al., 1969). After these observations, more theories of a transmissible agent identity were proposed, such as genetic information enclosed in a protein sheet (Latarjet et al., 1970), polysaccharides associated with membranes (Gibbons and Hunter, 1967) or genetic information protected by a molecule of the host origin (Bruce and Dickinson, 1987). Griffith suggested that the prion disease agent might be a protein able to self-replicate without a nucleic acid and proposed two candidate mechanisms to explain this phenomenon (Griffith, 1967). The first being a protein that acquired ability to trigger a reaction that is supressed under the normal

circumstances and creates a pathological event if switched on. The second is a spontaneous rise of an abnormal form of the protein normally present in an organism (Griffith, 1967). Griffith's hypotheses were not viewed favourably for another decade.

Many attempts were made to isolate and characterise the agent responsible for transmissible prion disease. Biochemical studies showed that the transmissible scrapie agent was inactivated by proteases which supported the original suggestion by Griffith for the involvement of a protein as the infectious agent for this disease. Subsequently, purification studies revealed that a partially PK-resistant protein of 27-30 kDa was isolated from infected hamster brains (Bolton et al., 1982, Prusiner et al., 1980, Prusiner, 1982). Importantly, the titre of infectious scrapie agent was found to correlate with the level of this PK-resistant protein (McKinley et al., 1983, DeArmond et al., 1985). These seminal studies led to the development of the prion hypothesis, which described the nature of the transmissible scrapie agent as proteinaceous particle (Prusiner, 1982).The protease resistant protein was termed PrP^{Sc}, where Sc stands for scrapie and its counterpart of similar molecular weight found in brains of healthy individuals was termed PrP^{C}, where C stands for cellular prion protein (Meyer et al., 1986, Oesch et al., 1985). Subsequently, the coding gene of PrP^{Sc} was identified as identical to that encoding PrP^{C} and is termed *PRNP* in humans and *Prnp* in mice. The two isoforms of PrP share the same amino acid sequence but have distinct biochemical and biophysical properties and adopt different conformation (Caughey et al., 1991, Caughey and Raymond, 1991, Stahl et al., 1993). It is now known that PrP may be PK-sensitive and PK-resistant (Sajnani et al., 2012, Thackray et al., 2007).

1.4 Structure of PrP

PrP^{C}, the normal cellular form of prion protein, is a membrane bound glycosylphosphatidylinositol (GPI)-anchored surface protein expressed ubiquitously but predominantly in neurons and glial cells in brain (Dormont, 2002, Cashman et al., 1990). The *PRNP* gene that encodes human PrP is located on chromosome 20 (Parchi and Gambetti, 1995). The PrP polypeptide chain consists of 253 amino acids with molecular weight around 35 to 36 kDa. Consistent with other membrane bound proteins, PrP^{C} is synthesised in the rough endoplasmic reticulum (ER) and transported via the Golgi apparatus onto the cell surface. During its biosynthesis, PrP^{C} undergoes a cascade of post-translational modifications such as N-terminal signal sequence cleavage, attachment of two oligosaccharide chains at asparagine residues 181 and 197, creation of an intramolecular disulphide bond between amino acid residues 179 and

214, and GPI-anchor attachment at position 231 after cleavage of C-terminal hydrophobic region (Turk et al., 1988, Billeter et al., 1997, Haraguchi et al., 1989). The molecular profile of PrP^C shown by western blot with an anti-PrP monoclonal antibody typically exhibits mono-, di- and un-glycosylated PrP (Rudd et al., 1999, Pan et al., 2002).

PrP^C has a flexible unstructured N-terminal domain with five highly conserved octapeptide repeats PHGGGWGQ that span amino acid residues 60 to 91 in the human prion protein which exhibits an affinity to Cu^{2+} ions (Aronoff-Spencer et al., 2000, Burns et al., 2002). Another two copper binding sites have been identified in the region of amino acid residues 92 to 115 in human PrP (Jackson et al., 2001, Qin et al., 2002). The structured C-terminal domain of PrP^C contains three alpha helices (α1, α2 and α3) and two short anti-parallel beta strands flanking α1 (Calzolai et al., 2005, Zahn et al., 2000). The α1 alpha helix spans from amino acid residues 147-155, α2 alpha helix spans from amino acid residues 176-177 and α3 alpha helix spans from amino acid residues 203-229. The helix α1 is flanked by β1 (amino acid residues 134 - 136) and β2 (amino acid residues 164 - 166). The globular structure of C-terminal region is supported by a disulphide bridge scaffold that links α2 and α3 helices (Billeter et al., 1997). The GPI-anchor of PrP^C is atypical as its core is modified by sialic acid addition (Stahl et al., 1992). The core structure of the PrP^C GPI-anchor is otherwise similar to that of common glycolipid-anchored proteins with an ethanolamine residue amide-bonded to the C-terminal amino acid, triple mannose residues, unacetylated glucosamine residue and a phosphoinositol molecule embedded in the outer leaf of the lipid bilayer (Harris, 1999).

Like other GPI-anchored proteins, PrP^C attaches to lipid rafts or cholesterol and sphingomyelin-rich domains on the membrane surface that provide a connection to other surface proteins and determine the metabolic fate of PrP^C (Critchley et al., 2004). After its attachment to a plasma membrane, PrP^C is continuously absorbed into the cell through clathrin-coated pits. PrP^C can be recycled via early endosomes back onto the cytoplasmic membrane, degraded in lysosomes via late endosomes or possibly converted into its pathological conformer PrP^{Sc} (Shyng et al., 1994).

1.5 The biology of PrP^C – the normal cellular form of PrP

The physiological role of PrP^C is still not completely clear. The fact that PrP^C is highly conserved between different species and ubiquitously expressed in these hosts suggested an essential role in cellular functions. The first attempt to elucidate its role was through a gene knock-out approach that generated mice that lacked PrP expression (Büeler et al., 1992). The main hallmark of this

$PrP^{-/-}$ animal model was their resistance to prion infection, which confirmed the key role of PrP in TSEs (Büeler et al., 1993). However, these $PrP^{-/-}$ mice did not show overt pathology or behavioural abnormalities (Büeler et al., 1992). Later on, the olfactory system was found to be disrupted in the $PrP^{-/-}$ mice and PrP^{C} was found to be critical for normal processing of sensory inputs by the olfactory system (Le Pichon et al., 2009). Many other PrP functions have been proposed for a physiological role of PrP^{C}, such as its involvement in anti-oxidation activities (Klamt et al., 2001, Wong et al., 2001, Haigh et al., 2015), mitochondrial biogenesis and morphology (Miele et al., 2002) or circadian rhythm maintenance (Tobler et al., 1997). Other studies have suggested that PrP^{C} plays a role in phagocytosis (de Almeida et al., 2005), synaptic function (Collinge et al., 1994), neuronal differentiation (Lima et al., 2007, Nuvolone et al., 2016) and neuroprotection (Carulla et al., 2015). Other proposed functions of PrP^{C} include a role in the immune system (Haddon et al., 2009, Gadotti and Zamponi, 2011) or in metal homeostasis (Tripathi et al., 2015, Cardova et al., 2017, Gasperini et al., 2016, Hornshaw et al., 1995). Based on the fact that copper ions rapidly stimulate PrP^{C} endocytosis, it has been hypothesised that PrP^{C} might serve as a receptor for an uptake of extracellular copper (Pauly and Harris, 1998). The Cu^{2+} ion is proposed to bind to PrP^{C} at the cellular surface and subsequently deliver it to an endocytic compartment where it dissociates from PrP^{C} to allow the latter to return back to the cell surface (Pauly and Harris, 1998, Harris, 1999).

1.6 The biology of PrP^{Sc} – the pathological form of PrP

PrP^{Sc} is the misfolded form of the cellular PrP with identical amino acid sequence and post translational modification states compared to PrP^{C} (Caughey and Raymond, 1991). PrP^{Sc} is characterised by its partial resistance to proteinase-K and phospholipase-C digestion (Bolton et al., 1982, Prusiner, 1982, Dormont, 2002). PrP^{Sc} is also insoluble in detergents and has a strong tendency to aggregate and polymerise (Dormont, 2002). While PrP^{C} comprises approximately forty percent alpha helix structure and just three percent beta sheet conformation, PrP^{Sc} consists of thirty percent alpha helix and forty percent beta sheet structure as supported by infrared spectroscopy (Caughey et al., 1991, Pan et al., 1993, Safar et al., 1993). Detailed structural analysis of PrP^{Sc} has been hampered because of its aggregated nature and insolubility in solution. However, amorphous PrP^{Sc} aggregates have been used to generate fibrils that can be analysed by transmission electron microscopy, atomic force microscopy or X-ray fibre diffraction analysis (Sim and Caughey, 2009, McKinley et al., 1986, Wille et al., 2009). The low resolution X-ray fibre diffraction analysis has helped to establish that the structure of PrP^{Sc} is characterised by a cross-

beta-sheet motif that resembles the one seen in amyloid fibrils (Wille et al., 2009). Another approach to characterise the structure of PrP^{Sc} was molecular threading analysis based on two-dimensional crystals of highly purified PrP^{Sc} that revealed trimers of left-handed beta-helical structure (Govaerts et al., 2004). Initial molecular dynamics simulations suggested that helix α2 and α3 of PrP remain intact during its conversion into PrP^{Sc} (DeMarco and Daggett, 2004). More recently, another conversion model proposed refolding of the C-terminal region of PrP^{Sc} by unwinding of helix α2 and α3 and was confirmed by experimental data (Cobb et al., 2007, Lu et al., 2007, Adrover et al., 2010). Additionally, it has been proposed that helix α2 and α3 helices may be involved in initial conversion of PrP^{C} to PrP^{Sc} (Chen and Thirumalai, 2013).

1.7 Animal prion diseases

1.7.1 Scrapie

Classical scrapie is probably the most studied prion disease to date and affects adult sheep and goats all over the world (Parry, 1960). Apart from the typical hosts of sheep and goats, scrapie can also affect mouflons (Jeffrey and González, 2007). Typical clinical signs of scrapie include itching and subsequent rubbing against objects resulting in a loss of fur, uncoordinated movement, hip swaying and weight loss, leading to the unavoidable death of an animal (Benestad et al., 2008, Vaccari et al., 2009, Goldmann, 2008). The incubation time of scrapie is 2 to 5 years long with death of the animal typically a few months after the onset of clinical signs. In terms of tissue neuropathology, spongiform vacuolation, astrogliosis and amyloid plaque presence occurs in the central nervous system (CNS) of affected animal. PrP^{Sc} can be detected in the CNS, spleen, lymphoid tissue, cell membrane, muscles, placenta and ileus tissues of animal with classical scrapie. Infectious scrapie prions can be found in faeces and secretions as well; this fact may facilitate the scrapie spread in a flock of sheep (Maddison et al., 2010a, Maddison et al., 2010b, Novakofski et al., 2005). Apart from classical scrapie, there has been identification of atypical scrapie (Nor98) (Benestad et al., 2003, Benestad et al., 2008, Fediaevsky et al., 2010). Atypical scrapie affects old sheep and is considered to be of a genetic or sporadic origin as it does not naturally transmit in flocks (Benestad et al., 2008, Tranulis et al., 2011). Atypical scrapie-affected sheep show ataxia, neuropil vacuolation and less prominent vacuolation in the brainstem and no PrP^{Sc} detectable in lymphoid tissue. The molecular profile of atypical scrapie PK-resistant PrP^{Sc} resembles that found in human prion disease GSS (Gretzschel et al., 2006). The 11kDa PK-resistant band of atypical scrapie PrP^{Sc} corresponds to the amino acid 90-153 which are

characterised by an 11 kDa protein fragment of ovine PrP, which corresponds to amino acid 82-146 of human PrP (Gretzschel et al., 2006, Salmona et al., 2003). The experimental transmission of atypical scrapie in ovine PrP transgenic mice has been successful but the evidence of transmission in the natural host has not been established (Simmons et al., 2007, Simmons et al., 2011, Le Dur et al., 2005).

Scrapie exhibits an autosomal recessive genetic disposition (Parry, 1960). There are polymorphisms in ovine PrP that influence susceptibility of sheep to either classical or atypical scrapie. The major scrapie associated polymorphisms are located at amino acid residues 136, 141, 154 and 171 (Goldmann, 2008, Goldmann et al., 1990, Clouscard et al., 1995). These polymorphisms believed to correlate with regions of PrP that undergo the conformation change during prion disease (Bossers et al., 1997). Polymorphisms that facilitate transmission of classical scrapie are $V^{136}L^{141}R^{154}Q^{171}$ (VRQ) and $A^{136}L^{141}R^{154}Q^{171}$ (ARQ), whereas the atypical scrapie transmission is associated with $A^{136}L^{141}R^{154}R^{171}$ (ARR), $A^{136}F^{141}R^{154}Q^{171}$ (AFRQ) and $A^{136}L^{141}H^{154}Q^{171}$ (AHQ) (Benestad et al., 2008, Hunter, 1997, Moum et al., 2005). Classical scrapie PrP genotypes are considered to be associated with resistance to atypical scrapie, and vice versa. This has led to a breeding programme to eradicate classical scrapie in the UK and central Europe (Ortiz-Pelaez et al., 2014).

1.7.2 Bovine spongiform encephalopathy

In 1986, a prion disease emerged in cattle in the UK. This disease was named classical bovine spongiform encephalopathy (BSE) or "mad cow disease" (Wells et al., 1987). Classical BSE is characterised by typical spongiform lesions in the brain of affected animals, as well as PK-resistant PrP^{Sc} (Prusiner et al., 1993, Hope et al., 1988). The extracts from BSE-affected cattle brains contained abnormal protein fibrils, similar to that in scrapie affected sheep brains that are derived from the pathological form of PrP (Kimberlin and Wilesmith, 1994).

The most probable source of classical BSE infection in cattle was identified as a nutrition supplement meat-and-bone meal (MBM) contaminated by brains of classical BSE affected animals that contained infectious PrP^{Sc} (Taylor and Woodgate, 1997, Nathanson et al., 1997). The route of classical BSE infection was found to be centripetal from the gut via the autonomic nervous system to the central nervous system. Primarily, the BSE-associated prions utilize principally sympathetic nerves and to a lesser extent parasympathetic structures (Kaatz et al., 2012).

Clinical symptoms of BSE involve abnormal posture, lack of coordination, difficulty in rising and loss of body weight (Braun, 2002). The prominent vacuolation and PrP^{Sc} accumulation are present in brain; in terminal stage of the disease, the pathology may spread to spinal cord, bone marrow, retina and tonsils (Novakofski et al., 2005). The average time for onset of clinical signs is 3.5 years with an incubation period of two to eight years (Sigurdson and Miller, 2003). Two atypical forms of BSE have been identified: L-type and H-type of BSE and H-type of BSE with distinct phenotypes and molecular pathology (Buschmann et al., 2004, Konold et al., 2012).

The epidemic of classical BSE in the UK began in 1986 and over the years, it affected close to four million cattle (Harman and Silva, 2009). Considerable attention focused on classical BSE as it became clear that this animal prion disease was associated with the emergence of variant CJD (vCJD) in humans (Prince et al., 2003). Human consumption of beef products contaminated by BSE has resulted in 230 confirmed cases of vCJD to date, including 177 in the UK since 1994 (Brown et al., 2001, Seed et al., 2018). This number of vCJD cases might not be finite as several studies predict more cases in the future (Brown et al., 2001, Seed et al., 2018).

1.7.3 Chronic wasting disease

Chronic wasting disease (CWD) affects free-ranging as well as captive cervids and was first identified in 1980s (Williams and Young, 1980, Williams and Young, 1992). Originally, CWD was thought to be restricted to North America (Mitchell et al., 2012). Nowadays, CWD distribution spans 14 states of USA and 2 Canadian provinces with additional CWD occurrences in South Korea, and more recently in Norway (Kim et al., 2005, Sigurdson, 2008, Benestad et al., 2016). The affected cervid species are mainly mule deer, white-tailed deer, red deer, sika deer, Rocky mountain elk and moose but CWD can affect a wide range of other cervids (Williams, 2005). CWD has been experimentally transmitted between cervids (Kurt and Sigurdson, 2016). A large spectrum of mammals have been successfully challenged by intracerebral inoculation of CWD, such as sheep, goats, cats, cattle and rodents as reviewed in (Gilch et al., 2011). However, natural inter-species transmission has not been observed to date (Imran and Mahmood, 2011a). The horizontal transmission of CWD in cervid populations is believed to occur through direct contact between affected animals or exposure to the same environmental infection (Sigurdson, 2008, Sigurdson and Miller, 2003). One possible environmental transmission of the prion agent is saliva (Haley et al., 2011). A confirmed pathway of CWD transmission is via uterine (Selariu et al., 2015). Infectious prions can be detected in cervid CNS tissue, the lymphoreticular system,

blood, muscles, uterus, pancreas, fat, retina and salivary glands (Race et al., 2009, Sigurdson, 2008, Spraker et al., 2010). The clinical signs of CWD are largely associated with weight loss and hence the name of the disease. The way CWD spread to Norway or other regions distant from the original endemic regions remains to be established. The possibilities include acquired disease that spread from North America or endemic disease (Benestad et al., 2016).

1.7.4 Prion disease in dromedary camels (CPD)

In 2018, an emergence of a new prion disease was detected in dromedary camels in Algeria (Babelhadj et al., 2018). The disease was detected during antemortem inspection at a camel slaughter house. Retrospectively, the prevalence of the disease in the dromedary camel population brought for slaughter was estimated to be 3.1 %. The origin of the disease has not been traced yet and the biochemical features of camel PrP^{Sc} do not correlate with BSE or sheep-passaged BSE. However, other possible origins, such as spread from scrapie-infected sheep cannot yet be ruled out. Further geographical distribution investigation of camel prion disease is required to understand its spread and to identify its origin (Babelhadj et al., 2018).

1.8 Human prion diseases

1.8.1 Creuztfeldt-Jakob disease

There are three aetiologies of CJD – sporadic (sCJD), genetic (gCJD) and acquired [iatrogenic (iCJD) and variant (vCJD)]. Sporadic CJD accounts for 85% cases of this human prion disease (Mead et al., 2003). Clinical signs, pathology and susceptibility to sCJD are influenced by polymorphisms in *PRNP* coding sequence. The homozygous polymorphism M129V was identified as a risk factor for sCJD development (Palmer et al., 1991) while the heterozygotes and homozygotes of valine polymorphism were found to develop more severe neuropathology than methionine homozygous patients (Hauw et al., 2000). The changes to cortical structures were found to be predominant in methionine homozygotes, whereas valine homozygotes exhibited deep gray matter pathology (Parchi et al., 1999). A different homozygous polymorphism E219K associated with increased sCJD incidence has been discovered in Japan (Shibuya et al., 1998). Myoclonus is the most typical clinical sign of sCJD and occurs in nearly 90% of CJD patients (Kretzschmar, 1993). Other clinical signs involve progressive dementia, cerebellar dysfunction, muscle incoordination, muscular atrophy and abnormal posture (Brownell and Oppenheimer, 1965, Kirschbaum, 1924). Subsequently the onset of reflex dysfunction, confusion and depression take place. The terminal stage of sCJD is typically characterized by an akinetic mutism (Belay,

1999). sCJD-associated pathology includes spongiosis, gliosis of grey matter, variable degrees of neuronal loss and punctate PrP^{Sc} immunostaining pattern (Gambetti et al., 2003a).

Genetic forms of CJD (gCJD) are linked to dominant point mutations in the human prion gene *PRNP*. gCJD was initially termed familial CJD (fCJD) but cases of this disease with no family history have been discovered and therefore the official name has changed to gCJD (Imran and Mahmood, 2011b). The incidence of gCJD amongst all CJD cases ranges from five to fifteen percent (Belay, 1999). The geographical/ethnic distribution of gCJD shows clusters of cases in Israel, Slovakia, Chile, Italy, Spain and Japan associated with polymorphisms in amino acid residues E200K, I210V, D178N and V180I (Nozaki et al., 2010, Gambetti et al., 2003b, Imran and Mahmood, 2011b). In human PrP protein sequence, the region within amino acid residues 51 to 91 comprises nonapeptide repeat PQGGGGWGQ and four octapeptide tandem repeats PHGGGWGQ (Imran and Mahmood, 2011b). The mutation D178N contributes towards the gCJD if linked with M129V polymorphism (Kretzschmar et al., 1995). The clinical signs of gCJD comprise progressive confusion, delusions, hallucinations, memory impairment followed by ataxia and myoclonus with a disease onset typically around 30 to 55 years of age (Mastrianni, 2010).

The iatrogenic form of CJD (iCJD) is an acquired disease linked to a surgical transfer of the infectious prion agent by contaminated human material of cadaveric origin (Brown et al., 2012). The major occurrences of iCJD have been associated with contaminated growth hormone and dura mater grafts originating from human cadavers with undiagnosed CJD. The first case of iCJD was linked to a corneal transplant in 1974 (Duffy et al., 1974) followed by cases caused by contaminated neurosurgical instruments (Brown et al., 2012). The growth hormone-linked outbreak exhibited mainly in France, UK and USA whereas dura mater graft linked infection was observed in Japan, South Korea, Austria and Netherlands (Chen and Dong, 2016).

Variant CJD (vCJD) is triggered by an oral intake of BSE contaminated material. This acquired disease has been identified amongst young people (16 years old) following the BSE epizootic in the UK. It was suggested from the experimental evidence that vCJD is related to consumption of BSE contaminated bovine products (Bruce et al., 1997). The clinical symptoms of vCJD are principally psychiatric and do resemble a typical CJD dementia or cerebellar ataxia (Will, 2003a, Will, 2003b). There is evidence that vCJD exhibits blood-borne infectivity and can be considered

a secondary iatrogenic CJD if transmitted by blood products from human to human (Brown et al., 2012, Dietz et al., 2007, Bishop et al., 2006).

1.8.2 Fatal familial insomnia

Fatal familial insomnia (FFI) is a rare, autosomal dominant genetic prion disease that affects principally the thalamus and is associated with sleep disorders of various manifestations (Mastrianni, 2010). FFI typically affects multiple members of families where an FFI-associated mutation in *PRNP* is inherited. The point mutation responsible for FFI is a substitution of aspartic acid at amino acid position 178 to asparagine (D178N) in conjunction with the methionine-valine polymorphism M129V (Lugaresi et al., 1986). So far, the disease has been reported in families within European countries, the USA, Japan, China and Morocco (Baldin et al., 2009).

FFI manifests in individuals aged 20 to 72 years with an average age of onset at 49 years old (Belay, 1999, Gambetti et al., 2003b). An average survival time for FFI patients spans from 8 to 72 months after the first clinical signs with an average survival time of 18.4 months. The most prominent clinical signs are disturbed sleep/wake patterns, insomnia, autonomic hyperactivity, myoclonus and ataxia (Montagna et al., 2003). The slow-wave and rapid-eye-movement sleep phases are reduced or lost in the more advanced stages of the disease when affected individuals develop hallucinations or coma (Medori and Tritschler, 1993, Medori et al., 1992). The loss of circadian rhythms in FFI is linked to decreased corticotrophin and increased cortisol secretion, as well as lower growth hormone, melatonin and prolactin secretion (Medori et al., 1992). In the early stages of FFI, the memory and attention are not affected but the deficit develops with time. Surprisingly, the majority of complex intellectual functions remain well preserved during onset and progression of FFI. The diagnosis of FFI is typically an electroencephalogram where the atypical sleep patterns accompanied by sympathetic hyperactivity are identified (Lugaresi et al., 1998).

Fatal insomnia can occur sporadically (sFI) as well when it does not exhibit any familial history (Montagna et al., 2003). Both types FFI and sFI have been found to have a potential for experimental transmission (Tateishi et al., 1995, Collinge et al., 1995).

1.8.3 Gerstmann-Straussler-Scheinker syndrome

Gerstmann–Sträussler–Scheinker syndrome (GSS) is associated with an autosomal dominant mutation in the *PRNP* gene. The incidence of GSS is approximately 1 in 100 million people per year (Belay, 1999).

The onset of GSS is usually in individuals aged between 30 to 60 years old and occurs with a slow progression of disease between an onset of clinical signs to the terminal disease around 3.5 and 9.5 years. The clinical signs of GSS include cerebellar ataxia, abnormal walking, dementia, dysarthria and parkinsonism (Imran and Mahmood, 2011b). Abnormal sleep and body temperature patterns may accompany the clinical manifestation (Provini et al., 2009). Polymorphisms in PrP associated with GSS include P102L, P105L, A117V, Y145X, Q160X, F198S, Q217R, Y218N, Y226X and Q227X (Jansen et al., 2010). In some forms of GSS, the PrP features a stop codon mutation, such as Y145X, Q160X, Y163X, Y226X, and Q227X, causing a C-terminal truncation and therefore an anchorless protein (Ghetti et al., 1996, Jansen et al., 2010, Jayadev et al., 2011).

The experimentally studied anchorless forms of mutant PrP generated GSS-like fragments and the amyloidogenesis role of anchorless PrP has been proposed (Zanusso et al., 2014). The M129V polymorphism in *PRNP* influences GSS disease phenotype; the most common cause of GSS is a combination of V129 and P102L polymorphisms that result in a prevalence of psychiatric disorders (Bianca et al., 2003). The neuropathological features associated with GSS are accompanied by amyloid plaques, spongiform changes, neuronal loss and astrocytic gliosis (Liberski et al., 2010).

1.9 Prion-like disease and prions

Protein misfolding neurodegenerative disorders are associated with conformational change of a protein that subsequently accumulates in the brain of affected individuals with resultant neurodegeneration accompanied by disease-specific clinical signs (Frost and Diamond, 2010). In prion disease the protein that misfolds is PrP^{C}, in Alzheimer's disease (AD) the protein is β-amyloid, in Parkinson's disease (PD) the protein is α-synuclein; and for Huntington's disease (HD) it has been found to be huntingtin protein (Brundin et al., 2010). Prion diseases are increasingly viewed as an important model for protein misfolding neurodegenerative diseases such as AD, PD and HD. They all exhibit a prion-like phenomenon evidenced by transcellular spread of misfolded disease-specific proteins, at least in experimental studies (Aguzzi and

Rajendran, 2009). In this context, understanding the mechanism of bona fide prion-induced neurotoxicity will therefore be relevant to human-specific protein misfolding neurodegenerative diseases (Kaufman and Diamond, 2013). This is an important area of research since its elucidation will provide strategies for therapeutic interventions, an important goal given the increasing world-wide aging population (Farooqui and Farooqui, 2009). However, the hallmark feature of *bona fide* prion diseases is their transmissibility between individuals of the same species and, in certain cases, between individuals of different species.

1.10 Prion protein conformational change and aggregation

Prion diseases are characterised by conformational change of PrP^{C} to PrP^{Sc} and subsequent aggregation of the prion disease-associated pathological form of PrP. To date, the location of PrP^{C} conformational change to PrP^{Sc} has not been fully identified. In genetic prion diseases, the pathogenic form of PrP presumably rises during its biosynthesis because of the mutation in amino acid sequence (Prusiner, 1998, Harris, 1999). In the case of acquired prion disease, the contact of exogenous PrP^{Sc} with endogenous PrP^{C} is required in order to trigger the accumulation of the pathogenic form of PrP (Prusiner, 1998). While the first contact between the two isoforms of PrP presumably occurs at the cell surface, the subsequent conversion can either take place immediately at the membrane or after endocytosis in endolysosomal structures or the ER (Shyng et al., 1993, Campana et al., 2005). Lipid rafts may play a role in the pathological conversion since PrP^{C} is released from the raft during endocytosis and is exposed to the negatively charged membrane (Sanghera and Pinheiro, 2002). Other suggestions have proposed that PrP^{C} simply accumulates on lipid rafts, which would increase the chance of a pathological conversion or that the lipid raft itself facilitates the conversion by the lipid chaperons present on its surface acting as cofactors (Campana et al., 2005).

Two mechanisms have been proposed for the conversion from PrP^{C} to PrP^{Sc} and its subsequent aggregation: the template-directed model (Griffith, 1967, Prusiner, 1991) and the nucleation-dependent model (Jarrett and Lansbury, 1993). The template-directed model proposes that the interaction between exogenous PrP^{Sc} and endogenous PrP^{C} triggers the pathological conformation shift from PrP^{C} to PrP^{Sc} (Prusiner et al., 1990, Telling et al., 1995). In this model, PrP^{Sc} acts as a matrix or a catalyst that imprints its structure onto PrP^{C}. There is a possibility for a role of a hypothetical chaperone that enables the conversion in the template-directed model (Huang et al., 1996). The nucleation-dependent model predicts the presence of a reversible

thermodynamic balance that requires high energy investment to ensure pathological conversion from PrP^{C} to PrP^{Sc}. In this model, the addition of PrP^{Sc} seed initiates PrP^{Sc} aggregation, recruitment of PrP^{C} into the nucleus and its subsequent conformational change into its pathological form. Possibly, this conversion involves some kind of PrP intermediates facilitating or enabling the process (Collinge, 2001). It is proposed that the seeds of PrP^{Sc} are highly organised and gradually create amyloid structures (Campana et al., 2005). The number of infectious nuclei increases by aggregate fragmentation that is essential for prion propagation (Piening et al., 2005). Subsequently, disease associated PrP can, on occasion accumulate into insoluble aggregates, so called prion plaques (Guo and Lee, 2014). These PrP^{Sc} protein aggregates may comprise of 8 to 20 nm wide filaments enriched for amyloid β-sheet structure.

1.11 Prion-induced neurodegeneration

Little is known about the role of the PrP^{Sc} in prion-induced neurodegeneration since examples exist where there is no detectable PrP^{Sc} present while the infectious prions are present (Collinge et al., 1995, Wille et al., 1996, Lasmézas et al., 1997, Shaked et al., 1999). According to the prion hypothesis, the transmissible infectious agent is composed mostly or solely of protein, namely PrP^{Sc}. The deposition of PrP^{Sc} has been co-localised with prion disease-linked neuropathological changes, such as spongiosis and neuronal death (Jendroska et al., 1991). However, in some cases, the level of PrP^{Sc} does not correlate with the degree of neurotoxicity. Murine PrP transgenic mice with the GSS P101L mutation exhibit typical prion disease symptoms but display low levels of PrP^{Sc} accumulation (Manson et al., 1999). Transgenic mice expressing anchorless PrP have shown disease-associated PrP accumulation but failed to exhibit any clinical symptoms (Chesebro et al., 2005). These results suggest that PrP^{Sc} might not be the only neurotoxic species causing prion disease-associated neurodegeneration.

During prion-induced neurodegeneration, PrP^{Sc} accumulation might occur in the endoplasmic reticulum (ER) (Lindholm et al., 2006). Disturbances in ER function caused by misfolded protein accumulation can cause ER stress, which may involve changes in Ca2+ homeostasis. The response of the ER is an attenuation of translation coupled with ER chaperone action and misfolded protein degradation. Once a certain level of ER stress is reached and maintained, cellular dysfunction and eventually cell death are presumably initiated. In PrP^{Sc}-treated neuroblastoma cells, increased calcium levels have been reported (Hetz et al., 2003). Subsequently, ER calcium stores were depleted by thapsigargin treatment, which in turn reduces

calcium levels (Hetz et al., 2003, Lindholm et al., 2006). This experiment suggested ER involvement in the PrP^{Sc}-associated pathology mechanisms. ER stress is able to activate signalling pathways such as the unfolded protein response (UPR) that acts against the effects of the original stress (Paschen and Frandsen, 2001, Breckenridge et al., 2003, Rao et al., 2004). The UPR is able to alter expression levels of different types of proteins, can inhibit protein synthesis to alleviate the burden upon the ER and can result in degradation of misfolded proteins (Paschen and Frandsen, 2001, Lindholm et al., 2006).

1.12 Cell-to-cell spread of prions

In several protein misfolding neurodegenerative diseases, misfolded protein may be recruited into intracellular aggregates that reside in the cytoplasm (Pearce et al., 2015). In the case of prion disease, most misfolded PrP is membrane bound, intracellular, or extracellular. This fact creates a biological conundrum as the misfolded protein aggregates are required to traffic from cell-to-cell to find a way from the donor cell to an acceptor one and to recruit the native form of protein. While viruses and bacterial pathogens have well known mechanisms of membrane trafficking, the cell-to-cell spread of prion proteins and their large-sized aggregates is not clearly defined (Aguzzi and Rajendran, 2009). There are two apparent steps required to transfer any pathological protein aggregate from cell-to-cell and that is exit from a donor cell and subsequent uptake by an acceptor cell (Costanzo and Zurzolo, 2013). The release of disease-associated PrP can be either passive as may occur during membrane leakage as a consequence of cell death. Alternatively, misfolded PrP may be released from cells through active secretion. The entry of disease-associated PrP into a recipient cell can be either through the penetration of the plasma membrane or via endocytosis. All of these steps would require the spread of prions through extracellular spaces. On the other hand, the intercellular spread of prions via tunnelling nanotubes (TNTs) has been proposed that would bypass extracellular prion transfer (Gousset et al., 2009, Rustom et al., 2004). In the case of PrP^{Sc}, there is evidence of its axonal transport to the nerve terminals along the neurons that would suggest its transfer through a synaptic gateway (Borchelt et al., 1994).

It is necessary to identify which cell types are involved in PrP^{Sc} trafficking and/or conversion as this has implications for therapeutic strategies. Multiple cell types have been found to be able to produce PrP^{Sc} *in vivo* and therefore might play a role in intercellular disease spread *in vivo*. These cell types are neurons, astrocytes and other glial cell types and lymphoreticular cells (Blättler et al., 1997, DeArmond et al., 1998, Diedrich et al., 1991, Race and Ernst, 1992). In the

case of peripheral prion infection, such as the result of oral exposure, the cooperation of several cell types is expected to be involved prior to neuroinvasion (Gerdes, 2009). It is believed that prions are able to cross the epithelial cell layer in the intestine and then use bone marrow-derived dendritic cells as a transporter to peripheral lymphoid tissue. The route from the periphery to the CNS has not been fully identified and no histopathological changes have been found in organs other than the CNS (Glatzel and Aguzzi, 2000). One of the explanations for a long incubation time of prion disease can be multiplication of prions in various locations. The main candidate for such a reservoir is the lymphoreticular system (LRS) as prion replication in lymphoid organs precedes that which occurs in CNS (Eklund et al., 1967). It is established that prion infectivity accumulates in lymph nodes as well as in intestinal Peyer's patches. After intragastric inoculation of scrapie prions to mice, Peyer's patches are the location of immediate prion replication followed by their replication in the spleen (Kimberlin and Walker, 1989). Others have discovered a different reservoir of infectivity in the peripheral nervous system, such as sensory and sympathetic ganglia (Groschup et al., 1999). In orally challenged hamsters with scrapie, PrP^{Sc} was detectable in enteric ganglia whereas after intraperitoneal injection of scrapie to hamsters, PrP^{Sc} was identified in both enteric and dorsal root ganglia (McBride and Beekes, 1999).

Since lymphoid tissue is involved in prion replication following peripheral exposure, there must be a specific cell type involved in prion propagation. It has been shown these cells are long lived, as established by an ionizing radiation study in mice, therefore making follicular dendritic cells (FDCs) the prime candidate cell type (Fraser and Farquhar, 1987). Experiments on mice with inactivated FDCs found an absence of prion replication after scrapie inoculation (Muramoto et al., 1993). Further studies have shown that prion accumulation relies on FDCs that express PrP^{C} (Brown et al., 1999). Immune system components seem to be required for prion infectivity transfer to the CNS (Glatzel and Aguzzi, 2000).

The transfer from the lymphoid tissues to nerves may occur through exosomes or the direct contact of molecules attached to a membrane of neighbouring cells where the PrP^{C} and PrP^{Sc} may come to contact (Kanu et al., 2002, Klöhn et al., 2013, Fevrier et al., 2004, Leblanc et al., 2017). Both neural loss and gliosis are associated with the accumulation of misfolded PrP. Separate astrocyte cultures are able to sustain efficient prion propagation (Cronier et al., 2004). Interestingly, astrocytes were found to be a primary site of prion accumulation (Victoria et al., 2016, Diedrich et al., 1991). The role of glial cells in prion spread is intensively studied as these

structures tightly surround neurons, have the possibility to migrate, and are connected to the vascular system creating a blood-brain gateway (Victoria et al., 2016). Activation of glial phagocytosis has been found to clear the protein aggregates and damaged neurons in various neurodegenerative diseases and CNS injuries (Mosher and Wyss-Coray, 2014, Burda and Sofroniew, 2014, Boillée et al., 2006, Pearce et al., 2015).

1.13 Topological forms of prion protein

PrP^C is predominantly a membrane tethered protein held in place by a GPI-anchor (Stahl et al., 1992). However, this protein is able to adopt various topological forms during its biogenesis. These different topological forms are believed to be generated in small amounts and comprise: 1) a secreted form that lacks a GPI-anchor that is released into the extracellular space (Hay et al., 1987b, Campana et al., 2007); 2) a cytosolic form that lacks both a GPI-anchor and an N-terminal signal peptide and therefore cannot be trafficked to the membrane and remains intracellular (Rane et al., 2004); 3) two different transmembrane forms where one comprises a glycosylated form of PrP and the other is an unglycosylated intermediate of similar transmembrane orientation that are both sensitive to protease digest (Hay et al., 1987a, Yost et al., 1990). The reason different topological forms arise might be due to inefficiency of the N-terminal signal peptide and subsequent failure of the protein to translocate into the lumen of the ER during biosynthesis (Rane et al., 2010, Stewart and Harris, 2003). PrP^C species with different topology have been proposed to be key neurotoxic intermediates in prion diseases (Stewart and Harris, 2003).

The secreted form of the PrP^C protein, PrP(ΔGPI), was first revealed in protein translation studies and was subsequently discovered in the medium of cultured cells, cerebrospinal fluid, serum and urine (Hay et al., 1987b, Borchelt et al., 1993, Parizek et al., 2001, Notari et al., 2012). The secreted and other truncated PrP forms can possibly arise by escape from glycolipidation, phospholipase-C cleavage or exosome-associated secretory processes (Borchelt et al., 1993, Parkin et al., 2004, Fevrier et al., 2004). It has been found that while the anchorless form of PrP adopts a protease-resistant form in cell-free systems, the same conformational change does not occur in cell culture experiments (Kocisko et al., 1994, Lawson et al., 2001, Rogers et al., 1993, Caughey and Raymond, 1991). Transgenic mouse models that express secreted PrP at a physiological level did not develop any striking pathology (Chesebro et al., 2005). In contrast, the overexpression of anchorless PrP above the physiological level resulted in spontaneous GSS-like

neurologic dysfunction, high infectivity and a high potential of cross-species transmissibility (Stöhr et al., 2011, Race et al., 2015, Thackray et al., 2012a). The amyloid deposition profile in anchorless PrP transgenic mice has been found to be angiocentric as opposed to the normal granular deposition of PrP^{Sc} in other mouse models of prion disease (Zanusso et al., 2014, Campana et al., 2007). Anchorless PrP has been described in patients with GSS which suggests this form of PrP has a role in prion-related neurotoxicity in these individuals (Jansen et al., 2010).

The cytosolic form of PrP^{C} protein, PrP(cyt), was found to accumulate in the cytosol in relatively low levels that are rapidly degraded (Rane et al., 2004). This PrP species accumulates in cells when treated by proteasome inhibitors and based on this observation the retro-translocation of the protein from the ER lumen has been proposed as a possible mechanism of cytosolic PrP generation (Stewart and Harris, 2003). PrP(cyt) has been proposed to be a neurotoxic intermediate and it was found to be able to misfold into a PrP^{Sc} analogue (Ma and Lindquist, 2002, Stewart and Harris, 2003). Mice transgenic for PrP(cyt) expression showed degeneration of cerebellar granule neurons and severe ataxia (Ma et al., 2002). In contrast to these observations, PrP(cyt) is not overtly toxic when expressed in *Drosophila* (Thackray et al., 2014b).

Transmembrane forms of PrP span the lipid bilayer using the highly conserved hydrophobic region that comprise amino acid residues 111 to 134 (Stewart and Harris, 2003). PrP can be orientated with either the N- or C-terminus protruding from the extracytoplasmic side of the membrane. These PrP species are part of a normal ER biosynthesis of a wild type PrP and are generated in small amounts (Harris, 2003). Some disease-linked mutations, such as A177V in human GSS, can increase the relative expression of the transmembrane form of PrP (Hegde et al., 1998).

All of these different topological forms of PrP^{C} might arise as a result of normal ER quality control mechanisms. Whether these different forms of PrP^{C} play any role in pathological conversion of the prion protein or the spread of infectious agent remains to be answered.

1.14 Prion strains

Different isolates of prion-infected material from the same species show different prion disease phenotypes when serially passaged in isogenic mice (Hill and Collinge, 2003). These various phenotypes are reflected as different neuropathologies and biochemical properties of PrP^{Sc} and are called prion strains. Each prion strain can be maintained through several passages in model animals. For conventional pathogens, disease strains represent a genetic variant or a subtype of

the moiety responsible for the disease. This concept is not valid in prion biology since prions lack a DNA-based genome and has been the main reason to doubt or refute the protein-only hypothesis (Chesebro, 1998). Under normal circumstances, different disease phenotypes are caused by a genetic mutation or polymorphism in a nucleic acid-based genome. With respect to prion diseases, it is assumed that alternative conformations of PrP^{Sc} are responsible for the strain phenomenon. Apart from PrP^{Sc} conformational change, other theories suggest different PrP^{Sc} glycosylation ratios may dictate prion strain properties (Collinge, 2001). Different prion strains trigger disease with conserved characteristics specific for each prion strain. These characteristics include incubation time, lesion profiles, clinical signs and PrP^{Sc} biochemical properties; these are maintained during serial passage, usually in mice.

The first observation of multiple variants of scrapie were described in experimentally infected goats that manifested either a scratching or drowsy phenotype (Pattison and Millson, 1961). Transmission of brain material from sheep that displayed these two different phenotypes to mice, resulted in distinct incubation periods for the onset of prion disease and unique lesion profiles in the murine brains (Fraser and Dickinson, 1973). Significantly, these properties were retained upon serial passage in the same mouse line. Similar phenomenon was also observed for sCJD isolates where the clinical and histopathological features diversified amongst these cases of human prion disease (Aucouturier et al., 1999). Moreover, vCJD can be considered a distinct prion strain as it differs from sCJD in many features such as age of disease onset, length of clinical course, amyloid plaque deposition and vacuolation profile (Bruce et al., 1997, Will et al., 1996). The prion strain responsible for vCJD in humans shares striking similarity with the agent responsible for BSE in cattle when both are passaged in wild type mice. This strongly supports the hypothesis of their shared origin (Hill et al., 1997).

There have been multiple attempts to elucidate the biochemical features of PrP^{Sc} that dictate prion strain-specific properties. It has been shown that PrP^{Sc} associated with FFI and genetic cases of CJD (gCJD) have different deglycosylated PK-resistant fragments of molecular mass of 19 kDa and 21 kDa, respectively (Monari et al., 1994, Parchi et al., 1996). After the transmission of FFI and gCJD to human PrP transgenic mice, PrP^{Sc} retained the molecular mass profiles seen in the original human isolates (Telling et al., 1996). The same phenomenon was discovered in hamster models of transmissible mink encephalopathy where two distinct phenotypes Hyper and Drowsy were biochemically different and conserved during prion propagation in a cell-free

environment (Bessen et al., 1995). PrP^{Sc} would appear to be able to alter its conformation in order to induce a particular disease phenotype with no change in the primary structure of PrP.

Prion strains can be only identified by transmission in isogenic hosts with subsequent phenotypic and molecular PrP^{Sc} readout. However, the molecular and biochemical readouts are increasingly used for prion strain typing (Aguzzi et al., 2007). One of the possible indicators can be a banding pattern of PrP in the western blot analysis. Sporadic CJD PrP^{Sc} exhibits a predominance of mono-glycosylated protein whereas di-glycosylated bands prevail in vCJD PrP^{Sc} (Collinge et al., 1996). Another indicator of prion strain identity is the PK-digest pattern as the cleavage sites of PrP^{Sc} might differ based on the conformation variation. After PK-digestion of L-type BSE, the resulting band appears to be lower than the PrP^{Sc} band of digested H-type BSE (Biacabe et al., 2004).

Various prion strains exhibit differential targeting of tissues and organs. There are two groups of organ tropism, neurotropic and lymphotropic (Aguzzi et al., 2007). Neurotropic prion strains, such as the prion strain responsible for classical BSE, primarily affect the CNS, as the lymphoid tissue contains prions just in the terminal stage of the disease (Sigurdson et al., 1999, Hilton et al., 2004, Heggebø et al., 2002). The lymphotropic prion strains, such as prions that cause vCJD, some scrapie strains and CWD, first target peripheral lymphoid structures before neuroinvasion (Sigurdson et al., 1999, Hilton et al., 2004, Heggebø et al., 2002, Aguzzi et al., 2007). In lymphotropic strains, both CNS and lymphoid tissues are targeted with the disease progression. The differences however are not absolute as the tissues are targeted to a different extent in each prion disease and between different prion strains (Aguzzi et al., 2007).

Another phenomenon tightly connected to prion strains is mutation of the transmissible agent. Strain mutation is triggered by conformation deviation during PrP^{Sc} propagation (Li et al., 2010). This deviation then spreads and creates a new prion strain with different biochemical and pathological characteristics. The reason for prion strain mutation is either an occurrence of a new shape of misfolded PrP that is then propagated or the presence of a mutated population of PrP present at a low titre in the original inoculum. Multiple prion strains of scrapie can be found in one isolate (Thackray et al., 2011, Solforosi et al., 2013, Kimberlin and Walker, 1978). Another disease where multiple prion strain coexistence was confirmed is sCJD (Polymenidou et al., 2005).

Prion strains and different prion diseases have various species compatibility that arises from a complex synergy of primary amino acid sequence, glycosylation patterns and PrP^{Sc} conformation structure, which collectively manifests itself as the species barrier (Moore et al., 2005, Pattison and Jones, 1968). The species barrier complicated the initial passaging of animal and human prions in rodent hosts as it prevented efficient transmission of prion disease (Aguzzi et al., 2007). The dissimilarity of PrP could be overcome by introduction of PrP transgenes into murine hosts that facilitated strain and disease research (Scott et al., 1989, Scott et al., 1997). The species barrier is now known to be dependent upon PrP amino acid sequence and the prion strain under analysis are congruent with the species form of the inoculum (Torres et al., 2014).

1.15 Synthetic prions

The experimental generation of synthetic prions that would act similarly to their natural counterparts is necessary to validate the prion hypothesis (Harris, 1999, Legname and Moda, 2017, Prusiner, 1982). The process of PrP^{C} conversion into PrP^{Sc} is of fundamental importance to assess the efficacy of therapeutic strategies able to interfere with this process. Prions appear to be defined exclusively by folding of a pathological isoform of PrP^{Sc} with no ivolvement of a DNA-based genome and alteration of PrP amino acid sequence (Moda et al., 2015). The ability of synthetic prions to induce pathology in animals would help to decipher pathological properties of the prion strains and confirm that these are enciphered in abnormal conformations of PrP associated with these infectious agents (Legname and Moda, 2017).

Initial attempts to assemble synthetic PrP^{Sc} fibrils and generate prion strains *de novo* were performed by the *in vitro* conversion of recombinant PrP into amyloid structures (Moda et al., 2015). In most cases, these fibrils were found to be infectious but not to the extent of *bona fide* prions, unless RNA or lipid molecules were added as cofactors during the *in vitro* conversion process (Wang et al., 2010, Makarava et al., 2010, Wang et al., 2017).

Subsequent studies utilised purified recombinant full-length mouse PrP in conjunction with common chemicals, such as guanidine hydrochloride, with or without the addition of sodium chloride or dithiothreitol to induce recombinant mouse PrP conversion into a pathological form, which was subsequently tested for pathogenicity upon *in vitro* cultured cell lines (Moda et al., 2015). The products generated were verified by inoculation of mouse hypothalamic cell line and neuroblastoma cell line with novel amyloid preparations. Several preparations of *in vitro* converted PrP exhibiting distinctive proteinase-resistant PrP material were shown to cause prion

strain-specific neuropathology when inoculated into mice (Moda et al., 2015). However, clinical signs typical of murine prion infection were not manifested in these mouse transmission studies.

More experiments with synthetic prions have to be carried out to elucidate the molecular events involved in PrP conversion, accumulation and propagation of mammalian prions. This is particularly important in order to further confirm the protein-only hypothesis that is currently favoured amongst prion biologists and also, synthetic prions might serve as a model system where the assembly mechanism and structural properties of the infectious agent could be elucidated (Schmidt et al., 2015). The strain identity, conformational diversity and other biological activities would also be able to be confirmed if the synthetic prions are assembled successfully.

1.16 The role of immune system in prion diseases

Acquired prion diseases are normally transmitted through oral exposure to prion-infected material (Wilesmith et al., 1991, Bruce et al., 1997, Hill et al., 1997). The proposed route of prion infection from the gastro intestinal tract to CNS involves transition through the lymphoreticular system. Transgenic mouse models revealed induction of follicular dendritic cells (FDCs) and subsequent upregulation of lymphotoxin α and β at the site of inflammation (Heikenwalder et al., 2005). Sheep with classical scrapie show PrP^{Sc} accumulation in mammary glands and simultaneous mastitis (Ligios et al., 2005). Also, PrP^{Sc} was detected in macrophages during classical scrapie (Herrmann et al., 2003). *In vitro* experiments revealed that peritoneal macrophages co-cultured with scrapie agent are able to reduce scrapie infectivity (Carp and Callahan, 1982). The role of macrophages in pathogenesis is not fully understood, however, depletion of macrophages in a murine model of scrapie caused higher mutant PrP accumulation in spleen and reduced incubation time (Beringue et al., 2000).

Prion diseases typically involve an increase of activated and phagocytic phenotype of microglia (Perry et al., 2002, Perry et al., 2010). Microglia were found to control repair and inflammatory processes and on the other hand, their potential to trigger neurotoxic pathways was revealed (Obst et al., 2017). The proliferation of microglia in prion disease is regulated by the activation of CSF1R gene – macrophage colony-stimulating factor 1 receptor (Olmos-Alonso et al., 2016, Obst et al., 2017). Prolonged inhibition of CSF1R in a murine model of AD pathology blocked proliferation of microglia and subsequently prevented synaptic neurodegeneration (Olmos-Alonso et al., 2016). The question that remains to be answered is if the microglia activation arises

as a consequence of misfolded protein accumulation or as a response to synaptic damage (Cunningham et al., 2003). Identification and subsequent manipulation of the components involved in the immune response to neurodegeneration might be a plausible route to develop therapeutics against neurodegenerative diseases, including prion disease (Stephenson et al., 2018).

1.17 Detection of prions

Prion disease in natural hosts, such as sheep, cattle or human, exhibit a long incubation time before clinical signs manifest. The years or decades long disease onset, outbred populations and ethical concerns render studies of prion-induced neurotoxicity in the natural hosts difficult. As a consequence, *in vitro* detection systems for PrP^{Sc} or *in vivo* detection of *bona fide* prion infectivity in animal models of these diseases are increasingly used in the study of mammalian prion disease.

1.17.1 *In vitro* detection systems of PrP^{Sc}

There have been numerous attempts aimed at the detection of PrP^{Sc} without a need for a lengthy bioassay in experimental animals. Unfortunately, the detection and quantification of PrP^{Sc} is difficult and few methods are able to reliably detect the pathological form of the prion protein. Due to the nature of nucleation-dependent prion replication, the *in vitro* detection systems are taking advantage of this *in vivo* process to replicate the conversion of PrP^{C} to PrP^{Sc} in the test tube (Barria et al., 2012).

The most widespread and well-established method of PrP^{Sc} detection is western blot coupled with PK-digestion (Rubenstein et al., 1986). The PrP^{Sc} protein typically exhibits resistance to digestion by proteinase-K in contrast to PrP^{C} that is fully digested. PK-digest results in a proteolytically truncated form of PrP^{Sc} with a characteristic band pattern formed at a molecular weight of 27 to 30 kDa when detected by western blot using anti-PrP monoclonal antibody (Stahl and Prusiner, 1991). The glycosylation ratio and therefore the position of bands on the western blot can help to discriminate different diseases and different prion strains (Collinge et al., 1996). Another common method of PrP^{Sc} detection *in vitro* is protein misfolding cyclic amplification (PMCA). This assay relies on cycles of accelerated prion replication and comprises two subsequent steps followed by PK-digest and western blot (Saborio et al., 2001). In the first step, the test homogenate that contains minute amounts of PrP^{Sc} is incubated with a high concentration of purified PrP^{C} that acts as a source of PrP for ongoing pathological conversion.

The second step of PMCA is a sonication phase that disturbs and multiplies the number of existing PrP^{Sc} nuclei present in the test sample without disturbing their ability to convert (Soto et al., 2002). New PrP^{Sc} molecules are generated in an exponential fashion, if the original sample contains PrP^{Sc} seeds. As little as one PrP^{Sc} seed is enough to be detected by PMCA (Saá et al., 2006). The final level of PrP^{Sc} in the sample can be detected by western blot after PK-digestion to reveal and quantify the presence of misfolded PrP.

Another, more recent method developed for detection of protein misfolding and aggregation is real-time quaking-induced conversion (RT-QuIC) assay (Atarashi et al., 2011a, Atarashi et al., 2011b). This assay is based on amplification of minute amounts of PrP^{Sc} in the presence of soluble recombinant PrP. Intermittent shaking is employed to enhance the seeding reaction of PrP conversion to PrP^{Sc} that aggregates and/or creates fibrils. In comparison to PMCA, RT-QuIC avoids PK-treatment coupled with western blot and employs the protocol of a previously established amyloid seeding assay (ASA) (Colby et al., 2007) that uses thioflavin T (ThT) fluorescence dye to quantify amyloid formation by fluorescence readings. This allows for a real time observation of the amplification cycles and if the endpoint titration is used, even the quantification of the PrP^{Sc} present in the infectious samples. RT-QuIC is particularly useful for the misfolded protein species that may be sensitive to PK-treatment and therefore not detectable by other methods (Shi et al., 2015, Colby et al., 2007).

1.17.2 *In vivo* detection systems of PrP^{Sc}

Large animal models

The only reliable method of detection of *bona fide* prion infectivity is bioassay in an experimental host. Bioassay is a method that allows us to study infectivity of prions *in vivo* and confirm prion disease transmissibility. Scrapie, as the first discovered animal prion disease, has been initially studied in its natural host, namely sheep. The transmission potential of scrapie was shown by inoculation of brain material from sheep that exhibited clinical signs of the disease into healthy sheep (Cuillé and Chelle, 1936). It has been found that BSE transmission from cattle to sheep is possible by intracerebral injection and BSE is able to exhibit the same lesion profile in the brain of sheep as it does in the original host (Foster et al., 1996). The BSE agent was tested for its transmission potential from cattle to sheep by blood transfusion (Houston et al., 2000). The results indicate that the glycoform pattern of PrP detected by western blot with anti-PrP monoclonal antibody in sheep is comparable to the one seen in cattle BSE. Ruminants in general

were extensively used to investigate transmissibility and differentiation of prion disease. Similarly, the experimental transmission of scrapie from sheep to cattle by intracerebral injection was confirmed in this large animal model and the scrapie transmission from sheep to cattle was deemed possible under experimental conditions (Gibbs et al., 1990). In cattle, the identification of PrP polymorphisms took place and E211K H-type BSE-associated polymorphism was described (Greenlee et al., 2012). The involvement of E211K was confirmed by experimental inoculation of E211K cattle with H-type BSE that revealed significantly reduced time to onset of clinical signs.

Another prion disease often studied in large animal hosts is CWD. In CWD research, deer models are sometimes employed to identify the routes of infection and to test diagnostic assays. Specifically, the routes of infection are under scrutiny as the way of prion transmission from animal to animal has not been verified. Using white-tailed deer as an animal model, the animals were exposed to CWD prions by either administration of saliva from CWD-positive animals, intraperitoneal blood injection, intracranial brain injection/aerosol administration or by sharing the environment with CWD prion-positive individuals (Davenport et al., 2018). After this experiment, it was concluded that prions can be horizontally transferred by saliva, as was suggested earlier by others (Davenport et al., 2018, Haley et al., 2011, Henderson et al., 2013). Saliva exposure remains the most likely mediator of deer-to-deer transmission of CWD. Other species used in CWD research often include other cervid species such as reindeer, mule-deer, white-tailed deer and elk (Sigurdson and Aguzzi, 2007, Cheng et al., 2016). However, with an advent of genetic engineering, transgenic models, specifically murine, are employed to substitute the large animal models. Transgenic mice can be tailored to harbour any species-specific PrP (ovine, bovine or cervid) and can then be used for bioassays.

Primate models

Shortly after the scrapie agent was categorised as a possible slow virus (Sigurdsson, 1954), the first human prion disease, kuru, was identified (Gajdusek and Zigas, 1957). Since kuru is a human disease, the need for animal models to study this condition arose and the first emerging animal model of human prion disease were primates, specifically chimpanzees. The transmission of kuru to chimpanzee was demonstrated in 1966 (Gajdusek et al., 1966), followed by CJD transmission to chimpanzees in 1968 (Gibbs et al., 1968). Primate animal models for prion disease were also utilised during the BSE epizootic in the UK when the link between bovine prions and vCJD was discovered through transmission studies that used macaque monkeys (Lasmézas et al., 1996). Macaques are probably the most widespread primate animal model in use, due to their

phylogenetic proximity to humans, genetic similarity, and methionine homozygosity in PrP amino acid position 129. The pathological phenotype in intracerebrally prion-inoculated macaques, such as specific distribution of brain vacuolation, was found to be extremely similar to the one vCJD exhibits in humans (Lasmézas et al., 1996, Lasmézas et al., 2001). Another primate model used for vCJD transmission studies was lemur. Lemurs orally challenged with BSE exhibited PrP^{Sc} in the gastrointestinal tract as well as in lymphoid tissues, confirming the theory of the oral transmission route of vCJD (Bons et al., 1999). Non-human primate models, including squirrel, spider, capuchin and African green monkey were utilized in comparison studies of prion strains (Parchi et al., 2010). Other studies, carried out in macaques, were performed to discover the zoonotic potential of prion diseases upon blood transfusion and to verify the risk of BSE by oral transmission in this host (Lasmézas et al., 2005, Lescoutra-Etchegaray et al., 2015). CWD research recently employed the macaque model as well. The potential of cervid to human inter-species CWD transmission was modelled in macaque to answer this important question (Race et al., 2018). The results obtained showed that CWD fails to cross the inter-species barrier and suggest that CWD is not transmissible to primates. Understandably, the experiments on primates are limited because of the ethical concerns, and additionally, due to their longevity and high cost (Brandner and Jaunmuktane, 2017).

Rodent models

The most developed and commonly used laboratory animals used to model prion disease are rodents (Wadsworth et al., 2010). The use of a bank vole as an experimental animal has been tested and this rodent has been identified as a universal acceptor for prions of different species (Chandler and Turfrey, 1972, Di Bari et al., 2008, Di Bari et al., 2013, Nonno et al., 2006, Watts et al., 2014). There are numerous studies where hamsters were used as experimental animals, moreover the incubation period of prion disease is shorter in hamster in comparison to mouse (Kimberlin and Walker, 1977, Prusiner et al., 1985, Meade-White et al., 2009). However, the mouse is considered more universal and is still preferred due to the use of various methods of murine genome manipulation (Kimberlin and Walker, 1977, Watts and Prusiner, 2014).

The majority of animal and human prion diseases have been studied using mouse experimental models (Bruce et al., 1997, Chiesa et al., 1998, Vascellari et al., 2012, Watts and Prusiner, 2014). One of the most important advancements of prion biology were made through the use of $PrP^{-/-}$ (knock-out) and PrP transgenic mice. It has been shown that $PrP^{-/-}$ mice cannot develop prion disease due to the lack of PrP (Büeler et al., 1993). Other studies dedicated to the assessment of

PrP^{Sc} toxicity have used graft transplants of tissue confirmed to contain high levels of PrP^{Sc} to $PrP^{-/-}$ mice (Brandner et al., 1996). PrP^{Sc} deposition and scrapie prion disease-associated neuropathology were evident in the grafted region, whereas there were no pathological changes in $PrP^{-/-}$ tissue. Since $PrP^{-/-}$ mice do not show any prion-induced pathology, this observation suggests that prion diseases are associated with a gain of function of PrP as it converts, or upon its conversion, into PrP^{Sc}. Ablation of PrP^{C} expression during an ongoing prion disease results in a reversal of prion-induced pathology (Mallucci et al., 2003, Mallucci et al., 2007). In this experiment, it has been shown that after the PrP^{C} depletion, neuronal loss was prevented and recovery continued despite the accumulation of PrP^{Sc} in glial cells (Mallucci et al., 2003). Collectively, these experiments suggested that PrP^{C} expression is essential for prion–mediated toxicity and that the neurotoxic agent forms during conversion of PrP^{C} to PrP^{Sc}.

PrP^{Sc} does not seem to be the neurotoxic form of the prion protein responsible for the neuropathology seen during the progression of prion diseases. Accordingly, there have been numerous studies using various transgenic mouse models to investigate the molecular mechanisms responsible for the prion-induced neurodegeneration. Transgenic mouse models with different PrP transgenes were able to trigger neuronal damage even in absence of PrP^{Sc} (Shmerling et al., 1998). Mice transgenic for N-terminal region truncated PrP showed severe ataxia and neuronal death that could be overturned by introduction of PrP^{C} into the same PrP transgenic mouse line. Another PrP form, ^{Ctm}PrP, orthologue to the PrP molecule developed during GSS in humans that shows a transmembrane localisation of its hydrophobic domain, exhibits scrapie-like neurodegeneration in absence of PrP^{Sc} (Hegde et al., 1998). Additionally, it has been suggested that the secretion of PrP from neurons may provide a mechanistic trigger for the neurotoxicity seen in some forms of familial prion disease (Tatzelt and Schätzl, 2007).

The genetic forms of prion diseases have been modelled in mice transgenic for human or humanised murine PrP (Hsiao et al., 1990, Chiesa et al., 1998, Chiesa et al., 2001, Harris et al., 2003, Dossena et al., 2008, Asante et al., 2009, Jackson et al., 2009, Jackson et al., 2013, Wadsworth et al., 2010, Chiesa et al., 2016). Different strategies have been adopted in order to introduce a PrP transgene into the murine genome, including the more common random integration of a transgene (RIT) (Dossena et al., 2008, Bouybayoune et al., 2015, Chiesa et al., 2016) or targeted gene knock-in approach (Jackson et al., 2009, Jackson et al., 2013). The RIT method gives rise to multiple founder mice lines, each with a different level of protein expression, which may be influenced by the number and position of integrated transgenes

(Kaczmarczyk and Jackson, 2015). The knock-in approach is a targeted genome modification where the protein expression corresponds to the natural expression level of a target protein and therefore the disease clinical signs develop later in life in comparison to RIT. Knock-in engineered mice transgenic for murine PrP carrying single codon mutations associated with familial CJD and FFI showed the spontaneous formation of transmissible prions (Jackson et al., 2009, Jackson et al., 2013).

Interestingly, an Alzheimer's disease mouse model studies suggest a role of PrP^{C} in prion-like neurodegeneration where the interaction between β-amyloid and PrP^{C} is suggested and the downstream toxicity of this interaction has been identified (Purro et al., 2018). This evidence suggests that PrP^{C} might be more involved and important in neurodegeneration more generally than previously thought.

While significant achievements in prion biology have been made using mouse as an experimental animal model, studies with the vertebrate host are relatively time-consuming, cumbersome and subject of ethical concerns. As a consequence, there is a need to develop more versatile and tractable animal models of mammalian prion disease.

Invertebrate models

Invertebrate hosts are increasingly employed in neurodegenerative research as animal models in order to discover the molecular mechanisms underpinning the aetiology of various human and animal diseases. Invertebrates typically have a simpler genome and one that can be more rapidly manipulated than in mammalian hosts. One of the most widespread organisms used for neurodegeneration studies is *Drosophila melanogaster*. The advanced state of genetics in the fruit fly enables researchers to readily manipulate the fly genome to study a spectrum of molecular mechanisms (Yoshihara et al., 2001). *Drosophila* has several features which lend itself to its use as an experimental organism. The most important advantages are its well characterised genome with many gene tailoring approaches established, its short lifespan and the ability to generate large numbers of flies to allow robust experimental data collection (Gavin et al., 2006, Ambegaokar et al., 2010). Moreover, the invertebrate brain is composed of similar neuronal types, circuits, ion channels and neurotransmitters as the mammalian brain (Littleton and Ganetzky, 2000). The cellular and molecular pathways of neurodegeneration are similar within invertebrates and mammalian natural hosts (Driscoll and Gerstbrein, 2003). For these reasons, a range of human neurodegenerative diseases have been modelled in *Drosophila* including

Alzheimer's disease (AD) (Wittmann et al., 2001) and Parkinson's disease (PD) (Feany and Bender, 2000).

1.18 *Drosophila* models of prion disease

Various attempts have been made over many years to develop a *Drosophila* model of mammalian prion disease. Early studies in this area investigated expression of full-length Syrian hamster prion protein in *Drosophila* (Raeber et al., 1995). This study showed that mammalian PrP could be successfully expressed in the fly. A variety of other studies have also expressed different species forms of PrP in *Drosophila* and have done so with little evidence of pathological prion formation and no evidence of prion transmissibility (Choi et al., 2010, Fernandez-Funez et al., 2009, Gavin et al., 2006, Murali et al., 2014).

A significant advance in the development of a *Drosophila* model of mammalian prion disease has been made by Thackray *et al.* who have successfully modelled transmissible scrapie disease in *Drosophila* (Thackray et al., 2012b, Thackray et al., 2012a, Thackray et al., 2014a). The system used by Thackray *et al.* involved the generation of ovine PrP transgenic *Drosophila* under expression control of the bi-partite UAS/GAL4 system (Brand and Perrimon, 1993). *Drosophila* transgenic for pan-neuronal expression of ovine PrP developed a neurotoxic phenotype after exposure to exogenous sheep scrapie prion inocula (Thackray et al., 2012b, Thackray et al., 2012a, Thackray et al., 2014a). This scrapie-infected neurotoxic phenotype in PrP transgenic *Drosophila* showed the cardinal signs of *bona fide* prion infection since it was accompanied by the accumulation of PK-resistant PrP and was transmissible to PrP transgenic recipients including ovine PrP transgenic mice (Thackray et al., 2016). These observations show that PrP transgenic *Drosophila* possess all of the necessary co-factors required for mammalian prion propagation and can be used to model mammalian prion disease.

The *Drosophila* model has been used to model inherited prion disease such as GSS (Gavin et al., 2006, Choi et al., 2010, Murali et al., 2014). While *Drosophila* transgenic for PrP with GSS-associated mutations develop clinical signs and neuropathology, *bona fide* transmission of spontaneously formed prions has not been demonstrated. It remains to be shown that *Drosophila* can be used as a valid model of spontaneous generation of infectious prions with all the hallmarks of prion disease.

1.19 *Drosophila* genetics

The use of *Drosophila* as a genetic model organism was initiated by Thomas Hunt Morgan during his investigation of chromosomal theory of inheritance (St Johnston, 2002). The flies were initially used for their short generation time, ease of use and production of big numbers of progeny. Subsequently, the advantages of simple genetics and presence of external features that can be genetically manipulated to represent mutant phenotypes were discovered. The techniques evolved rapidly and allowed *Drosophila* to become one of the most tractable multicellular organisms used for genetic analysis (Rubin and Lewis, 2000). A large number of developmental processes were found to be conserved between *Drosophila* and vertebrates. With an expansion of sequencing techniques, *Drosophila* was one of the first organisms to be used for genomic analysis (Adams et al., 2000). The fruit fly genome consists of approximately 15,000 genes and there is twice as many human homologous genes in the fly genome than in the genome of another widely used model organism *Caenorhabditis elegans* (Friedman and Hughes, 2001). Out of all 287 human disease-associated genes, 197 genes have their *Drosophila* counterpart (Fortini et al., 2000). Using *Drosophila* transgenesis, it is possible to incorporate genes that are not naturally present in the *Drosophila* genome; the human disease-associated transgenes can exhibit very similar symptoms after transgenic expression in the fly (Ambegaokar et al., 2010, Feany and Bender, 2000, Martin et al., 2014). The transgenic *Drosophila* can be successfully used to investigate various basic biological questions such as identification of a gene function or gene involvement in a specific process (St Johnston, 2002).

1.20 Aims and objectives of the project

1) Generation and characterisation of PrP transgenic *Drosophila* to provide alternative approach towards neurodegeneration research
2) Verification of PrP expression levels in *Drosophila* and testing different expression drivers to this extent
3) Investigation of neurodegeneration and its impact in both acquired and genetic prion disease modelled in PrP transgenic *Drosophila*
    a. Observation of early changes in synaptic architecture of PrP transgenic *Drosophila* larvae after scrapie prion inoculation
    b. Investigation of cellular or neuronal populations involved in prion-induced neurodegeneration by biochemical and phenotypical studies in PrP^{C}/PrP^{Sc} chimeric flies

2 Materials and methods

2.1 Plasmids

The pUASTattB plasmids (Bischof et al., 2007) and pJFRC19- MUH plasmids (Pfeiffer et al., 2010) were kindly provided by Dr Alana Thackray, University of Cambridge, UK. The plasmid maps can be seen in **Figure 1**. The pBSKSII-Mo3F4PrP and pBSKSII-HaPrP plasmids were kindly provided by Dr Walker Jackson, DZNE, Germany (Jackson et al., 2013).

2.2 Recombinant prion proteins

VRQ and ARQ recombinant prion protein (Thackray et al., 2003, Thackray et al., 2004) was kindly provided by Dr. Alana Thackray, Department of Veterinary Medicine, University of Cambridge, UK.

2.3 *Drosophila melanogaster*

The various PrP transgenic *Drosophila* used or generated in this thesis are listed in **Tables 1-4** in the first results chapter. All fly lines generated in this thesis were created in collaboration with Dr. Alana Thackray, University of Cambridge, UK. My contribution can be seen from the figures in this thesis as these were all generated by myself. The ovine PrP transgenic fly lines (topological forms of PrP on chromosome 2 under the GAL4-UAS control) generated prior to this research project were kindly supplied by Dr Alana Thackray, University of Cambridge, UK (Thackray et al., 2012b, Thackray et al., 2012a, Thackray et al., 2014b, Thackray et al., 2014a). Stable fly stocks were maintained by conventional fly crosses as balanced fly lines. All fly lines were raised on standard cornmeal media (Lewis, 1960) at 25°C (unless stated otherwise) at low to medium density. The complete list of *Drosophila* genotypes used throughout the project can be seen in **Appendix 8.1.**

The *Drosophila* transgenesis vector pUASTattB was used to generate flies with a PrP transgene on chromosome 2 of the fly genome, while pJFRC19-MUH was used to generate flies with a PrP transgene inserted on chromosome 3 (with an exception of human PrP transgenic flies where pUASTattB was used for both chromosome 2 and 3 transgenesis). The complete list of DNA sequences of transgenes used throughout the project can be seen in **Appendix 8.2.**

2.4 Construction of PrP transgenic flies with insect signal peptide

The generation of *Drosophila* transgenic for murine 3F4 PrP (Mo3F4PrP) and hamster PrP (HaPrP) with a fly leader peptide were underway in this thesis, as well as the human and cervid PrP transgenic flies that were created in the same manner. The method is explained using hamster and mouse 3F4 PrP transgene as an example. The only difference between the generation of the human and cervid PrP transgenes were the primers used (full list of primers used throughout the project can be seen in **Appendix 8.3**). The ovine chromosome 3 PrP transgenic flies were created from existing chromosome 2 ovine PrP transgenes by PCR and RE-digest to be able to ligate these into pJFRC19-MUH plasmid. More details about making the other transgenes can be found in the results section.

The mouse and hamster PrP transgenes for insertion into the *Drosophila* genome were prepared by PCR that generated a DNA fragment encoding the mature form of murine PrP (amino acid residues 23 – 231) or hamster PrP (amino acid residues 23-232) with DNA that encoded an insect secretion signal peptide at the 5' end and a species-specific GPI signal peptide at the 3'end. PCR was carried out using substrate pBSKSII plasmid DNA that contained Mo3F4PrP insert (amino acids 1 – 231) or HaPrP insert (amino acids 1 – 232) and oligonucleotide primers MoPD1F for mouse and HaPD1F for hamster PrP with MoRI reverse primer for mouse and HaFI reverse primer for hamster PrP in the presence of *Pfu* DNA polymerase (Promega). The PCR reaction conditions consisted of an initial denaturation at 95°C for 2 minutes followed by 30 cycles of denaturation at 95°C for 30 seconds, primer annealing at 55°C for 30 seconds and extension at 72°C for 2 min. The final extension of PCR products was carried out at 72°C for 7 minutes.

The second step of PCR was carried out using a product of the first PCR as a substrate. The oligonucleotide primers PD2F with MoRI reverse primer for mouse and HaFI reverse primer for hamster PrP were used. The 788 bp product of the second PCR comprised DNA encoding an insect secretion signal peptide at 5' end followed by DNA encoding either mouse (residues 23 – 231) or hamster PrP (residues 23 – 232) and the DNA encoding a species-specific PrP GPI anchor sequence (amino acid residues 233 – 256) at 3' end. The reaction conditions of the second round of PCR were identical. The PCR primers PD2F and reverse HaRI and MoRI contained *EcoRI* and *XhoI* restriction sites, respectively, that allowed directional cloning of the 788 bp PCR product into the *Drosophila* transgenesis vector pUASTattB. Reverse HaRI and MoRI primers contained

a stop codon ahead of the *XhoI* restriction site. If the PrP transgene was intended for an insertion into pJFRC19-MUH plasmid, the *XbaI* and *XhoI* restriction enzymes would be used.

Each PrP transgene construct was restriction enzyme digested, subsequently ligated into pUAStattB (or pJFRC19-MUH) and rescued by transformation in DH5α bacteria. pUAST-PrP or pJFRC-PrP plasmids were isolated from large-scale cultures by QIAprep Spin Maxiprep Kits (QIAGEN) for subsequent *Drosophila* transgenesis. The purified plasmids were sequenced to verify their identity.

2.5 Restriction enzyme digest of plasmid DNA

pUAST-Mo3F4PrP and pUAST-HaPrP were subjected to restriction digest with the enzymes *EcoRI* and *XhoI*. The restriction enzyme buffer used was RE buffer H (Promega). The RE digest was carried out at 37°C for 90 minutes and the reaction was stopped at 80°C for 10 minutes.

RE digest reaction mix:

Sterile deionised water	10.4 µl
20x digestion buffer H	2 µl
Plasmid DNA (1 µg/sample)	0.5 µl
EcoRI (1U/µl)	1 µl
XhoI (1U/µl)	1 µl
Final reaction volume	20 µl

The same protocol was employed in case of pJFRC19-MUH plasmid with a difference of the restriction enzymes *XbaI* and *XhoI* used here.

The reaction product and a PCR products of PrP transgenes from a previous part were run on 2% low melting point agarose gel (Invitrogen) prepared in 1x TAE buffer [40 mM Tris, 20 mM acetic acid, 1 mM EDTA, pH 8.4] that contained 0.5 µg/ml ethidium bromide. The DNA Hyper Ladder I (10 kb, BIOLINE) was loaded in a volume of 5 µl. The gel was run at 80V/50 minutes. DNA bands were visualised by UV transillumination and the bands of our interest were extracted from the gel following the QIAquick Gel Extraction Kit protocol (QIAGEN). Sterile deionised water was used for a product elution. DNA was quantified using NanoDrop.

2.6 Ligation of PrP transgenes into the pUASTattB or pJFRC19-MUH vector

Ligation reaction was carried out at 18°C overnight to obtain pUASTattB-MoPrP or pUASTattB-HaPrP (with insect signal peptide) plasmid. The same protocol would be applied in case of pJFRC19-MUH-PrP.

Ligation reaction mix:

Sterile deionised water	8.1 µl
25ng of pUAST (pJFRC) vector	1.76 µl
75 ng of PrP insert	5.14 µl
5x T4-DNA ligase buffer	4 µl
1U of T4 DNA-ligase	1 µl
Final reaction volume	20 µl

2.7 Preparation of calcium-competent DH5α

A glycerol stock of Escherichia coli DH5α was kindly provided by Dr Alana Thackray (University of Cambridge). An aliquot of non-transformed DH5α bacteria in 50% glycerol stock was mixed with 200µl of LB-broth, and streaked onto an LB-plate prior to incubation at 37°C overnight. A single colony was picked and transferred to 10 ml of LB-broth, incubated with vigorous shaking (250 rpm) at 37°C for 16 hours. A 100µl aliquot of the overnight bacterial culture was transferred to 100 ml of fresh LB-broth and incubated at 37°C with vigorous shaking (250 rpm) until an OD_{600}=0.35-0.4 was reached. The culture was aliquoted into pre-chilled 50 ml Falcon tubes and left on ice for 30 minutes. Bacteria were pelleted by centrifugation at 6 000 g at 4°C for 20 minutes in a Beckmann-Coulter Allegra 15R centrifuge. The bacterial pellet was re-suspended in 10 ml of pre-chilled 0.45µm filter-sterilised 100 mM $CaCl_2$ and pelleted again by centrifugation. Finally, the pellet was re-suspended in 4 ml of pre-chilled sterile 100 mM $CaCl_2$. One ml of sterile glycerol was added to the solution and 200 µl aliquots of calcium-competent DH5α were frozen at -80°C. The viability of cells was verified by cultivation on LB and LB-Amp plates.

2.8 Transformation of calcium-competent cells

One µl of ligation reaction mix was transferred to 200µl calcium competent DH5α cells and the solution was kept on ice for 20 minutes. The cells were heat-shocked in 42°C water bath/2 minutes and then quenched on ice/2 minutes. Pre-warmed LB-broth (with or without 100µg/ml Ampicillin) was added to the mix and incubated for 90 minutes at 37°C/250 rpm. The samples

were spread on LB and LB-Amp plates and incubated overnight at 37°C to verify the transformation. The transformants were subsequently produced in large scale and the plasmids were isolated using QIAprep Spin Maxiprep Kits (QIAGEN) for subsequent *Drosophila* transgenesis.

2.9 pUASTattB- and pJFRC19-MUH-PrP-mediated transgenesis in *Drosophila*

The pUASTattB-PrP *Drosophila* transgenesis was performed by BestGene® (California, USA) using fly embryos micro-injection technique (**Figure 2** in the first results chapter). The pJFRC19-MUH-PrP transgenesis was performed at the Department of Genetics (University of Cambridge) using the same method. The standard protocol for fly transgenesis was employed (Muhammad, 2012). Pole regions of one-hour old embryos of *Drosophila* (G0) were injected by pUASTattB-PrP or pJFRC19-MUH-PrP plasmids. The integration process was mediated by PhiC31 integrase delivered in the form of mRNA as a part of the recipient fly line genotype.

2.10 Validation of transgenesis in PrP transgenic *Drosophila*

After the generation of PrP transgenic flies in collaboration with Dr. Alana Thackray, University of Cambridge, UK, I went on to validate and characterise the PrP transgenic *Drosophila*. All subsequent experiments were performed solely by myself. The presence of a correct variant of PrP transgene sequence in each appropriate fly line was confirmed by PCR amplification using insert specific primers. The fly heads were dissected by incubation (5 minutes) of plastic vials containing flies in liquid-nitrogen and decapitated by vortexing. The fly head homogenates were prepared by homogenizing 5 fly heads in 25 µl of PK-lysis buffer (10 mM Tris/HCl, pH 8; 1 mM EDTA; 25mM NaCl; 200 µl/ml proteinase-K). The samples were homogenised by plastic hand-held homogeniser, incubated at 37°C for 30 minutes and at 80°C for 10 minutes to stop the reaction. The primers specific for regions immediately 5' and 3' to the ends of the PrP transgene were used (primer sequences in **Appendix 8.3**). Subsequent DNA sequence analysis of the PCR product was used to confirm the correct PrP construct in each appropriate fly line using the vector specific primers pUAST-F and -R or pJFRC-F and –R.

2.11 Cre-mediated excision of the RFP cassette from PrP transgenic *Drosophila*

The transgenic flies generated were carrying a red fluorescent protein (RFP) cassette flanked by *loxP* sites in their genome. PrP transgenic fly lines were subjected to the following fly crosses and G3 flies were crossed to maintain stable stocks of RFP-excised *Drosophila*.

G0: male w; M{PrP, 3xP3-RFP.attP}ZH-51D X female y w; P{Cre}1b; Sco/CyO

G1: male y w; P{Cre}1b; (RFP-)PrP/CyO X female w; Sco/SM6a

G2: male w; (RFP-)PrP/SM6a X female w; Sco/SM6a

G3: male w; (RFP-)PrP/SM6a X female w; (RFP-)PrP/SM6a

2.12 Chromosome balancing and construction of dual PrP flies

Recombination between homologous chromosomes has to be prevented to avoid any fragmentation of the transgene during crossing-over. This is carried out by crossing the PrP transgenic fly line with a balancer fly line to create heterozygous flies that have the PrP transgene on one chromosome while the balancer chromatid is placed on the other one as seen in **Figure 3** in the first results chapter. The details of chromosome balancing and its use are explained in detail in the appropriate results section.

2.13 Construction of dual PrP transgenic flies

In case of dual PrP expressing flies construction, two consecutive crosses were carried out. The first one to re-balance the existing PrP transgenic flies in order to immediately assemble balanced stock while the second cross of the two chosen PrP transgenic fly genotypes was performed. The crossing scheme can be seen in **Figure 15** in the first results chapter and the detailed process is again explained in the appropriate results section.

2.14 Fly head collection

Drosophila melanogaster anaesthetised and culled by freezing at -20°C were used for the fly head collection. Whole flies placed in sealed Eppendorf tubes were snap-frozen in liquid nitrogen for 5 minutes and decapitated by vigorous vortexing for 30 seconds. Since the fly neck is one of the weakest spots on the *Drosophila* body, the head snaps off the thorax in a clean manner after freezing and is possible to be collected. The fly heads have characteristic globular shape and are easy to recognise from the torsos and other debris that consist of fly legs and wings. Fly heads

were sorted on the piece of aluminium foil, counted and collected with a fine paintbrush. The fly heads were stored at -20°C for later use.

2.15 Bicinchoninic acid assay (BCA)

Five male fly heads were used per each well on the 96-well plate for BCA. Each sample was prepared by homogenising 10 fly heads (5 heads for the first well plus 5 to be diluted down in the series) in 12 µl of AEBSF lysis buffer [50 mM Tris/HCl, pH 7.5, 100 mM NaCl, 0.5 % Nonidet P40 and 1 mM 4-(2-aminoethyl) benzenesulfonyl fluoride (AEBSF)] by Eppendorf plastic hand-held pestles. After sonication on ice (10 min), two aliquots of the supernatant were taken out to achieve 5 fly head equivalent in 5 µl of a solution in the first well. From the second well onwards, the samples were further titrated in half steps with the dilution medium 50mM sodium acetate. Each sample was prepared in triplicate. The Pierce™ BCA Protein Assay Kit (Thermo Fisher Scientific) protocol was followed and BSA solution was used as a standard. The starting BSA dilution was 2 mg/ml per well. The plates were incubated at 37°C for 90 min and read at 490 nm in regular intervals during the course of assay development. The results were interpolated, quantified and plotted in GraphPad Prism 6.

2.16 SDS-Polyacrylamide gel electrophoresis and western blot

Recombinant PrP and PrP expressed in *Drosophila* were analysed by SDS-polyacrylamide gel electrophoresis (SDS-PAGE) and western blot detection using anti-PrP monoclonal antibodies. The fly head homogenates were prepared in AEBSF lysis buffer and 1 µl of lysis buffer was used per 1 fly head. Fly heads were homogenised using hand held Eppendorf pestles and sonicated on ice for 10 minutes. The fly larvae homogenates were prepared from 5 whole second instar larvae in 10 µl AEBSF by hand held Eppendorf pestles and sonicated on ice for 10 minutes. The samples were mixed with 2x Laemmli buffer (Sigma Aldrich), heated at 80°C for 10 minutes, cooled on ice and centrifuged at 13 000 g for 10 minutes. Supernatant was collected and loaded onto an SDS-PAGE gel.

SDS-PAGE gel composition (for 2 gels):

	12% resolving gel	5% stacking gel
Deionised water	4.3 ml	2.87 ml
Acrylamide (40%)	3 ml	500 µl
1.5 M Tris:HCl (pH 8.8)	2.5 ml	x
1 M Tris:HCl (pH 6.8)	x	500 µl
10% SDS (sodium dodecyl sulphate)	100 µl	40 µl
10% APS (ammonium persulphate)	100 µl	40 µl
TEMED (tetramethylethylenediamine)	8 µl	8 µl

SDS-PAGE was carried out using a 12% resolving gel and 5% stacking gel in all cases. Protein samples to be analysed were mixed with 2x Laemmli buffer (Sigma Aldrich) loaded in 10 µl per track (or 5µl in the case of protein markers). Electrophoresis was carried out at 180 V for 50 minutes. The proteins were transferred to nitrocellulose membrane by blotting at 45mA/90 minutes. The membrane was blocked overnight in 5% non-fat milk (in 1x TBST) [50 mM Tris.HCl, pH 7.4, 150 mM NaCl, 0.1% Tween 20], washed in 1x TBST for thirty minutes and subsequently incubated with Sha31 primary monoclonal antibody (1:2000) in 1% non-fat milk in 1x TBST per membrane for 1 hour at 18˚C. The washing step was repeated and the membrane was probed with 1:2000 HRP in 1% milk in 1x TBST for an hour. Finally, the membrane was washed in 1x TBST. Visualisation of protein bands was carried out in ChemiDoc Imaging System (BioRad) using Enhanced Chemiluminescence method with standard ECL solutions.

2.17 Investigation of PK-resistance of mammalian brain homogenates

The ovine VRQ/VRQ scrapie-free normal brain homogenate and VRQ/VRQ 0005 scrapie positive 10% (w/v) brain homogenates in PBS (pH 7.4) were kindly provided by Dr Alana Thackray as well as 10% (w/v) murine CD1, ME7, C57BL/6 and RML brain homogenates in PBS (pH 7.4). The homogenates were treated with 32 µg/ml of PK at 37°C for times ranging from 30 minutes to 120 minutes (the non-PK-treated samples were subjected to the same conditions). The PK-digest was stopped by addition of 2x Laemmli buffer (Sigma Aldrich), heated at 80°C for 5 minutes, cooled on ice and centrifuged at 13 000 g for 10 minutes. Supernatant was collected and loaded onto an SDS-PAGE gel to be subjected to a SDS-PAGE and a western blot, as described earlier.

2.18 Investigation of PK-resistance of PrP transgenic flies

For PK-digest followed by SDS-PAGE and western blot, the lysis buffer used was AEBSF free [50 mM Tris/HCl, pH 7.5, 100 mM NaCl and 0.5 % Nonidet P40] used in volume of 1 µl per fly head. After homogenisation with plastic Eppendorf pestle, the samples were sonicated on ice for 10 minutes and then subjected to the PK-digest protocol. The samples were diluted by PBS (pH 7.3) to achieve 9 µl of solution per sample, treated by 1 µl of various PK concentrations ranging from 1 to 5 µg of PK per ml (in the final solution) and incubated at 37°C for 30 minutes (the non-PK-treated samples were subjected to the same conditions). The PK-digest was stopped by addition of 2x Laemmli buffer (Sigma Aldrich), heated at 80°C for 5 minutes, cooled on ice and centrifuged at 13 000 g for 10 minutes. Supernatant was collected and loaded onto an SDS-PAGE gel to be subjected to a SDS-PAGE and a western blot, as described earlier.

2.19 Capture-detector ELISA

The fly head homogenates for capture-detector ELISA were prepared in the AEBSF lysis buffer in a volume of 1 µl per fly head. The fly heads were homogenised using hand held Eppendorf pestles, centrifuged at 13 000 g for 5 minutes, resuspended and then loaded into wells including the debris. The dilution medium used to achieve 50 µl of solution per well was PBS (pH 7.4).

The 96 well plate was first coated by 50 µl of 20 ng/µl purified anti-PrP capture antibody 245 in PBS (pH 7.4) per well and incubated at 4°C overnight. Each well was washed with 150 µl of PBS (pH 7.4) and blocked by 150 µl of 5% milk (Marvel) in PBS (pH 7.4) at 18°C/600 rpm for 60 minutes. The plate was washed two times in 150 µl of PBS-T [0.1% tween in PBS pH 7.4] per well and coated with 50 µl of antigen (fly head homogenate or recombinant protein) in PBS (pH 7.4) per well. The antigen incubation was carried out at 18°C/600 rpm for 60 minutes. Each well was then washed three times with 150 µl of PBS (pH 7.4). The incubation with biotinylated secondary anti-PrP antibody SAF32 was performed by pipetting 50 µl of 1 ng/µl of SAF32 in PBS (pH 7.4) into each well and incubation at 18°C/600 rpm for 60 minutes. The wells were washed twice by 150 µl of PBS-T per well and incubated with 50 µl of streptavidin alkaline phosphatase conjugate (1:3000 in PBS ph 7.4) (Sigma Aldrich) at 18°C/600 rpm for 60 minutes. The wells were then washed by 150 µl of PBS-T per well and equilibrated by 100 µl of ELISA buffer [0.05M glycine, 0.03M NaOH, 0.25mM MgCl2 and 0.25mM ZnCl in distilled water] per well at 18°C for 1 minute. Finally, 100 µl of 0.5mg/ml p-nitrophenyl phosphate in ELISA buffer was added to each well and incubated at 37°C while measuring the OD 415 nm on an ELISA plate reader every 10

or 15 minutes for up to 90 minutes. The results were interpolated, quantified and plotted in GraphPad Prism 6.

2.20 Verification of LexA-mediated targeted gene expression

LexA mediated targeted gene expression was assessed by fluorescence microscopy. Various 57C10-GAL4/targeted LexA dual driver fly lines (kindly provided by Dr Matthias Landgraf, Department of Zoology, University of Cambridge) were crossed with fluorescent reporter fly lines carrying UAS-GFP (green fluorescent protein) and/or LexAop-td-Tomato red protein (red fluorescent protein). The specific fluorescent reporter fly lines and single/dual driver fly lines used for this experiment are listed in **Appendix 8.1**. Resultant 1st instar *Drosophila* larvae were harvested and visualised as whole mounts by Zeiss AxioPhot epifluorescence microscope. The images were analysed and merged using Fiji 2.0.2 (ImageJ) program.

2.21 Lethality tracing experiment

The 57C10-n-Syb-LexA cross was subjected to lethality tracing experiment to discover the developmental stage of the fly lethality. The cascade of crosses was performed to enable the fluorescent visualisation of PrP expression (details of a cross in **Appendix 8.4**). The progeny was visualised by Zeiss AxioPhot epifluorescence microscope. The first instar larvae that exhibited solely the red fluorescence were collected and transferred onto a fresh agar plate. The control larvae with both red and yellow fluorescence were put aside to another plate as a control. The mixed population of test and control fluorescent larvae was left to hatch on an agar plate as well. The larvae development was monitored daily until the adults appeared or no living larvae/flies were left. The experiment was set up in two repeats.

2.22 Neuromuscular junction (NMJ) analysis

The fly crosses, scrapie inoculation, dissection and immunostaining of *Drosophila* larvae to visualise NMJs were performed by Dr. Alana Thackray, University of Cambridge, UK, Dr. Matthias Landgraf and Dr. Matthew Oswald, Department of Zoology, University of Cambridge, UK prior to the start of my PhD programme. The methods used are described in **Appendix 8.5**.

2.22.1 Imaging and data analysis

NMJs were visualised using Leica SP5 upright confocal microscope using a 63x/NA1.3 glycerol immersion objective. Multi-channel images were obtained and subsequently analysed using Fiji 2.0.2 (ImageJ) program with a bespoke NMJ Buddy plugin (coded by Richard Burton, Gurdon

Institute, and kindly provided by Dr Matthias Landgraf, Department of Zoology, University of Cambridge, UK). Synaptic architecture and overall morphology of single aCC motoneurons innervating dorsal acute muscle 1 (DA1) located at abdominal hemi segments A4 and A5 on a left and a right hand side of a dorsal line (A4R, A4L and A5R) in prion exposed and normal brain homogenate exposed larvae (n≥25 NMJs analysed per treatment group).

Upon first inspection, NMJs were classified into three distinct phenotypic classes based on overall visual appearance: linear NMJs - that comprised only two main neuronal branches with majority of their length stretched along the proximal edge of muscle DA1; non-linear NMJs that comprise more than two long neuronal branches that may/or may not be parallel to the edge of muscle DA1 and irregular NMJs that comprised relatively short length, bent or twisted neuronal branches of a "damaged" appearance. The irregular NMJ phenotype do not appear to be caused by dissection as this genotype-specific phenomenon was present in multiple independently dissected groups of *Drosophila* larvae. The NMJ shape irregularities and fragmentation appear to be a result of a genotype-specific toxicity.

Subsequently, each NMJ was also assessed for number of synaptic boutons (distinct spherical varicosities along the NMJ branch), synaptic bouton area (area of synaptic bouton varicosities measured by NMJ Buddy plug-in), number of active zones (neurotransmitter release puncta labelled with Bruchpilot marker), number of neuronal branches (two or more boutons off of the primary nerve terminal and any subsequent branches off of these secondary branches), number of satellite boutons (extensions of one bouton off the nerve branch), neuronal cable length (as shown in **Figure 3** in the results section) and NMJ spread (as shown in **Figure 3** in the results section)) together with measurement of DA1 muscle surface area (calculated by multiplication of muscle length with muscle width using Fiji 2.0.2 (ImageJ) program). Some of the collected data was then subjected to normalisation to average DA1 muscle area of each treatment group to correct for subtle differences in larval size of each category with regards to the actual size of innervated muscle (Miller et al., 2012). The normalisation was performed by dividing mean control muscle surface area by the mean experimental muscle surface area and multiplication of the result by the bouton count or active zone count specific for the test sample.

NMJ synaptic architecture data were analysed in a PrP genotypic manner (comparison of combined control and prion-inoculated values between different PrP genotypes) by one-way ANOVA and by paired analysis of control and prion-inoculated values within individual PrP

genotypes by unpaired t-test. Statistical analysis was carried out and visualised using GraphPad Prism 6.

2.23 Protein misfolding cyclic amplification (PMCA)

PMCA is a method that allows *in vitro* replication of any PrP^{Sc} present in the sample (Lacroux et al., 2012). The method consists of incubation step where the contact of PrP^{C} substrate and a potential PrP^{Sc} seed takes place and the polymers of PrP^{Sc} are formed (Barria et al., 2012). The second step includes sonication that breaks down the aggregates to increase the number of PrP^{Sc} nuclei. This process is cyclic to amplify any PrP^{Sc} present in the sample to be able to detect it by western blot coupled with PK-digest. PMCA analysis kindly performed by Dr. Olivier Andreoletti (INRA, Toulouse, France) and the method is described in **Appendix 8.5**.

To carry out PMCA, 20 fly heads were homogenised in 20 µl of PBS (pH 7.4) with plastic Eppendorf pestles. The homogenisation process was quick (below 5 minutes) and performed on ice. The samples were then sonicated for 10 minutes and centrifuged at 13 000 g for 10 minutes. The supernatant was transferred into a fresh tube and sent for PMCA analysis.

2.24 Real-time quaking-induced conversion (RT-QuIC)

RT-QuIC is considered to be similarly sensitive as animal bioassays (Wilham et al., 2010, Atarashi et al., 2011a, Orrú et al., 2015). The method is based on intermittent shaking of samples that (might) contain PrP^{Sc} with recombinant PrP^{C} substrate. The aggregation and fibril formation is induced in the solution, if the PrP^{Sc} is present. In contrast to PMCA, the PK-digest and western blot phases are replaced here with Thioflavin-T (ThT) fluorescence dye that is incorporated in the aggregates while these are formed. Therefore, this method is suitable even for PK-sensitive species of misfolded PrP and allows for real time quantification of aggregate formation (Atarashi et al., 2011a, Peden et al., 2014).

The samples for RT-QuIC were prepared by homogenising 10 fly heads in 10 µl of calcium- and magnesium-free PBS [1mM EDTA; 150 mM NaCl; 0.5% Triton X-100 and 1X Complete Mini EDTA-free Protease Inhibitor Cocktail (Roche)]. The fly heads were homogenised with plastic hand-held homogenisers (Eppendorf) and the homogenates were centrifuged at 420 g for 5 minutes. The supernatant was collected and immediately frozen at -80°C. The samples were subjected to RT-QuIC by Dr. Marcelo A. Barria Matus (National CJD Research and Surveillance Unit, Edinburgh) and the method is described in **Appendix 8.5**.

2.25 *Drosophila* survival assay

Freshly hatched fly progeny of selected genotypes (list of dual PrP transgenic fly crosses with dual drivers can be seen in **Appendix 8.6**) were collected every two days and allowed to mate for 24 hours. Thirty females per fly genotype were then separated into 3 tubes of 10 flies (triplicates) containing standard cornmeal medium (Lewis, 1960). In case of 57C10-GAL4 ; repo-LexA cross, there were just 18 flies collected per fly genotype (triplicates of six). The flies were maintained at 22°C and flipped into fresh tubes 3 times a week while the number of dead flies was recorded at the same time (Crowther et al., 2005). The survival curves were assembled in GraphPad Prism 6 using Kaplan-Meier plots. The statistical analysis was performed using student t-test in GraphPad Prism 6.

3 Chapter 1 - Construction and characterisation of mammalian PrP transgenic flies

3.1 Introduction

Prion diseases exhibit a long incubation time before onset of clinical signs in the natural host, such as sheep, cattle or human. The outbred populations, late onset and the ethical concerns render studies of prion-induced neurotoxicity in the natural hosts difficult. To overcome this problem, animal models are increasingly used to study prion-induced neurodegeneration, as well as other neurodegenerative disease-associated pathology.

To date, the most commonly used animals for prion research are rodents (Wadsworth et al., 2010). Various species of rodents were tested and used as experimental animals. The use of a bank vole has been tested and this rodent has been identified as a universal acceptor for prions of different species (Chandler and Turfrey, 1972, Nonno et al., 2006, Di Bari et al., 2008, Watts et al., 2014). There are numerous studies where hamsters were used as experimental animals (Kimberlin and Walker, 1977, Prusiner et al., 1985, Meade-White et al., 2009). However, the mouse is considered more universal and is still the preferred animal model due to the array of methods used for murine genome manipulation (Kimberlin and Walker, 1977, Watts and Prusiner, 2014).

Mouse experimental models have been used to study the majority of animal and human prion diseases (Bruce et al., 1997, Chiesa et al., 1998, Vascellari et al., 2012, Watts and Prusiner, 2014). Specifically, the $PrP^{-/-}$ (knock-out) and PrP transgenic mice enabled various breakthroughs in prion biology. Collectively, these experiments using transgenic mice helped to elucidate that PrP^{C} expression plays a crucial role in prion–mediated toxicity and that the neurotoxic agent forms during conversion of PrP^{C} to PrP^{Sc}.

Apart from acquired prion disease, the genetic forms of prion disease have been modelled in mice transgenic for human or humanised murine PrP (Hsiao et al., 1990, Chiesa et al., 1998, Chiesa et al., 2001, Harris et al., 2003, Dossena et al., 2008, Asante et al., 2009, Jackson et al., 2009, Wadsworth et al., 2010, Jackson et al., 2013, Chiesa et al., 2016). There are multiple approaches towards murine genome manipulation to introduce a PrP transgene to the acceptor organism. The two main methods involve commonly used random integration of a transgene (RIT) (Dossena et al., 2008, Bouybayoune et al., 2015, Chiesa et al., 2016) and more specific targeted

gene knock-in approach (Jackson et al., 2009, Jackson et al., 2013). Knock-in engineered mice transgenic for murine PrP carrying single codon mutations associated with familial CJD and FFI showed the spontaneous formation of transmissible prions (Jackson et al., 2009, Jackson et al., 2013). In contrast, studies using the same transgene but the RIT method of murine genome manipulation did not identify any transmissible prions even though the disease-specific clinical signs have developed (Dossena et al., 2008, Bouybayoune et al., 2015).

While significant achievements in prion biology have been made using mouse as an experimental animal model, studies with vertebrate hosts are time-consuming, cumbersome and subject of ethical concerns. Therefore, there is a need to develop more versatile and tractable animal models of mammalian prion disease. To discover the molecular mechanisms underpinning the aetiology of various human and animal diseases, invertebrate animal models are increasingly employed in neurodegenerative research. The use of invertebrates in research is more time efficient and their simple genetics allows for easier gene manipulation and discovery of mechanisms involved in neurodegeneration.

One of the most common organisms used for neurodegeneration studies is *Drosophila melanogaster*. *Drosophila* has several features which lend itself to its use as an experimental organism (Yoshihara et al., 2001). The most significant advantages are its well characterised genome with many gene tailoring approaches established, its short lifespan and the ability to generate large numbers of flies to allow robust experimental data collection (Gavin et al., 2006, Ambegaokar et al., 2010). The cellular and molecular pathways involved in the process of neurodegeneration seem to be highly similar within invertebrates and mammalian natural hosts (Driscoll and Gerstbrein, 2003). The invertebrate brain is composed of similar neuronal types, circuits, ion channels and neurotransmitters (Littleton and Ganetzky, 2000). A wide range of human neurodegenerative diseases has already been modelled in *Drosophila* including Alzheimer's disease (AD) (Wittmann et al., 2001) and Parkinson's disease (PD) (Feany and Bender, 2000).

The biggest advantage of the *Drosophila* model is its ability to express the protein of interest in a spatiotemporal, restricted manner in a transgenic animal (Brand and Perrimon, 1993, Jenett et al., 2012). The directed expression helps to analyse genes involved in disease development, nervous system circuits, or carry a disease-associated mutation (Jenett et al., 2012). This specificity is allowed by the two-component system of site-specific integration and targeted gene expression

in *Drosophila*. The driver systems are based on the transgenic construct that drives expression of a site-specific transcriptional activator with binding sites positioned upstream of a responder gene (Pfeiffer et al., 2010). The transcriptional activator must be naturally absent in *Drosophila* genome to specifically express only the gene of interest and therefore the transcription activators come from different species. This system enables directed expression of a target gene in distinct tissues, cell types or subtypes (Brand and Perrimon, 1993).

The binary system enables separation of a target gene from its transcriptional activator and therefore creation of transgenic lines that trigger protein expression upon crossing with a respective driver. Both components are stored in libraries and are used to induce various expression patterns in the fly. The only limitation of this precise manipulation is the number of cell type-specific or tissue-specific driver lines available (Brand and Perrimon, 1993).

To drive the expression of the transgene, the transcriptional activator must be placed upstream from the gene of interest. Therefore, the transgene is inserted into one of the vectors that contain a transcriptional activator compatible with the driver system used. The most widely used plasmid for the GAL4-UAS system is pUAST*attB* (Bischof et al., 2007). The pUAST*attB* was designed to allow GAL4-dependent direct expression of a gene of choice in the tissue of choice. The gene sequence is subcloned into a polylinker (contains unique restriction sites) that is positioned upstream of the SV40 small t intron and polyadenylation site and downstream of five tandemly arrayed GAL4 binding sites, hsp70 TATA box and a transcriptional start (Brand and Perrimon, 1993). This non-viral P-element vector contains the *white+* marker followed by a *loxP* site, UAS sequence promoter and *attB* site that recombines with the *attP* site present in the recipient fly genome.

Another widely used expression system is LexA-lexAop. For LexA-lexAop there are different plasmids available, such as pJFRC19-MUH (pJFRC19-13XLexAop2-IVS-myr::GFP). The LexA-lexAop plasmids are constructed similarly as the pUAST*attB* vectors but with various alterations to the number and type of promoters present in a sequence. The pJFRC19-MUH contains 13 LexAop2 sites and hsp70 basal promoter upstream from the gene sequence and the SV40 terminator downstream of an insertion site. The insertion site initially contains myr::GFP gene (with green fluorescence) which is excised and replaced by the gene of interest. The landing site in the recipient fly genome is the *attP2* site *su(Hw)attP2* that again allows φC31 integration (Groth et al., 2004).

To generate transgenic *Drosophila melanogaster*, the transgene of interest needs to be constructed and integrated into the fly genome. One of the most reliable methods of transgene targeted integration is the germ-line transformation of *Drosophila* via transposable elements using φC31 integrase (Groth et al., 2004, Thorpe and Smith, 1998, Bischof et al., 2007). The serine integrase from bacteriophage φC31 mediates sequence-directed recombination of phage attachment site (*attP*) in the *Drosophila* genome and bacterial attachment site (*attB*) present in a transgenesis vector (Thorpe et al., 2000). In comparison to other systems available, such as *Cre/loxP* or FLP/FRT, φC31 integrase mediates exclusively the integration and not the excision reaction (Bischof et al., 2007). The transformation efficiency is elevated by the presence of an endogenous source of φC31 integrase to avoid co-injection of φC31 integrase mRNA. To increase the specificity even further, a *white*$^{+}$ mini gene-based reconstitution system is employed to enable visual selection of precise *attP* targeted integration by the red eye colouration of the fly and prevent rare nonspecific integration event (Bischof et al., 2007).

The *attP* sites in the *Drosophila* genome were designed to avoid any interference of commonly used markers and transposon systems and were precisely mapped throughout all four fly chromosomes to determine any intergenic locations of a transgene. The *attP* landing site M{3xP3-RFPattP} has been created with certain features facilitating its use for fly transgenesis (Bischof et al., 2007). Apart from the *attP* docking site for an *attB*-containing plasmid, the red fluorescent protein (RFP) is present in the construct which drives strong red fluorescence expression in the fly eye under the control of an artificial 3xP3 promoter. The RFP presence does not interfere with the *white+* marker and thanks to the RFP cassette flanked by *loxP* sites, the marker can be easily excised using *Cre* recombinase-mediated excision that targets *loxP* sites. The site-specific integration into a recipient fly genome enables quantitative comparison of different genes inserted at the same genomic location (Pfeiffer et al., 2010).

Transgenic *Drosophila* were first utilised as a prion disease animal model when the full-length Syrian hamster prion protein was expressed in this system (Raeber et al., 1995). Due to different glycosylation mechanisms in *Drosophila,* the relative molecular weight of prion protein has been observed to be lower than in mammalian hosts. Other features such as successful membrane attachment of PrP to the cellular surface were found to be conserved between mammalian hosts and the fruit fly.

Some of the PrP transgenic *Drosophila* systems used in research, represented mere overexpression of mammalian PrP in the fly with little evidence of pathological prion formation and no evidence of prion transmissibility (Choi et al., 2010, Fernandez-Funez et al., 2009, Gavin et al., 2006, Murali et al., 2014). Significant progress in the development of a *Drosophila* model of mammalian prion disease has been made by Thackray *et al.*, who have successfully modelled transmissible scrapie disease in *Drosophila* (Thackray et al., 2014a, Thackray et al., 2012b, Thackray et al., 2012a). The system used by Thackray *et al.* involved the generation of ovine PrP transgenic *Drosophila* under expression control of the bi-partite UAS/GAL4 system and the same system is utilised in this project (Brand and Perrimon, 1993). *Drosophila* transgenic for ovine PrP that is pan-neuronally expressed develop a neurotoxic phenotype after exposure to exogenous sheep scrapie prion inoculum (Thackray et al., 2014a, Thackray et al., 2012b, Thackray et al., 2012a). This scrapie infected neurotoxic phenotype in PrP transgenic *Drosophila* has shown signs of *bona fide* prion infection since it was found to be accompanied by the accumulation of PK-resistant mutant PrP as well as being transmissible to PrP transgenic recipient ovine PrP transgenic mice (Thackray et al., 2014a, Thackray et al., 2012b, Thackray et al., 2012a, Thackray et al., 2014b).

The use of *Drosophila melanogaster* is not limited to basic prion research; it has proven possible to use PrP transgenic flies to detect infectious prion proteins in blood plasma of pre-clinical stage scrapie affected sheep (Thackray et al., 2016). This bioassay allows for rapid and efficient blood or plasma screening to detect prion disease associated protein and it can be further developed to be applicable to other prion diseases, such as vCJD. These studies show that PrP transgenic *Drosophila* do not lack the necessary co-factors required for mammalian prion propagation and can be used to model mammalian prion disease.

Apart from acquired prion disease, the *Drosophila* model has been used to model inherited prion disease such as GSS on multiple occasions (Gavin et al., 2006, Choi et al., 2010, Murali et al., 2014). The phenotype and neuropathology associated with prion disease have developed in the majority of cases but the *bona fide* transmissible properties of mutant prion protein were not found in these models. It remains to be shown that *Drosophila* can be used as a valid model of spontaneous generation of infectious prions with all the hallmarks of prion disease. Progress in this respect has been made by Thackray *et al.* (parts in this project as well) where humanised mouse and hamster FFI- and CJD-associated PrP transgenes successfully generated by Jackson *et*

al. were utilised for *Drosophila* transgenesis (Thackray et al., 2017, Jackson et al., 2009, Jackson et al., 2013).

This chapter describes the process of fly transgenesis, transgene and transgenesis vector construction and various approaches towards verification of the flies generated. The aim of the fly lines constructed was to test a hypothesis that the mutant prion protein can spontaneously transmit from cell-to-cell in a *Drosophila* model of inherited prion disease. In the other chapters of this thesis, intercellular transmissibility will be tested by co-expression of disease-associated PrP in small populations of cells or neurons and pan-neuronal expression of the native form of cellular PrP in *Drosophila* CNS. This is enabled by construction of dual PrP transgenic flies that harbour PrP of two genotypes – cellular and prion disease-associated on both chromosomes 2 and 3. The proteins will then be simultaneously expressed under the control of a double expression driver to achieve independent and specific expression of PrP in separate cell or neuron types. The transmission of the disease-associated phenotype and its neuropathology will then be tested by molecular biology methods. It is important to address this issue, since if successful, it might provide an important new model for genetically controlled protein misfolding neurodegenerative disease.

3.2 Results

3.2.1 Construction and characterisation of mammalian PrP transgenic flies

To study prion-associated neurodegeneration in an invertebrate host, the transgenesis of *Drosophila melanogaster* was performed to incorporate a mammalian PrP transgene. Naturally, the fruit fly is devoid of any PrP orthologue. Therefore, PrP transgenes of various origin were used to construct a fly model of PrP expression to make comparisons based on their sequence differences and species of origin. The fly lines generated contained PrP transgenes associated with either a cellular form of PrP that is naturally present in mammalian brains and is not associated with an onset of any disease, PrP carrying a polymorphism associated with susceptibility or resistance to prion disease or a transgene with a mutation directly causing spontaneous prion-associated misfolding.

The list of all PrP transgenic flies used or generated in collaboration with Dr. Alana Thackray, University of Cambridge, UK during this project can be seen in **Table 1** for humanised murine and hamster PrP transgenic flies, **Table 2** for ovine PrP transgenic flies, **Table 3** for human PrP transgenic flies and **Table 4** for cervid PrP transgenic flies.

In this chapter, the process of fly transgenesis is explained as well as the basis of chromosome balancing. The procedure of transgene generation, incorporation into vectors and their isolation is explained (work carried out in collaboration with Dr. Alana Thackray, University of Cambridge, UK). The resulting PrP transgenic fly lines are then verified for the presence of a transgene and its sequence is confirmed (work carried out by myself). Later, the process of double PrP balancing is described as I also made dual PrP transgenic flies.

3.2.2 Transgenesis vectors used for *Drosophila* PrP transgenesis

Two different vectors were used for fly transgenesis – pUASTattB and pJFRC-MUH (pJFRC19-13XLexAop2-IVS-myr::GFP). The plasmid maps of both vectors can be seen in **Figure 1.** Both plasmids can be cut with a pair of restriction enzymes to allow for transgene integration of a similarly cut PrP construct. For pUASTattB plasmid, the restriction enzymes of our choice were *XhoI* and *EcoRI* and for pJFRC-MUH, the restriction enzymes used were *XbaI* and *XhoI.* The successful transgene integration manifests by ampicillin resistance of resulting *DH5α* colonies. After plasmid isolation, both types of plasmids act as *Drosophila* expression vectors that recombine with *attP* specific sites in *Drosophila* genome and therefore allow site-specific

integration of a PrP transgene. The easy detection of vector insertion is facilitated by the subsequent change of the fly phenotype. After the successful insertion, both plasmids result in red eye coloration in the successfully modified PrP transgenic *Drosophila* progeny.

The pUASTattB plasmid is used for transgene expression under the control of UAS-GAL4 system. In the majority of flies generated in this project, the pUASTattB vector is used for chromosome 2 incorporation. The human PrP transgenic flies are the only exception where pUASTattB plasmid is used for chromosome 3 transgenesis. The pJFRC-MUH plasmid expresses a protein of choice under the control of the LexA-lexAop system and in this project, the system is used for chromosome 3 fly transgenesis. Both expression systems and their function will be described in detail in the next chapter.

3.2.3 Fly transgenesis and chromosome balancing

The pUASTattB or pJFRC-MUH plasmid carrying the PrP insert of our choice (details in the latter chapters) was injected into the posterior end of one hour old *Drosophila* embryos derived from the 51D recipient fly line for chromosome 2 incorporation or AttP2 recipient fly line for chromosome 3 incorporation. For successful germ line transgenesis, the transgene must be taken up by the pole cells that are predestined to become germ cells. The plasmids incorporate into the *Drosophila* genome by a process of homologous recombination between a single landing attP site in the *Drosophila* genome and a unique attB site in the plasmid genome. The site-specific recombination is enabled by *PhiC31* integrase that is delivered in the form of mRNA along with the plasmids. The process of fly transgenesis can be seen in **Figure 2.**

The recipient fly lines have white^{-}/white^{-} genotype coding for white-eye colouration. The plasmids carry a white^{+} mini gene that produces red-eye colouration. The inheritance of the PrP transgene is therefore marked by the presence of the dominant white^{+} mini gene that causes a red-eye colouration in all successive fly generations that carry the transgene of our interest. The fly transgenesis was performed by BestGene Inc. or by the Department of Genetics microinjection service.

To prevent recombination between homologous chromosomes that might cause fragmentation of the PrP transgene during crossing-over, the stable stock is generated by introduction of balancers. The balancer fly lines carry inverted chromatids tagged by a phenotypic marker to easily recognize the balancer chromosome. Their inverted sequence prevents recombination due to the lack of homology and it preserves an intact gene when placed at the same position of the

homologous chromosome. The balancer fly line used carries two phenotypic markers – CyO (curly wings) and if (irregular facet). After crossing with a PrP transgenic fly, the red eyed flies with curly wings were collected to ensure the presence of both balancer and a PrP transgene (with white^{+} mini gene). The stable stocks were then maintained by brother-sister mating and two phenotypes occured in the progeny – PrP/CyO that carried a phenotypic marker or PrP/PrP that lacked a phenotypic marker (the combination of CyO/CyO genotype is lethal) in all subsequent generations. The scheme of fly balancing can be seen in **Figure 3**.

3.2.4 Generation of murine 3F4 and hamster PrP transgenes

In this project, the murine 3F4 and hamster PrP transgenic flies were used to model spontaneous PrP misfolding that arises from different polymorphisms in the PrP gene. Plasmids containing inserts of murine 3F4 or hamster PrP transgene that carried single codons associated with inherited forms of human prion diseases (CJD and FFI) were obtained from Dr Walker Jackson (DZNE, Germany). Murine PrP was engineered to contain the L108M and V111M substitutions creating the 3F4 epitope, whereas hamster PrP carries the 3F4 epitope naturally. The identical constructs have been used to successfully model inherited human prion diseases in mouse (Jackson et al., 2009, Jackson et al., 2013). In studies presented here, murine 3F4 and hamster PrP transgenes were constructed with species specific or insect signal peptide. The transgenes were than aimed for transgenesis either on *Drosophila* chromosome 2 or 3. *Drosophila* transgenic for these constructs were generated in collaboration with Dr. Alana Thackray, University of Cambridge, UK and characterised by myself. The parts performed by me are shown in the result figures in this thesis.

The original murine 3F4 or hamster PrP transgenes received were contained in pBSKSII plasmids. The murine 3F4 and hamster inserts contained species specific signal peptide and their list can be seen in **Table 5**. The plasmids supplied were verified using a PCR with PrP specific primers MoFI and MoRI for murine 3F4 constructs and HaFI and HaRI primers for hamster constructs. The primers used carried *EcoRI* and *XhoI* restriction sites (list of primers in **Appendix 8.3**) and bind to to the 3' and 5' end of each appropriate insert sequence in the pBSKSII plasmid series (**Figure 4**). The expected size of mouse and hamster PrP PCR products was 761 bp which corresponds to the result obtained.

The PCR product was then purified and used as an insert for pUASTattB plasmid construct to generate pUAST-PrP with species specific signal peptide to be used for *Drosophila* transgenesis.

The verification of *Drosophila* transgenesis was performed first using PrP specific primers MoFI and MoRI for murine 3F4 constructs and HaFI and HaRI primers for hamster constructs (**Figure 5**). The expected size of mouse and hamster PrP PCR products was 761 bp which corresponds to the result obtained. A second verification was performed using pUASTattB plasmid specific primers flanking the PrP insertion site applied to the fly head homogenates to amplify the products for sequencing (**Figure 6**). The product of expected size 1.1kB was obtained. The sequencing was successful and confirmed the expected insert sequence in all cases. The full-length sequences of all PrP transgenes can be found in **Appendix 8.2.** The new fly lines were balanced to achieve stable stocks and maintained an intact PrP transgene.

To compare the expression levels of PrP with different signal peptides in the *Drosophila* system, murine 3F4 and hamster PrP inserts with insect signal peptide were constructed. Previously made ovine PrP transgenic *Drosophila* (Thackray et al., 2012b, Thackray et al., 2012a, Thackray et al., 2014a) contain insect signal peptide as opposed to the transgenes received from Dr Walker Jackson (DZNE, Germany) that contain murine or hamster signal peptide. The comparison of expression levels in identical fly genotypes with a difference solely in the signal peptide can help identify an impact of the insect signal peptide species on the PrP expression levels in *Drosophila.*

The pUAST-Mo3F4 and pUAST-Ha PrP constructs were used for a preparation of PrP insert with insect signal peptide. The first step was PCR amplification of the PrP transgene and synthesis of the first part of a fly leader peptide (**Figure 7**) using semi-nested PCR with MoPD1F and MoRI (or HaPD1F and HaRI) primers (**Figure 8**). A PCR product of expected size 743 bp was obtained and used for the second step of semi-nested PCR to generate a full-length insect signal peptide PrP transgene (**Figures 9 and 10**). The forward primer (PD2F) used to generate the insect signal peptide carried an *EcoRI* restriction site and the reverse primers (MoRI or HaRI) carried an *XhoI* restriction site. A PCR product of expected size 788 bp was obtained in all appropriate reactions.

The mouse 3F4 WT transgenes with DNA encoding an insect signal peptide were purified and digested by *EcoRI* and *XhoI* restriction enzymes. The *Drosophila* transgenes and pUASTattB vector were *EcoRI* and *XhoI* digested. The RE digest products (PrP and pUASTattB) were run on low melting point agarose gel and bands of interest were isolated (**Figure 11**). The expected size of the PrP transgene was 758 bp and the size of the pUASTattB plasmid was 8.489 kB. The

results are shown for mouse 3F4 WT sample but the same procedure was carried out to generate hamster PrP transgenic flies as well.

The transgene containing the mouse 3F4 or hamster PrP constructs was then ligated to the pUASTattB vector, rescued in *DH5α* bacteria and isolated from large scale culture. The presence of the correct PrP transgene in each pUASTattB vector was verified by PCR (**Figure 12**). A PCR product of expected size 788 bp was observed. The identity of a transgene was confirmed by DNA sequence analysis (sequence in **Appendix 8.2**).

The pUASTattB-PrP constructs with insect specific signal peptide were purified and used for *Drosophila* transgenesis by embryonal microinjection. The samples that went forward for fly embryonal microinjection were hamster WT and CJD. The verification of *Drosophila* transgenesis was then performed using PCR with pUASTattB plasmid specific primers flanking the PrP insertion site applied to the fly head homogenates to amplify the products for sequencing (**Figure 13**). The expected product of 788 bp was observed and subsequent sequencing confirmed the expected insert sequence in all cases. The full-length sequences of all PrP transgenes can be found in **Appendix 8.2.** The new fly lines were then balanced to achieve stable stocks and maintain an intact PrP transgene.

To achieve a simultaneous but independent expression of PrP from both chromosome 2 and 3, the PrP transgenic flies with a PrP insert on chromosome 3 were constructed to enable this experiment. The flies with PrP insert on chromosome 3 were prepared in similar manner as the chromosome 2 transgenic flies except for use of the transgenesis vector pJFRC-MUH (**Figure 1**). This vector triggers expression under the LexA-lexAop system and the insertion of PrP is enabled by use of PrP specific primers Chr3haFxho1 and Chr3haRxba1 carrying restriction enzyme sites *XbaI* and *XhoI* (list of primers in **Appendix 8.3**) and treatment of both insert PCR product and pJFRC-MUH plasmid with the same restriction enzymes. The purifed product was then used for fly transgenesis and the fly genotype was verified by PCR with pJFRC-F and –R primers that flank the PrP insert and allow for sequencing (**Figure 14**). The sequencing was successful and confirmed the expected insert sequence in all cases. The full-length sequences of all PrP transgenes can be found in **Appendix 8.2.** The new fly lines were balanced to achieve stable stocks and maintain an intact PrP transgene.

The double PrP transgenic flies were assembled using two consecutive crosses of the chromosome 2 PrP transgenic flies and chromosome 3 PrP transgenic flies of our interest. The

hamster WT PrP transgenic fly (hamster signal peptide) on chromosome 2 was combined with hamster CJD PrP transgenic fly (hamster signal peptide) on chromosome 3 to achieve a dual PrP fly. The first step was double balancing of both PrP transgenic flies by crossing them with double CyO / if ; MKRS / TM6b balancer (Department of Genetics stock, University of Cambridge, UK). After collection of the double balanced progeny of the opposite phenotype, the final cross to assemble the double PrP transgenic fly was made. The detail of the crosses can be seen in **Figure 15.** Overview of all existing PrP transgenic *Drosophila* with mouse 3F4 and hamster PrP transgenes can be seen in **Table 1**.

3.2.5 Generation of ovine PrP transgenes

Drosophila transgenic for topological variants of ovine PrP have been previously generated by Dr. Alana Thackray: a) VRQ(GPI) – a membrane bound form of ovine PrP; b) VRQ(ΔGPI) – a secreted anchorless form of ovine PrP (associated with human GSS); c) VRQ(cyt) – a cytosolic form of ovine PrP which is anchorless and does not possess a signal peptide sequence (Thackray et al., 2012b, Thackray et al., 2012a, Thackray et al., 2014a). These VRQ topological variant fly lines carry the PrP transgene with insect signal peptide on chromosome 2 at the fly genome under the control of GAL4-UAS driver system.

During the course of this thesis, PrP transgenic flies VRQ(GPI) and VRQ(ΔGPI) with the PrP transgene inserted on chromosome 3 under the control of the LexA-lexAop operator were generated. Ovine PrP primers VRQm-F and –R specific for VRQ(GPI) transgenic flies and VRQs-F and VRQs-R primers specific for VRQ(ΔGPI) carrying restriction enzyme sites XbaI and XhoI (list of primers in **Appendix 8.3**) were used to prepare the PrP inserts for fly transgenesis. The result of a PCR can be seen in **Figure 16** and the reaction products of expected size 795 bp for VRQ(GPI) transgenic fly DNA and 781 bp for VRQ(ΔGPI) transgenic fly DNA were obtained. Subsequently, the treatment of both PrP insert PCR products and pJFRC-MUH plasmid with the XbaI and XhoI restriction enzymes was performed. The ligated and purified product was then used for fly transgenesis. The transgenic fly genotype was verified by PCR with pJFRC-F and –R primers that flank the PrP insert and allow for sequencing. The results of PCR for VRQ(GPI) can be seen in **Figure 17** and the results for VRQ(ΔGPI) can be seen in **Figure 18**. The sequencing was successful and confirmed the expected insert sequence in all cases. The full-length sequences of all PrP transgenes can be found in **Appendix 8.2.**

The double PrP transgenic flies were assembled using two consecutive crosses of the chromosome 2 PrP transgenic flies and chromosome 3 PrP transgenic flies of our interest. The VRQ(GPI) transgenic fly on chromosome 2 was combined with VRQ(ΔGPI) transgenic fly on chromosome 3 to achieve a dual PrP fly. The first step was double balancing of both PrP transgenic flies by crossing them with double CyO / if ; MKRS / TM6b balancer (Department of Genetics stock, University of Cambridge, UK). After collection of the double balanced progeny of the opposite phenotype, the final cross to assemble the double PrP transgenic fly was made. The cross is explained in **Figure 15**. Overview of all existing PrP transgenic *Drosophila* with ovine PrP transgenes can be seen in **Table 2.**

3.2.6 Generation of human PrP transgenes

The human PrP transgenes were generated to model the homozygous or heterozygous combinations of polymorphisms that affect susceptibility to acquired prion disease. The polymorphisms generated were either V129 or M129 PrP amino acid substitutions. By simultaneous expression of both transgenes from chromosomes 2 and 3, the polymorphisms V129/V129, M129/M129 or heterozygous M129/V129 and V129/M129 were achieved.

The human PrP transgenes were generated by the same procedure as murine and hamster PrP transgenes with insect signal peptide (semi-nested PCR, **Figures 7-10**). The human PrP transgenes contain insect signal peptide and human GPI-anchor. The primers used for transgene preparation were HuPrP-PDF1 and HuPrP-R in the first step and PD2F with HuPrP-R in the second step and carried *EcoRI, XbaI* and *XhoI* restriction sites (list of primers in **Appendix 8.3**).

Similarly to the murine and hamster transgenes, the PCR products were purified and used as inserts for pUASTattB plasmid constructs to generate pUAST-PrP with insect signal peptide to be used for *Drosophila* transgenesis on chromosome 2. The verification of *Drosophila* transgenesis was performed using pUASTattB plasmid specific primers flanking the PrP insertion site applied to the fly head homogenates to amplify the products for sequencing (**Figure 19**). The product of expected size 1.1 kB was obtained. The sequencing was successful and confirmed the expected insert sequence in all cases. The full-length sequences of all PrP transgenes can be found in **Appendix 8.2.**

To achieve simultaneous expression of PrP from both chromosome 2 and 3, the human PrP transgenic flies with PrP inserted on chromosome 3 were constructed to enable this experiment. The flies with a PrP insert on chromosome 3 were prepared in a similar manner as the

chromosome 2 transgenic flies. The pUASTattB vector was employed for chromosome 3 transgenesis as the expression of both transgenes is jointly under the control of UAS-GAL4 system. The purifed plasmid was used for fly transgenesis and the fly genotype was verified by PCR with pUAST-F and –R primers that flank the PrP insert and allow for sequencing (**Figure 20**). The sequencing was successful and confirmed the expected insert sequence in all cases. The full-length sequences of all PrP transgenes can be found in **Appendix 8.2**. The new fly lines were balanced to achieve stable stocks and maintained an intact PrP transgene.

The double PrP transgenic flies were assembled using two consecutive crosses of the chromosome 2 PrP transgenic flies and chromosome 3 PrP transgenic flies of our interest. The human PrP transgenic fly with PrP on chromosome 2 was combined with human PrP transgenic fly with PrP on chromosome 3 to achieve dual PrP fly. The first step was double balancing of both PrP transgenic flies by crossing them with double CyO / if ; MKRS / TM6b balancer (Department of Genetics stock, University of Cambridge, UK). After collection of the double balanced progeny of the opposite phenotype, the final cross to assemble the double PrP transgenic fly was made. The scheme of the crosses can be seen in **Figure 15**. Overview of all existing PrP transgenic *Drosophila* with human PrP transgenes can be seen in **Table 3.**

3.2.7 Generation of cervid PrP transgenes

The cervid PrP (white-tailed deer) transgenes were generated to simulate the polymorphisms that affect susceptibility to acquired prion disease. The polymorphisms generated were either S138 or N138 PrP amino acid substitutions.

The cervid PrP transgenes were generated by the same procedure as human PrP transgenic flies. The cervid PrP transgenes contain insect signal peptide and cervid GPI-anchor. The primers used were PD1FCerPrP and CerPrPR1 for the first PCR step and PD2F and CerPrPR1 for the second PCR step. The primers carried *EcoRI, XbaI* and *XhoI* restriction sites (list of primers in **Appendix 8.3**).

After the PCR purification, the products were used as inserts for pUASTattB plasmid constructs to generate pUAST-PrP with insect signal peptide to be used for *Drosophila* transgenesis. The verification of *Drosophila* transgenesis was performed using pUASTattB plasmid specific primers flanking the PrP insertion site applied to the fly head homogenates to amplify the products for sequencing **(Figure 21**). The product of expected size 781 kB was obtained. The sequencing was successful and confirmed the expected insert sequence in all cases. The full-

length sequences of all PrP transgenes can be found in **Appendix 8.2.** The new fly lines were balanced to achieve stable stocks and maintained an intact PrP transgene. Overview of all existing PrP transgenic *Drosophila* with cervid PrP transgenes can be seen in **Table 4.**

3.3 Discussion

This chapter describes construction and validation of all PrP transgenic flies used for PrP expression and protein-misfolding experiments. PrP inserts of various species were used in transgenesis to model different genetic prion diseases or sensitivity of PrP transgenic *Drosophila* to exogenous prion disease.

As stated before, there have been some PrP transgenic *Drosophila* models assembled and used to model prion disease in the past (Raeber et al., 1995, Murali et al., 2014, Choi et al., 2010, Thackray et al., 2012a, Thackray et al., 2014a). To a certain extent, the *Drosophila* models of neurodegeneration are successful. On the other hand, there has been a lot of discrepancy in the approach towards this task, resulting in models that do not reflect a real situation in mammalian models.

The majority of the *Drosophila* models used, rely on the fact that the cellular form of PrP triggers misfolding when overexpressed (Choi et al., 2010, Fernandez-Funez et al., 2009, Gavin et al., 2006, Murali et al., 2014). Unfortunately, this event is not typical for the host organisms harbouring PrP prone to prion disease. Under normal circumstances, the onset of prion disease arises either from genetic mutation in the PRNP gene, transmission of exogenous prion disease or sporadic occurrence of a disease through a one-time event of protein misfolding (Aguzzi et al., 2008). There is no evidence for prion disease arising from PrP overexpression in the host organism, therefore, the conclusions drawn from such models cannot be considered a source of universally applicable experimental data. The processes that lead to the onset of misfolding and/or neurodegeneration might not be identical to those that arise during the *bona fide* prion infection.

In prion research, new models and especially those easy to assemble and fast to test are needed. The majority of clinical diagnostic tests for prion-disease still rely on the use of sentient experimental animals, such as mice (Taguchi et al., 2003). Infectivity, the most important feature of prions, cannot be precisely processed *in vitro* so far. The long interval between inoculation and disease onset hampers the investigation and deems the bioassay in mice impractical. This

renders the whole process complicated, costly and lengthy. Patients are condemned to wait for the results of their tests for months in uncertainty. If there was an adequate method to test for prions *in vitro* or use a faster *in vivo* method, it would solve a pressing problem in the field of prion diagnostics. By developing the fly models further, the opportunity opens for efficient substitutes of mice-based *in vivo* diagnostics.

It has been established that *bona fide* prion disease can be modelled in *Drosophila* and substitute the lengthy *in vivo* assay in mice (Thackray et al., 2016). In this project, the wide approach of making various PrP transgenic flies with transgenes of different species origin and genotype/polymorphism was adopted. The boundaries of the fly research need to be pushed and introducing more opportunities to study different features of prion disease may well be a way of wider adoption of this versatile model.

The approach used here employed either genetically manipulated *PRNP* that carried a mutation associated with known human prion disease, or the PrP^{C} transgenic flies that were infected with prion disease exogenously. As well as acquired prion disease that has already been confirmed in *Drosophila* models (Thackray et al., 2012b, Thackray et al., 2012a, Thackray et al., 2014a, Thackray et al., 2016), recently, the genetic form of prion disease was successfully modelled in *Drosophila* by our group (Thackray et al., 2017).

In this chapter, the process of preparation of various fly transgenes, integration into plasmids, fly transformation and verification of the generated flies are described. Five different species of PrP were successfully used as transgenes in this thesis: hamster (**Figures 4-10, 13 and 14**), mouse 3F4 (humanised) (**Figures 4-6, 11 and 12**), ovine (**Figures 16-18**), human (**Figures 19 and 20**) and cervid (**Figure 21**). The method of transgene generation was similar in all transgenic fly lines prepared with minor adjustments.

PCR-enabled modifications were employed to adjust the transgenes to the need of this project. In the first section, the semi-nested PCR was successfully used to create PrP transgenic flies with insect signal peptide (mouse 3F4 and hamster PrP), (**Figures 7-14**). This approach allowed for design and synthesis of the signal peptide using a combination of two different forward primers. These two primers created the new insect signal peptide attached to the PrP DNA sequence. The incorporation of insect signal peptide into mouse 3F4 and hamster sequences was employed to be able to compare PrP expression patterns between different transgenic flies that have been generated in our lab. The original mouse 3F4 and hamster transgenes created by Dr. Walker

Jackson contained species-specific signal peptide - murine signal peptide for mouse 3F4 transgene and hamster signal peptide for hamster PrP transgene (**Figures 4-6**), whereas the previously generated ovine PrP flies contained insect signal peptide (**Figure 16-18**). To investigate the expression profiles between different species of PrP, this inclusion enabled the direct comparison of influence of signal peptide origin on its expression profile. Another comparison provided by using the species-specific and insect signal peptide is a comparison of the influence of signal peptide identity on the protein expression profile. If the expression levels are found to be different, this effect would be caused by the difference in signal peptide.

Apart from different species of PrP and their variability of signal peptide identity, there were various topological forms of PrP employed in this study. The topological forms, apart from a standard membrane bound form of PrP, are the secreted form of ovine PrP that lacks a GPI-anchor and a cytosolic form of ovine PrP that lacks both GPI-anchor and signal peptide sequence. To introduce flies that can simultaneously express two different genotypes of PrP, even more variance was brought into the fly experiments by utilising two different fly chromosomes (2 and 3) as carriers of PrP. The difference of the expression profile triggered from chromosome 2 and chromosome 3 can therefore be investigated.

Species	Signal peptide	Topological variant	Chromosome
Mouse 3F4	Murine	Membrane bound	2
Hamster	Hamster	Membrane bound	2+3
Hamster	Insect	Membrane bound	2
Ovine	Insect	Membrane bound	2+3
Ovine	Insect	Secreted	2+3
Ovine	Insect	Cytosolic	2
Human	Insect	Membrane bound	2+3
Cervid	Insect	Membrane bound	2

Table 6. List of all categories of PrP transgenic flies generated in this thesis.
All fly lines generated can be compared to each other based on the combination of these categories

Some of the fly models made by other research groups have gone a bit further by utilizing the *Drosophila* codon usage system (Fernandez-Funez et al., 2017). This codon optimisation however resulted in accelerated progression of any protein expression-linked pathology and caused lethality when pan-neuronally expressed in flies (personal communication with Dr. Pedro Fernandez-Funez and (Fernandez-Funez et al., 2017). The approach of keeping the codon usage system authentic for the PrP insert results in a slower progression of pathology and therefore a higher chance to successfully model prion-associated neurodegeneration (Thackray et al., 2012a, Thackray et al., 2014a, Thackray et al., 2017).

The method of site-specific single transgene integration of PrP sequence into the fly genome was successfully confirmed in all cases in this chapter. All the amplified DNA sequences were sequenced and compared against the expected sequence to confirm their identity. The next step will be verification of targeted PrP expression and/or co-expression in these flies after crossing with the respective fly drivers.

4 Chapter 2 - Targeted protein expression in PrP transgenic *Drosophila*

4.1 Introduction

An integral part of the success of *Drosophila* as an experimental animal model is the ability to express any gene of interest in a specific population of cells in a transgenic animal (Brand and Perrimon, 1993, Jenett et al., 2012). This directed transgene expression allows the analysis of genes that play a role in normal development or pathology (Jenett et al., 2012). In addition, this invertebrate host allows the analysis of genes that harbour disease-specific mutations.

The spatially restricted expression of a specific transgene in *Drosophila* is enabled by the invention of two-component systems. These systems rely on site-specific integration of a transgene inserted in the specific vector and targeted gene expression in *Drosophila*. The transgenic construct drives the expression of a site-specific transcriptional activator, for example GAL4, and the second part of a construct, such as UAS, that has its binding sites positioned upstream of a responder transgene (for example PrP) (Pfeiffer et al., 2010).

The transgene is inserted into one of the specific vectors containing the transcriptional activator compatible with the driver system used. The most widely used plasmid for the GAL4-UAS system is pUASTattB (Bischof et al., 2007). An alternative is the LexA-lexAop system where there are different plasmids available, such as pJFRC19-MUH (pJFRC19-13XLexAop2-IVS-myr::GFP).

The binary systems allow separation of a target gene from its transcriptional activator through the creation of distinct transgenic fly lines, which allow transgene expression only after the experimental introduction of the two separate components in the same fly line as a result of conventional fly crossing. This helps to avoid the potential toxic effect of long term transgene expression on the maintenance of fly stocks. In the cells that produce GAL4, the UAS is activated and the gene that is inserted under its control is turned on and starts producing its resulting protein. Different drivers have different patterns of GAL4 expression as they use different cell specific promoters and therefore they drive the transgene expression under the UAS control in different subpopulations of cells. Both components, drivers and transgenic fly lines, can create libraries and can be used to induce various expression patterns in the fly. The only limitation of this precise manipulation are the cell type-specific or tissue-specific driver lines available (Brand and Perrimon, 1993).

Multiple expression driver fly lines exist that allow the triggering of a targeted expression of a gene of interest in a tissue or cell specific manner. The systems theoretically allow for any gene to be expressed in any cell type at any developmental stage (del Valle Rodríguez et al., 2012). Currently, there are three main independent binary expression systems in *Drosophila melanogaster*: GAL4-UAS, LexA-LexAop and QF-QUAS. The QF-QUAS system is not employed in this thesis and more info can be found in (Potter et al., 2010).

The GAL4-UAS binary expression system uses the yeast GAL4 transcriptional activator expressed in a specific pattern as its first component (Brand and Perrimon, 1993). The GAL4 protein has been characterised in detail for its DNA binding properties and transcriptional activation potential (Ptashne, 1988). The GAL4 binding site was also optimized for its high affinity binding by mutagenesis (Webster et al., 1988). The second component of this system is a UAS promoter silent in the absence of GAL4 (Brand and Perrimon, 1993). The UAS promoter is the stably integrated pUAST-based responder construct repressible by the presence of GAL80 protein (Ma and Ptashne, 1987, Klueg et al., 2002). The gene of interest under the control of the UAS promoter is therefore expressed specifically in regions with GAL4 presence. There are a number of available GAL4-promoter fusions and enhancer trap insertion lines that can be used as tailored solutions for any kind of experiment (Hayashi et al., 2002). The applications of the GAL4-UAS system are diverse and involve cell-specific ectopic gene expression with selective activation of any cloned gene, genetic mutant rescue, gene overexpression, RNA interference screens and therefore it has been used in numerous developmental studies (del Valle Rodríguez et al., 2012, Southall and Brand, 2008).

The second independent expression system developed for use in *Drosophila* is LexA-LexAop binary system (Lai and Lee, 2006). The LexA repressor, protein of 202 amino acids, regulates DNA damage SOS response in *Escherichia coli* (Walker, 1984). The LexA consists of DNA-binding and dimerization domains (Pfeiffer et al., 2010). In this two component system, the LexA operator (LexAop) from the bacterial transcription factor is activated by the binding of LexA protein. LexA DNA-binding motifs (LexAop) are located upstream of the target gene (Little and Mount, 1982). The LexA C-terminal DNA-binding domain is derived either from a GAL4 bacterial transcription factor or a strong activation domain VP16 of herpes simplex virus (Triezenberg et al., 1988, Sadowski et al., 1988). When the VP16 LexA driver is used, the expression may be triggered independently on the GAL4 system. Moreover, the fused LexA DNA-binding domain with attached VP16 activation domain is one of the strongest known to

date that allows transcription of transgenes that contain LexAop motifs (del Valle Rodríguez et al., 2012, Szüts and Bienz, 2000, Lai and Lee, 2006). The LexA system is a complementary system often used in conjunction with the GAL4-UAS system to create complex *in vivo* models of gene expression mosaics and to refine patterns of gene expression (Lai and Lee, 2006, Shang et al., 2008, Pfeiffer et al., 2010). The only limitation of the LexA-LexAop system is the lower availability of enhancer trap and promoter fusion lines than in the case of the GAL4-UAS system (del Valle Rodríguez et al., 2012).

The detailed list of *Drosophila* driver systems used in this thesis, their effectors, function, targets and species of origin can be seen in **Table 7**.

In this chapter, the PrP expression in various PrP transgenic flies generated in the thesis is verified. Two different expression systems UAS-GAL4 and LexA-LexAop were utilised in this study and various cells or tissues were used for protein expression targeting. The list of all the driver fly lines used in the thesis can be seen in **Table 8**. The drivers were used as independent systems in cases where the PrP transgene was inserted in a single copy or in conjunction with other driver systems in the case of the dual PrP transgenic flies. Dual PrP fly transgenesis allows for the expression of two different types of protein in one fly. The combination of drivers then determined the target of each PrP subtype expression.

First, the total protein expression in PrP transgenic flies was established by bicinchoninic acid assay (BCA) to be able to draw a conclusion about the protein contents in one fly head. Subsequently, the western blots (WB) with anti-PrP monoclonal antibody Sha31 were performed to verify PrP expression in all the fly lines generated and to verify the drivers that were used. The dual drivers were additionally tested by fluorescent microscopy when the Tomato Red and/or Green Fluorescent Protein (GFP) were expressed under the control of these drivers. The fluorescence patterns were investigated in order to verify their ability to target protein expression. To quantify the level of PrP expressed in the PrP transgenic flies, Capture-Detector Enzyme-linked immunosorbent assay (CD-ELISA) was employed. This thesis chapter shows various PrP expression levels in PrP transgenic flies and verifies fly ability to express a foreign protein. A set of novel dual fly driver lines of UAS-GAL4 and LexA-LexAop were established and tested in this chapter.

In the last chapter of this thesis, the flies generated here will be tested further for their misfolded protein content and their ability to develop and transmit prion disease. These novel PrP

transgenic flies coupled with the use of novel dual driver fly lines will be used to probe the cell-to-cell spread mechanisms in dual PrP transgenic flies and their disease-associated phenotypes.

4.2 Results

4.2.1 Total protein content in *Drosophila* heads

To establish the PrP expression levels in the transgenic *Drosophila* lines used in this study, fly head homogenates were routinely prepared as described in the **Materials and methods 2.16**. The drivers utilised here, target protein expression to various places in the CNS. Therefore, fly head homogenate, where the miscellaneous proteins expressed in the fly body as well as possible inhibitors are minimised, is an ideal material for protein assays. Initially, the total protein content in one fly head had to be established to see if the total protein content was comparable amongst different homogenate preparations to ensure reproducibility and also to test genotypic differences if there were any.

Bovine serum albumin (BSA) was used as a standard to estimate the protein content in the unknown samples. The 51D control non-PrP-transgenic flies and ARQ ovine PrP transgenic flies were used for the BCA to see whether the total protein contents in the heads change with the fly genotype. ARQ transgenic flies express relatively high levels of protein whereas the 51D flies do not express PrP. The data in **Figure 22** show a titration of fly head homogenates of two different genotypes and their average protein expression compared to the BSA standard curve. All fly head homogenates were prepared in triplicate and the difference of the protein content between the samples of the same genotype were analysed by one-way ANOVA to draw a conclusion of the comparability of fly head homogenates. The resulting P value was 0.5377, which means the differences of protein content amongst the repeats were not statistically significant ($P > 0.05$). However, when the same dilutions of fly head homogenates were compared between 51D and ARQ genotype by two-tailed t-test, the P value was 0.0339, which means that the difference was statistically significant ($P < 0.05$). The total protein expression per one fly head of 51D fly has been established at 1.32 μg (±0.0151) and total protein expression per one fly head of ARQ PrP transgenic fly has been established at 1.39 μg (±0.0098). The difference of the expression level between the genotypes has been calculated at 5.4%. After the total protein measurement, the PrP expression profile in each PrP transgenic *Drosophila* genotype has been investigated by western blot. Some of the differences in PrP expression levels were further quantified by capture-detector ELISA.

4.2.2 Verification of dual expression fly drivers by fluorescent markers

In order to test the spatial expression targeting of dual drivers prior to crossing with PrP transgenic flies, the LexA and dual Gal4/LexA driver lines were crossed with single or dual GFP and td-Tomato red fluorescent reporters. Fluorescent microscopy was employed in this experiment to analyse expression patterns in the larvae of their progeny. The drivers tested were crossed with Td-Tom (Tomato Red) fluorescent protein transgenic flies or green fluorescent protein (GFP) transgenic flies or their combination in a form of dual fluorescent protein transgenic flies to observe the protein expression patterns in *Drosophila* larval CNS as explained in **Materials and methods 2.20.** All the fluorescent reporter fly lines and dual driver fly lines used for this experiment are listed in **Appendix 8.1.**

The first LexA driver fly line to be tested for the targeted expression of fluorescent protein was 57C10-LexA which expresses the protein of interest pan-neuronally. The data in **Figure 23** show the expression pattern of 57C10-LexA pan-neuronal driver crossed (separately) with Td-Tom or GFP reporter that both exhibit uniform CNS expression in *Drosophila* larvae. Subsequently, targeted fluorescent protein expression in glial cells induced by the repo-LexA dual driver was investigated in 57C10-GAL4 ; repo-LexA driver. The data in **Figure 24** show the repo-LexA-driven expression of GFP in glial cells (apart from midline glia) encapsulating the CNS and simultaneous 57C10-GAL4 pan-neuronal expression of td-Tomato red protein in the CNS. The repo-LexA GFP expression spreads into the peripheral glia as well. Next, fluorescent protein expression was investigated in a 57C10-GAL4 ; iav-LexA dual driver fly. The 57C10-GAL4 drives the td-Tomato red protein expression pan-neuronally in the CNS and simultaneously, iav-LexA drives an expression of GFP in sensory neurons of chordotonal organs (**Figure 25**). The iav-LexA GFP expression is targeted to the peripheral nerves as well. Another driver tested was a 57C10-GAL4 ; 71A10-LexA dual driver fly. The td-Tomato expression under GAL4 control was found to be pan-neuronal and GFP expression under 71A10-LexA control was targeted to unknown classes of interneurons solely amongst CNS (**Figure 26**). Subsequently, the 57C10-GAL4 ; 72F11-LexA system was investigated. This dual driver fly line induced 72F11-LexA expression of GFP in basin interneurons (postsynaptic partners of the chordotonal and class IV multidendritic sensory organs) coupled with td-Tomato red protein expression under the control of 57C10-GAL4 pan-neuronal driver. The data in **Figure 27** show the 57C10-GAL4 ; 72F11-LexA controlled expression of both fluorescent proteins targeted to the CNS and some non-specific expression of GFP that can be seen around the CNS. The situation is similar in the

57C10-GAL4 ; 20B01-LexA driver fly expressing td-Tomato red protein pan-neuronally under the control of 57C10-GAL4 in CNS and GFP expression driven to basin interneurons (postsynaptic partners of the chordotonal sensory organs) under the control of 20B01-LexA (**Figure 28**). 20B01-LexA drives non-specific GFP expression in peripheral cells surrounding the CNS.

Collectively, the results verify targeted expression of fluorescent proteins by the 57C10-LexA single driver and multiple dual GAL4/LexA drivers used in the thesis. The PrP expression patterns are expected to be identical to the ones seen here, when the same drivers are used for PrP transgenic fly line crosses.

4.2.3 PrP expression in PrP transgenic *Drosophila*

The fly lines created by transgenesis have been previously tested by PCR and DNA sequencing to verify the transgene presence and identity. To confirm the ability to express PrP in transgenic *Drosophila*, the PrP transgenic flies were crossed with their respective drivers to initiate PrP expression. The detailed *Drosophila* mating schemes can be seen in **Figure 29.**

For the initial testing of PrP transgenic flies with a transgene under the control of the UAS-GAL4 system, the pan-neuronal elav-GAL4 driver line was used. For the flies generated with a transgene regulated by the LexA-lexAop system, the drivers triggered expression of PrP in various cellular subsets, such as interneurons or glial cells.

PrP expression in mouse 3F4 and hamster PrP transgenic flies

Mouse 3F4 and hamster UAS-PrP (chromosome 2) transgenic flies with species specific signal peptide sequence were crossed with elav-GAL4 driver and subjected to western blot analysis to detect the PrP expression levels. The western blot data for 5 day old flies transgenic for murine 3F4 PrP can be seen in **Figure 30** and the data for hamster PrP can be seen in **Figure 31**. The double band of mono-glycosylated PrP of 29 kDa is present in all genotypes of both murine 3F4 and hamster PrP transgenic flies. The expression levels of mouse 3F4 and hamster PrP appear to be higher than VRQ(GPI) ovine PrP expression levels under the same elav-GAL4 driver (as shown in **Figures 30 and 31**).

The PrP concentration was measured using a Capture-detector ELISA in mouse 3F4 wild type and hamster wild type PrP transgenic flies. The data in **Figure 32** show the absorbance values for both PrP transgenic fly genotypes as well as for 51D control flies. The samples were prepared in

triplicate to verify the PrP content in fly head homogenates. The average PrP content in one mouse 3F4 wild type fly head was established at 5.8 ng (±0.0241) whereas the hamster PrP wild type flies showed 6.7 ng (±0.009) of PrP per head. The hamster PrP transgenic flies exhibited significantly higher expression of PrP ($P = 0.0042$) than mouse 3F4 flies. The 51D control flies with no PrP transgene showed significantly lower absorbance values ($P < 0.0001$) than mouse 3F4 or hamster PrP expressing flies; that correlates with the lack of PrP in their genomes (**Figure 32**).

The hamster wild type and hamster CJD PrP transgenic flies with insect signal peptide were generated and balanced to obtain a stable stock. The males of the hamster WT and CJD were crossed with elav-GAL4 driver and subjected to western blot analysis to detect PrP expression profile. The western blot data for 5 day old flies transgenic for hamster WT and CJD PrP can be seen in **Figure 33**. Multiple lines per each genotype were tested by western blot and the line M1 for hamster WT with insect signal peptide and line M2 for hamster CJD with insect signal peptide were found to express PrP. The double band of mono-glycosylated PrP of 29 kDa is present in both M1 WT and M2 CJD hamster PrP transgenic fly lines. The expression level and profile of hamster PrP transgenic flies with hamster (species-specific) signal peptide and hamster PrP transgenic flies with insect signal peptide appeared to be identical under the same elav-GAL4 driver (**Figure 33**).

Hamster CJD PrP transgenic flies with hamster signal peptide with the PrP gene on chromosome 3 were constructed to enable the assembly of dual PrP flies. The hamster CJD-LexAop inserted on chromosome 3 of the fly genotype was crossed to repo-LexA driver to express hamster CJD PrP. As a control, hamster CJD with a PrP gene on chromosome 2 under the control of pan-neuronal GAL4 driver was used. The repo-LexA drives expression of hamster CJD on chromosome 3 in glial cells and the western blot analysis shows a double band of mono-glycosylated PrP at 29 kDa, the 57C10-GAL4 expression of hamster CJD from chromosome 2 shows an identical molecular profile but what appears to be a higher PrP expression (**Figure 34**). The expression of hamster CJD PrP from chromosome 3 under the LexA control was verified.

Once the dual PrP transgenic flies with a UAS-PrP transgene on chromosome 2 and a second LexAop-PrP transgene on chromosome 3 were generated, they were crossed with various dual PrP drivers (combination of GAL4 and LexA driver system). The general crossing scheme of the dual PrP flies with dual drivers is explained in detail in **Figure 35**. This crossing scheme is universal for all dual drivers used throughout the thesis, unless stated otherwise.

The hamster wild type and hamster CJD dual PrP transgenic flies with hamster signal peptide were assembled and balanced to obtain a stable stock. The males of the hamster WT-UAS ; CJD-LexAop dual flies were crossed with females of the dual expression drivers and collected at 5 days of age for a western blot analysis. The dual drivers used were 57C10-GAL4 ; **repo**-LexA, 57C10-GAL4 ; **GMR**-LexA and 57C10-GAL4 ; **iav**-LexA. These dual drivers are able to express hamster WT and CJD from chromosome 2 and chromosome 3 simultaneously. The 57C10-GAL4 ; repo-LexA drives expression of hamster WT on chromosome 2 pan-neuronally, expression of hamster CJD on chromosome 3 in the glial cells and dual expression of hamster WT and CJD pan-neuronally and in glial cells, respectively. The 57C10-GAL4 ; GMR-LexA drives expression of hamster WT on chromosome 2 pan-neuronally, expression of hamster CJD on chromosome 3 in the eyes and dual expression of hamster WT and CJD pan-neuronally and in the eyes, respectively. The 57C10-GAL4 ; iav-LexA drives expression of hamster WT on chromosome 2 pan-neuronally, expression of hamster CJD on chromosome 3 in the interneurons of postsynaptic partners of chordotonal organs and dual expression of hamster WT and CJD pan-neuronally and in interneurons, respectively. The western blot analysis in **Figure 36** shows a double band of mono-glycosylated PrP at 29 kDa in all cases. However, the 57C10-GAL4 pan-neuronal expression of hamster WT from chromosome 2 appears to show higher PrP levels than repo-LexA, GMR-LexA and iav-LexA expression of hamster CJD from chromosome 3. The hamster CJD (chromosome 3) expression levels appear to be in the order: repo-LexA > GMR-LexA > iav-LexA. In case of co-expression of hamster WT and CJD under the control of 57C10-GAL4 ; repo-LexA, 57C10-GAL4 ; GMR-LexA and 57C10-GAL4 ; iav-LexA, the PrP expression levels seem to be elevated above levels of both individually expressed WT and CJD. This result shows that the dual PrP flies are able to express both hamster WT and hamster CJD simultaneously under the control of dual GAL4/LexA drivers (**Figure 36**).

PrP expression in ovine PrP transgenic flies

As a control for the latter experiments in this thesis, the ovine PrP transgenic flies with PrP on chromosome 2 were crossed with the pan-neuronal elav-GAL4 driver and collected at 5 days of age for western blot analysis. The data in **Figure 37** show all VRQ ovine topological forms of PrP driven by elav-GAL4 pan-neuronal driver. The expected molecular weight of glycosylated VRQ(GPI) PrP is 29 kDa whereas the expected molecular weight of VRQ(ΔGPI) and VRQ(cyt) PrP is 26 kDa. The secreted form of PrP displays a double band of PrP.

The VRQ ovine PrP expressed by elav-GAL4 in all its topological forms was quantified by Capture-detector ELISA. The results in **Figure 38** show the absorbances measured for chromosome 2 ovine PrP transgenic flies VRQ(GPI), VRQ(ΔGPI) and VRQ(cyt) as well as for 51D control, non-PrP-trangenic flies. The samples were prepared in triplicate to verify the PrP content in fly head homogenates. The average PrP content for one VRQ(GPI) fly head was calculated as 0.2 ng (±0.00159); this result corresponds to the western blot results that show a VRQ(GPI) band of a relatively low intensity (**Figure 37**). The average PrP content in one VRQ(ΔGPI) fly head was established at 1.5 ng (±0.31359) when expressed from chromosome 2; the result correlates with western blot analysis that appears to exhibit the highest PrP content in the VRQ(ΔGPI) topological form of ovine PrP (**Figures 37 and 38**). The VRQ(cyt) fly head homogenate measured by ELISA showed 0.1 ng (±0.00239) of PrP per head which is disconnected from the actual PrP levels observed in western blot analysis. The fact that VRQ(cyt) cannot be quantified by CD-ELISA was described in Thackray *et al.* (Thackray et al., 2014b). However, all topological forms of ovine PrP expressed in the fly resulted in significantly different PrP levels when compared to each other ($P < 0.005$), as well as all ovine PrP transgenic flies exhibited significantly higher PrP expression than 51D negative control flies ($P < 0.0001$), as expected.

Once the ovine VRQ(GPI) and VRQ(ΔGPI) PrP transgenic *Drosophila* with PrP on chromosome 3 under the control of LexA driver were generated, the initial step was to test their pan-neuronal LexA expression using the 57C10-LexA driver. The expected fractions of fly progeny of this cross were: 1) curly wing and stubble bristle flies; 2) curly wing and normal bristle flies; 3) normal wing and stubble bristle flies and 4) normal wing and normal bristle flies (which is the PrP expressing fraction of this cross). The progeny fraction that carries a phenotype associated with PrP expression was absent from the total progeny as shown in **Table 9**. The resultant phenotypes of the progeny appeared as thirds, which points to lethality phenomenon when PrP was expressed pan-neuronally under the control of the strong 57C10-LexA driver fly line.

In response to the previous result, the VRQ gene on chromosome 3 and 57C10-LexA driver fly cross was subjected to a lethality tracing experiment to discover the developmental stage at which the fly dies. A specific fly cross that involved VRQ(GPI) flies coupled with a fluorescent marker allowed PrP expression to be observed in 57C10-LexA driven flies. The progeny (larvae) combinations visualised by fluorescent microscopy can be seen in **Figure 39**. The *Drosophila* larvae with Td-Tom red fluorescence in the CNS and an absence of YFP yellow fluorescence in

the eye were the ones expressing PrP pan-neuronally. The flies with YFP eye fluorescence or combined YFP eye and CNS Td-Tom red fluorescence had no PrP expression. The larvae development was monitored and the data are shown in **Table 10**. Larvae and adults with PrP expression transferred onto a separate test plate showed behaviour changes such as reduced agar penetrating ability and no ability to fly. The PrP expressing adults were practically immobile after their emergence from pupal cases and the survival rate of these PrP expressing flies was 40 - 45% when compared to the control, given that larvae of this genotype were separated from the other fractions of the progeny. The one to three days old adults (survivors) with PrP expression were subjected to a western blot analysis to investigate the PrP expression levels (**Figure 40**). The level of PrP expressed under the control of the LexA pan-neuronal driver was extremely high and might indeed be the cause of the lethality. The mixed population of PrP expressing larvae and control larvae maintained on the same agar plate gave rise to no PrP transgenic adults upon hatching (data not shown). The weaker PrP expressing flies/larvae were not able to survive and compete with control flies in a standard population of progeny.

After the failure to produce flies that express PrP under the control of LexA pan-neuronally, the cellular subset-specific LexA driver fly lines were crossed with PrP transgenic flies with VRQ PrP on chromosome 3 to investigate the efficiency of their expression. The dual driver lines tested were 71A10-LexA, 72F11-LexA, iav-LexA, repo-LexA and GMR-LexA. The western blot data of the crosses can be seen in **Figure 41**. The most intensive band appeared in the case of VRQ(GPI) crossed with repo-LexA driver which drives expression in glial cells. The VRQ(GPI) PrP expression level under repo-LexA control seemed to be high in comparison to elav-GAL4 driven VRQ(GPI) expression and even VRQ(ΔGPI) under the control of elav-GAL4. The bands are visible in the case of VRQ(GPI) flies driven by the iav-LexA driver and their relatively low intensity is consistent with the fact that PrP expression in *Drosophila* is restricted to the sensory neurons of the chordotonal organs neuronal subset as seen in **Figure 25**. The second highest expression level appears to be exhibited by GMR-LexA driven PrP expression in the eye. The band patterns of the LexA subset specific drivers coupled with VRQ(GPI) resemble those from the VRQ(GPI) PrP gene on chromosome 2 where the band appears around 29 kDa. The 71A10-LexA driver did not show any PrP expression and 72F11-LexA driver showed a faint band at the detection level limit of a western blot. This may be due to the small proportion of interneurons where the PrP expression is driven by these LexA driver lines as seen in **Figures 26 and 27**. PrP expression was successfully confirmed in iav-LexA, repo-LexA and GMR-LexA driven

constructs. The expression levels are tightly correlated to the cellular or neuronal population in which the PrP is expressed. The highest expression levels seems to be exhibited in repo-LexA driven flies which corresponds with the number of glial cells present in the fly CNS.

To quantify the amount of PrP expressed in ovine PrP positive flies with a transgene on chromosome 3 under the control of LexA drivers, a Capture-detector ELISA was performed. The iav-LexA and repo-LexA drivers were selected for the assay as these were expressing the lowest detectable and the highest levels of PrP expressed, respectively (as seen in **Figure 41**). The results in **Figure 42** show the absorbances measured for chromosome 3 ovine PrP transgenic VRQ(GPI) flies as well as for the attP2 control, non-PrP-trangenic flies. The average PrP content for one VRQ(GPI)-iav-LexA fly head was calculated as 0.3 ng (±0. 0.02937); this seem to correspond to the western blot results that showed a VRQ(GPI)-iav-LexA band of a relatively low intensity (**Figure 41**). The average PrP content in one VRQ(GPI)-repo-LexA fly head was established at 5.0 ng (±0.019287); the results correlate with a western blot analysis that appear to show the highest PrP content in VRQ(GPI)-repo-LexA fly heads (**Figure 41**). The results in **Figure 42** suggest that the PrP expression levels are significantly different between the PrP transgenic fly genotypes ($P < 0.0001$). The PrP absorbance values are also significantly elevated in VRQ(GPI)-iav-LexA driven flies ($P = 0.0027$) and VRQ(GPI)-repo-LexA driven flies ($P < 0.0001$) when compared to 51D negative control flies.

After testing the single ovine PrP transgenic flies, dual PrP transgenic flies were generated and crossed with dual 57C10-GAL4/subset specific-LexA drivers. The dual PrP transgenic fly genotypes generated and verified here were VRQ(GPI)-UAS ; VRQ(ΔGPI)-LexAop and their controls. To test the simultaneous expression of VRQ(GPI)-UAS ; VRQ(ΔGPI)-LexAop, three dual drivers previously found to express detectable levels of PrP in the neuronal or cellular subsets under the control of LexA were tested: 57C10-GAL4 ; **GMR**-LexA, 57C10-GAL4 ; **repo**-LexA and 57C10-GAL4 ; **iav**-LexA. The fly head homogenates were prepared from 5 days old *Drosophila* males. The data in **Figure 43** show that all drivers are able to drive both single and dual PrP expression.

The 57C10-GAL4 ; GMR-LexA driven flies show VRQ(GPI)-UAS pan-neuronal expression band at 29 kDa. In the case of VRQ(ΔGPI)-LexAop, the band is formed at the position of 26 kDa and seemed to be less intense than its pan-neuronal VRQ(GPI)-UAS counterpart. When the dual PrP expression of VRQm-UAS and VRQm-LexAop is triggered both pan-neuronally and in the

Drosophila eye, the PrP band at 29 kDa is formed and its expression levels appear to be elevated above both VRQm-UAS and VRQs-LexAop, as expected. The VRQ(GPI)-UAS ; VRQ(ΔGPI)-LexAop simultaneous expression under the control of the 57C10-GAL4 ; GMR-LexA driver results in a dual band pattern of VRQ(GPI)-UAS at 29 kDa and VRQ(ΔGPI)-LexAop at 26 kDa as expected. The VRQ(ΔGPI)-LexAop band appeared to show a higher PrP expression level when expressed along with VRQ(GPI)-UAS pan-neuronally; the expression levels were lower when the same protein is expressed alone (**Figure 43**).

The 57C10-GAL4 ; repo-LexA driven flies show VRQ(GPI)-UAS pan-neuronal expression band at 29 kDa. In the case of VRQ(ΔGPI)-LexAop, the band is formed at the position of 26 kDa and appears to be more intense than its pan-neuronal VRQ(GPI)-UAS counterpart. When the dual PrP expression of VRQ(GPI)-UAS and VRQ(GPI)-LexAop is triggered both pan-neuronally and in the *Drosophila* glial cells, the PrP band at 29 kDa is formed and its expression levels seem to be elevated above both VRQ(GPI)-UAS and VRQ(ΔGPI)-LexAop, as expected. The VRQ(GPI)-UAS ; VRQ(ΔGPI)-LexAop simultaneous expression under the control of the 57C10-GAL4 ; repo-LexA driver results in a dual band pattern of VRQ(GPI)-UAS at 29 kDa and VRQ(ΔGPI)-LexAop at 26 kDa. Both VRQ(GPI)-UAS and VRQ(ΔGPI)-LexAop bands seem to retain their expression levels regardless of their independent or simultaneous expression (**Figure 43**).

The 57C10-GAL4 ; iav-LexA driven flies show VRQ(GPI)-UAS pan-neuronal expression band at 29 kDa. In case of VRQ(ΔGPI)-LexAop, the band is formed at the position of 26 kDa and seems to be less intense than its pan-neuronal VRQ(GPI)-UAS counterpart. When the dual PrP expression of VRQm-UAS and VRQm-LexAop is triggered both pan-neuronally and in the *Drosophila* sensory neurons, the PrP band at 29 kDa is formed and its expression levels seem to be elevated above both VRQm-UAS and VRQs-LexAop, as expected. The VRQ(GPI)-UAS ; VRQ(ΔGPI)-LexAop simultaneous expression under the control of 57C10-GAL4 ; iav-LexA driver results in a dual band pattern of VRQ(GPI)-UAS at 29 kDa and VRQ(ΔGPI)-LexAop at 26 kDa. Both VRQ(GPI)-UAS and VRQ(ΔGPI)-LexAop bands seem to retain their expression levels regardless of their independent or simultaneous expression (**Figure 43**).

Nevertheless, these result show that dual PrP transgenic flies are able to express both VRQ(GPI) and VRQ(ΔGPI) simultaneously under the control of various dual GAL4/LexA drivers.

PrP expression in human PrP transgenic flies

Two genotypes (M129 and V129) of chromosome 2 human PrP transgenic flies with insect signal peptide were generated and verified by western blot. Since both M129 and V129 are under the control of UAS, the flies were crossed with an elav-GAL4 pan-neuronal driver to test the PrP expression levels. In **Figure 44**, the data for all the human PrP fly lines generated can be seen. The PrP band formed around 26-29 kDa can be seen in all cases and there seem to be no differences in the position or intensity of the PrP bands between different fly lines or the two genotypes. Since the human PrP expression levels are relatively high, the intense PrP band does not reveal that it consists of two bands at approximate size of 29 and 26 kDa as seen in **Figure 45**. PrP expression was confirmed in all human PrP transgenic fly lines generated.

The same genotypes, M129 and V129, of human PrP transgenic flies with insect signal peptide were generated with a transgene inserted on chromosome 3. In contrast to all the previous flies generated with a transgene on chromosome 3, the human PrP flies do not require to be expressed independently from chromosomes 2 and 3 (detailed explanation in the next paragraph). Therefore, the M129 and V129 on chromosome 3 are under the control of UAS-GAL4 system, as well as their chromosome 2 counterparts. To test the PrP expression levels of chromosome 3 human PrP transgenic *Drosophila*, the cross with elav-GAL4 fly line was performed. The data in **Figure 45** show the PrP expression levels in chromosome 3 human PrP transgenic flies, compared to chromosome 2 PrP transgenic flies. The results suggests that there is a difference in PrP expression levels when human PrP is expressed from chromosome 2 or 3. The PrP band positions are identical in all the flies analysed here. Chromosome 2 human PrP transgenic flies seem to exhibit higher PrP levels than chromosome 3 human PrP transgenic flies (**Figure 45**).

To simulate the homozygous and heterozygous genotypes present in humans, dual human PrP transgenic flies were generated. In humans, the polymorphisms at amino acid position 129 influence the susceptibility to acquired prion diseases. The combinations generated to be able to model human PrP polymorphisms in the fly were homozygous M129/M129 and V129/V129 and heterozygous M129/V129 and V129/M129 (chromosome 2/chromosome 3, respectively). The data in **Figure 46** show that the dual PrP flies seem to express higher amounts of PrP than single human PrP transgenic flies when crossed with elav-GAL4 driver. The double band of PrP at approximately 29 and 26 kDa is present again. In the case of the M129/V129 combination, the expression level appear to be at the same level as a single M129 expression level. However, during multiple repeats of this western blot, the expression levels were found to be similar across

the genotypes and seemed to be elevated above the level of single PrP expression (data not shown). The dual human PrP transgenic flies were successfully verified for their dual PrP expression.

To compare PrP expression in human PrP transgenic flies with a transgene on chromosome 2, 3 or their combination, the Capture-detector ELISA was performed. The data in **Figure 47** show the ELISA absorbances of samples from human M129 on chromosome 2, M129 on chromosome 3, V129 on chromosome 2, V129 on chromosome 3 and a combination of M129/M129 on both chromosomes, as well as for 51D control flies. The average PrP content in one M129 fly head was established at 4.5 ng (±0.09405) when expressed from chromosome 2 whereas M129 on chromosome 3 showed 3.2 ng (±0.02121) of PrP per head. The average PrP content in one V129 fly head was established at 3.9 ng (±0.00919) when expressed from chromosome 2 whereas V129 on chromosome 3 showed 2 ng (±0.01061) of PrP per head. Simultaneous expression of M129/M129 from both chromosomes resulted in 5.2 ng (±0.02616) of PrP being expressed. The dual human PrP transgenic flies exhibited higher PrP content than single human PrP transgenic flies as previously suggested by the western blot (**Figure 46**). However, the PrP levels were not statistically significant from that expressed by M129 on chromosome 2 ($P = 0.0572$). Otherwise, the PrP levels were significantly different between all groups of flies (see the P values in **Figure 47**). As a confirmation of a western blot of chromosome 2 and 3 human PrP transgenic flies (**Figure 46**), the CD-ELISA showed significantly lower PrP concentrations when the human PrP is expressed from chromosome 3 when compared to chromosome 2 expressing flies (**Figure 47**). The PrP absorbance values are also significantly elevated in all PrP transgenic flies, when compared to 51D negative control flies (M129 ch2: $P = 0.0015$, M129 ch3: $P = 0.0002$, V129 ch2: $P < 0.0001$, V129 ch3: $P < 0.0001$ and M129/M129: $P < 0.0001$).

PrP expression in cervid PrP transgenic flies

Two genotypes (S138 and N138) of chromosome 2 cervid (white-tailed deer) PrP transgenic flies with insect signal peptide were generated and verified by western blot. In cervids, the homozygous polymorphisms in amino acid position 138 influence the susceptibility to acquired prion diseases. Both S138 and N138 were placed under the control of UAS and the flies were crossed with elav-GAL4 pan-neuronal driver to test the PrP expression levels. In **Figure 48**, the data for all cervid PrP transgenic fly lines generated can be seen. The PrP band that formed around 29 kDa can be seen in all cases and there seem to be no differences in the position or

intensity of the PrP bands between different fly lines of the two genotypes. The PrP expression was confirmed in all cervid PrP transgenic fly lines generated.

4.3 Discussion

The use of *Drosophila* as an experimental animal for modelling neurodegenerative disease was initiated in 1998, when HD and Spinocerebellar ataxia were successfully reproduced in the fly (Jackson et al., 1998, Warrick et al., 1998). Since the *Drosophila* genome lacks a PrP orthologue, the fly seems to be an ideal organism to investigate gain-of-function mechanisms that might be associated with misfolding of PrP (Fernandez-Funez et al., 2017). Once the UAS-GAL4 system was introduced in the fly model, it allowed for expression of foreign PrP transgenes more readily (Brand and Perrimon, 1993, Deleault et al., 2003). Neurodegeneration modelling in *Drosophila* has become more common and the first models of prion disease have emerged, such as mouse-derived GSS-associated P101L PrP transgene that triggers neurodegenerative changes in PrP transgenic flies (Gavin et al., 2006). Later on, wild type hamster PrP was expressed in *Drosophila* which causes spontaneous neurodegeneration and accumulation of misfolded proteins (Fernandez-Funez et al., 2009). The robust expression levels of wild type PrP in *Drosophila* seem to enable accumulation of pathological conformers and produce neurotoxicity but there is a lack of proteinase-K resistant protein formed (Fernandez-Funez et al., 2009, Fernandez-Funez et al., 2017). In 2012, *Drosophila* models of ovine PrP variants emerged (Thackray et al., 2012b, Thackray et al., 2012a). These ovine PrP models have shown the potential for prion disease transmissibility and development of prion-like material upon exposure to scrapie material in *Drosophila* (Thackray et al., 2014a, Thackray et al., 2012a). Another phenomenon successfully studied in ovine PrP transgenic flies is the influence of topological variants of PrP (membrane-bound, secreted and cytosolic PrP expressed from the same genomic locus) on the toxicity developed in flies (Thackray et al., 2014b, Thackray et al., 2014a). The secreted VRQ(ΔGPI) form of PrP was found to be the most toxic and exhibited a spontaneous locomotor defect in the absence of prion exposure that was transmissible to PrP transgenic flies (Thackray et al., 2014a). While the membrane-bound ovine PrP VRQ(GPI) transgenic *Drosophila* constructed by Thackray *et al.* produced neurotoxicity solely after prion-exposure, as would be expected, PrP transgenic flies developed by other research groups exhibited neurodegeneration even when just the wild type PrP was expressed (Thackray et al., 2014a, Murali et al., 2014). Both the murine wild type and GSS-associated P101L PrP expressed in cholinergic neurons of *Drosophila* showed progressive locomotor dysfunction in these genotypes (Murali et al., 2014). In *Drosophila* models, the goal is to achieve physiological levels of protein expression to successfully generate a

model that faithfully represents events responsible for prion-induced neurodegeneration in mammalian hosts.

Mouse 3F4, hamster, ovine, human and cervid (white-tailed deer) PrP transgenic flies were generated and this chapter describes the methods of verification and quantification of their protein expression levels and profiles. The fly expression drivers used for targeted protein expression in the GAL4 and LexA fly systems were verified as well, for their use in PrP transgenic *Drosophila* crosses.

In the first stage, the total amount of protein in single fly heads was measured. Since a lot of comparisons of PrP expression levels are based on the fly head homogenate analyses, the comparability of protein contents of the fly head-derived homogenates were evaluated. A BCA assay was employed to measure the protein content of the fly head homogenates prepared in independent repeats and from two different fly genotypes – 51D with no PrP expression and the ARQ ovine transgenic fly genotype with PrP expression (**Figure 22**). The BCA data showed that the homogenate preparation resulted in reproducible protein content amongst the same genotype as one-way ANOVA statistical analysis exhibited P = 0.5377, which is not a statistically significant P value. This showed that the homogenates prepared from the equal amount of heads could be directly compared. When two different genotypes ARQ ovine PrP transgenic flies and 51D negative control flies were compared, the statistics exhibited P = 0.0339, which is a statistically significant P value. The total protein content of the 51D genotype was found to be approximately 5.7% lower than in the ARQ PrP transgenic flies. This difference could be partially caused by the additional PrP expression in ARQ PrP transgenic flies. The total amount of protein per fly head averages around 1.38 ng. Based on the BCA data, the homogenate preparation seems to be a robust method that yields comparable amounts of total protein and therefore, the fly head homogenates used for other assays can be considered comparable, as long as equal numbers of fly heads are used throughout the samples.

Prior to the set-up of crosses that trigger PrP expression in the PrP transgenic flies, the new single and dual driver fly lines were tested for their spatial expression of PrP. The novel LexA- and GAL4-mediated dual driver fly lines investigated here were characterised initially by their ability to allow simultaneous expression through the regulated expression of fluorescent marker probes. The various dual driver fly lines were shown to permit both pan-neuronal, sensory or intermediate neuron and glial cell expression of the target fluorescent probe. All drivers that have

been used showed a successful expression of fluorescent proteins at the larval stage that enabled verification of the dual expression drivers (**Figures 23-28**). The expression pattern of the fluorescent protein in repo-LexA driven larvae showed the presence of fluorescence in peripheral glia (**Figure 24**) and iav-LexA driven larvae showed fluorescent protein in peripheral nerves (**Figure 25**). The protein expression in the periphery did not influence the function of our drivers and was expected to take place. The visualisation of protein expression patterns revealed some non-specific expression out of the CNS in 72F11-LexA driven larvae (**Figure 27**) and 20B01-LexA driven larvae (**Figure 28**). This was not expected and might be a result of a non-specific function of these drivers. These experiments confirmed the utility of the dual driver system and the specificity of the driver fly lines. The majority of the drivers used in the thesis have not previously been used for adult fly expression, only for third-instar larval expression in *Drosophila*. This thesis provides evidence that expression in *Drosophila* adults using dual drivers is possible, at least for the dual driver genotypes tested here.

Western blot analyses were performed to verify the ability of PrP transgenic flies to express PrP. The flies generated here were PrP transgenic flies with PrP originating from different species and carrying various mutations or polymorphisms predisposing them to disease susceptibility or even spontaneous disease development. To enable the simultaneous expression of two types of PrP in one fly (PrP^{C} and PrP^{Sc} orthologues), PrP transgenic *Drosophila* with PrP transgene insertion on chromosome 2, chromosome 3 and dual PrP transgenic flies with PrP on both chromosomes 2 and 3 were assembled and their PrP expression was tested.

In the first stage, the mouse 3F4 PrP and hamster PrP transgenic flies with species specific signal peptide were tested for their expression of PrP from chromosome 2 under the control of the elav-GAL4 driver. The expression levels of all mouse 3F4 (**Figure 30**) and hamster PrP (**Figure 31**) transgenic fly genotypes – wild type, FFI and CJD - were of a similar level, apart from the hamster CJD that exhibited a lower level of PrP expression. However, the hamster CJD PrP levels expressed in *Drosophila* were found to be comparable with other hamster genotypes when the western blot was repeated (Thackray et al., 2017). Hamster PrP expression seemed to be generally higher than PrP in the mouse 3F4 transgenic flies as measured by CD-ELISA (**Figure 32**).

The insect signal peptide hamster PrP transgenic flies were constructed to verify the impact of the identity (origin) of the signal peptide on the levels of PrP expression. The insect signal peptide hamster PrP transgenic flies were generated to replace the hamster signal peptide hamster PrP

flies that previously showed a lower locomotor activity even in their WT genotype when compared to 51D control flies (Thackray et al., 2017). **Figure 33** shows that there was no observable difference in the PrP expression levels between the hamster WT and hamster CJD PrP transgenic flies with different signal peptides. The hypothesis that the identity of signal peptide might be the contributing factor of lower or higher PrP expression levels in PrP transgenic *Drosophila* was refuted in this case as the PrP levels seemed to be comparable. The actual impact of insect signal peptide on their locomotor ability remains to be established in future.

Hamster CJD PrP transgenic flies with hamster signal peptide were constructed to enable the expression of spontaneously misfolding protein from chromosome 3 simultaneously with a normal cellular form of prion protein from chromosome 2 at the later stages of the project. PrP expression from chromosome 3 under the repo-LexA control (eye expression) was successfully tested by a western blot as seen in **Figure 34**. The expression level of the same protein (hamster CJD-associated PrP) was found to be lower when expressed in glial cells under the repo-LexA control in contrast to the one pan-neuronally expressed under the 57C10-GAL4 control. It seems that the glial cell-specific expression was less efficient than neuronal expression in the case of the hamster PrP transgenic flies.

The next step to take was verification of dual PrP transgenic flies containing hamster WT PrP on chromosome 2 under the GAL4 control and hamster CJD on chromosome 3 under the LexA control of repo, GMR and iav dual drivers (**Figure 36**). The pan-neuronal expression levels of hamster WT seemed to be uniform amongst the three different dual drivers, as expected. The subset-specific hamster CJD expression levels seemed to be in order: repo-LexA > GMR-LexA > iav-LexA. The highest expression levels were apparently exhibited in repo-LexA driven flies and corresponded with the number of glial cells present in the fly CNS, as seen by the fluorescent reporter images (**Figures 24-28**). The protein expression levels are expected to correlate with the number of cells in which they are expressed. In dual hamster PrP expressing flies, the PrP expression levels appeared to be elevated above levels of both individually expressed WT and CJD, as expected. These results showed the versatility of a fly model and the efficiency of the subset specific single or dual expression (**Figure 36**).

The topological variants of ovine PrP were constructed and verified in the past and the elav-GAL4 expression in this project was shown merely to compare the other PrP transgenic fly expression levels with these well-known standards (**Figure 37**) (Thackray et al., 2014a). The fact

that VRQ(cyt) cannot be quantified by ELISA (**Figure 38**) was already described in Thackray, *et al.,* 2014 and the result was verified by conformation-dependent immunoassay (CDI) (Thackray et al., 2014b). The assumption is that the VRQ(cyt) might adopt a distinct conformation from other topological forms of ovine PrP. After denaturation with guanidine and subsequent CDI, the VRQ(cyt) becomes recognizable. Apparently, epitopes of VRQ(cyt) are normally not accessible and the denaturation step is required to uncover them (Thackray et al., 2014b). The reason for this might be caused by VRQ(cyt) not being subjected to post-translational modifications as the cytosolic VRQ fails to enter the ER. The protein folding and stability is likely to be influenced by the lack of glycosylation and initiation of disulphide bond, however, the VRQ(cyt) expression was not found to be detrimental in the fly system (Thackray et al., 2014b).

To directly compare PrP expression from chromosomes 2 (GAL4) and 3 (LexA), the pan-neuronal expression of ovine PrP from chromosome 3 under the 57C10-LexA control was performed. Unfortunately, PrP detection was prevented by the fact that such high PrP expression levels were detrimental to the fly, as seen by the progeny fractions in **Table 9**; the PrP expression fraction was absent from the progeny.

The lethality tracing experiment was therefore set up, to discover at what stage of the *Drosophila* development the PrP expression becomes lethal. Surprisingly, the larvae of the PrP expressing fluorescent phenotype emerged from the eggs and develop to the first instar with no obvious problems (**Figure 39**), later on, they were separated from the other fluorescent phenotypes to observe their further development. When kept separately, 40% of the larvae (compared to non-PrP transgenic control) actually developed into adults (**Table 10**). However, the adults emerging were not able to fly or even fully shed their pupal cases. The situation in the mixed population of PrP and non-PrP transgenic larvae replicated the lethality phenomenon, as larvae cannibalism caused eradication of the weaker PrP-expressing larvae. PrP-expressing survivors tested by western blot (**Figure 40**) confirmed the extremely high PrP levels expressed driven by the LexA pan-neuronal driver. The high PrP level was predicted to be the cause of lethality in this genotype.

Instead of the pan-neuronal driver, tissue or cellular subset specific LexA-drivers were utilised to express ovine PrP from chromosome 3 PrP transgenic flies (**Figure 41**). Expression was successfully confirmed in the case of iav-LexA, repo-LexA and GMR-LexA drivers. The 71A10- and 72F11-LexA drivers did not show PrP expression above the western blot detection level.

This could be caused by either a small number of cells in which the PrP was expressed or by the inability of protein expression in the *Drosophila* adult stage. Further quantification of the PrP expression levels by CD-ELISA showed nearly 17 times lower PrP expression levels in the iav-LexA driven flies than in the strongest repo-LexA driven flies (**Figure 42**).

In an attempt to visualise dual PrP expression of VRQ(GPI) from chromosome 2 under GAL4 control and VRQ(ΔGPI) from chromosome 3 under LexA control, the dual pan-neuronal GAL4 and subset specific LexA drivers were employed. The results here confirmed the ability to co-express two types of PrP. However, in contrast to hamster PrP expression in **Figure 36**, the results were not as clear-cut in ovine PrP dual transgenic flies (**Figure 43**). There seemed to be a difference between pan-neuronal PrP expression levels of VRQ(GPI)-UAS in the case of 57C10-GAL4 ; repo-LexA driver and the other two drivers used. The expression patterns triggered by 57C10-GAL4 ; repo-LexA driver seemed to be reverted in both VRQ(GPI) that appeared to show lower PrP expression levels, and VRQ(ΔGPI) that seemed to show PrP levels elevated above the ones of GMR-LexA and iav-LexA drivers. This band pattern was maintained in the dual VRQ(GPI) ; VRQ(ΔGPI) PrP expressing fly as well. In the case of elav-GAL4 driven expression of VRQ(GPI), the levels of this topological form of protein seemed to be always lower than in VRQ(ΔGPI) and VRQ(cyt). Therefore, the lower pan-neuronal expression as seen in the 57C10-GAL4 ; repo-LexA cross was expected. On the other hand, the VRQ(ΔGPI) expression took place in smaller cellular subsets and for this reason, the VRQ(GPI) pan-neuronal expression might have been above the level of VRQ(ΔGPI), which it was not. There is no clear explanation for this phenomenon and it remains to be investigated in detail in future. Moreover, in the GMR-LexA driven dual PrP fly, the VRQ(ΔGPI) expression level is elevated above the level of the same protein expressed separately. The reason for this changed band pattern might be the interference of pathological misfolding presumably taking place in this dual PrP fly with the protein metabolism that results in a rise of anchorless PrP species (**Figure 43**).

The human PrP transgenic flies were assembled both with a transgene on chromosome 2 or 3 and on both chromosomes. In contrast to the ovine, mouse 3F4 and hamster PrP transgenic flies that have independent expression under two different drivers, the human PrP transgenic flies were prepared to express both polymorphisms of the transgenes pan-neuronally under the control of the elav-GAL4 driver. In human populations, V129 and M129 polymorphisms exist in 3 variants. Homozygous carriers have either V129/V129 or M129/M129 on both their homologous chromosomes, heterozygous carriers have a combination of V129/M129 on their

homologous chromosomes. To simulate this situation in the fly system, the flies expressing combinations of V129 and M129 from chromosomes 2 and 3 were assembled and simultaneous dual PrP expression under the elav-GAL4 driver was tested by western blot and CD-ELISA. The human transgenic flies of all genotypes had a similar PrP expression level (**Figure 44**), with the difference in the PrP levels expressed from chromosome 2 and chromosome 3 (**Figure 45**). The dual PrP transgenic flies showed higher PrP expression both on western blot and by CD-ELISA (**Figures 46 and 47**). The M129/V129 genotype that appeared to have lower levels of PrP expression, similar to the single M129 PrP expressing flies, was tested again and the expression levels were found to be similar to the other genotypes and seemed to be elevated above the level of single PrP expression (data not shown). In humans, the heterozygotes M129/V129 have the different polymorphisms on homologous chromosomes; the combinations of M129/V129 and V129/M129 were introduced into *Drosophila* to make sure these two combinations have the same properties and can be used interchangeably. The CD-ELISA quantification (**Figure 47**) did not show a double amount of PrP in dual PrP flies but their expression level was slightly increased in comparison to the single PrP expressing flies (not statistically significant difference between M129 chromosome 2 and M129/M129 dual PrP flies; $P = 0.0572$). For M129/M129 dual expressing flies, the sum of the concentrations of PrP M129 chromosome 2 and M129 chromosome 3 indicated the final PrP concentration should reach 7.7 ng per fly head. PrP concentration in M129/M129 was measured at 5.2 ng per head by CD-ELISA and was still increased above that of the M129 single PrP transgenic fly with 4.5 ng of PrP per head. The human PrP transgenic flies were constructed towards the end of my project and therefore were not used for any more experiments. In future, these will be used for transmission studies of CWD, CPD and vCJD to test the transmissibility potential of these diseases.

The cervid PrP transgenic flies were successfully verified by western blot and the expression levels were found to be comparable for both polymorphisms N138 and S138 of cervid PrP transgenic flies. The cervid PrP appears to be in its mono-glycosylated form as a single band at a position of 29 kDa was present in all cases. When compared to ovine, murine 3F4, hamster or human PrP expressed in the fly, cervid PrP expression profile resembled that of membrane-bound ovine PrP transgenic flies the most. All the other PrP species showed different molecular weight bands of un-glycosylated PrP. The cervid PrP transgenic flies were constructed towards the end of my project and therefore were not used for any more experiments. In future, these will

be used for transmission studies of CWD, as its transmissibility potential to human or ovine PrP transgenic flies is not clear at the moment.

To conclude, efficient PrP expression was seen in all tested genotypes under the control of both single and dual GAL4 and LexA drivers and further experiments could be carried out using the newly constructed single or dual PrP transgenic flies.

5 Chapter 3 - Acquired and spontaneous prion-induced pathology in PrP transgenic *Drosophila*

5.1 Introduction

One of the most widespread organisms used for neurodegeneration studies is *Drosophila melanogaster*. Human prion diseases are exceptionally problematic to study in the natural host and research in *Drosophila* helps to rapidly gain insight into the molecular mechanisms that underlie their pathogenesis (Rincon-Limas et al., 2010). *Drosophila* research has already proven to be advantageous as the genetic suppressors of neurodegeneration were successfully identified using this organism (Fernandez-Funez et al., 2000, Bilen and Bonini, 2007, Cao et al., 2008). The *Drosophila* invertebrate model shows conservation of the molecular chaperones and pathways in protein aggregation and degradation that have been confirmed in mammals (Rincon-Limas et al., 2010).

Modelling prion disease in *Drosophila* was found to be challenging by many, as the initial attempts to induce prion-associated neurodegeneration in the fruit fly did not result in neuropathology (Raeber et al., 1995). The heat pulse inducible system of protein expression was employed in this study and that might have been a reason why sustained high levels of PrP were not achieved. Later attempts suggested that the fly cannot accumulate pathological forms of PrP in the brain due to clearance mechanisms specific for *Drosophila* (Deleault et al., 2003). When GSS-associated PrP was used for fly transgenesis (P101L), brain degeneration and PrP aggregation were reported but the accumulated proteins were neither detergent-insoluble nor PK-resistant (Gavin et al., 2006). Some models developed later, relied on PrP overexpression and subsequent spontaneous initiation of protein misfolding (Fernandez-Funez et al., 2009). In this model, detergent-insolubility took place after sarcosyl treatment but the protein remained PK-sensitive. The models of ovine PrP transgenic *Drosophila* later developed by Dr Thackray were able to replicate the majority of the hallmark features associated with prion diseases (Thackray et al., 2012b, Thackray et al., 2012a, Thackray et al., 2014b, Thackray et al., 2014a, Thackray et al., 2016, Thackray et al., 2017).

To follow up on the previous models generated in our lab, the goal of this thesis was to establish a model that would allow for dissection of molecular mechanisms involved in prion-induced neurodegeneration. In vertebrates, synaptic loss or dysfunction precedes onset of clinical signs within ongoing prion disease (Mallucci et al., 2003, Mallucci et al., 2007) and is considered to be a

common feature in the early stages of neurodegenerative diseases in general (Scheff and Price, 2006, Li et al., 2003, Cunningham et al., 2003, Henstridge et al., 2018). The synapse was found to be an early pathological target in numerous nervous system disorders including amyotrophic lateral sclerosis (ALS), Charcot-Marie-Tooth disease (CMT), spinal muscular atrophy (SMA) or Huntington's disease (HD) (Rozas et al., 2011, Henstridge et al., 2018). The cellular and molecular pathways of neurodegeneration are similar within invertebrates and mammalian natural hosts (Driscoll and Gerstbrein, 2003, Katz et al., 2013). Moreover, the invertebrate brain is composed of similar neuronal types, circuits, ion channels and neurotransmitters (Littleton and Ganetzky, 2000, Katz et al., 2013, Wolfram and Baines, 2013, Frank, 2014).

The murine or *Drosophila* larval neuromuscular junction (NMJ) visualisation is a precise tool that facilitates direct observation of early neuropathology phenotypes in the context of the whole organism (Sleigh et al., 2014). Many laboratories studying diseases of the nervous system in *Drosophila* have focused on the NMJ as a model synapse (Davis and Müller, 2015, Harris and Littleton, 2015, Frank et al., 2013). The NMJ is a specialised synapse formed between a motor neuron and a somatic muscle fibre (Landgraf and Thor, 2006). The arrangement of 30 body-wall muscles per mid-abdominal hemisegment in the *Drosophila* larva has been well characterized (Nose, 2012). The general pattern of innervation is that each muscle is innervated uniquely by a motor neuron that forms comparatively big (type 1b) varicosities (boutons) (Budnik et al., 2006). In addition, groups of dorsal, ventral and external muscles are jointly co-innervated by a common exciter motor neuron with relatively smaller (type 1s) boutons and another common neuromodulatory motor neuron. Thus, most muscles have synapses formed by multiple axons of various shapes and sizes (Lee et al., 2008, Johansen et al., 1989, Landgraf and Thor, 2006). The NMJ analysis is an established model system that has been used extensively for the analysis of synaptic structure, function, development and plasticity (Miller et al., 2012, Jan and Jan, 1976, Keshishian et al., 1996, Frank et al., 2013, Davis and Müller, 2015, Harris and Littleton, 2015). NMJ architecture changes can be analysed relatively easily due to their segmentally repeated and stereotypic morphology (Packard et al., 2003, Ruiz-Cañada and Budnik, 2006, Collins and DiAntonio, 2007, Miller et al., 2012, Landgraf and Thor, 2006).

In this thesis, larval *Drosophila* NMJs were used to probe prion-induced synaptic phenotype. Regulation of synaptic activity, both formation and function, relies on similar molecular mechanisms in *Drosophila* and vertebrates (Keshishian et al., 1996, Featherstone and Broadie, 2000, Miller et al., 2012). Significantly, molecules identified in studies of *Drosophila* NMJ

development are conserved in vertebrates (Vactor et al., 1993). For example, larval NMJ synapses in *Drosophila* contain ionotropic glutamate receptors (GluRs), which are homologous to mammalian AMPA-glutamate receptors and their postsynaptic scaffolds resemble mammalian counterparts (Menon et al., 2013). In addition, the *Drosophila* motor system is highly accessible, can be analysed using single cell resolution and the arrangement of motor neurons innervating body muscles in *Drosophila* larvae have been described in detail (Brent et al., 2009, Johansen et al., 1989, Landgraf and Thor, 2006). These attributes underpin the use of the *Drosophila* NMJ synapse to model mammalian prion-induced neurodegeneration in the CNS.

It was therefore decided to investigate synaptic architecture of various topological variants of PrP transgenic and/or prion-exposed *Drosophila* in order to provide a phenotypic analysis of prion-induced neurotoxicity and begin to establish the molecular basis of this neurodegenerative process. This strategy was supported by evidence that the physiological function of PrP involves interaction with synapsin during clathrin-coated pit mediated synaptic membrane internalisation (Spielhaupter and Schätzl, 2001, Shyng et al., 1994, Shyng et al., 1995). In this context, conversion of PrP to its pathological form during a prion disease may induce synaptic dysfunction by perturbation of neurotransmitter vesicle release or endocytosis (Robinson et al., 2014). In the first part of this chapter, the aCC motor neuron of NMJ that innervates dorsal acute muscle 1 (DA1) is analysed. This motor neuron is considered to have a pioneer role in DA1 innervation and is thought to guide the other motor neuron subclasses along the intersegmental motor nerve (Jacobs and Goodman, 1989, Sánchez-Soriano and Prokop, 2005, Thomas et al., 1984, Fujioka et al., 2003, Lin et al., 1995, Garces and Thor, 2006). The model system used here will be sheep scrapie prion infection of ovine PrP transgenic *Drosophila* of different genotypes at the larval stage (Thackray et al., 2014a, Thackray et al., 2012b).

Prion-induced synaptic neurodegeneration was just one aspect investigated here. Another question asked in this thesis was how the transcellular spread of misfolded PrP that spontaneously arises in the fly model functions and what cell types might be involved in this process. The dissection of this phenomenon was enabled by the construction of PrP transgenic flies associated with spontaneous prion-induced misfolding. Specifically, the construction of dual PrP transgenic flies that co-express both conformers of PrP in two distinct populations of cells or neurons was advantageous in the effort to identify the mechanism of spreading. A similar strategy was used in a Huntington's disease *Drosophila* model, where the transcellular spread of protein aggregates was observed (Babcock and Ganetzky, 2015). The initial neuronal population

where the mutant huntingtin was expressed proved to play an important role, as the pattern of aggregate deposition after spreading was unique for each of the populations. As the flies aged, the mutant huntingtin aggregates were found to accumulate in multiple regions of fly brain where they caused neuronal loss. It has been identified that the spreading requires active internalisation as the neuronal loss was halted when endocytosis was blocked (Babcock and Ganetzky, 2015).

The goal of my experiment was to test a similar approach in prion-induced neurodegeneration spontaneously arising in *Drosophila*. Dual PrP transgenic flies were used for this purpose where the pathological form of PrP is expressed either in the fly eye, glial cells or sensory neurons of chordotonal organs while the wild type form of PrP is expressed pan-neuronally, serving as a substrate for misfolding. The levels of infectivity were detected in young and old flies to see if misfolding and/or transcellular spread takes place and how different the misfolded protein levels are between the dual PrP fly genotypes. The existence of any toxic effect caused by PrP misfolding on the fly will be tested by comparison of the survival of dual PrP transgenic *Drosophila* to their negative control counterparts. Since the exogenous infection of flies by scrapie show transcellular spread of misfolded PrP from the periphery to the CNS, it was expected that a similar situation would occur in the brain, where the mutant form of PrP is taken up by neurons (Thackray et al., 2014a, Thackray et al., 2016). There are different ways of cell-to-cell spread proposed for prion diseases. One of them is an involvement of tunnelling nanotubes that can take up intracellular or membrane bound vesicles harbouring PrP^{Sc} and make an intracellular shift from one cell to another (Gousset et al., 2009, Encalada et al., 2011, Magalhães et al., 2005). Tunnelling nanotubes are able to transmit PrP^{Sc} in various neuronal and non-neuronal cell lines. In this project, the transmission between different types of cells, such as glial cells and neurons, will be investigated; the transmission between two different brain cell types will cast light onto the possibility of prion transmission between such cells. Another proposed way of prion transmission is by exosomes that carry PrP^{C} or PrP^{Sc} on their membrane and therefore initiate the contact between the two conformers, therefore facilitating their conversion (Klöhn et al., 2013). Simple contact of two cells may be a chance for prion intercellular transmission according to some sources (Kanu et al., 2002) but is refuted by others (Paquet et al., 2007b). Other suggestions for PrP^{Sc} spread are "cell painting", where the GPI-anchored protein travels from the cell surface to another cell's surface and attaches there (Paquet et al., 2007b, Paquet et al., 2007a) or microvesicle involvement (Mattei et al., 2009). The fact that seems to prevent intercellular prion spread by simple release and uptake is the absence of GPI-cleaving

enzyme PIPLC that has not been identified in prion disease (Caughey et al., 1990, Stahl et al., 1990). The last option for prion spread is involvement of anchorless PrP species, that act as intermediaries of the pathological conversion (Stöhr et al., 2011). This phenomenon was further explored in this chapter, as the ovine PrP used as a source of misfolded protein in the experiment lacks a GPI-anchor and is therefore secreted. This fact increases the chance of any observable cell-to-cell spread of prion disease and is a way to discover anchorless PrP involvement. The time-course of PrP^{Sc} spread is unknown as well; it might happen either continuously with the progressing prion aggregation or in the early stages of an infection, as the first wave followed by aggregation in later stages. Since a lot of features of the process of cell-to-cell spread remain to be discovered, the advances made in this chapter would be really valuable in this respect.

The goal of this chapter was to investigate both acquired and spontaneous prion-induced neurotoxicity in *Drosophila*. In the acquired prion disease fly model of ovine scrapie, the subcellular events were investigated using the NMJ as a model synapse. This was carried out to investigate early morphology and synaptic architecture changes that were influenced by prion-induced neurodegeneration. Using PrP transgenic flies harbouring single codon mutations associated with human genetic prion disease, the spontaneous prion-induced PK-resistance was investigated. Lastly, the transcellular spread of misfolded PrP was analysed through the use of dual PrP transgenic flies by *in vitro* methods and an *in vivo* survival assay.

5.2 Results

5.2.1 Absence of PrP in the non-transgenic *Drosophila* host

Drosophila melanogaster is naturally devoid of any PrP orthologues and is considered to be unable to accumulate or propagate prions. To verify this fact, the presence of PrP was investigated. The results in the previous chapters confirm the lack of PrP by PCRs, western blots and CD-ELISAs. Our negative control 51D and attP2 flies did not show any PrP expression throughout the experiments performed in this thesis. The data in representative **Figure 49** show that there was no detectable PrP expression in 51D flies crossed to either elav-GAL4 pan-neuronal driver or repo-GAL4 glial driver flies. In ovine VRQ(GPI) PrP transgenic flies, used as a positive control, the PrP is clearly detected in the elav-GAL4 cross by the presence of a 29 kDa band.

More assays that underpin the fact that *Drosophila* flies do not express PrP and do not act as mechanical vectors after exogenous prion inoculation were performed by Dr. Alana Thackray in the past and are described in **Appendix 8.5.8**.

5.2.2 Acquired prion disease modelled in *Drosophila* larvae

The ability of ovine PrP transgenic flies to express PrP and propagate prions were tested extensively by Thackray *et al.* (Thackray et al., 2012b, Thackray et al., 2012a, Thackray et al., 2014b, Thackray et al., 2014a, Thackray et al., 2016, Thackray et al., 2018a, Thackray et al., 2018b). The studies tested the presence of misfolded PrP, behavioural changes of prion infected *Drosophila*, transmissibility potential and strain specificity of a prion infection in the PrP transgenic flies or the possibility to use flies as a rapid bioassay for potentially prion-infected blood (Thackray et al., 2014a, Thackray et al., 2016, Thackray et al., 2018a, Thackray et al., 2018b). The adult *Drosophila* is able to develop *bona fide* prion infection but the neuronal-level changes underlying prion-induced neurodegeneration were not looked upon yet. In this thesis, a novel method to detect early neurodegenerative changes in *Drosophila* larvae was verified.

The experiment was performed to uncover whether or not expression of mutated transmissible forms of PrP, when expressed in single neurons of *Drosophila*, led to changes in their synaptic connections. The larval stage of *Drosophila* inoculated with scrapie was used for this experiment (genotypes of PrP transgenic flies and driver used can be seen **Appendix 8.5.2**). To this end, multiple topological forms of VRQ PrP were targeted to *Drosophila* aCC and RP2 motor neurons via the GAL4 /UAS-PrP binary expression system (Brand and Perrimon, 1993, Fujioka et al., 2003, Pfeiffer et al., 2010) and the experimental ovine PrP (VRQ) transgenic fly larvae were fed on scrapie infected sheep brain homogenate at 1% w/v until the late third instar wandering larval stage. The experiment focused on structural aspects of synaptic architecture of neuromuscular junctions (NMJs) as a general synapse model. 51D non-PrP transgenic *Drosophila* were used as negative controls and they were fed on food that contained either prion-infected or normal brain homogenate. Three NMJs of aCC motor neurons in abdominal hemi segments A4 and A5 on the left and right side (A4R, A4L and A5R) were analysed by confocal microscopy in each dissected larva (**Figure 50**).

Gross morphology changes in VRQ expressing Drosophila larvae

As the first step, all the collected NMJ confocal images were closely inspected to observe any common changes in their overall morphology. Based on this observation across my data pool,

NMJs were grouped into three categories based on their overall gross morphology, which were termed "linear", "non-linear" and "irregular". Linear NMJs comprise two main neuronal branches with the majority of their length stretched along the proximal edge of DA1 muscle. Non-linear NMJs exhibit more than two long neuronal branches that may or may not be parallel to the edge of the DA1 muscle. Irregular NMJs show relatively short length, bent or twisted neuronal branches. Representative examples of these NMJs and their overall morphology were revealed by anti-HRP immunostaining (**Figure 51**). Gross morphological classes of NMJs revealed different ratios across the analysed treatment groups. The data in **Table 11** show the percentage of NMJ categories for each PrP transgenic fly line. Larvae in which mis-expression of cytoplasmically localised VRQ was targeted to the aCC and RP2 motor neurons by VRQ(cyt) had the largest proportion of "irregular" shaped aCC NMJ terminals. This gross morphological phenotype was common to both prion inoculated and normal brain homogenate inoculated animals. The other VRQ larvae genotypes investigated exhibited the largest percentage of linear NMJs, apart from the VRQ(ΔGPI) inoculated treatment group, where the non-linear NMJs were the most prevalent. The control 51D genotype was found to be associated with a linear NMJ morphology.

Neuronal architecture analysis of VRQ expressing Drosophila larvae

After the overall gross morphology analysis, a detailed neuronal architecture analysis was performed to investigate and quantify NMJ terminal architecture changes observed in each NMJ. The methodology of quantification can be seen in **Figure 52**. To quantify the changes in neuronal architecture amongst the genotypes and their treatment groups, statistical analyses were performed. The comparison of results amongst three different genotypes of VRQ PrP transgenic flies and 51D control flies was performed using ordinary one-way ANOVA (GraphPad Prism 6). The comparison of treatment groups (normal brain homogenate and prion inoculated) was performed for each genotype by the two-tailed unpaired t-test (GraphPad Prism 6). The results of statistical analyses were plotted and the data groups showing significant difference from 51D control transgenic flies and between genotypes or treatment groups are shown here.

The area of each DA1 muscle innervated by aCC motor neurons involved in our study was calculated based on its width and length (**Figure 50**). The muscle area was then used to normalise quantified categories of NMJ architecture to compensate for the individual size difference of each larva. The area of DA1 muscle of VRQ(cyt) genotype was significantly smaller than all other PrP transgenic and 51D transgenic *Drosophila* genotypes (**Figure 53A**). This change in DA1 area

could potentially have been caused by the smaller extent of stretching of larvae of this genotype while dissecting and not by naturally smaller DA1 muscle area of this genotype as we found out by another dissection experiment (data not shown). In other words, this may have been caused by operator inconsistency or error.

After the treatment groups of each genotype were compared (**Figure 53B**), there was a significant decrease of DA1 muscle area in the VRQ(GPI) prion-inoculated treatment group compared to the control group of the same genotype. In this case, it might be caused by a reduced muscle size in the prion-treated group, as the DA1 muscle area of respective control and prion-inoculated treatment groups were found to be similar across the sample range. However, it is fair to point out that there is no way to exclude the unequal muscle stretching again.

The DA1 muscle area was later used to normalize results of other quantified categories to account for potential differences in animal size, as represented by the size of DA1 muscles. The comparison between genotypes was made more difficult after normalisation of results to DA1 area due to the inconsistent muscle stretching between the VRQ(cyt) genotype and other genotypes (**Figure 53A**). However, the comparison between control and inoculated treatment groups of each genotype can be considered valid, as the muscles were stretched to the same extent in each pair of treatment groups of a particular genotype. A significant difference in DA1 muscle area was found between treatment groups of VRQ(GPI) (**Figure 53B**).

The total number of synaptic boutons per aCC NMJ was counted and compared. The bouton count revealed no variation between genotypes of aCC motor neurons expressing different variants of PrP (**Figure 54A**). The overall number of boutons did not differ significantly from the "51D" control genotype, which represents the same genetic background to experimental animals, though without any PrP transgene insertions. However, the comparison between control (normal brain homogenate treated) and prion-treated group of each PrP genotype showed significant increase in the number of boutons per NMJ in VRQ(cyt) *Drosophila* larvae after prion inoculation (**Figure 54B**). The number of boutons in other treatment groups of PrP transgenic or 51D *Drosophila* was not influenced by prion inoculation.

The raw bouton count was then normalised to the average area of muscle DA1 in each genotype/treatment group and the results were compared between control and prion-inoculated treatment groups of each genotype (**Figure 55A**). Only the VRQ(cyt) prion-treated group exhibited a significant increase in bouton count. Other treatment groups across the range of

analysed genotypes did not show any significant differences in bouton count after normalisation for muscle size. The single bouton area comparison between treatment groups was performed by normalisation of bouton area to the number of synaptic boutons (**Figure 55B**). The single bouton area was found to be significantly reduced after prion-exposure in VRQ(cyt) and VRQ(GPI) PrP transgenic larvae.

In the next step, the presence of satellite boutons was evaluated and quantified. The comparison of the number of satellite boutons was assessed (**Figure 56**). The expression of VRQ(cyt) led to a significantly increased number of satellite boutons when compared to all other genotypes (**Figure 56A**). However, this did not appear to be a prion-treatment triggered phenomenon as this also manifested in the absence of prion inoculation and there was no difference between the control normal brain homogenate and prion-inoculated treatment group of this genotype (**Figure 56B**).

The total number of active zones was quantified for each NMJ, following visualisation with staining for the active zone protein Bruchpilot using the monoclonal antibody nc82 (Wagh et al., 2006) (**Figure 57**). The comparison of active zone counts between genotypes showed a decreased number of active zones in VRQ (ΔGPI) in contrast to all other genotypes as seen by the data in **Figure 57A**. The number of active zones of the VRQ(GPI) genotype was increased when compared to the 51D genotype. The data divided into treatment groups exhibited a decline in the number of active zones in the VRQ(GPI) when prion-inoculated (**Figure 57B**). The VRQ(cyt) active zone count was significantly increased after prion inoculation.

The last category analysed was active zone count normalised to average DA1 muscle area (**Figure 58**). The comparison between genotypes (**Figure 58A**) showed a significantly decreased number of active zones after normalisation in the VRQ(ΔGPI) and significantly increased number of active zones in the VRQ(cyt) genotype. The number of active zones per μm^2 of DA1 muscle area was found to be significantly enhanced after prion-exposure in VRQ(ΔGPI) and VRQ(cyt) PrP transgenic larvae (**Figure 58B**).

5.2.3 Genetic prion disease modelled in *Drosophila*

Mouse 3F4 and hamster PrP expression under different conditions in PrP transgenic flies

The PrP transgenic *Drosophila* expressing humanised murine (with 3F4 epitope) or hamster PrP with mutations associated with spontaneously arising human prion disease CJD and FFI were

tested for their PrP expression under various conditions. The fact that adult *Drosophila* were able to express PrP at detectable levels was verified in the previous chapter. Here, larval PrP expression is investigated as well as the adult expression influenced by the fly age and maintenance temperature. The data in **Figure 59** show the expression profile of PrP at the larval stage of *Drosophila* development. The expression levels seemed to be comparable to the PrP expressed in the adult stage of PrP transgenic *Drosophila*. There was no obvious downregulation or upregulation of PrP expression, validating that the PrP expression is present from an extremely early stage of fly development. The NMJ analysis performed in the previous section is based on the phenomenon of PrP expression at the larval stage as well. Since larval PrP expression levels appear to be similar to the adult ones, prion-induced neurodegeneration can be observed at the early stages of fly development.

In the next step, PrP transgenic flies of different ages were compared to see the impact of their age on PrP expression levels. The data in **Figure 60** show the comparison of PrP expression profiles in five day old flies and 16 day old flies. The western blot analysis did not appear to show an increase of PrP expression in 16 days old flies, the expression levels in both 5 days old flies and 16 day old flies seemed to be comparable.

The influence of maintenance temperature in the CO_2 incubators where the flies were kept on PrP expression levels was tested in the next stage. Typically, the flies for immediate experiments were kept at 25°C, whereas the fly stocks were kept at 18-20°C. The lower temperature slows down fly development but it is not known if this slower development impacts protein expression levels. The PrP expression levels of flies of the same age kept either at 20°C or 25°C were compared in **Figure 61**. The expression levels did not seem to be influenced by the temperature as the PrP levels detected appeared to be equal between the treatment groups, based on the western blot results.

Proteinase-K resistance of misfolded PrP of mammalian origin

PrP^{Sc} expression in mammalian hosts exhibits typical profiles of PrP glycosylation and PK-resistance. To be able to compare our PrP transgenic flies of different genotypes to the authentic prion expression profiles in mammals, western blot analyses coupled with PK-digestion were performed on ovine and murine brain homogenates. The PK-resistance of misfolded $PrP^{(Sc)}$ was expected to be a result of a stabilisation of β-sheets by denaturation and is one of the major signs of prion disease in mammals.

The ovine New Zealand-derived VRQ/VRQ brain homogenates were utilised as a scrapie-free control and the classical scrapie-infected ovine VRQ/VRQ SE1848/0005 homogenates from terminally ill sheep that were identified by routine statutory surveillance were subjected to PK-digestion and subsequent western blot analysis to observe the mammalian PrP banding profile and its PK-resistance properties. The data in **Figure 62** show a PK-digest of an ovine VRQ/VRQ control and scrapie-affected brain homogenates to compare the expression profiles and PK-resistance of PrP. The VRQ/VRQ control brain homogenate shows lack of resistance to PK, with the three bands typical for mammalian PrP that represent a mixture of di-glycosylated (35 kDa), mono-glycosylated (30 kDa) and non-glycosylated (27 kDa) PrP reduced to a single faint band at a position of 25 kDa after PK-treatment. If treated for longer, this band disappears completely (data not shown). The scrapie-positive VRQ/VRQ ovine brain homogenates show a change in the banding pattern after 32 μg/ml PK-treatment. The densest bands were seen at position 27-30 kDa which are PrP^{Sc}-associated molecular weights with an additional intense band at position of 16 kDa. PK-resistance is evident even after 120 minutes of PK-digestion.

A similar situation took place in the case of PrP^{Sc} in transgenic mice. The control PrP mouse lines CD1 and C57BL6 used as negative control samples and prion-inoculated mouse lines positive for ME7 or RML mouse-adapted scrapie prion strains were PK-digested and analysed by western blot. The data in **Figure 63** show the PK-resistance in control and prion-inoculated mouse brain homogenates. Again, the PrP banding profile exhibits three bands that represent mixture of di-glycosylated (35 kDa), mono-glycosylated (30 kDa) and non-glycosylated (27 kDa) PrP. After 32 μg/ml PK-digest, the control samples CD1 and C57BL show an absence of PK-resistant material, whereas the ME7 and RML inoculated mouse brain homogenates show a shift in molecular weight towards 27-30 kDa PrP^{Sc}-associated bands with an additional intense band at position of 16 kDa. In both ovine VRQ/VRQ and murine PrP transgenic brain homogenates, there is a clear difference between the negative control groups without scrapie and scrapie-positive samples after PK-treatment. The scrapie-positive brains show PK-resistant material in all cases and confirm that a similar blotting profile is conserved amongst different mammalian species.

Proteinase-K resistance of mouse 3F4 and hamster PrP transgenic flies associated with human genetic prion disease

In PrP transgenic *Drosophila*, PrP PK-resistance is not always present even though there is the presence of infectivity. The PK-resistant fraction of PrP fully reappears when the prion infection is passaged from flies to mice (Thackray et al., 2018a). Mammalian PrP transgenic flies were

subjected to PK-digestion followed by western blot to detect levels of PK-resistance. The genotypes investigated were wild type PrP transgenic flies, not associated with any spontaneous protein misfolding, and then FFI and CJD associated PrP transgenic flies that spontaneously misfold and therefore PK resistance is expected to be present in these genotypes. The data in **Figure 64** show PK-treatment of mouse 3F4 PrP variants expressed in *Drosophila*. The wild type fly head homogenates showed PK sensitivity as the PrP was almost completely digested when PK-treated by 1 - 2 μg/ml of PK and detected by western blot probed with anti-PrP monoclonal antibody Sha31. The same treatment with 1 - 2 μg/ml of PK revealed high levels of PK-resistance in the mouse 3F4 FFI fly genotype and mild PK-resistance in the case of mouse 3F4 CJD fly samples. The PK-treatment concentrations used (1 - 2 μg/ml PK) were relatively low in comparison to the PK levels used to treat mammalian tissues (32 μg/ml PK) but the concentrations were enough to completely digest the wild type PrP expressed in the fly. PK-digestion of hamster PrP transgenic flies resulted in mild PK-resistance of both FFI and CJD variants in comparison to wild type PrP transgenic flies where the digest was complete after PK treatment of 4 - 5 μg/ml (**Figure 65**). The PK concentrations used for digestion of hamster PrP transgenic flies were higher than in mouse 3F4 transgenic flies (4 - 5 μg/ml PK) but still relatively low in contrast to the PK concentration used for PrP expressed in mammals (32 μg/ml PK). Collectively, these observations showed that variants of mouse 3F4 and hamster PrP were successfully expressed in *Drosophila*, and that PrP mutations associated with genetic prion disease affect the molecular properties of the PrP when it is expressed in the fly. Mild PK-resistance was seen in the majority of cases of human prion disease-associated mouse 3F4 and hamster PrP expressed in transgenic flies.

5.2.4 Cell-to-cell spread of prions modelled in *Drosophila*

In the next stage, the dual ovine PrP expressing flies were used to investigate cell-to-cell transmissibility potential of spontaneously misfolding PrP expressed simultaneously with a normal form of PrP in the fly. Dual expression drivers of different subset specific combinations of LexA expression were used in this experiment coupled with pan-neuronal Gal4 expression. The pan-neuronal component of the driver system was 57C10-GAL4 which is an orthologue of elav-GAL4 system.

Pan-neuronal PrP expression in dual PrP transgenic flies

Since the pan-neuronal expression was triggered by an elav-GAL4 driver in all other previous cases, the expression levels had to be compared to see if there was any difference in the amount of PrP expressed under its control. The data in **Figure 66** show that the elav-GAL4 and 57C10-GAL4 expression levels result in the same expression profile with slightly elevated PrP levels expressed by the 57C10-GAL4 driver. This expression level difference (quantitation) is further investigated in **Table 12**. The data show that the PrP levels expressed under the control of 57C10-GAL4 driver were elevated above the expression levels of the elav-GAL4 driven expression. On average, the expression is 23% higher in the case of 57C10-GAL4 than that in elav-GAL4. The expression under the control of 57C10-GAL4 is efficient and can be used as a comparable pan-neuronal driver of PrP expression.

Proteinase-K resistance of misfolded PrP in dual PrP transgenic flies

To model spontaneous PrP misfolding and cell-to-cell spread of the pathological conformational change in the *Drosophila* model, dual ovine PrP transgenic flies were used. The spontaneously misfolding genotype used was VRQ(ΔGPI) that is a secreted form of PrP observed to cause neurotoxicity and a transmissible phenotype in transgenic *Drosophila*. VRQ(ΔGPI) lacks a GPI anchor and can be considered an orthologue to GSS-associated PrP in human prion disease. The dual expression of VRQ(GPI) pan-neuronally and VRQ(ΔGPI) in a cellular subset were expected to initiate cell-to-cell transmission of misfolded PrP. The data in **Figure 67** show the PK-treatment of 30 day old flies that express VRQ(GPI) PrP pan-neuronally simultaneously with VRQ(ΔGPI) expressed in the *Drosophila* eye by GMR-LexA driver. In contrast to the experiment with mouse 3F4 and hamster misfolded PrP of FFI and CJD genotype, there was no PK resistance detected in the VRQ(GPI) and VRQ(ΔGPI) dual transgenic fly.

Detection of misfolded PrP in dual PrP transgenic flies

The PK-sensitive protein might still be able to trigger pathological misfolding resulting in neurotoxicity. To verify the presence of misfolded protein able to initiate pathological conversion of PrP in the fly model, protein misfolding cyclic amplification (PMCA) was performed. Flies of age 5 days and 30 days were compared in this assay to see if the misfolded protein accumulates as the flies aged. The level of misfolded PrP was expected to be higher in 30 day old flies than in 5 day old flies due to the VRQ(ΔGPI) template directed misfolding that

employs VRQ(GPI) that is abundant in fly brain, if the cell-to-cell transmission of prions takes place in this model.

The PMCA results were negative in all cases and did not detect any misfolded PrP. The positive control of 30 days old scrapie-infected ovine VRQ(GPI) and negative flies with non-PrP transgenic flies also failed to be detected by PMCA. In previous experiments performed by Dr Alana Thackray, the misfolded PrP in positive control 30 days old scrapie-infected ovine VRQ(GPI) flies was successfully detected (Thackray et al., 2014a). The list of samples subjected to PMCA and the results can be seen in **Table 13**. The standard PMCA protocol performed by Dr. Olivier Andreoletti (INRA, Toulouse, France) failed to detect seeding activity in dual PrP transgenic fruit fly homogenates.

A similar set of samples (**Table 14**) was subjected to the real-time quaking-induced conversion (RT-QuIC) protein misfolding assay. The flies of age 5 days and 30 days were compared in this assay to see if the misfolded protein accumulates as the flies aged. The level of misfolded PrP was expected to be higher in 30 day old flies than in 5 day old flies due to the VRQ(ΔGPI) template directed misfolding that employs VRQ(GPI) that is abundant in fly brain, if the cell-to-cell transmission of prions takes place in our model. The results of RT-QuIC were all negative, including the positive control 30 days old scrapie-infected ovine VRQ(GPI) flies. The detailed results show some false positive samples. On one occasion, VRQ(GPI)-UAS ; VRQ(GPI)-LexAop x 57C10-GAL4 ; repo-LexA sample resulted in a positive result when diluted at the 10^{-1} after RT-QuIC reaction with a lag time of 13 hours. The lag time of 13 hours is close to that expected for a sporadic CJD positive control (6.5 hours). However, the same sample was then retested and both repeat runs yielded a negative result. The other 6 samples that have shown positive results did so in the time of more than 60 hours of the assay and all of them were either 51D negative controls or 5 day old flies where the protein misfolding would not be expected. The details of the false positive samples can be seen in **Table 15**. The standard RT-QuIC protocol used by Dr. Marcelo A. Barria Matus (NCJDRSU, Edinburgh) failed to detect seeding activity in dual PrP transgenic fruit fly homogenates.

Phenotypic assay of spontaneous neurotoxicity in dual PrP transgenic flies

It is established that the survival of PrP transgenic *Drosophila* is compromised by the accumulation of disease-associated PrP as a consequence of prion infection in these flies (Thackray *et al.,* 2012a). Accordingly, the survival of VRQ(GPI) and VRQ(ΔGPI) PrP co-

expressing flies under the control of the dual 57C10-GAL4 and LexA cell-specific drivers (repo, iav or GMR) were subjected to survival analysis to investigate whether this phenotypic assay could detect cell-to-cell spread of disease-associated PrP in the *Drosophila* brain. To do so, groups of dual PrP transgenic *Drosophila* were maintained under regular fly husbandry conditions and their survival recorded on a regular basis.

The data in **Figure 70** show that there was a significantly accelerated decline in survival of dual ΔGPI/wild type PrP flies in comparison to the dual wild type PrP control flies. This accelerated decline was evident in 57C10-GAL4 ; repo-LexA flies that expressed ΔGPI in glial cells ($P = 0.0022$) or in 57C10-GAL4 ; iav-LexA flies that expressed ΔGPI in interneurons ($P = 0.0249$), with wild type PrP co-expressed pan-neuronally in both cases.). In contrast, no significant accelerated decline in survival was observed when ΔGPI PrP was expressed in the fly eye with co-expression of wild type PrP pan-neuronally ($P = 0.3416$) when compared to GPI PrP co-expressed in both subsets. The magnitude of the accelerated decline was significantly greater in flies that expressed ΔGPI PrP in glial cells and interneurons compared to those that expressed this form of the prion protein in the fly eye ($P < 0.0001$) simultaneously with pan-neuronal expression of wild type PrP. The comparison of survival ability between 57C10-GAL4 ; repo-LexA and 57C10-GAL4 ; iav-LexA co=expressing ΔGPI PrP and wild type PrP resulted in significantly reduced survival of 57C10-GAL4 ; repo-LexA ($P = 0.0003$). The difference of the survival ability was evaluated by two-tailed t test comparison of the survival results throughout the whole assay.

The data in **Figure 69** show the survival curves for the control groups of flies used in this experiment. A significant decline in survival was observed in 57C10-GAL4 ; iav-LexA flies that expressed ΔGPI PrP in interneurons ($P < 0.0001$), with no other form of PrP expression in the same fly line compared to the response observed for wild type PrP control flies. In addition, the non-PrP transgenic control fly line 51D/AttP2 also exhibited an accelerated decline in survival when expressed pan-neuronally and in interneurons compared to the response observed for dual wild type PrP transgenic fly control ($P = 0.0254$). The remainder of the single or dual PrP control flies did not show an accelerated decline in their survival compared to their respective control group.

5.3 Discussion

The objective of this chapter was to investigate acquired and spontaneous pathological prion formation in PrP transgenic flies of various genotypes. Acquired prion-induced neurodegeneration was investigated at the larval level to be able to observe and describe any early scrapie-induced synapse neurodegeneration in the neuromuscular junction (NMJ) of PrP transgenic *Drosophila* larvae. The PrP transgenic flies were then used to model spontaneous misfolding associated with FFI and CJD in the case of mouse 3F4 and hamster PrP transgenic flies and an orthologue of GSS-associated PrP in the case of secreted ovine PrP transgenic flies. Apart from a simple expression of spontaneously misfolding PrP in the fly system, the simultaneous dual PrP expression, where one form of PrP serves as a template for pathological misfolding and the other serves as a substrate, was exploited here. The attempt to express the cellular PrP and misfolded PrP in one fly was made, to discover if, and how, the transcellular spread of misfolded protein works in the fly system.

The *Drosophila* model is considered, and was confirmed here, to be devoid of any PrP orthologues as seen by the results in the first result section (**Figures 49 + Appendix 8.5.8 - figures A and B**). This initial step was essential to be able to link the results obtained with the PrP transgene and not the presence of *Drosophila* PrP. Control 51D *Drosophila* do not express PrP. Any detected PrP-induced neurodegeneration in our model is therefore caused solely by the presence of an additional PrP transgene artificially inserted into the *Drosophila* genome.

Since all the previous experiments performed by Dr Alana Thackray in our lab were performed on adult flies and involved investigation of phenotypic changes in the flies and detection of PrP misfolding, without detailed studies of the prion-induced synaptic degeneration, the next step taken in this thesis was investigation of synaptic neurodegeneration in *Drosophila*. The *Drosophila* larvae were used in this experiment due to their lack of opacity and therefore ability to visualise fluorescent staining in synapses of dissected specimens. Neuromuscular junction (NMJ) analysis was carried out to identify and describe changes of NMJ morphology associated with various PrP transgenic fly genotypes and an onset of prion infection in PrP transgenic *Drosophila* larvae. The PrP transgenic *Drosophila* genotypes comprised three different topological variants of PrP – membrane bound VRQ(GPI), secreted VRQ(ΔGPI) and cytosolic VRQ(cyt) form of PrP. The high expression of PrP has been specifically targeted to the NMJs of aCC and RP2 motor neurons and the flies were orally exposed to either scrapie VRQ/VRQ

infected brain material as a source of infectious agent causing neurodegeneration or a normal (scrapie-free) sheep brain homogenate of the same genotype. The late third instar wandering *Drosophila* larvae were harvested, dissected, immunostained and analysed by confocal microscopy.

This project focused on structural aspects of synaptic architecture of neuromuscular junctions (NMJs) and their changes upon PrP expression and prion-exposure. The presence of PrP expression in mammalian hosts has been confirmed in cortico-cerebellar neurons as well as in NMJs (Robinson et al., 2014, Herms et al., 1999). Specifically, the neuronal location of PrP was reported along long axons and presynaptic and postsynaptic terminals in various prion models (Moya et al., 2000, Um et al., 2012, Um et al., 2013, Robinson et al., 2014). It has been indicated that the loss of synapses or their dysfunction precede the clinical signs of neurodegenerative diseases (Mallucci et al., 2007, Mallucci et al., 2003). A broad range of NMJ morphology changes were found to take place in the early stages of neurodegeneration (Scheff and Price, 2006, Li et al., 2003, Cunningham et al., 2003). Therefore it was hypothesized that NMJ morphology changes might be observable in the larval stage of *Drosophila* and these changes of NMJ architecture, associated with prion-related neurodegeneration, have been analysed and quantified in this study.

The initial step of NMJ analysis was an evaluation of gross NMJ morphology. Three distinctive overall morphology phenotypes of the motor neuron within individual NMJs of PrP transgenic *Drosophila* could be discerned: "linear", "non-linear", or "irregular" (**Figure 51**). The non-linear and irregular NMJ phenotypes were viewed as those associated with synaptic plasticity, either growth or neurodegeneration of this neuronal substructure (Moloney et al., 2014). When the number of the various morphological NMJ phenotypes was assessed within *Drosophila* larvae it was evident that differences existed between PrP genotypes and between prion-exposed and control treatment groups within a particular PrP genotype. These morphological observations of NMJ phenotype suggested that PrP genotype and prion infection could affect synaptic architecture and therefore synaptic activity. In the next step, detailed NMJ parameters, such as the number of boutons and satellite boutons within each larval NMJ, were assessed in larvae of different PrP transgenic *Drosophila* genotypes. This analysis was based on the observation and quantification of different parameters of NMJ architecture and its comparison between PrP transgenic *Drosophila* larvae genotypes and their treatment groups.

The first step of detailed synaptic architecture analysis was to determine the area of DA1 muscle innervated by the respective aCC motor neuron (**Figure 53**). It has been found that VRQ(cyt) larvae were stretched to a lesser extent than other genotypes involved in the study (**Figure 53A**). Therefore, the comparison of categories dependent on the extent of stretching could not be properly performed between genotypes. Comparison between treatment groups was possible, as the stretching was comparable amongst each genotype (**Figure 53B**). The quantified data of NMJ morphology were normalised to DA1 muscle area to account for the area innervated by the aCC motor neuron where possible (**Figure 55 and 58**); this analysis was not performed between genotypes due to the different extent of stretching in VRQ(cyt) transgenic larvae.

After the DA1 muscle area measurement, individual categories of NMJ morphology were quantified. The analysis uncovered that some of the differences appeared to be a general effect of topological PrP expression, other differences were triggered by prion exposure. The membrane bound form of PrP VRQ(GPI) containing the GPI anchor is the closest to the naturally occurring mammalian prions expressed in the original hosts. Previous studies did not report any prominent NMJ structural changes in VRQ(GPI) analogues in PrP transgenic or prion-infected *Drosophila* larvae (Robinson et al., 2014). In our analysis, the overall NMJ morphology of VRQ(GPI) expressing flies did not point to any changes in control or prion inoculated treatment group when compared to the control 51D genotype. The large proportion of linear NMJs suggested no large structural reorganization after prion exposure. The changes found in detailed NMJ analysis were sometimes contradictory in contrast to the more prominent NMJ architecture changes of VRQ(cyt). The VRQ(GPI) genotype was found to be associated with a significantly reduced single bouton area (**Figure 55B**). The number of active zones in both the control and inoculated treatment group was increased in comparison to the 51D control genotype (**Figure 57A**) and the number of active zones was found to be decreased after prion inoculation in contrast to the control group of the same genotype (**Figure 57B**). The reduction of bouton size and decrease in active zone count after prion exposure might be the sign of an onset of prion pathology where the loss of active zones causes impairment of synaptic transmission (Nishimune, 2012). However, the decrease in number of active zones was found to be contradictory to the increase of the same in the VRQ(cyt) genotype after prion inoculation.

VRQ(ΔGPI) PrP transgenic *Drosophila* larvae express a secreted form of PrP that lacks a glycosylphosphatidylinositol (GPI) anchor sequence. This genotype exhibits spontaneous formation of transmissible prion pathology with no previous prion exposure (Thackray et al.,

2014a). The VRQ(ΔGPI) genotype showed changes in overall NMJ morphology where the number of irregular NMJs was found to be reduced in comparison to other PrP variants (**Table 11**). Furthermore, larvae of prion-exposed VRQ(ΔGPI) transgenic *Drosophila* showed a difference in the proportion of linear and non-linear NMJs compared to those seen in non-prion exposed larvae of the same genotype. In terms of detailed neuronal architecture of VRQ(ΔGPI) expressing flies, the most prominent change observed was a significantly reduced active zone count in this genotype (**Figure 57A**) and an increased number of active zones per μm^2 of DA1 muscle when VRQ(ΔGPI) was expressed in motor neurons of *Drosophila* larvae that were fed prion-inoculated food (**Figure 58B**). The raw active zone count was elevated after prion exposure as well but the increase was not statistically significant **(Figure 57B)**. The VRQ(ΔGPI) genotype showed an array of pathological changes to the NMJ structure. The result for this genotype would however be expected to be similar in both control and prion inoculated larvae, as the locomotor defects in adult *Drosophila* of VRQ(ΔGPI) were evident and rapid in both treatment groups (Thackray et al., 2014a). The elevated number of active zones and their higher density might be an early effect of prion inoculation as the spontaneously triggered pathology in VRQ(ΔGPI) develops later in the life of *Drosophila*.

The VRQ(cyt) PrP transgenic *Drosophila* larvae express a cytosolic form of PrP that does not attach to the membrane nor is secreted into the extracellular space. It has been demonstrated that the cytosolic form of PrP does not enter the secretory pathway due to the lack of a C-terminal GPI-anchor and N-terminal signal peptide (Ma and Lindquist, 2002, Ma et al., 2002). This protein stays in the cytosol and its conformation differs from the two other genotypes of VRQ PrP (Thackray et al., 2014a, Thackray et al., 2014b). Phenotypic studies observed normal behaviour in control VRQ(cyt) PrP transgenic flies compared to 51D and other VRQ transgenic fly genotypes. After prion exposure, the locomotor ability of VRQ(cyt) transgenic flies declined rapidly and significantly compared to 51D and the prion-exposed transgenic VRQ(GPI) genotype (Thackray et al., 2014a, Thackray et al., 2014b). The VRQ(cyt) PrP naturally occurs in various neuronal subpopulations and due to the difference in its conformation and location it may have altered susceptibility to aggregation (Mironov et al., 2003). The neurons that comprise this form of PrP may play a significant role in prion disease pathogenesis. The overall morphology analysis of *Drosophila* transgenic for VRQ(cyt) displayed an altered proportion of NMJ morphologies compared to the VRQ(GPI) transgenic *Drosophila* or control 51D flies (**Table 11**). Most noticeably, larvae of VRQ(cyt) PrP transgenic flies were characterized by an increase of irregular

phenotype NMJs. There did not appear to be a difference in the morphology of NMJs from prion-exposed and control VRQ(cyt) PrP transgenic *Drosophila*. The morphological observations were consistent with a general consequence of intracellular prion protein expression in the case of VRQ(cyt) transgenic *Drosophila*. It was observed in VRQ(cyt) that the number of synaptic boutons was significantly elevated after prion exposure above that seen in control larvae of the same genotype (**Figure 54B**). The raw bouton count was then normalised to the average area of DA1 muscle and the VRQ(cyt) prion-treated group still exhibited a significant increase in bouton count (**Figure 55A**). Moreover, the average area of a single bouton (bouton area normalised to the raw number of boutons) in VRQ(cyt) PrP transgenic larvae was found to be significantly reduced (**Figure 55B**). The number of satellite boutons associated with larval NMJs from the VRQ(cyt) transgenic flies showed an increase compared to the number seen in 51D control *Drosophila* and all other genotypes (**Figure 56A**), whereas there was no significant difference observed between control and prion inoculated treatment groups of the same genotype (**Figure 56B**). The number of active zones in VRQ(cyt) prion inoculated larvae was found to be elevated in contrast to the control group of the same genotype (**Figure 57B**). After the normalisation of data to DA1 muscle area, the number of active zones was found to be significantly enhanced when prion-infected in VRQ(cyt) PrP transgenic larvae (**Figure 58**). The toxicity developed in this genotype apparently arises through different molecular pathways than in other PrP genotypes as confirmed by the NMJ analysis results. Smaller and more numerous boutons located in irregularly shaped NMJs suggest an ongoing prion-related pathology. The results of the prion-exposed VRQ(cyt) larvae treatment group are consistent with reported results in Alzheimer's disease where smaller and disintegrated boutons appeared as a consequence of human Tau protein overexpression (Chee et al., 2005). The change of structure seems to originate from inhibition of synaptic transport by Tau protein as an early sign of pathological processes and formation of neurofibrillary tangles. My findings in the prion-inoculated VRQ(cyt) PrP transgenic *Drosophila* larvae of structural changes correspond to the assumption that Tau uses soluble cytosolic forms of the same protein as the mediators of neurotoxicity (Feuillette et al., 2010).

To conclude, the NMJ morphology changes were found to be unique for each of the genotypes of PrP transgenic *Drosophila* larvae. The perturbations of various measurement categories were recorded and analysed to reflect the impact of neurodegeneration caused by either spontaneous or inoculation triggered pathology. The spectra of analysed changes in NMJ architecture of all

three different PrP transgenic *Drosophila* genotypes were found to be broad and sometimes difficult to define. One of the reasons might be that the impact on *Drosophila* larvae might not be observable due to the early stage of prion pathology. The process of neurodegeneration is extremely complicated and may have various stages in its development; this phenomenon would explain sometimes contradictory results from my analysis. However, the most prominent NMJ architecture changes have been found in the VRQ(cyt) genotype larvae as its nature is unique amongst other genotypes studied here. It appears that the cytosolic form of the PrP molecule might indeed play a role as a neurotoxicity mediator (Li et al., 2011). This study was designed to contribute to the sparse knowledge of prion related pathology and to enable yet another method of experimental analysis of prion infected invertebrate hosts. NMJ analysis might provide an insight into the early progress of prion related neurodegeneration.

The spontaneous generation of prion-associated misfolding in *Drosophila* was investigated in the next section of the thesis using mouse 3F4 and hamster PrP transgenic flies. Initially, *Drosophila* of different ages and generated under different conditions were investigated to observe the impact of these conditions on their expression profiles. The PrP expression level of murine 3F4 PrP transgenic flies did not seem to be influenced by the age of flies (**Figures 59 and 60**). The PrP expression apparently peaks at the larval stage and remains similar at 5 and 16 days of age. Interestingly, the PrP expression pattern in larvae is apparently showing the same intensity and glycosylation pattern as in the adult flies. Previously, glycosylation in PrP transgenic *Drosophila* larvae was reported as missing (Robinson et al., 2014) which does not seem to be the case here. The unchanged PrP expression level in the later times of *Drosophila* life might be caused by metabolism of PrP and a function of its promoter. Oxidative metabolism can generate high amounts of reactive oxygen species which can then cause protein damage and interfere with normal cell metabolism and halt PrP expression (Gasperini and Legname, 2014, Esiri, 2007). The maintenance temperature does not influence the PrP expression levels, even though fly development is protracted at the lower temperature (**Figure 61**). The glycosylation pattern and PrP levels are not altered by the fly age nor the maintenance temperature which proves an enormous stability of the fly expression system and reproducibility of results generated using the *Drosophila* model.

To be able to compare the glycosylation patterns and PK-resistance of mammalian PrP transgenic flies, the mammalian brain tissue homogenates were subjected to western-blot protein detection and PK-digestion. As expected, the three bands typical for mammalian PrP that

represent a mixture of di-glycosylated (35 kDa), mono-glycosylated (30 kDa) and non-glycosylated (27 kDa) PrP were evident. After PK-treatment, these were reduced to a single faint band at a position of 25 kDa, if the sample did not contain misfolded prions. The scrapie-positive brain homogenates showed a change in the expression pattern after PK-treatment to the highest expression level at 27-30 kDa (PrP^{Sc}-associated molecular weights) with an additional intense band at 16 kDa. This pattern appeared in both ovine and murine brains (**Figures 62 and 63**). The same experiment was carried out for mouse 3F4 and hamster PrP transgenic flies of wild type, FFI and CJD genotypes. PrP transgenic *Drosophila* with either a CJD- or FFI-associated mutation showed a mild resistance to PK compared with the respective wild type PrP protein (**Figures 64 and 65**). A similar PK-resistance has been shown for mo3F4P101L PrP when expressed in *Drosophila* (Choi et al., 2010). These observations are consistent with the ability of mutations associated with genetic forms of human prion disease to affect stability and biochemistry of PrP (Billeter et al., 1997, Liemann and Glockshuber, 1999, Dossena et al., 2008, Bouybayoune et al., 2015, Hill et al., 2006) or to transit into the secretory pathway (Dossena et al., 2008, Bouybayoune et al., 2015, Petersen et al., 1996, Drisaldi et al., 2003) when expressed in *Drosophila*.

Prior to this research project, the spontaneous and transmissible toxicity developed in CJD and FFI-associated mouse 3F4 and hamster PrP transgenic flies were investigated (Thackray et al., 2017). The mouse 3F4 and hamster PrP transgenic flies were subjected to phenotypic assay to monitor the climbing ability dependent on their PrP genotype. The climbing ability locomotor assay performed by Dr. Alana Thackray (Thackray et al., 2017) has shown a declined locomotor ability of both mouse 3F4 and hamster FFI and CJD-associated PrP transgenic flies in comparison to the negative control 51D flies and the wild type PrP expressing flies in the majority of cases. In some cases, there was not a significant difference between the climbing ability of the wild type and FFI genotype as can be seen in (Thackray et al., 2017). The data suggest that mouse 3F4 and hamster PrP transgenic flies that carry mutations linked to spontaneous development of human prion disease are able to develop a neurotoxic phenotype. Moreover, the fly-to-fly transmission of the neurotoxic phenotype was shown to be possible using fly head homogenates prepared from the same fly genotypes that were orally transmitted to the wild type mouse 3F4 or hamster PrP transgenic flies. In the case of CJD-associated PrP transgenic fly homogenates, the significantly reduced climbing ability took place upon the oral exposure to this inoculum. The same situation took place in mouse 3F4 FFI inoculum but not in

the hamster FFI inoculum, where there was no significant difference observed. The transmission studies helped to clarify that the FFI and CJD-associated PrP transgenic flies were not just able to spontaneously generate toxicity but also generate toxicity transmissible from individual to individual that accumulated with time (Thackray et al., 2017).

Based on this knowledge, the dual PrP flies were constructed to enable monitoring of cell-to-cell spread of misfolded prions in PrP transgenic *Drosophila.* The first experiment assessed 57C10-GAL4 expression when compared to the standard elav-GAL4 PrP expression (**Figure 66**). The protein levels detected in the case of 57C10-GAL4 were approximately 23% higher than elav-GAL4. This fact improves the chance of success of dual PrP flies as there is more PrP substrate present in the fly brain, and therefore a better chance to be able to detect prion-associated misfolding in the dual PrP transgenic flies **(Table 12).**

After simultaneous pan-neuronal expression of VRQ(GPI) and targeted expression of VRQ(ΔGPI) in the eye, the PK-digest was performed to compare murine and hamster FFI and CJD PrP results (**Figures 64 and 65**) with the (GSS-orthologue) secreted ovine PrP in **Figure 67**. The band pattern clearly shows the dual expression of VRQ(GPI) at 29 kDa and VRQ(ΔGPI) PrP at 26 kDa. After PK-digest, there seemed to be no PK-resistance present in this model (**Figure 67**). In GSS, the unglycosylated PK-resistant fragment is typically found at 7 to 14 kDa, depending on the GSS-associated mutation the organism carries (Yang et al., 2009, Piccardo et al., 2001). In the dual VRQ(GPI) and VRQ(ΔGPI) fly, there was no PK-resistant fragment present and therefore not even a mild PK-resistance was detected in this case, corresponding to the data from VRQ(ΔGPI) subjected to PMCA that did not show any PK-resistance (Thackray et al., 2014a).

In order to detect minute amounts of misfolded PrP that were predicted to arise in the dual PrP fly model upon the contact of VRQ(ΔGPI) with ubiquitous VRQ(GPI), the PMCA was employed. The negative result of VRQ(ΔGPI) was expected to be avoided in this case as the material detected is misfolded VRQ(GPI) and not the original VRQ(ΔGPI). Unfortunately, the assay failed to detect any misfolded proteins in my samples (**Table 13**). The positive control of scrapie prion-exposed VRQ(GPI) flies aged 30 days did not give a positive result either. This might be caused by either a mistake in the sample preparation, sample transport or storage conditions or the mistake in the PMCA protocol, as the same flies were already confirmed positive by PMCA in the past (Thackray et al., 2014a). The hypothetical reason for the negative PMCA results of the test

samples include the fact that the process of misfolding is template-directed and the VRQ(GPI) substrate acquires the VRQ(ΔGPI) conformational form; the PK-sensitivity is then present again in the newly formed misfolded PrP. The prion strain theory is not clear on this topic as sometimes the substrate actually influences the conformation and therefore the strain properties are not necessarily identical to the prion seed used (Morales, 2017). In the case investigated here, the PK-sensitivity might have been passed from VRQ(ΔGPI) prion seed to VRQ(GPI) substrate. Even though the VRQ(ΔGPI) is an agent capable of spontaneous misfolding and infectivity spreading from fly-to-fly, it would be unable to generate PK-resistance in misfolded VRQ(GPI) and therefore it would fail to be identified using PMCA. However, since the control samples yielded negative results as well, this explanation is not valid on this occasion.

An alternative method of misfolded protein detection was employed to avoid the PK-sensitivity influence on the result. The real-time quaking-induced conversion (RT-QuIC) method used here is based on continuous measurement of fluorescence triggered by Thioflavin T incorporation into misfolded PrP aggregates (Atarashi et al., 2011a). The samples used included the positive control of 30 days old scrapie prion-exposed VRQ(GPI) flies that were found to be positive in PMCA (Thackray et al., 2014a). The positive control was used for assay optimisation but unfortunately, the results were negative in all three attempts made. All the test samples were subjected to RT-QuIC but there was no sample that would be positive for prion aggregation in the standard time or throughout the repeats (**Table 14**). Some samples yielded positive results after a long reaction time (more than 65 hours in contrast to the ordinary assay time of 6.5 hours). None of these would be expected to exhibit prion-associated misfolding as they were either 51D negative controls or flies of an age of 5 days (**Table 15**). There are multiple reasons that can explain the failure to detect misfolded proteins in this case. The most obvious one is the use of standard protocol at NCJDRSU, Edinburgh, where the recombinant hamster PrP is used as a substrate for misfolding. Since the samples subjected to RT-QuIC are ovine PrP transgenic, the incompatibility of these molecules could be the reason for the negative result. The RT-QuIC assay was not previously optimised for scrapie infected sheep samples at NCJDRSU, as they focus on human prion diseases and that can be another pitfall. Of course, the sample preparation and transport might be the reason as well.

Both *in vitro* assays yielded negative results despite the fact that both VRQ(GPI) and VRQ(ΔGPI) are simultaneously expressed in the fly model as proven by the western blots. If the failure of both assays is caused by the dual PrP transgenic *Drosophila* model itself, the cell-to-cell spread of

misfolded prions is not taking place and neither are the protein aggregates formed. To test this assumption, the *Drosophila* longevity assay was performed to observe the impact of prion-induced neurodegeneration on lifespan of dual PrP transgenic *Drosophila*.

The same genotypes of flies that have been used for RT-QuIC were tested in a survival assay. Previous phenotypic studies, for example negative geotaxis climbing assay, have been used to show the effect of accumulation of disease-associated PrP in the fly (Thackray *et al.,* 2012b, Thackray *et al.,* 2012a, Thackray *et al.,* 2014b, Thackray *et al.,* 2014a, Thackray *et al.,* 2016, Thackray *et al.,* 2017). A prion-based survival assay is built upon the fact that PrP^{Sc} accumulation in prion-infected PrP^{C} positive hosts triggers neurodegeneration, neuronal loss and leads to premature death of the individual (Soto and Satani, 2011). Accordingly, it was hypothesised that dual PrP transgenic *Drosophila* would show a shortened lifespan as a consequence of template-directed prion misfolding of wild type PrP induced by ΔGPI PrP.

A significant decline in *Drosophila* survival was observed in dual ΔGPI/wild type PrP transgenic *Drosophila*, in contrast to control dual wild type PrP flies (**Figure 68**). This was seen in *Drosophila* with expression of ΔGPI PrP in glial cells or in interneurons, with wild type PrP co-expressed pan-neuronally in both cases. A more severe effect was seen in dual PrP *Drosophila* where ΔGPI PrP was expressed in glial cells compared to flies with this form of mutant PrP expressed in interneurons. This may be because glial cells are distributed throughout the fly brain and interneurons are limited cellular subset, providing a greater initial source of disease-associated PrP in the former case. The pan-neuronal expression of wild type PrP and simultaneous expression of ΔGPI PrP in the fly eye did not seem to affect fly survival. The apparent lack of effect upon fly survival in this case may reflect a difference in the ability of ΔGPI PrP to spread to CNS neurons from fly eye cells compared to glia or interneurons. Alternatively, the misfolding of ΔGPI PrP in the fly eye may be different compared to glia or interneurons, rendering this prion protein conformer less toxic. A third alternative is that the kinetics of spread of ΔGPI PrP from the fly eye differs from that of glia or interneurons and that a longer time is required in order to see any phenotypic effect.

As expected, ΔGPI PrP expressed alone from either glial cells or interneurons in *Drosophila* affected survival of the fly (**Figure 69**). When ΔGPI PrP was expressed in interneurons alone, the magnitude of the accelerated decline was greater than that compared to expression solely in glial cells. These observations suggest that the particular subset of interneurons used in these dual PrP

experiments play a prominent role in *Drosophila* survival and that expression of ΔGPI PrP and wild type PrP in these cells compromises their normal function. When ΔGPI PrP was expressed in glial cells with co-expression of wild type PrP pan-neuronally, an accelerated loss of survival was seen compared to flies with anchorless PrP expressed in glial cells alone. It is assumed that ΔGPI PrP secreted from glial cells initiates wild type PrP misfolding pan-neuronally resulting in the accelerated decline in survival. The assumption is that the interaction of wild type PrP expressed in neurons and misfolded PrP expressed in glial cells initiates misfolding of the prion protein in neurons and therefore causes a greater decline in survival ability. An alternative situation may exist in the case of interneuronal expression of ΔGPI and dual PrP expression pan-neuronally (which includes the interneuronal subset) with wild type PrP. In this case, wild type PrP may cause a neuroprotective effect within the interneurons, which needs to be overwhelmed by accumulation of misfolded PrP. In this scenario, the neuroprotective effect of PrP within interneurons would have to be different from other neurons, since this effect is not seen in dual PrP flies with ΔGPI PrP expressed from glial cells and wild type PrP expressed pan-neuronally. Despite the difficulties in explaining all of the data, this novel PrP transgenic *Drosophila* study does appear to show evidence of cell-to-cell spread of misfolded disease-associated PrP. This preliminary experiment provides encouragement for future work with this interesting *Drosophila* model.

The research into the cell-to-cell transmission of spontaneously generated prions can be a useful tool for understanding molecular mechanisms underlying this process. Under experimental conditions, when the aggregated protein inoculum is administered *in vivo*, the pathology is induced not just around the inoculation site but also spreads into synaptically connected brain regions that might be quite spatially distant (Guo and Lee, 2014, Luk et al., 2012, Masuda-Suzukake et al., 2013). The knowledge gained from this model might be advantageous for identifying the mechanism of prion disease transfer between different brain cell types, from periphery to CNS, from one individual to another individual or species to species. If the cell-to-cell spread proves to be possible in this or similar models, the gene silencing can be used as a rapid tool to identify genes involved in this process. The findings would help to identify the relationship between intercellular spread of misfolded proteins and the pathogenesis of neurodegenerative diseases in general (Guo and Lee, 2014). Since the dual hamster wild type and CJD PrP transgenic fly was constructed towards the end of this project, there was not an opportunity to test this system in a similar experiment. The experiment will be carried out in

future as this combination might acquire PK-resistance necessary for PMCA testing and therefore enable an easy detection of levels of misfolded PrP. The use of hamster WT and CJD-associated PrP in one fly system might result in a more severe phenotype, as the PrP expression levels are higher in hamster PrP transgenic flies than in ovine PrP transgenic flies used for the dual PrP expression experiment in this project.

6 Final discussion

The World Health Organisation classifies neurodegenerative diseases, including those caused by protein misfolding, as one of the greatest present day problems for public health (Aarli et al., 2006, WHO, 2017). It is important to understand the aetiology of these diseases in order to be able to develop targeted treatment to alleviate the suffering they cause. To study neurodegenerative disease in detail, it is necessary to utilise animal models of these conditions in order to identify cellular and biochemical pathways responsible for their pathogenesis (McGurk et al., 2015). For this reason, various experimental animal systems have been used extensively to study neurodegenerative diseases. The invertebrate *Drosophila melanogaster* is one of the animal models increasingly used for this in mammalian protein misfolding neurodegeneration research as it is a genetically well-characterised species that lends itself to the dissection of the processes involved or impaired in such conditions (Hirth, 2010). The relative ease of transgenesis in the fly has enabled insertion of practically any gene of interest into the *Drosophila* genome and its expression in a spatially restricted manner (Brand and Perrimon, 1993). This has allowed the creation of *Drosophila* fly lines with mutated endogenous genes or exogenous genes that are associated with different mammalian neurodegenerative disease conditions. The short lifespan of the fly, as well as the large number of progeny that can be generated, enable large-scale screens of pathological processes.

Early studies on the genetics of neurodegeneration were carried out in *Drosophila* through phenotypic studies initiated by deletion of orthologous genes in the fly that are associated with neurodegeneration in humans, and which could be successfully compensated by transgenesis with their human counterpart (Luo et al., 1992). Subsequently, flies that exhibited progressive neurodegeneration in the CNS were identified during *Drosophila* mutagenesis experiments (Min and Benzer, 1999). These flies were found to have a reduced life span that was accompanied by pathology in distinct regions of the brain. The fact that neurodegeneration can be triggered in this invertebrate host reinforces the notion that mechanisms involved in CNS integrity are highly conserved between *Drosophila* and mammalian species (Akassoglou et al., 2004, Lu and Vogel, 2009). *Drosophila* models have been developed for multiple protein misfolding neurodegenerative diseases such as Huntington's disease (Tsuda et al., 2005, Bilen et al., 2006, Raj and Sarkar, 2017), Parkinson's disease (Scherzer et al., 2003, Auluck et al., 2002, Kontopoulos et al., 2006, Mohite et al., 2018), Alzheimer's disease (Tsuda and Lim, 2018, Fulga et al., 2007,

Martín-Peña et al., 2018) or prion disease, such as Creutzfeldt-Jakob disease (Thackray et al., 2017), Gerstmann–Sträussler–Scheinker syndrome (Choi et al., 2010, Gavin et al., 2006, Murali et al., 2014), fatal familial insomnia (Thackray et al., 2017) and scrapie (Thackray et al., 2012b, Thackray et al., 2012a, Thackray et al., 2014a, Thackray et al., 2018a).

Prion diseases are distinct from other protein misfolding neurodegenerative conditions since they are transmissible between individuals of the same or different species. Moreover, infectious prions are strikingly different when compared to conventional pathogens, such as bacteria or viruses, since they lack a nucleic acid-based genome. The infectious agent associated with the transmissible form of prion diseases PrP^{Sc}, is considered to be an abnormal conformer of the ubiquitously expressed normal conformer of this protein PrP^{C} (Prusiner, 1982). Typical molecular biology techniques, such as PCR or DNA-based hybridization, are not able to detect the prions since the infectious agent lacks nucleic acid. As a consequence, the only reliable method to detect prion infectivity relies on bioassay performed in a suitable experimental animal (Thackray et al., 2018b). The transmissibility of infectious prions is one of the main hallmarks of *bona fide* prion diseases, although some of these conditions are difficult to transmit to an experimental host. Rodent animal models have been extensively used for prion bioassays, since large animals exhibit long incubation times for the onset of clinical signs of prion disease (Chandler and Turfrey, 1972). In addition to mice, hamsters and bank-voles are also used to measure prion infectivity in many instances (Brandner and Jaunmuktane, 2017). However, even in rodents, the onset of clinical signs of terminal prion disease can take months or even years to appear following inoculation with test material. This invariably leads to slow progress with mammalian prion bioassays and has led to increasing ethical debate about the use of vertebrate animal models to study prion diseases.

Thus, use of a less sentient host such as *Drosophila* would be a welcome addition to the range of animal hosts used to assess mammalian prion infectivity. In this context, it has recently been shown that scrapie-exposed ovine PrP transgenic *Drosophila* can rapidly replicate *bona fide* mammalian prions that are transmissible to a mammalian host (Thackray et al., 2018a). This confirms the use of *Drosophila* as a valid animal model of mammalian prion disease and shows that this invertebrate host contains all the co-factors necessary for authentic mammalian prion replication. In this thesis, existing ovine PrP transgenic *Drosophila* have been investigated in an attempt to address the mechanism of prion-induced neurotoxicity. In addition, various new PrP transgenic *Drosophila* have been characterised that allow an expansion in the range of diversity

of these novel invertebrates for prion disease analysis. Collectively, these studies have contributed to the establishment of *Drosophila* to model mammalian prion disease and provide new avenues for prion disease research.

One of the goals of this thesis was to attempt to dissect prion-induced changes at the neuronal level in PrP transgenic *Drosophila*. Previous studies have shown that PrP^{Sc} accumulates in the brain of prion-exposed PrP transgenic *Drosophila* and that this is accompanied by a prion-induced phenotype in the fly (Thackray et al., 2012a, Thackray et al., 2014a, Thackray et al., 2016, Thackray et al., 2018a). The presence and extent of neuronal damage in this invertebrate prion model remains to be established. Therefore, synapse damage was modelled at the neuromuscular junction (NMJ) of PrP transgenic *Drosophila* larvae as a candidate method to investigate neurodegeneration in the fly. This approach has already been successfully employed in *Drosophila* model of Alzheimer's disease (Mhatre et al., 2014) and Parkinson's disease (West et al., 2015).

To detect and quantify the early neuronal changes in prion-exposed PrP transgenic *Drosophila*, confocal microscopy analysis of NMJs in *Drosophila* larvae was employed. The observations from these experiments showed numerous early-onset changes to the overall and detailed morphology of NMJ architecture. These changes to the NMJ structures were not only influenced by prion-inoculation but were also dependent upon the topography of PrP expression in the fly. Specifically, *Drosophila* transgenic for cytosolic PrP showed the highest level of observable prion-induced neuropathological changes. This may imply the rapid onset of neurodegeneration associated with this PrP form and its possible involvement in the process of prion-induced neurotoxicity as suggested by other studies (Li et al., 2011, Ma et al., 2002, Mironov et al., 2003, Thackray et al., 2014b). The NMJ analysis in this thesis was performed on exogenously prion-inoculated ovine PrP transgenic flies. The early changes seen in prion-exposed *Drosophila* might be better observable in flies that model genetic forms of prion disease, since the mutant form of PrP is expressed from the start of their development and can be made to do so pan-neuronally, thereby enhancing prion-induced toxicity. PrP expression is fully established in the *Drosophila* 2^{nd} instar larval stage as shown in **Figure 59**, therefore, the NMJ analysis of genetic prion disease, such as CJD or FFI modelled in *Drosophila* larvae might be the next step to take in order to observe and quantify the synaptic changes taking place during prion disease.

Studies carried out in this thesis have contributed to the development of a genetic model of prion disease in the fly. Using site-directed mutagenesis, PrP transgenes that harbour a single codon mutation associated with genetic CJD and FFI human prion disease were successfully inserted into the fly genome and expressed pan-neuronally (Thackray et al., 2017). In the natural host, CJD and FFI-associated mutations cause spontaneous PrP misfolding with resultant prion disease without exposure to exogenous prions. The *Drosophila* models of genetic prion disease provide novel systems to correlate prion-induced changes with those seen in acquired models of prion disease in the fly.

The proof-of-principle for the use of mutant PrP transgenic *Drosophila* was provided by phenotypic and biochemical analysis of CJD and FFI flies (Thackray et al., 2017). Spontaneous prion-induced neurodegeneration in CJD- and FFI-associated PrP transgenic *Drosophila* was detected by a progressive decline in locomotor ability that manifested in both fly lines. Importantly, this toxic phenotype was found to be transferrable to recipient *Drosophila* that expressed wild type PrP (Thackray et al., 2017). The FFI and CJD-associated transmissible neurotoxicity resembled that observed in the case of exogenous scrapie-inoculation of ovine PrP transgenic flies (Thackray et al., 2012b, Thackray et al., 2012a, Thackray et al., 2014b, Thackray et al., 2014a, Thackray et al., 2016, Thackray et al., 2018a). Additionally, CJD and FFI PrP transgenic *Drosophila* showed the presence of a mildly PK-resistant form of PrP (as seen in **Figures 64 and 65**). Mildly PK-resistant PrP was observed in genetic prion disease modelled in the mouse P101L PrP transgenic flies (Choi et al., 2010, Gavin et al., 2006). These data suggest that the spontaneous formation of pathological PrP associated with mammalian prion disease can be generated in mutant PrP transgenic *Drosophila*.

In murine models of genetic prion disease, contradictory results have been obtained with respect to the spontaneous generation of transmissible prions. The murine models of FFI, CJD and GSS established by Choi and colleagues using random transgene integration showed neurological illness and misfolded prion protein without transmission of prion disease (Choi et al., 2010). However, other transgenic mice generated by a knock-in approach that harbour PrP transgenes associated with CJD and FFI prion disease in humans were able to replicate both neurological illness and prion transmissibility (Jackson et al., 2013). The difference in transgene integration may be the reason for divergence between these different mouse disease models.

To take the *Drosophila* model one step further, the ultimate goal of this thesis was to create a PrP-transgenic fly, where it was possible to observe cell-to-cell transmission of prions in the brain of *Drosophila* CNS and identify cell populations and genes involved in this process. In acquired and sporadic prion disease, pathology spreads through the CNS by template-directed misfolding of PrP^{C} upon contact with PrP^{Sc} (Aguzzi et al., 2008). The process by which this occurs is not clear and the mechanisms involved in such transcellular spread need to be fully elucidated. One way to model this situation in *Drosophila* is to trigger simultaneous expression of PrP^{C} and PrP^{Sc} in the same fly, where PrP^{C} is expressed panneuronally throughout the CNS and PrP^{Sc} is generated and released from a smaller subpopulation of cells or neurons. This would be expected to allow disease-associated PrP to migrate from a site of origin to the other cells that initially only contain PrP^{C}.

A similar experiment was performed in a fly model of Hungtington's disease, where dual transgenic *Drosophila* were used to investigate a role of phagocytic glia in the uptake and clearance of glutamine-rich aggregates formed by a pathogenic fragment of huntingtin protein (Pearce et al., 2015). In this fly model, the mutated huntingtin was expressed in a single class of olfactory neurons in antennae while the wild type huntingtin was expressed in glial cells. Use of this dual expression model enabled identification of a role of the *Draper* signalling pathway in conversion and phagocytic glia neuroprotection in neurodegenerative disease (Pearce et al., 2015). A similar approach was taken in Alzheimer's disease where *Drosophila* transgenic for two forms of amyloid-beta (Aβ) that are co-expressed in different neuronal clusters were employed to observe the accelerated formation and propagation of amyloid pathology throughout the fly brain (Sowade and Jahn, 2017). In this recent study, it was discovered that small amounts of disease-related and fast-aggregating Aβ species were able to induce the deposition of an abundant and normally soluble Aβ variant and therefore initiate Aβ-induced pathology. Moreover, fly survival was reduced as a result of the neurotoxicity that arises in this model (Sowade and Jahn, 2017). Both of these dual transgenic fly models can be considered a proof-of-concept of modelling the spread of misfolded protein-induced neurotoxicity *in vivo* in an intact *Drosophila* CNS.

The use of *Drosophila* that model genetic prion disease, such as CJD or FFI, would seem to be an ideal system to study the transcellular spread of prions because of the ability to target mutated and wild type PrP expression to defined cell populations. However, the generation of such dual PrP expressing fly lines was not completed in time for use in experiments within this thesis. In an

attempt to study transcellular spread of prions in PrP transgenic *Drosophila*, experiments in this thesis utilised flies that were transgenic for the secreted form of ovine PrP that lacks a GPI-anchor [PrP(ΔGPI)] expressed either in *Drosophila* glial cells, sensory neurons of chordotonal organs or fly eyes. Anchorless PrP has already been described as being able to trigger spontaneous neurotoxicity in ovine PrP(ΔGPI) transgenic *Drosophila* (Thackray et al., 2014a). Moreover, the neurotoxic phenotype was transmissible to *Drosophila* that were transgenic for wild type ovine PrP. This model can be considered analogous to human GSS, which is associated in some cases with mutations, such as Q227X or Y226X, that lead to an absence of the PrP GPI-anchor (Jansen et al., 2010). It was hypothesised that accumulation of disease-associated PrP, in the form of anchorless PrP, would lead to a release of the material from its original site to the other cellular compartment. This was expected to lead to a conversion of wild type PrP into disease-associated PrP, as occurs upon *in vivo* transmission of ΔGPI PrP fly head material (Thackray et al., 2014a).

In order to detect disease-associated PrP potentially present in dual PrP transgenic flies, *in vitro* amplification techniques were used to analyse the material. The method of choice for amplification of misfolded PrP was protein misfolding cyclic amplification (PMCA). In PMCA reactions, a PrP^{C}-containing substrate is combined with a seed of PrP^{Sc}, following repeated cycles of incubation and sonication, the amount of PrP^{Sc} increases to levels where it can be detected by biochemical methods, typically as PK-resistant PrP^{Sc} on a western blot. As shown by data in **Table 13**, PMCA did not detect any disease-associated PrP in head homogenate from ΔGPI/wild type dual PrP *Drosophila*. One possibility for these negative results was that disease-associated PrP was amplified by the PMCA reaction but the material was not sufficiently PK-resistant to be detected because of the relatively high level of Proteinase K used in the protocol. This may be the case as shown by the results in **Figure 67** that show both membrane bound ovine VRQ PrP and secreted ovine VRQ PrP in the dual transgenic fly were PK-sensitive. Other possible explanations for why the PMCA assay yielded negative results for these particular samples was that the assay was not optimised for disease-associated secreted PrP or there was a mistake in sample preparation or sample transport conditions. Neither of these explanations can be successfully ruled out at this point. However, the PMCA data obtained in this thesis correlate with the lack of PMCA reactivity for head homogenates prepared from ΔGPI PrP flies directly (Thackray, A.M., unpublished observations).

To circumvent the PMCA, another *in vitro* amplification method termed RT-QuIC was employed. The readout for RT-QuIC readout does not depend on PK-resistance but rather Thioflavin-T incorporation into PrP aggregates (Atarashi et al., 2011a). It was decided that this method could be a suitable alternative to assess potentially PK-sensitive disease-associated PrP samples. Dual PrP transgenic flies that expressed wild type and ΔGPI simultaneously in different cellular subsets were subjected to RT-QuIC and the results can be found in **Table 14.** None of the fly lines analysed were identified as positive in RT-QuIC, apart from the apparently false positive samples that can be seen in **Table 15**. However, the positive control of wild type ovine PrP transgenic flies exposed to scrapie material that were previously confirmed positive by PMCA did not exhibit any aggregation during RT-QuIC assay either. The negative results here can be explained by multiple theories. In RT-QuIC, hamster recombinant PrP was used as a substrate, which might not be a compatible substrate for the ovine PrP seed. Another reason might be that the RT-QuIC protocol was not optimised for *Drosophila* samples and therefore failed to react in this case. In addition, it cannot be excluded that a mistake in sample preparation or sample transport conditions occurred.

Due to the lack of biochemical detection of disease-associated PrP *in vitro*, the ΔGPI/wild type dual PrP flies were assessed by an *in vivo* survival assay. The survival assay performed in this thesis (**Figures 68 and 69)** showed an accelerated decline in survival of *Drosophila* that expressed a combination of mutant PrP in glial or interneuronal cells together with pan neuronal expression of wild type PrP. *Drosophila* with mutant PrP expression in the eye and simultaneous expression of wild type PrP in neurons failed to show any significant accelerated decline in the survival. This may suggest that differences in PrP misfolding may occur dependent upon topological expression of the mutant prion protein used here, or that there are differences in the mechanism of cell-to-cell spread of misfolded PrP between different cell types. While the small sample size of flies used in this particular experiment may have had some influence upon its outcome, the preliminary data obtained do provide encouraging support for further studies in this important area of prion biology. Future experiments should be aimed at repeating this study with an increase in both the sample size and time of the survival assay.

It is expected that with refinement, detection of disease-associated PrP and its spreading in dual PrP transgenic *Drosophila* will become possible. This will validate the use of dual PrP transgenic flies for a more extensive and detailed search for genetic modifiers of prion-induced neurodegeneration through omic approaches including pathway-targeting analyses. The use of

PrP transgenic *Drosophila* as an animal model has certain advantages for this type of study: its ease of transgenesis, simple genetics and assays available for dissection of pathological mechanisms involved. Fly models of neurodegenerative disorders have already been used to help to identify genetic suppressors of neurodegeneration (Fernandez-Funez et al., 2000).

The candidate of choice for a transcriptomic analysis is RNA-sequencing. This approach can be used to compare differential gene expression between exogenously prion-infected or spontaneously prion-positive and control flies. A comparison of gene expression between these experimental groups will identify upregulated or downregulated candidate genes responsible for, or triggered by, neurodegeneration (Khalifé et al., 2011). Using bioinformatics analysis tools, the identified genes can be assembled *in silico* into pathways relevant to the disease process. Components of the pathways identified can then be used as candidates for gene silencing or as pharmaceutical targets (Benetti et al., 2012). These downstream experiments are important to confirm that the genes identified by RNA-sequencing play the role in the pathological processes. With a wide range of PrP transgenic flies of different species origin with distinct topological transgene expression, and differential disease aetiology, such as acquired, genetic or sporadic, the RNA-sequencing techniques can be used to uncover features of prion-induced neurodegeneration.

It will be important to validate changes in gene expression by the addition of proteomic analysis that would investigate protein expression profiles in order to help elucidate prion-induced neurodegeneration in PrP transgenic *Drosophila*. Typically, mass spectrometry is a method of choice for proteomic analysis (Moore et al., 2014). Genes identified by transcriptomic and proteomic analyses should always be confirmed by reverse transcription PCR (RT-PCR) to verify the up- or downregulation of a candidate gene in comparison to the control PrP transgenic fly. Comparison of transcriptomics and proteomics analysis can provide important answers on the topic of genes that are not translated into proteins and therefore are not expressed (Edfors et al., 2016). Important intervention checkpoints in biochemical pathways can be identified using this comparison as the prion disease-associated pathology can be the reason for the suppressed gene expression (Ghazalpour et al., 2011).

Previous transcriptomic studies carried out in mice have suggested disruption of synaptic transmission, calcium homeostasis, lipid metabolism, metal-binding protein folding and protein degradation (Jang et al., 2010, Hwang et al., 2009, Sorensen et al., 2008, Xiang et al., 2004, Booth

et al., 2004, Skinner et al., 2006, Moore et al., 2014). When genomic and proteomic analyses were combined using genetic CJD diseased human brain tissue, similar disruptions were discovered but were also complemented with mitochondrial and glucose metabolism imbalances (Xiang et al., 2004, Gawinecka et al., 2010, Gawinecka et al., 2013, Gawinecka et al., 2012, Moore et al., 2014). Specific proteins that have been found to be upregulated in prion diseases, such as vimentin or α-2-macroglobulin, also appear to be upregulated in Alzheimer's and Parkinson's disease (Moore et al., 2014, Levin et al., 2009, Van Gool et al., 1993). This suggests that the general response may be similar in different protein misfolding diseases. This further suggests that identified chemical interventions may affect more than one form of protein misfolding neurodegenerative disease.

Strategies aimed at the development of genetic or chemical interventions that may halt or retard prion disease can readily be performed in *Drosophila.* This animal species lends itself to gene silencing or pharmaceutical treatment. *Drosophila* is an ideal animal species to perform silencing of a gene of interest due to the existence of available RNA interference (RNAi) fly lines that can be readily used for this purpose. The Bloomington *Drosophila* Stock Centrum is an established source of experimental *Drosophila* that comprises fly collections capable of genome-wide silencing. The RNAi silencing relies on the binding of a small RNA molecule homologous to a sequence within a target gene mRNA (Kavi et al., 2005). The creation of this dsRNA molecule triggers destruction of target gene mRNA by an RNA-induced silencing complex (RISC), specifically Dicer ribonuclease enzyme, and therefore silencing of the targeted gene. The first successful use of this method for gene silencing was performed in a *Caenorhabditis elegans* model and the development of this method was awarded with the Nobel Prize (Fire et al., 1998). Unfortunately, the same method cannot be applied to mammalian cells as the dsRNA cleavage does not take place. However, there are adjustments to this method, such as inclusion of short interfering RNA (siRNA) that can induce sequence-specific silencing in a similar manner in mammalian cells (Elbashir et al., 2001).

The effect of RNAi-targeted gene silencing in the fly could be investigated for its effect upon prion-induced phenotypic behaviour (e.g. the climbing ability assay or survival assay) and disease-associated PrP accumulation. The rescue or improvement of a prion-induced phenotype would imply that the targeted gene is involved in prion-induced pathology and could be used as a possible target for disease intervention. Of course, since *Drosophila* is an invertebrate host, any identified targets would have to be confirmed in a mammalian model before drawing any further

conclusions. To date, no study using RNAi fly lines to silence genes involved in prion-induced neurodegeneration have been carried out. The use of RNAi gene silencing is a logical step to be taken using the diverse set of PrP transgenic *Drosophila* described in this thesis. Such studies may be expected to result in significant advancements of PrP transgenic *Drosophila* research and prion research in general. Previous attempts to perform similar analyses in mice were able to identify candidate genes involved in prion-induced neurodegeneration but these still have to be verified (Nuvolone et al., 2017, White et al., 2008). Gene silencing in mice is a lengthy process and the ease of use of PrP transgenic *Drosophila* can result in the identification of new candidates for prion disease therapy more rapidly.

After target identification, potential drug therapies can be tested in the PrP transgenic *Drosophila* model. Several therapeutic compounds that were approved for human therapy were tested on *Drosophila* and the results were encouraging as the molecular mechanisms in mammals and *Drosophila* are similar or even identical (Fernández-Hernández et al., 2016). Even though PrP is not a native *Drosophila* protein, the validity of compounds tested in PrP transgenic *Drosophila* is underpinned by fly and human genome homology of 60% amongst human disease-related genes (Rubin et al., 2000). In comparison to *in vitro* cell culture drug screening, the *in vivo* screening in *Drosophila* is more complex and can allow for the implementation of more sophisticated screening methods (Fernández-Hernández et al., 2016). Less complex *in vitro* screens often render results that are not validated when tested *in vivo*, therefore, use of *Drosophila* can increase the probability of success and contribute to the cost-effectiveness of the process. In contrast to mammalian models, drug administration in *Drosophila* is carried out typically by the oral route. The drug is usually mixed into fly food and the administration starts as early as the *Drosophila* larval stage. Drug administration can be continued throughout the adult life of a *Drosophila* to mimic the situation of mammalian hosts.

Fly-based drug screening was successfully used for the discovery of epithelial malignant growth or intestinal tumour treatment (Markstein et al., 2014, Willoughby et al., 2013). Drug optimisation studies in *Drosophila* have helped to improve the efficiency of the selected compounds and reduce their side effects (Dar et al., 2012, Fernández-Hernández et al., 2016). In neurodegeneration research, the Huntington's disease fly model was used to test an effect of histone deacetylase inhibitors (Steffan et al., 2004, Rincon-Limas et al., 2010). A *Drosophila* model of tauopathy was used for the screening of mTOR inhibitors and autophagy inducer pharmaceuticals (Berger et al., 2006). NAD+ precursor nicotinamide riboside was found to

alleviate neuronal loss in the Parkinson's disease fly model (Schöndorf et al., 2018) and feeding low-dose morphine was able to rescue motor function and prolong *Drosophila* lifespan in this disease model (Wang et al., 2018).

An ideal for anti-neurodegeneration drug treatment would be the discovery of a compound that is non-toxic and effective against different neurodegenerative diseases. Accordingly, there is a significant interest in compounds that naturally occur in foods or the environment and may have a positive effect on slowing down disease pathology in a relatively safe manner. These natural products are usually antioxidants that can be isolated from a number of aromatic plants or spices (Beg et al., 2018, Abolaji et al., 2018, Ma et al., 2017). In a *Drosophila* model of Alzheimer's disease, the effect of the antioxidant kaempferol, or extracts of gardenia, were tested and discovered to be potential therapeutic agents for this neurodegenerative disease (Beg et al., 2018, Ma et al., 2017). Similarly, a Parkinson's disease (PD) *Drosophila* model was employed in drug effect studies where cabergoline alginate nanocomposite, asiatic acid, genistein or resveratrol were identified and verified as efficient drug candidates for this condition (Abolaji et al., 2018, Khanam et al., 2018, Ding et al., 2018, Siddique et al., 2018).

In prion research, *Drosophila* drug screening is still in its infancy, however, a CJD fly model was used to test for drugs that induce Hsp70 and suppress neurotoxicity (Zhang et al., 2014). The candidate drugs used for this purpose were the Hsp90 inhibitor, geldanamycin derivative alvespimycin (17-DMAG) and glucocorticoid dexamethasone. Surprisingly, treatment with both compounds separately did not result in a change of pathological phenotype while combined treatment with both drugs resulted in a 50% decrease of total expression levels of PrP and therefore lower levels of neurotoxicity and partially rescued *Drosophila* locomotor ability. However, these compounds were found to have numerous downsides, such as high toxicity and low solubility (Zhang et al., 2014). These pharmacological features render their use problematic in human medicine. Two other anti-prion compounds 6-aminophenanthridine (6AP), an inhibitor of the protein folding activity of the ribosome (Pang et al., 2013), and guanabenz acetate (GA), an antihypertensive drug with anti-prion activity (Tribouillard-Tanvier et al., 2008), were shown to alleviate phenotypes in the oculopharyngeal muscular dystrophy *Drosophila* model (Barbezier et al., 2011).

Currently, there are very few compounds clinically available for human prion disease management (Zhang et al., 2014). Therapies are based on passive immunisation by antibodies

specific for the N-terminal unstructured domain of PrP, as C-terminal specific antibodies have been deemed toxic (Sonati et al., 2013, Herrmann et al., 2015). The problem with antibody-based therapy is achievement of a high concentration of the anti-PrP antibodies in the brain (Zhang et al., 2014).

Recently, the possibility of neurodegeneration treatment by repurposed drugs has been investigated in mice (Halliday et al., 2017). Two candidate drugs already approved for human use were identified by phenotypic screens to be able to alter PERK/eIF2α-P signalling. This signal transduction pathway maintains protein synthesis and it has been shown that its overactivation leads to decreased protein synthesis that causes neuronal loss in neurodegenerative disorders (Radford et al., 2015, Moreno et al., 2012). Both candidate drugs, trazodone hydrochloride and dibenzoylmethane, were able to reverse the reduction of protein synthesis *in vitro* and *in vivo* as shown in mice models of Alzheimer's disaese and prion disease (Halliday et al., 2017). Alprenolol hydrochloride, a β-adrenergic blocker used in hypertension management, has been identified as another candidate anti-prion compound from the collection of existing approved drugs (Miyazaki et al., 2018). These candidate anti-prion compounds could easily be tested *in vivo* using PrP transgenic *Drosophila*.

The PrP transgenic *Drosophila* developed and investigated in this thesis may serve many purposes in drug-based anti-prion research. With advances in engineering and robotics, fly maintenance and monitoring has the potential to be fully automated allowing an increase of their standard medium-throughput screening to high-throughput. Monitoring the flies for their phenotype automatically, using camera systems coupled with automatic image analysis would enable wide screens of multiple diseases, fly genetic backgrounds or prion strains and their direct comparison at the same time.

Another use of PrP transgenic *Drosophila* is their ability to serve as a bioassay for prion infectivity. The bioassay of prions in *Drosophila* could serve as a new standard for prion infectivity assessment and replace, where appropriate, the use of rodents since this invertebrate host appears to be more sensitive than the traditional mouse bioassay (Thackray *et al.*, 2016). The *Drosophila* bioassay shows a limit of detection at $\geq 10^{-10}$ fold dilution of scrapie-infected sheep brain homogenate, whereas the mouse bioassay has a limit of detection of 10^{-6} fold dilution of the same inoculum (Thackray *et al.*, 2016). The time needed to complete a rodent bioassay ranges between multiple months and years, whereas the fly-based bioassay of prions can be performed

in approximately 6 weeks (Thackray *et al.*, 2018b). These observations highlight the utility of the PrP transgenic *Drosophila* for use as a rapid and efficient bioassay for mammalian prion infectivity. For example, experiments with human PrP transgenic flies of different genotypes can reveal the potential of CJD or vCJD transmission or even transmission of animal prion diseases, such as chronic wasting disease (CWD) or camel prion disease (CPD), to humans. With regards to CPD, the transmissibility of this new prion disease has not yet been reported (Babelhadj et al., 2018) and the transmission of CPD to ovine, bovine, cervid and human PrP transgenic flies might be a rapid and feasible solution to identify the risk of inter-species transmission. Since dromedary camels are not kept separately from other wild life species, the inter-species transmissibility and zoonotic potential is something that should be investigated at the earliest opportunity. This might help with identification of the disease source, such as whether it has an adapted-scrapie or BSE strain origin and with the risk of transmission and potential geographical spread of this newly discovered disease.

Another use of a sensitive and rapid *Drosophila* prion bioassay would be in assessment of prion infectivity in blood. To date, the full extent of the presence of BSE-derived vCJD in the human population is unknown (Llewelyn et al., 2004, Peden et al., 2004). Since the 1980s, there have been stringent selection criteria applied to blood donors to exclude anyone who underwent corneal transplant or growth hormone treatments originating from pituitary extract to avoid the vCJD transmission via blood transfusion (Boulton, 2003). Approximately eight percent of confirmed vCJD patients in the UK have been reported as former blood donors, therefore, the blood recipients might be at risk as well. The transmission of BSE and scrapie by blood was confirmed in sheep models (Houston et al., 2000) and the outcome of these transmission studies suggests that the risk of transmission, even from fractionated or leucocyte depleted blood, might be similar in the case of the vCJD agent (Boulton, 2003).

It is important to point out that PrP transgenic *Drosophila* that express misfolded prions fall under the containment level 2 safety level category in the case of scrapie, while CWD or human prion disease models require containment level 3. These precautions are in place to avoid any inadvertent release of prion-exposed flies and were enforced throughout the experiments conducted in this thesis. An important feature to highlight in *Drosophila*-based research is its ability to replace or reduce the use of more sentient hosts in experimental studies. Making a transgenic rodent, which is the most commonly used experimental animal in neurodegenerative research, demands prolonged housing and regular maintenance. Neurodegeneration research is

associated with cognitive and sensory pathologies that need to manifest in the animals towards the end of their life in order for them to be sacrificed and analysed. To conduct research on vertebrates, such as rodents, primates or other large species is problematic and brings irrevocable animal welfare issues. However, at the basic research level, use of *Drosophila* could be viewed as more ethical. The routine bioassays and initial drug screenings are definitely two feasible goals for a use of PrP transgenic *Drosophila* in this respect. Obviously, some approaches will inevitably require validation in mammalian hosts later on before clinical trials in humans. PrP transgenic *Drosophila* can detect pre-clinical blood samples (Thackray et al., 2016). Pre-clinical vCJD blood donors pose a risk of transmission to the blood recipients and the routine screening for the vCJD pathological agent in blood is another example of the utility of the fly bioassay. *In vitro* methods might not be able to detect the low titre of prion infectivity and therefore, the *Drosophila* prion bioassay is an ideal candidate for replacement of lengthy mammalian bioassays that is able to amplify minute amounts of misfolded PrP in the blood sample.

6.1 Conclusion

In this research project, multiple PrP transgenic *Drosophila* were characterised and verified with a goal to provide novel invertebrate models for the relatively rapid study of mammalian prion disease. The fly lines established here (see **Tables 1, 2, 3 and 4**), allowed the elucidation of cellular and molecular processes associated with prion-induced neurotoxicity. Moreover, *in vivo* transcellular spread of misfolded PrP was investigated here to discover if it is possible to model this situation in *Drosophila.* To this end, *Drosophila* transgenic for various species forms of mammalian PrP were characterised at the biochemical, synaptic and phenotypic level. All genotypes of ovine, hamster, humanised murine 3F4, cervid and human PrP transgenic flies used here were verified for their PrP expression on multiple occasions and on some occasions under two independent fly expression systems. The relative PrP expression levels in the PrP transgenic fly models were found to be species-specific with the highest expression in human PrP transgenic flies and the lowest expression levels in ovine PrP transgenic flies; specifically the order was: human ≥ hamster ≥ murine 3F4 > cervid ≥ ovine PrP. PrP expression did not have a detrimental effect on *Drosophila,* since there was no spontaneous neurotoxicity in any fly line that expressed a wild type form of the prion protein. In the acquired prion disease model of scrapie, the subcellular events of synaptic neurodegeneration were studied using the NMJ as a synapse model in the scrapie-exposed ovine PrP transgenic *Drosophila* larvae with prion-induced neurodegeneration targeted to NMJs. This was the first step to observe the direct impact of

prion-induced neurodegeneration on the fly. The analysis showed that prion-exposed larval NMJs displayed altered morphology or synaptic architecture that were influenced by the topological expression of PrP.

Using hamster and humanised murine 3F4 PrP transgenic flies that harboured single codon mutations associated with human genetic prion disease, it was possible to investigate the development of a spontaneous prion-induced transmissible neurotoxic phenotype (Thackray et al., 2017). Moreover, this prion-induced phenotype was accompanied by accumulation of a mildly PK-resistant form of PrP.

The transcellular spread of misfolded PrP was analysed through the use of dual PrP transgenic *Drosophila*. These fly lines expressed secreted PrP(ΔGPI) that harboured a mutation similar to a genetic form of human GSS prion disease and wild type PrP in different neuronal subsets. The ability of mutant PrP to initiate misfolding of wild type PrP in these fly lines was investigated by *in vitro* protein conversion and *in vivo* by fly survival assays. The results of these experiments show that the secreted form of ovine PrP is difficult to detect *in vitro*. However, a preliminary *in vivo* survival assay showed that the VRQ(GPI) and PrP(ΔGPI) dual PrP transgenic flies show an accelerated decline in survival in comparison to control flies when the pathological form of PrP was expressed in glial cells or interneurons of postsynaptic partners of chordotonal organs in *Drosophila*. This suggest there might be a neuronal uptake of material from glial cells in PrP transgenic *Drosophila* model as well as from neuronal subsets.

The experiments carried out in this thesis have helped to demonstrate that many features associated with mammalian prion diseases can be replicated in PrP transgenic *Drosophila*. This versatile invertebrate animal model provides new methodologies for the rapid investigation of protein misfolding-induced neurodegeneration and allows us to benefit from multiple fly-specific advantages, such as simple genetics and short lifespan. The ease of fly transgenesis and their well-understood genome can play an important role in elucidation of genetic modifiers of prion replication and prion-induced neurotoxicity. The PrP transgenic fly lines studied in this thesis can be used for many future projects and help to address a range of important questions in prion biology.

7 References

Aarli, J. A., Dua, T., Janca, A. and Muscetta, A. 2006. Neurological Disorders. Public Health Challenges, World Health Organization. Geneva.

Abolaji, A. O., Adedara, A. O., Adie, M. A., Vicente-Crespo, M. and Farombi, E. O. (2018) 'Resveratrol prolongs lifespan and improves 1-methyl-4-phenyl-1,2,3,6-tetrahydropyridine-induced oxidative damage and behavioural deficits in *Drosophila* melanogaster', *Biochem Biophys Res Commun.*

Adams, D. H., Caspary, E. A. and Field, E. J. (1969) 'The incorporation of [3H]thymidine, [14C]orotic acid, [14C]uridine-diphosphoglucose and [14C]glucosamine into a post-ribosomal fraction of normal and scrapie-affected mouse brain and spleen', *J Gen Virol,* 4(1), pp. 89-100.

Adams, M. D. and Celniker, S. E. and Holt, R. A. and Evans, C. A. and Gocayne, J. D. and Amanatides, P. G. and Scherer, S. E. and Li, P. W. and Hoskins, R. A. and Galle, R. F. and George, R. A. and Lewis, S. E. and Richards, S. and Ashburner, M. and Henderson, S. N. and Sutton, G. G. and Wortman, J. R. and Yandell, M. D. and Zhang, Q. and Chen, L. X. and Brandon, R. C. and Rogers, Y. H. and Blazej, R. G. and Champe, M. and Pfeiffer, B. D. and Wan, K. H. and Doyle, C. and Baxter, E. G. and Helt, G. and Nelson, C. R. and Gabor, G. L. and Abril, J. F. and Agbayani, A. and An, H. J. and Andrews-Pfannkoch, C. and Baldwin, D. and Ballew, R. M. and Basu, A. and Baxendale, J. and Bayraktaroglu, L. and Beasley, E. M. and Beeson, K. Y. and Benos, P. V. and Berman, B. P. and Bhandari, D. and Bolshakov, S. and Borkova, D. and Botchan, M. R. and Bouck, J. and Brokstein, P. and Brottier, P. and Burtis, K. C. and Busam, D. A. and Butler, H. and Cadieu, E. and Center, A. and Chandra, I. and Cherry, J. M. and Cawley, S. and Dahlke, C. and Davenport, L. B. and Davies, P. and de Pablos, B. and Delcher, A. and Deng, Z. and Mays, A. D. and Dew, I. and Dietz, S. M. and Dodson, K. and Doup, L. E. and Downes, M. and Dugan-Rocha, S. and Dunkov, B. C. and Dunn, P. and Durbin, K. J. and Evangelista, C. C. and Ferraz, C. and Ferriera, S. and Fleischmann, W. and Fosler, C. and Gabrielian, A. E. and Garg, N. S. and Gelbart, W. M. and Glasser, K. and Glodek, A. and Gong, F. and Gorrell, J. H. and Gu, Z. and Guan, P. and Harris, M. and Harris, N. L. and Harvey, D. and Heiman, T. J. and Hernandez, J. R. and Houck, J. and Hostin, D. and Houston, K. A. and Howland, T. J. and Wei, M. H. and Ibegwam, C. and Jalali, M. and Kalush, F. and Karpen, G. H. and Ke, Z. and Kennison, J. A. and Ketchum, K. A. and Kimmel, B. E. and Kodira, C. D. and Kraft, C. and Kravitz, S. and Kulp, D. and Lai, Z. and Lasko, P. and Lei, Y. and Levitsky, A. A. and Li, J. and Li, Z. and Liang, Y. and Lin, X. and Liu, X. and Mattei, B. and McIntosh, T. C. and McLeod, M. P. and McPherson, D. and Merkulov, G. and Milshina, N. V. and Mobarry, C. and Morris, J. and Moshrefi, A. and Mount, S. M. and Moy, M. and Murphy, B. and Murphy, L. and Muzny, D. M. and Nelson, D. L. and Nelson, D. R. and Nelson, K. A. and Nixon, K. and Nusskern, D. R. and Pacleb, J. M. and Palazzolo, M. and Pittman, G. S. and Pan, S. and Pollard, J. and Puri, V. and Reese, M. G. and Reinert, K. and Remington, K. and Saunders, R. D. and Scheeler, F. and Shen, H. and Shue, B. C. and Sidén-Kiamos, I. and Simpson, M. and Skupski, M. P. and Smith, T. and Spier, E. and Spradling, A. C. and Stapleton, M. and Strong, R. and Sun, E. and Svirskas, R. and Tector, C. and Turner, R. and Venter, E. and Wang, A. H. and Wang, X. and Wang, Z. Y. and Wassarman, D. A. and Weinstock, G. M. and Weissenbach, J. and Williams, S. M. and WoodageT and Worley, K. C. and Wu, D. and Yang, S. and Yao, Q. A. and Ye, J. and Yeh, R. F. and Zaveri, J. S. and Zhan, M. and Zhang, G. and Zhao, Q. and Zheng, L. and Zheng, X. H. and Zhong, F. N. and Zhong, W. and Zhou, X. and Zhu, S. and Zhu, X. and Smith, H. O. and Gibbs, R. A.

and Myers, E. W. and Rubin, G. M. and Venter, J. C. (2000) 'The genome sequence of *Drosophila* melanogaster', *Science,* 287(5461), pp. 2185-95.
Adrover, M., Pauwels, K., Prigent, S., de Chiara, C., Xu, Z., Chapuis, C., Pastore, A. and Rezaei, H. (2010) 'Prion fibrillization is mediated by a native structural element that comprises helices H2 and H3', *J Biol Chem,* 285(27), pp. 21004-12.
Aguzzi, A., Heikenwalder, M. and Polymenidou, M. (2007) 'Insights into prion strains and neurotoxicity', *Nat Rev Mol Cell Biol,* 8(7), pp. 552-61.
Aguzzi, A., Sigurdson, C. and Heikenwaelder, M. (2008) 'Molecular mechanisms of prion pathogenesis', *Annu Rev Pathol,* 3, pp. 11-40.
Aguzzi, A. and Rajendran, L. (2009) 'The transcellular spread of cytosolic amyloids, prions, and prionoids', *Neuron,* 64(6), pp. 783-90.
Akassoglou, K., Malester, B., Xu, J., Tessarollo, L., Rosenbluth, J. and Chao, M. V. (2004) 'Brain-specific deletion of neuropathy target esterase/swisscheese results in neurodegeneration', *Proc Natl Acad Sci U S A,* 101(14), pp. 5075-80.
Alper, T., Cramp, W. A., Haig, D. A. and Clarke, M. C. (1967) 'Does the agent of scrapie replicate without nucleic acid?', *Nature,* 214(5090), pp. 764-6.
Ambegaokar, S. S., Roy, B. and Jackson, G. R. (2010) 'Neurodegenerative models in *Drosophila*: polyglutamine disorders, Parkinson disease, and amyotrophic lateral sclerosis', *Neurobiol Dis,* 40(1), pp. 29-39.
Aronoff-Spencer, E., Burns, C. S., Avdievich, N. I., Gerfen, G. J., Peisach, J., Antholine, W. E., Ball, H. L., Cohen, F. E., Prusiner, S. B. and Millhauser, G. L. (2000) 'Identification of the Cu2+ binding sites in the N-terminal domain of the prion protein by EPR and CD spectroscopy', *Biochemistry,* 39(45), pp. 13760-71.
Asante, E. A., Gowland, I., Grimshaw, A., Linehan, J. M., Smidak, M., Houghton, R., Osiguwa, O., Tomlinson, A., Joiner, S., Brandner, S., Wadsworth, J. D. and Collinge, J. (2009) 'Absence of spontaneous disease and comparative prion susceptibility of transgenic mice expressing mutant human prion proteins', *J Gen Virol,* 90(Pt 3), pp. 546-58.
Atarashi, R., Sano, K., Satoh, K. and Nishida, N. (2011a) 'Real-time quaking-induced conversion: a highly sensitive assay for prion detection', *Prion,* 5(3), pp. 150-3.
Atarashi, R., Satoh, K., Sano, K., Fuse, T., Yamaguchi, N., Ishibashi, D., Matsubara, T., Nakagaki, T., Yamanaka, H., Shirabe, S., Yamada, M., Mizusawa, H., Kitamoto, T., Klug, G., McGlade, A., Collins, S. J. and Nishida, N. (2011b) 'Ultrasensitive human prion detection in cerebrospinal fluid by real-time quaking-induced conversion', *Nat Med,* 17(2), pp. 175-8.
Aucouturier, P., Kascsak, R. J., Frangione, B. and Wisniewski, T. (1999) 'Biochemical and conformational variability of human prion strains in sporadic Creutzfeldt-Jakob disease', *Neurosci Lett,* 274(1), pp. 33-6.
Auluck, P. K., Chan, H. Y., Trojanowski, J. Q., Lee, V. M. and Bonini, N. M. (2002) 'Chaperone suppression of alpha-synuclein toxicity in a *Drosophila* model for Parkinson's disease', *Science,* 295(5556), pp. 865-8.
Babcock, D. T. and Ganetzky, B. (2015) 'Transcellular spreading of huntingtin aggregates in the *Drosophila* brain', *Proc Natl Acad Sci U S A,* 112(39), pp. E5427-33.
Babelhadj, B., Di Bari, M. A., Pirisinu, L., Chiappini, B., Gaouar, S. B. S., Riccardi, G., Marcon, S., Agrimi, U., Nonno, R. and Vaccari, G. (2018) 'Prion Disease in Dromedary Camels, Algeria', *Emerg Infect Dis,* 24(6).
Baldin, E., Capellari, S., Provini, F., Corrado, P., Liguori, R., Parchi, P., Montagna, P. and Cortelli, P. (2009) 'A case of fatal familial insomnia in Africa', *J Neurol,* 256(10), pp. 1778-9.

Barbezier, N., Chartier, A., Bidet, Y., Buttstedt, A., Voisset, C., Galons, H., Blondel, M., Schwarz, E. and Simonelig, M. (2011) 'Antiprion drugs 6-aminophenanthridine and guanabenz reduce PABPN1 toxicity and aggregation in oculopharyngeal muscular dystrophy', *EMBO Mol Med,* 3(1), pp. 35-49.

Barria, M. A., Gonzalez-Romero, D. and Soto, C. (2012) 'Cyclic amplification of prion protein misfolding', *Methods Mol Biol,* 849, pp. 199-212.

Beg, T., Jyoti, S., Naz, F., Rahul, Ali, F., Ali, S. K., Reyad, A. M. and Siddique, Y. H. (2018) 'Protective effect of kaempferol on the transgenic *Drosophila* model of Alzheimer's disease', *CNS Neurol Disord Drug Targets.*

Belay, E. D. (1999) 'Transmissible spongiform encephalopathies in humans', *Annu Rev Microbiol,* 53, pp. 283-314.

Benestad, S. L., Sarradin, P., Thu, B., Schönheit, J., Tranulis, M. A. and Bratberg, B. (2003) 'Cases of scrapie with unusual features in Norway and designation of a new type, Nor98', *Vet Rec,* 153(7), pp. 202-8.

Benestad, S. L., Arsac, J. N., Goldmann, W. and Nöremark, M. (2008) 'Atypical/Nor98 scrapie: properties of the agent, genetics, and epidemiology', *Vet Res,* 39(4), pp. 19.

Benestad, S. L., Mitchell, G., Simmons, M., Ytrehus, B. and Vikøren, T. (2016) 'First case of chronic wasting disease in Europe in a Norwegian free-ranging reindeer', *Vet Res,* 47(1), pp. 88.

Benetti, F., Gustincich, S. and Legname, G. (2012) 'Gene expression profiling and therapeutic interventions in neurodegenerative diseases: a comprehensive study on potentiality and limits', *Expert Opin Drug Discov,* 7(3), pp. 245-59.

Berger, Z., Ravikumar, B., Menzies, F. M., Oroz, L. G., Underwood, B. R., Pangalos, M. N., Schmitt, I., Wullner, U., Evert, B. O., O'Kane, C. J. and Rubinsztein, D. C. (2006) 'Rapamycin alleviates toxicity of different aggregate-prone proteins', *Hum Mol Genet,* 15(3), pp. 433-42.

Beringue, V., Demoy, M., Lasmézas, C. I., Gouritin, B., Weingarten, C., Deslys, J. P., Andreux, J. P., Couvreur, P. and Dormont, D. (2000) 'Role of spleen macrophages in the clearance of scrapie agent early in pathogenesis', *J Pathol,* 190(4), pp. 495-502.

Bessen, R. A., Kocisko, D. A., Raymond, G. J., Nandan, S., Lansbury, P. T. and Caughey, B. (1995) 'Non-genetic propagation of strain-specific properties of scrapie prion protein', *Nature,* 375(6533), pp. 698-700.

Biacabe, A. G., Laplanche, J. L., Ryder, S. and Baron, T. (2004) 'Distinct molecular phenotypes in bovine prion diseases', *EMBO Rep,* 5(1), pp. 110-5.

Bianca, M., Bianca, S., Vecchio, I., Raffaele, R., Ingegnosi, C. and Nicoletti, F. (2003) 'Gerstmann-Sträussler-Scheinker disease with P102L-V129 mutation: a case with psychiatric manifestations at onset', *Ann Genet,* 46(4), pp. 467-9.

Bilen, J. and Bonini, N. M. (2007) 'Genome-wide screen for modifiers of ataxin-3 neurodegeneration in *Drosophila*', *PLoS Genet,* 3(10), pp. 1950-64.

Bilen, J., Liu, N., Burnett, B. G., Pittman, R. N. and Bonini, N. M. (2006) 'MicroRNA pathways modulate polyglutamine-induced neurodegeneration', *Mol Cell,* 24(1), pp. 157-63.

Billeter, M., Riek, R., Wider, G., Hornemann, S., Glockshuber, R. and Wüthrich, K. (1997) 'Prion protein NMR structure and species barrier for prion diseases', *Proc Natl Acad Sci U S A,* 94(14), pp. 7281-5.

Bischof, J., Maeda, R. K., Hediger, M., Karch, F. and Basler, K. (2007) 'An optimized transgenesis system for *Drosophila* using germ-line-specific phiC31 integrases', *Proc Natl Acad Sci U S A,* 104(9), pp. 3312-7.

Bishop, M. T., Hart, P., Aitchison, L., Baybutt, H. N., Plinston, C., Thomson, V., Tuzi, N. L., Head, M. W., Ironside, J. W., Will, R. G. and Manson, J. C. (2006) 'Predicting susceptibility and incubation time of human-to-human transmission of vCJD', *Lancet Neurol,* 5(5), pp. 393-8.

Blättler, T., Brandner, S., Raeber, A. J., Klein, M. A., Voigtländer, T., Weissmann, C. and Aguzzi, A. (1997) 'PrP-expressing tissue required for transfer of scrapie infectivity from spleen to brain', *Nature,* 389(6646), pp. 69-73.

Boillée, S., Yamanaka, K., Lobsiger, C. S., Copeland, N. G., Jenkins, N. A., Kassiotis, G., Kollias, G. and Cleveland, D. W. (2006) 'Onset and progression in inherited ALS determined by motor neurons and microglia', *Science,* 312(5778), pp. 1389-92.

Bolton, D. C., McKinley, M. P. and Prusiner, S. B. (1982) 'Identification of a protein that purifies with the scrapie prion', *Science,* 218(4579), pp. 1309-11.

Bons, N., Mestre-Frances, N., Belli, P., Cathala, F., Gajdusek, D. C. and Brown, P. (1999) 'Natural and experimental oral infection of nonhuman primates by bovine spongiform encephalopathy agents', *Proc Natl Acad Sci U S A,* 96(7), pp. 4046-51.

Booth, S., Bowman, C., Baumgartner, R., Sorensen, G., Robertson, C., Coulthart, M., Phillipson, C. and Somorjai, R. L. (2004) 'Identification of central nervous system genes involved in the host response to the scrapie agent during preclinical and clinical infection', *J Gen Virol,* 85(Pt 11), pp. 3459-71.

Borchelt, D. R., Koliatsos, V. E., Guarnieri, M., Pardo, C. A., Sisodia, S. S. and Price, D. L. (1994) 'Rapid anterograde axonal transport of the cellular prion glycoprotein in the peripheral and central nervous systems', *J Biol Chem,* 269(20), pp. 14711-4.

Borchelt, D. R., Rogers, M., Stahl, N., Telling, G. and Prusiner, S. B. (1993) 'Release of the cellular prion protein from cultured cells after loss of its glycoinositol phospholipid anchor', *Glycobiology,* 3(4), pp. 319-29.

Bossers, A., Belt, P. B. G. M., Raymond, G. J., Caughey, B., de Vries, R. and Smits, M. A. (1997) 'Scrapie susceptibility-linked polymorphisms modulate the in vitro conversion of sheep prion protein to protease-resistant forms', *Proc Natl Acad Sci U S A,* 94(10), pp. 4931-6.

Boulton, F. (2003) 'The impact of variant CJD on transfusion practices in the UK', *Transfus Apher Sci,* 28(2), pp. 107-16.

Bouybayoune, I., Mantovani, S., Del Gallo, F., Bertani, I., Restelli, E., Comerio, L., Tapella, L., Baracchi, F., Fernández-Borges, N., Mangieri, M., Bisighini, C., Beznoussenko, G. V., Paladini, A., Balducci, C., Micotti, E., Forloni, G., Castilla, J., Fiordaliso, F., Tagliavini, F., Imeri, L. and Chiesa, R. (2015) 'Transgenic fatal familial insomnia mice indicate prion infectivity-independent mechanisms of pathogenesis and phenotypic expression of disease', *PLoS Pathog,* 11(4), pp. e1004796.

Brand, A. H. and Perrimon, N. (1993) 'Targeted gene expression as a means of altering cell fates and generating dominant phenotypes', *Development,* 118(2), pp. 401-15.

Brandner, S., Isenmann, S., Raeber, A., Fischer, M., Sailer, A., Kobayashi, Y., Marino, S., Weissmann, C. and Aguzzi, A. (1996) 'Normal host prion protein necessary for scrapie-induced neurotoxicity', *Nature,* 379(6563), pp. 339-43.

Brandner, S. and Jaunmuktane, Z. (2017) 'Prion disease: experimental models and reality', *Acta Neuropathol,* 133(2), pp. 197-222.

Braun, U. (2002) '[Clinical signs and diagnosis of BSE]', *Schweiz Arch Tierheilkd,* 144(12), pp. 645-52.

Breckenridge, D. G., Germain, M., Mathai, J. P., Nguyen, M. and Shore, G. C. (2003) 'Regulation of apoptosis by endoplasmic reticulum pathways', *Oncogene,* 22(53), pp. 8608-18.

Brent, J. R., Werner, K. M. and McCabe, B. D. (2009) '*Drosophila* larval NMJ dissection', *J Vis Exp,* (24).

Brown, K. L., Stewart, K., Ritchie, D. L., Mabbott, N. A., Williams, A., Fraser, H., Morrison, W. I. and Bruce, M. E. (1999) 'Scrapie replication in lymphoid tissues depends on prion protein-expressing follicular dendritic cells', *Nat Med,* 5(11), pp. 1308-12.

Brown, P., Brandel, J. P., Sato, T., Nakamura, Y., MacKenzie, J., Will, R. G., Ladogana, A., Pocchiari, M., Leschek, E. W. and Schonberger, L. B. (2012) 'Iatrogenic Creutzfeldt-Jakob disease, final assessment', *Emerg Infect Dis,* 18(6), pp. 901-7.

Brown, P., Will, R. G., Bradley, R., Asher, D. M. and Detwiler, L. (2001) 'Bovine spongiform encephalopathy and variant Creutzfeldt-Jakob disease: background, evolution, and current concerns', *Emerg Infect Dis,* 7(1), pp. 6-16.

Brownell, B. and Oppenheimer, D. R. (1965) 'AN ATAXIC FORM OF SUBACUTE PRESENILE POLIOENCEPHALOPATHY (CREUTZFELDT-JAKOB DISEASE)', *J Neurol Neurosurg Psychiatry,* 28, pp. 350-61.

Bruce, M. E. and Dickinson, A. G. (1987) 'Biological evidence that scrapie agent has an independent genome', *J Gen Virol,* 68 (Pt 1), pp. 79-89.

Bruce, M. E., Will, R. G., Ironside, J. W., McConnell, I., Drummond, D., Suttie, A., McCardle, L., Chree, A., Hope, J., Birkett, C., Cousens, S., Fraser, H. and Bostock, C. J. (1997) 'Transmissions to mice indicate that 'new variant' CJD is caused by the BSE agent', *Nature,* 389(6650), pp. 498-501.

Brundin, P., Melki, R. and Kopito, R. (2010) 'Prion-like transmission of protein aggregates in neurodegenerative diseases', *Nat Rev Mol Cell Biol,* 11(4), pp. 301-7.

Budnik, V., Gorczyca, M. and Prokop, A. (2006) 'Selected methods for the anatomical study of *Drosophila* embryonic and larval neuromuscular junctions', *Int Rev Neurobiol,* 75, pp. 323-65.

Burda, J. E. and Sofroniew, M. V. (2014) 'Reactive gliosis and the multicellular response to CNS damage and disease', *Neuron,* 81(2), pp. 229-48.

Burns, C. S., Aronoff-Spencer, E., Dunham, C. M., Lario, P., Avdievich, N. I., Antholine, W. E., Olmstead, M. M., Vrielink, A., Gerfen, G. J., Peisach, J., Scott, W. G. and Millhauser, G. L. (2002) 'Molecular features of the copper binding sites in the octarepeat domain of the prion protein', *Biochemistry,* 41(12), pp. 3991-4001.

Buschmann, A., Biacabe, A. G., Ziegler, U., Bencsik, A., Madec, J. Y., Erhardt, G., Lühken, G., Baron, T. and Groschup, M. H. (2004) 'Atypical scrapie cases in Germany and France are identified by discrepant reaction patterns in BSE rapid tests', *J Virol Methods,* 117(1), pp. 27-36.

Büeler, H., Aguzzi, A., Sailer, A., Greiner, R. A., Autenried, P., Aguet, M. and Weissmann, C. (1993) 'Mice devoid of PrP are resistant to scrapie', *Cell,* 73(7), pp. 1339-47.

Büeler, H., Fischer, M., Lang, Y., Bluethmann, H., Lipp, H. P., DeArmond, S. J., Prusiner, S. B., Aguet, M. and Weissmann, C. (1992) 'Normal development and behaviour of mice lacking the neuronal cell-surface PrP protein', *Nature,* 356(6370), pp. 577-82.

Calzolai, L., Lysek, D. A., Pérez, D. R., Güntert, P. and Wüthrich, K. (2005) 'Prion protein NMR structures of chickens, turtles, and frogs', *Proc Natl Acad Sci U S A,* 102(3), pp. 651-5.

Campana, V., Caputo, A., Sarnataro, D., Paladino, S., Tivodar, S. and Zurzolo, C. (2007) 'Characterization of the properties and trafficking of an anchorless form of the prion protein', *J Biol Chem,* 282(31), pp. 22747-56.

Campana, V., Sarnataro, D. and Zurzolo, C. (2005) 'The highways and byways of prion protein trafficking', *Trends Cell Biol,* 15(2), pp. 102-11.

Cao, W., Song, H. J., Gangi, T., Kelkar, A., Antani, I., Garza, D. and Konsolaki, M. (2008) 'Identification of novel genes that modify phenotypes induced by Alzheimer's beta-amyloid overexpression in *Drosophila*', *Genetics,* 178(3), pp. 1457-71.

Cardova, A., Adam, P., Mariani, S., Richtera, L., Heger, Z., Labuda, J., Minunni, M. and Adam, V. (2017) 'Electrochemical and optical study of metallothionein interactions with prion proteins', *J Pharm Biomed Anal,* 140, pp. 355-361.

Carp, R. I. and Callahan, S. M. (1982) 'Effect of mouse peritoneal macrophages on scrapie infectivity during extended in vitro incubation', *Intervirology,* 17(4), pp. 201-7.

Carulla, P., Llorens, F., Matamoros-Angles, A., Aguilar-Calvo, P., Espinosa, J. C., Gavín, R., Ferrer, I., Legname, G., Torres, J. M. and del Río, J. A. (2015) 'Involvement of PrP(C) in kainate-induced excitotoxicity in several mouse strains', *Sci Rep,* 5, pp. 11971.

Cashman, N. R., Loertscher, R., Nalbantoglu, J., Shaw, I., Kascsak, R. J., Bolton, D. C. and Bendheim, P. E. (1990) 'Cellular isoform of the scrapie agent protein participates in lymphocyte activation', *Cell,* 61(1), pp. 185-92.

Caughey, B., Neary, K., Buller, R., Ernst, D., Perry, L. L., Chesebro, B. and Race, R. E. (1990) 'Normal and scrapie-associated forms of prion protein differ in their sensitivities to phospholipase and proteases in intact neuroblastoma cells', *J Virol,* 64(3), pp. 1093-101.

Caughey, B. and Raymond, G. J. (1991) 'The scrapie-associated form of PrP is made from a cell surface precursor that is both protease- and phospholipase-sensitive', *J Biol Chem,* 266(27), pp. 18217-23.

Caughey, B. W., Dong, A., Bhat, K. S., Ernst, D., Hayes, S. F. and Caughey, W. S. (1991) 'Secondary structure analysis of the scrapie-associated protein PrP 27-30 in water by infrared spectroscopy', *Biochemistry,* 30(31), pp. 7672-80.

Chandler, R. L. and Turfrey, B. A. (1972) 'Inoculation of voles, Chinese hamsters, gerbils and guinea-pigs with scrapie brain material', *Res Vet Sci,* 13(3), pp. 219-24.

Chee, F. C., Mudher, A., Cuttle, M. F., Newman, T. A., MacKay, D., Lovestone, S. and Shepherd, D. (2005) 'Over-expression of tau results in defective synaptic transmission in *Drosophila* neuromuscular junctions', *Neurobiol Dis,* 20(3), pp. 918-28.

Chen, C. and Dong, X. P. (2016) 'Epidemiological characteristics of human prion diseases', *Infect Dis Poverty,* 5(1), pp. 47.

Chen, J. and Thirumalai, D. (2013) 'Helices 2 and 3 are the initiation sites in the PrP(C) → PrP(SC) transition', *Biochemistry,* 52(2), pp. 310-9.

Cheng, Y. C., Hannaoui, S., John, T. R., Dudas, S., Czub, S. and Gilch, S. (2016) 'Early and Non-Invasive Detection of Chronic Wasting Disease Prions in Elk Feces by Real-Time Quaking Induced Conversion', *PLoS One,* 11(11), pp. e0166187.

Chesebro, B. (1998) 'BSE and prions: uncertainties about the agent', *Science,* 279(5347), pp. 42-3.

Chesebro, B., Trifilo, M., Race, R., Meade-White, K., Teng, C., LaCasse, R., Raymond, L., Favara, C., Baron, G., Priola, S., Caughey, B., Masliah, E. and Oldstone, M. (2005) 'Anchorless prion protein results in infectious amyloid disease without clinical scrapie', *Science,* 308(5727), pp. 1435-9.

Chiesa, R., Piccardo, P., Ghetti, B. and Harris, D. A. (1998) 'Neurological illness in transgenic mice expressing a prion protein with an insertional mutation', *Neuron,* 21(6), pp. 1339-51.

Chiesa, R., Pestronk, A., Schmidt, R. E., Tourtellotte, W. G., Ghetti, B., Piccardo, P. and Harris, D. A. (2001) 'Primary myopathy and accumulation of PrPSc-like molecules in peripheral tissues of transgenic mice expressing a prion protein insertional mutation', *Neurobiol Dis,* 8(2), pp. 279-88.

Chiesa, R., Restelli, E., Comerio, L., Del Gallo, F. and Imeri, L. (2016) 'Transgenic mice recapitulate the phenotypic heterogeneity of genetic prion diseases without developing

prion infectivity: Role of intracellular PrP retention in neurotoxicity', *Prion,* 10(2), pp. 93-102.

Choi, J. K., Jeon, Y. C., Lee, D. W., Oh, J. M., Lee, H. P., Jeong, B. H., Carp, R. I., Koh, Y. H. and Kim, Y. S. (2010) 'A *Drosophila* model of GSS syndrome suggests defects in active zones are responsible for pathogenesis of GSS syndrome', *Hum Mol Genet,* 19(22), pp. 4474-89.

Clouscard, C., Beaudry, P., Elsen, J. M., Milan, D., Dussaucy, M., Bounneau, C., Schelcher, F., Chatelain, J., Launay, J. M. and Laplanche, J. L. (1995) 'Different allelic effects of the codons 136 and 171 of the prion protein gene in sheep with natural scrapie', *J Gen Virol,* 76 (Pt 8), pp. 2097-101.

Cobb, N. J., Sönnichsen, F. D., McHaourab, H. and Surewicz, W. K. (2007) 'Molecular architecture of human prion protein amyloid: a parallel, in-register beta-structure', *Proc Natl Acad Sci U S A,* 104(48), pp. 18946-51.

Colby, D. W., Zhang, Q., Wang, S., Groth, D., Legname, G., Riesner, D. and Prusiner, S. B. (2007) 'Prion detection by an amyloid seeding assay', *Proc Natl Acad Sci U S A,* 104(52), pp. 20914-9.

Collinge, J., Whittington, M. A., Sidle, K. C., Smith, C. J., Palmer, M. S., Clarke, A. R. and Jefferys, J. G. (1994) 'Prion protein is necessary for normal synaptic function', *Nature,* 370(6487), pp. 295-7.

Collinge, J., Palmer, M. S., Sidle, K. C., Gowland, I., Medori, R., Ironside, J. and Lantos, P. (1995) 'Transmission of fatal familial insomnia to laboratory animals', *Lancet,* 346(8974), pp. 569-70.

Collinge, J., Sidle, K. C., Meads, J., Ironside, J. and Hill, A. F. (1996) 'Molecular analysis of prion strain variation and the aetiology of 'new variant' CJD', *Nature,* 383(6602), pp. 685-90.

Collinge, J. (1999) 'Variant Creutzfeldt-Jakob disease', *Lancet,* 354(9175), pp. 317-23.

Collinge, J. (2001) 'Prion diseases of humans and animals: their causes and molecular basis', *Annu Rev Neurosci,* 24, pp. 519-50.

Collinge, J. and Clarke, A. R. (2007) 'A general model of prion strains and their pathogenicity', *Science,* 318(5852), pp. 930-6.

Collins, C. A. and DiAntonio, A. (2007) 'Synaptic development: insights from *Drosophila*', *Curr Opin Neurobiol,* 17(1), pp. 35-42.

Costanzo, M. and Zurzolo, C. (2013) 'The cell biology of prion-like spread of protein aggregates: mechanisms and implication in neurodegeneration', *Biochem J,* 452(1), pp. 1-17.

Cotto, E., André, M., Forgue, J., Fleury, H. J. and Babin, P. J. (2005) 'Molecular characterization, phylogenetic relationships, and developmental expression patterns of prion genes in zebrafish (Danio rerio)', *FEBS J,* 272(2), pp. 500-13.

Critchley, P., Kazlauskaite, J., Eason, R. and Pinheiro, T. J. (2004) 'Binding of prion proteins to lipid membranes', *Biochem Biophys Res Commun,* 313(3), pp. 559-67.

Cronier, S., Laude, H. and Peyrin, J. M. (2004) 'Prions can infect primary cultured neurons and astrocytes and promote neuronal cell death', *Proc Natl Acad Sci U S A,* 101(33), pp. 12271-6.

Crowther, D. C., Kinghorn, K. J., Miranda, E., Page, R., Curry, J. A., Duthie, F. A., Gubb, D. C. and Lomas, D. A. (2005) 'Intraneuronal Abeta, non-amyloid aggregates and neurodegeneration in a *Drosophila* model of Alzheimer's disease', *Neuroscience,* 132(1), pp. 123-35.

Cuillé, J. and Chelle, P. L. (1936) 'La maladie dite tremblante due mouton est-elle inocuable?', *Comptes rendus de l'academie des sciences,* 203, pp. 1552-1554.

Cuillé, J. a. C., P. (1939) 'Transmission expérimental de la tremblante chez lachévre', *Comptes rendu de l'Academie des Sciences,* (208), pp. 1058-1060.

Cuillé, J. P. L. (1936) 'La maladie dite tremblante due mouton est-elle inocuable?', *Comptes rendus de l'academie des sciences,* 203, pp. 1552-1554.
Cunningham, C., Deacon, R., Wells, H., Boche, D., Waters, S., Diniz, C. P., Scott, H., Rawlins, J. N. and Perry, V. H. (2003) 'Synaptic changes characterize early behavioural signs in the ME7 model of murine prion disease', *Eur J Neurosci,* 17(10), pp. 2147-55.
Dar, A. C., Das, T. K., Shokat, K. M. and Cagan, R. L. (2012) 'Chemical genetic discovery of targets and anti-targets for cancer polypharmacology', *Nature,* 486(7401), pp. 80-4.
Davenport, K. A., Mosher, B. A., Brost, B. M., Henderson, D. M., Denkers, N. D., Nalls, A. V., McNulty, E., Mathiason, C. K. and Hoover, E. A. (2018) 'Assessment of Chronic Wasting Disease Prion Shedding in Deer Saliva with Occupancy Modeling', *J Clin Microbiol,* 56(1).
Davis, G. W. and Müller, M. (2015) 'Homeostatic control of presynaptic neurotransmitter release', *Annu Rev Physiol,* 77, pp. 251-70.
de Almeida, C. J., Chiarini, L. B., da Silva, J. P., E Silva, P. M., Martins, M. A. and Linden, R. (2005) 'The cellular prion protein modulates phagocytosis and inflammatory response', *J Leukoc Biol,* 77(2), pp. 238-46.
DeArmond, S. J., McKinley, M. P., Barry, R. A., Braunfeld, M. B., McColloch, J. R. and Prusiner, S. B. (1985) 'Identification of prion amyloid filaments in scrapie-infected brain', *Cell,* 41(1), pp. 221-35.
DeArmond, S. J., Mobley, W. C., DeMott, D. L., Barry, R. A., Beckstead, J. H. and Prusiner, S. B. (1998) 'Changes in the localization of brain prion proteins during scrapie infection', *Neurology,* 50(1), pp. 1271-80; discussion 2.
del Valle Rodríguez, A., Didiano, D. and Desplan, C. (2012) 'Power tools for gene expression and clonal

analysis in *Drosophila*', *Nature Methods,* 9(1), pp. 47-55.
Deleault, N. R., Dolph, P. J., Feany, M. B., Cook, M. E., Nishina, K., Harris, D. A. and Supattapone, S. (2003) 'Post-transcriptional suppression of pathogenic prion protein expression in *Drosophila* neurons', *J Neurochem,* 85(6), pp. 1614-23.
DeMarco, M. L. and Daggett, V. (2004) 'From conversion to aggregation: protofibril formation of the prion protein', *Proc Natl Acad Sci U S A,* 101(8), pp. 2293-8.
Di Bari, M. A., Chianini, F., Vaccari, G., Esposito, E., Conte, M., Eaton, S. L., Hamilton, S., Finlayson, J., Steele, P. J., Dagleish, M. P., Reid, H. W., Bruce, M., Jeffrey, M., Agrimi, U. and Nonno, R. (2008) 'The bank vole (Myodes glareolus) as a sensitive bioassay for sheep scrapie', *J Gen Virol,* 89(Pt 12), pp. 2975-85.
Di Bari, M. A., Nonno, R., Castilla, J., D'Agostino, C., Pirisinu, L., Riccardi, G., Conte, M., Richt, J., Kunkle, R., Langeveld, J., Vaccari, G. and Agrimi, U. (2013) 'Chronic wasting disease in bank voles: characterisation of the shortest incubation time model for prion diseases', *PLoS Pathog,* 9(3), pp. e1003219.
Diedrich, J. F., Bendheim, P. E., Kim, Y. S., Carp, R. I. and Haase, A. T. (1991) 'Scrapie-associated prion protein accumulates in astrocytes during scrapie infection', *Proc Natl Acad Sci U S A,* 88(2), pp. 375-9.
Dietz, K., Raddatz, G., Wallis, J., Müller, N., Zerr, I., Duerr, H. P., Lefèvre, H., Seifried, E. and Löwer, J. (2007) 'Blood transfusion and spread of variant Creutzfeldt-Jakob disease', *Emerg Infect Dis,* 13(1), pp. 89-96.
Ding, H., Xiong, Y., Sun, J., Chen, C., Gao, J. and Xu, H. (2018) 'Asiatic Acid Prevents Oxidative Stress and Apoptosis by Inhibiting the Translocation of α-Synuclein Into Mitochondria', *Front Neurosci,* 12, pp. 431.

Dormont, D. (2002) 'Prion diseases: pathogenesis and public health concerns', *FEBS Lett,* 529(1), pp. 17-21.

Dossena, S., Imeri, L., Mangieri, M., Garofoli, A., Ferrari, L., Senatore, A., Restelli, E., Balducci, C., Fiordaliso, F., Salio, M., Bianchi, S., Fioriti, L., Morbin, M., Pincherle, A., Marcon, G., Villani, F., Carli, M., Tagliavini, F., Forloni, G. and Chiesa, R. (2008) 'Mutant prion protein expression causes motor and memory deficits and abnormal sleep patterns in a transgenic mouse model', *Neuron,* 60(4), pp. 598-609.

Drisaldi, B., Stewart, R. S., Adles, C., Stewart, L. R., Quaglio, E., Biasini, E., Fioriti, L., Chiesa, R. and Harris, D. A. (2003) 'Mutant PrP is delayed in its exit from the endoplasmic reticulum, but neither wild-type nor mutant PrP undergoes retrotranslocation prior to proteasomal degradation', *J Biol Chem,* 278(24), pp. 21732-43.

Driscoll, M. and Gerstbrein, B. (2003) 'Dying for a cause: invertebrate genetics takes on human neurodegeneration', *Nat Rev Genet,* 4(3), pp. 181-94.

Duffy, P., Wolf, J., Collins, G., DeVoe, A. G., Streeten, B. and Cowen, D. (1974) 'Letter: Possible person-to-person transmission of Creutzfeldt-Jakob disease', *N Engl J Med,* 290(12), pp. 692-3.

Edfors, F., Danielsson, F., Hallström, B. M., Käll, L., Lundberg, E., Pontén, F., Forsström, B. and Uhlén, M. (2016) 'Gene-specific correlation of RNA and protein levels in human cells and tissues', *Mol Syst Biol,* 12(10), pp. 883.

Eklund, C. M., Kennedy, R. C. and Hadlow, W. J. (1967) 'Pathogenesis of scrapie virus infection in the mouse', *J Infect Dis,* 117(1), pp. 15-22.

Elbashir, S. M., Harborth, J., Lendeckel, W., Yalcin, A., Weber, K. and Tuschl, T. (2001) 'Duplexes of 21-nucleotide RNAs mediate RNA interference in cultured mammalian cells', *Nature,* 411(6836), pp. 494-8.

Encalada, S. E., Szpankowski, L., Xia, C. H. and Goldstein, L. S. (2011) 'Stable kinesin and dynein assemblies drive the axonal transport of mammalian prion protein vesicles', *Cell,* 144(4), pp. 551-65.

Esiri, M. M. (2007) 'Ageing and the brain', *J Pathol,* 211(2), pp. 181-7.

Farooqui, T. and Farooqui, A. A. (2009) 'Aging: an important factor for the pathogenesis of neurodegenerative diseases', *Mech Ageing Dev,* 130(4), pp. 203-15.

Feany, M. B. and Bender, W. W. (2000) 'A *Drosophila* model of Parkinson's disease', *Nature,* 404(6776), pp. 394-8.

Featherstone, D. E. and Broadie, K. (2000) 'Surprises from *Drosophila*: genetic mechanisms of synaptic development and plasticity', *Brain Res Bull,* 53(5), pp. 501-11.

Fediaevsky, A., Maurella, C., Nöremark, M., Ingravalle, F., Thorgeirsdottir, S., Orge, L., Poizat, R., Hautaniemi, M., Liam, B., Calavas, D., Ru, G. and Hopp, P. (2010) 'The prevalence of atypical scrapie in sheep from positive flocks is not higher than in the general sheep population in 11 European countries', *BMC Vet Res,* 6, pp. 9.

Fernandez-Funez, P., Nino-Rosales, M. L., de Gouyon, B., She, W. C., Luchak, J. M., Martinez, P., Turiegano, E., Benito, J., Capovilla, M., Skinner, P. J., McCall, A., Canal, I., Orr, H. T., Zoghbi, H. Y. and Botas, J. (2000) 'Identification of genes that modify ataxin-1-induced neurodegeneration', *Nature,* 408(6808), pp. 101-6.

Fernandez-Funez, P., Casas-Tinto, S., Zhang, Y., Gómez-Velazquez, M., Morales-Garza, M. A., Cepeda-Nieto, A. C., Castilla, J., Soto, C. and Rincon-Limas, D. E. (2009) 'In vivo generation of neurotoxic prion protein: role for hsp70 in accumulation of misfolded isoforms', *PLoS Genet,* 5(6), pp. e1000507.

Fernández-Hernández, I., Scheenaard, E., Pollarolo, G. and Gonzalez, C. (2016) 'The translational relevance of *Drosophila* in drug discovery', *EMBO Rep,* 17(4), pp. 471-2.

Fernandez-Funez, P., Sanchez-Garcia, J. and Rincon-Limas, D. E. (2017) '*Drosophila* models of prionopathies: insight into prion protein function, transmission, and neurotoxicity', *Curr Opin Genet Dev,* 44, pp. 141-148.

Feuillette, S., Miguel, L., Frébourg, T., Campion, D. and Lecourtois, M. (2010) '*Drosophila* models of human tauopathies indicate that Tau protein toxicity in vivo is mediated by soluble cytosolic phosphorylated forms of the protein', *J Neurochem,* 113(4), pp. 895-903.

Fevrier, B., Vilette, D., Archer, F., Loew, D., Faigle, W., Vidal, M., Laude, H. and Raposo, G. (2004) 'Cells release prions in association with exosomes', *Proc Natl Acad Sci U S A,* 101(26), pp. 9683-8.

Fire, A., Xu, S., Montgomery, M. K., Kostas, S. A., Driver, S. E. and Mello, C. C. (1998) 'Potent and specific genetic interference by double-stranded RNA in Caenorhabditis elegans', *Nature,* 391(6669), pp. 806-11.

Fischer, J. A., Giniger, E., Maniatis, T. and Ptashne, M. (1988) 'GAL4 activates transcription in *Drosophila*', *Nature,* 332(6167), pp. 853-6.

Fortini, M. E., Skupski, M. P., Boguski, M. S. and Hariharan, I. K. (2000) 'A survey of human disease gene counterparts in the *Drosophila* genome', *J Cell Biol,* 150(2), pp. F23-30.

Foster, J. D., Bruce, M., McConnell, I., Chree, A. and Fraser, H. (1996) 'Detection of BSE infectivity in brain and spleen of experimentally infected sheep', *Vet Rec,* 138(22), pp. 546-8.

Frank, C. A. (2014) 'Homeostatic plasticity at the *Drosophila* neuromuscular junction', *Neuropharmacology,* 78, pp. 63-74.

Frank, C. A., Wang, X., Collins, C. A., Rodal, A. A., Yuan, Q., Verstreken, P. and Dickman, D. K. (2013) 'New approaches for studying synaptic development, function, and plasticity using *Drosophila* as a model system', *J Neurosci,* 33(45), pp. 17560-8.

Fraser, H. and Dickinson, A. G. (1973) 'Scrapie in mice. Agent-strain differences in the distribution and intensity of grey matter vacuolation', *J Comp Pathol,* 83(1), pp. 29-40.

Fraser, H. and Farquhar, C. F. (1987) 'Ionising radiation has no influence on scrapie incubation period in mice', *Vet Microbiol,* 13(3), pp. 211-23.

Friedman, R. and Hughes, A. L. (2001) 'Pattern and timing of gene duplication in animal genomes', *Genome Res,* 11(11), pp. 1842-7.

Frost, B. and Diamond, M. I. (2010) 'Prion-like mechanisms in neurodegenerative diseases', *Nat Rev Neurosci,* 11(3), pp. 155-9.

Fujioka, M., Emi-Sarker, Y., Yusibova, G. L., Goto, T. and Jaynes, J. B. (1999) 'Analysis of an even-skipped rescue transgene reveals both composite and discrete neuronal and early blastoderm enhancers, and multi-stripe positioning by gap gene repressor gradients', *Development,* 126(11), pp. 2527-38.

Fujioka, M., Lear, B. C., Landgraf, M., Yusibova, G. L., Zhou, J., Riley, K. M., Patel, N. H. and Jaynes, J. B. (2003) 'Even-skipped, acting as a repressor, regulates axonal projections in *Drosophila*', *Development,* 130(22), pp. 5385-400.

Fulga, T. A., Elson-Schwab, I., Khurana, V., Steinhilb, M. L., Spires, T. L., Hyman, B. T. and Feany, M. B. (2007) 'Abnormal bundling and accumulation of F-actin mediates tau-induced neuronal degeneration in vivo', *Nat Cell Biol,* 9(2), pp. 139-48.

Féraudet, C., Morel, N., Simon, S., Volland, H., Frobert, Y., Créminon, C., Vilette, D., Lehmann, S. and Grassi, J. (2005) 'Screening of 145 anti-PrP monoclonal antibodies for their capacity to inhibit PrPSc replication in infected cells', *J Biol Chem,* 280(12), pp. 11247-58.

Gadotti, V. M. and Zamponi, G. W. (2011) 'Cellular prion protein protects from inflammatory and neuropathic pain', *Mol Pain,* 7, pp. 59.

Gajdusek, D. C. and Zigas, V. (1957) 'Degenerative disease of the central nervous system in New Guinea; the endemic occurrence of kuru in the native population', *N Engl J Med,* 257(20), pp. 974-8.

Gajdusek, D. C., Gibbs, C. J. and Alpers, M. (1966) 'Experimental transmission of a Kuru-like syndrome to chimpanzees', *Nature,* 209(5025), pp. 794-6.

Gambetti, P., Kong, Q., Zou, W., Parchi, P. and Chen, S. G. (2003a) 'Sporadic and familial CJD: classification and characterisation', *Br Med Bull,* 66, pp. 213-39.

Gambetti, P., Parchi, P. and Chen, S. G. (2003b) 'Hereditary Creutzfeldt-Jakob disease and fatal familial insomnia', *Clin Lab Med,* 23(1), pp. 43-64.

Garces, A. and Thor, S. (2006) 'Specification of *Drosophila* aCC motoneuron identity by a genetic cascade involving even-skipped, grain and zfh1', *Development,* 133(8), pp. 1445-55.

Gasperini, L. and Legname, G. (2014) 'Prion protein and aging', *Front Cell Dev Biol,* 2, pp. 44.

Gasperini, L., Meneghetti, E., Legname, G. and Benetti, F. (2016) 'In Absence of the Cellular Prion Protein, Alterations in Copper Metabolism and Copper-Dependent Oxidase Activity Affect Iron Distribution', *Front Neurosci,* 10, pp. 437.

Gavin, B. A., Dolph, M. J., Deleault, N. R., Geoghegan, J. C., Khurana, V., Feany, M. B., Dolph, P. J. and Supattapone, S. (2006) 'Accelerated accumulation of misfolded prion protein and spongiform degeneration in a *Drosophila* model of Gerstmann-Sträussler-Scheinker syndrome', *J Neurosci,* 26(48), pp. 12408-14.

Gawinecka, J., Cardone, F., Asif, A. R., De Pascalis, A., Wemheuer, W. M., Schulz-Schaeffer, W. J., Pocchiari, M. and Zerr, I. (2012) 'Sporadic Creutzfeldt-Jakob disease subtype-specific alterations of the brain proteome: impact on Rab3a recycling', *Proteomics,* 12(23-24), pp. 3610-20.

Gawinecka, J., Dieks, J., Asif, A. R., Carimalo, J., Heinemann, U., Streich, J. H., Dihazi, H., Schulz-Schaeffer, W. and Zerr, I. (2010) 'Codon 129 polymorphism specific cerebrospinal fluid proteome pattern in sporadic Creutzfeldt-Jakob disease and the implication of glycolytic enzymes in prion-induced pathology', *J Proteome Res,* 9(11), pp. 5646-57.

Gawinecka, J., Nowak, M., Carimalo, J., Cardone, F., Asif, A. R., Wemheuer, W. M., Schulz-Schaeffer, W. J., Pocchiari, M. and Zerr, I. (2013) 'Subtype-specific synaptic proteome alterations in sporadic Creutzfeldt-Jakob disease', *J Alzheimers Dis,* 37(1), pp. 51-61.

Gerdes, H. H. (2009) 'Prions tunnel between cells', *Nat Cell Biol,* 11(3), pp. 235-6.

Ghazalpour, A., Bennett, B., Petyuk, V. A., Orozco, L., Hagopian, R., Mungrue, I. N., Farber, C. R., Sinsheimer, J., Kang, H. M., Furlotte, N., Park, C. C., Wen, P. Z., Brewer, H., Weitz, K., Camp, D. G., Pan, C., Yordanova, R., Neuhaus, I., Tilford, C., Siemers, N., Gargalovic, P., Eskin, E., Kirchgessner, T., Smith, D. J., Smith, R. D. and Lusis, A. J. (2011) 'Comparative analysis of proteome and transcriptome variation in mouse', *PLoS Genet,* 7(6), pp. e1001393.

Ghetti, B., Piccardo, P., Spillantini, M. G., Ichimiya, Y., Porro, M., Perini, F., Kitamoto, T., Tateishi, J., Seiler, C., Frangione, B., Bugiani, O., Giaccone, G., Prelli, F., Goedert, M., Dlouhy, S. R. and Tagliavini, F. (1996) 'Vascular variant of prion protein cerebral amyloidosis with tau-positive neurofibrillary tangles: the phenotype of the stop codon 145 mutation in PRNP', *Proc Natl Acad Sci U S A,* 93(2), pp. 744-8.

Gibbons, R. A. and Hunter, G. D. (1967) 'Nature of the scrapie agent', *Nature,* 215(5105), pp. 1041-3.

Gibbs, C. J., Gajdusek, D. C., Asher, D. M., Alpers, M. P., Beck, E., Daniel, P. M. and Matthews, W. B. (1968) 'Creutzfeldt-Jakob disease (spongiform encephalopathy): transmission to the chimpanzee', *Science,* 161(3839), pp. 388-9.

Gibbs, C. J., Safar, J., Ceroni, M., Di Martino, A., Clark, W. W. and Hourrigan, J. L. (1990) 'Experimental transmission of scrapie to cattle', *Lancet,* 335(8700), pp. 1275.
Gilch, S., Chitoor, N., Taguchi, Y., Stuart, M., Jewell, J. E. and Schätzl, H. M. (2011) 'Chronic wasting disease', *Top Curr Chem,* 305, pp. 51-77.
Glatzel, M. and Aguzzi, A. (2000) 'Peripheral pathogenesis of prion diseases', *Microbes Infect,* 2(6), pp. 613-9.
Goldmann, W. (2008) 'PrP genetics in ruminant transmissible spongiform encephalopathies', *Vet Res,* 39(4), pp. 30.
Goldmann, W., Hunter, N., Foster, J. D., Salbaum, J. M., Beyreuther, K. and Hope, J. (1990) 'Two alleles of a neural protein gene linked to scrapie in sheep', *Proc Natl Acad Sci U S A,* 87(7), pp. 2476-80.
Gousset, K., Schiff, E., Langevin, C., Marijanovic, Z., Caputo, A., Browman, D. T., Chenouard, N., de Chaumont, F., Martino, A., Enninga, J., Olivo-Marin, J. C., Männel, D. and Zurzolo, C. (2009) 'Prions hijack tunnelling nanotubes for intercellular spread', *Nat Cell Biol,* 11(3), pp. 328-36.
Govaerts, C., Wille, H., Prusiner, S. B. and Cohen, F. E. (2004) 'Evidence for assembly of prions with left-handed beta-helices into trimers', *Proc Natl Acad Sci U S A,* 101(22), pp. 8342-7.
Greenlee, J. J., Smith, J. D., West Greenlee, M. H. and Nicholson, E. M. (2012) 'Clinical and pathologic features of H-type bovine spongiform encephalopathy associated with E211K prion protein polymorphism', *PLoS One,* 7(6), pp. e38678.
Gretzschel, A., Buschmann, A., Langeveld, J. and Groschup, M. H. (2006) 'Immunological characterization of abnormal prion protein from atypical scrapie cases in sheep using a panel of monoclonal antibodies', *J Gen Virol,* 87(Pt 12), pp. 3715-22.
Griffith, J. S. (1967) 'Self-replication and scrapie', *Nature,* 215(5105), pp. 1043-4.
Groschup, M. H., Beekes, M., McBride, P. A., Hardt, M., Hainfellner, J. A. and Budka, H. (1999) 'Deposition of disease-associated prion protein involves the peripheral nervous system in experimental scrapie', *Acta Neuropathol,* 98(5), pp. 453-7.
Groth, A. C., Fish, M., Nusse, R. and Calos, M. P. (2004) 'Construction of transgenic *Drosophila* by using the site-specific integrase from phage phiC31', *Genetics,* 166(4), pp. 1775-82.
Guo, J. L. and Lee, V. M. (2014) 'Cell-to-cell transmission of pathogenic proteins in neurodegenerative diseases', *Nat Med,* 20(2), pp. 130-8.
Haddon, D. J., Hughes, M. R., Antignano, F., Westaway, D., Cashman, N. R. and McNagny, K. M. (2009) 'Prion protein expression and release by mast cells after activation', *J Infect Dis,* 200(5), pp. 827-31.
Hadlow, W. J. (1959) 'Scrapie and kuru', *Lancet,* pp. 298-290.
Haigh, C. L., Tumpach, C., Drew, S. C. and Collins, S. J. (2015) 'The Prion Protein N1 and N2 Cleavage Fragments Bind to Phosphatidylserine and Phosphatidic Acid; Relevance to Stress-Protection Responses', *PLoS One,* 10(8), pp. e0134680.
Haley, N. J., Mathiason, C. K., Carver, S., Zabel, M., Telling, G. C. and Hoover, E. A. (2011) 'Detection of chronic wasting disease prions in salivary, urinary, and intestinal tissues of deer: potential mechanisms of prion shedding and transmission', *J Virol,* 85(13), pp. 6309-18.
Halliday, M., Radford, H., Zents, K. A. M., Molloy, C., Moreno, J. A., Verity, N. C., Smith, E., Ortori, C. A., Barrett, D. A., Bushell, M. and Mallucci, G. R. (2017) 'Repurposed drugs targeting eIF2α-P-mediated translational repression prevent neurodegeneration in mice', *Brain,* 140(6), pp. 1768-1783.

Haraguchi, T., Fisher, S., Olofsson, S., Endo, T., Groth, D., Tarentino, A., Borchelt, D. R., Teplow, D., Hood, L. and Burlingame, A. (1989) 'Asparagine-linked glycosylation of the scrapie and cellular prion proteins', *Arch Biochem Biophys,* 274(1), pp. 1-13.

Harman, J. L. and Silva, C. J. (2009) 'Bovine spongiform encephalopathy', *J Am Vet Med Assoc,* 234(1), pp. 59-72.

Harris, D. A. (1999) 'Cell biological studies of the prion protein', *Curr Issues Mol Biol,* 1(1-2), pp. 65-75.

Harris, D. A. (2003) 'Trafficking, turnover and membrane topology of PrP', *Br Med Bull,* 66, pp. 71-85.

Harris, D. A., Chiesa, R., Drisaldi, B., Quaglio, E., Migheli, A., Piccardo, P. and Ghetti, B. (2003) 'A murine model of a familial prion disease', *Clin Lab Med,* 23(1), pp. 175-86.

Harris, K. P. and Littleton, J. T. (2015) 'Transmission, Development, and Plasticity of Synapses', *Genetics,* 201(2), pp. 345-75.

Hauw, J. J., Sazdovitch, V., Laplanche, J. L., Peoc'h, K., Kopp, N., Kemeny, J., Privat, N., Delasnerie-Lauprêtre, N., Brandel, J. P., Deslys, J. P., Dormont, D. and Alpérovitch, A. (2000) 'Neuropathologic variants of sporadic Creutzfeldt-Jakob disease and codon 129 of PrP gene', *Neurology,* 54(8), pp. 1641-6.

Hay, B., Barry, R. A., Lieberburg, I., Prusiner, S. B. and Lingappa, V. R. (1987a) 'Biogenesis and transmembrane orientation of the cellular isoform of the scrapie prion protein [published errratum appears in Mol Cell Biol 1987 May;7(5):2035]', *Mol Cell Biol,* 7(2), pp. 914-20.

Hay, B., Prusiner, S. B. and Lingappa, V. R. (1987b) 'Evidence for a secretory form of the cellular prion protein', *Biochemistry,* 26(25), pp. 8110-5.

Hayashi, S., Ito, K., Sado, Y., Taniguchi, M., Akimoto, A., Takeuchi, H., Aigaki, T., Matsuzaki, F., Nakagoshi, H., Tanimura, T., Ueda, R., Uemura, T., Yoshihara, M. and Goto, S. (2002) 'GETDB, a database compiling expression patterns and molecular locations of a collection of Gal4 enhancer traps', *Genesis,* 34(1-2), pp. 58-61.

Hegde, R. S., Mastrianni, J. A., Scott, M. R., DeFea, K. A., Tremblay, P., Torchia, M., DeArmond, S. J., Prusiner, S. B. and Lingappa, V. R. (1998) 'A transmembrane form of the prion protein in neurodegenerative disease', *Science,* 279(5352), pp. 827-34.

Heggebø, R., Press, C. M., Gunnes, G., González, L. and Jeffrey, M. (2002) 'Distribution and accumulation of PrP in gut-associated and peripheral lymphoid tissue of scrapie-affected Suffolk sheep', *J Gen Virol,* 83(Pt 2), pp. 479-89.

Heikenwalder, M., Zeller, N., Seeger, H., Prinz, M., Klöhn, P. C., Schwarz, P., Ruddle, N. H., Weissmann, C. and Aguzzi, A. (2005) 'Chronic lymphocytic inflammation specifies the organ tropism of prions', *Science,* 307(5712), pp. 1107-10.

Henderson, D. M., Manca, M., Haley, N. J., Denkers, N. D., Nalls, A. V., Mathiason, C. K., Caughey, B. and Hoover, E. A. (2013) 'Rapid antemortem detection of CWD prions in deer saliva', *PLoS One,* 8(9), pp. e74377.

Henstridge, C. M., Sideris, D. I., Carroll, E., Rotariu, S., Salomonsson, S., Tzioras, M., McKenzie, C. A., Smith, C., von Arnim, C. A. F., Ludolph, A. C., Lulé, D., Leighton, D., Warner, J., Cleary, E., Newton, J., Swingler, R., Chandran, S., Gillingwater, T. H., Abrahams, S. and Spires-Jones, T. L. (2018) 'Synapse loss in the prefrontal cortex is associated with cognitive decline in amyotrophic lateral sclerosis', *Acta Neuropathol,* 135(2), pp. 213-226.

Herms, J., Tings, T., Gall, S., Madlung, A., Giese, A., Siebert, H., Schürmann, P., Windl, O., Brose, N. and Kretzschmar, H. (1999) 'Evidence of presynaptic location and function of the prion protein', *J Neurosci,* 19(20), pp. 8866-75.

Herrmann, L. M., Cheevers, W. P., Davis, W. C., Knowles, D. P. and O'Rourke, K. I. (2003) 'CD21-positive follicular dendritic cells: A possible source of PrPSc in lymph node macrophages of scrapie-infected sheep', *Am J Pathol,* 162(4), pp. 1075-81.

Herrmann, U. S., Sonati, T., Falsig, J., Reimann, R. R., Dametto, P., O'Connor, T., Li, B., Lau, A., Hornemann, S., Sorce, S., Wagner, U., Sanoudou, D. and Aguzzi, A. (2015) 'Prion infections and anti-PrP antibodies trigger converging neurotoxic pathways', *PLoS Pathog,* 11(2), pp. e1004662.

Hetz, C., Russelakis-Carneiro, M., Maundrell, K., Castilla, J. and Soto, C. (2003) 'Caspase-12 and endoplasmic reticulum stress mediate neurotoxicity of pathological prion protein', *EMBO J,* 22(20), pp. 5435-45.

Hill, A. F. and Collinge, J. (2003) 'Subclinical prion infection in humans and animals', *Br Med Bull,* 66, pp. 161-70.

Hill, A. F., Desbruslais, M., Joiner, S., Sidle, K. C., Gowland, I., Collinge, J., Doey, L. J. and Lantos, P. (1997) 'The same prion strain causes vCJD and BSE', *Nature,* 389(6650), pp. 448-50, 526.

Hill, A. F., Joiner, S., Beck, J. A., Campbell, T. A., Dickinson, A., Poulter, M., Wadsworth, J. D. and Collinge, J. (2006) 'Distinct glycoform ratios of protease resistant prion protein associated with PRNP point mutations', *Brain,* 129(Pt 3), pp. 676-85.

Hilton, D. A., Sutak, J., Smith, M. E., Penney, M., Conyers, L., Edwards, P., McCardle, L., Ritchie, D., Head, M. W., Wiley, C. A. and Ironside, J. W. (2004) 'Specificity of lymphoreticular accumulation of prion protein for variant Creutzfeldt-Jakob disease', *J Clin Pathol,* 57(3), pp. 300-2.

Hirth, F. (2010) '*Drosophila* melanogaster in the study of human neurodegeneration', *CNS Neurol Disord Drug Targets,* 9(4), pp. 504-23.

Hope, J., Reekie, L. J., Hunter, N., Multhaup, G., Beyreuther, K., White, H., Scott, A. C., Stack, M. J., Dawson, M. and Wells, G. A. (1988) 'Fibrils from brains of cows with new cattle disease contain scrapie-associated protein', *Nature,* 336(6197), pp. 390-2.

Hornshaw, M. P., McDermott, J. R., Candy, J. M. and Lakey, J. H. (1995) 'Copper binding to the N-terminal tandem repeat region of mammalian and avian prion protein: structural studies using synthetic peptides', *Biochem Biophys Res Commun,* 214(3), pp. 993-9.

Houston, F., Foster, J. D., Chong, A., Hunter, N. and Bostock, C. J. (2000) 'Transmission of BSE by blood transfusion in sheep', *Lancet,* 356(9234), pp. 999-1000.

Hsiao, K. K., Scott, M., Foster, D., Groth, D. F., DeArmond, S. J. and Prusiner, S. B. (1990) 'Spontaneous neurodegeneration in transgenic mice with mutant prion protein', *Science,* 250(4987), pp. 1587-90.

Huang, Z., Prusiner, S. B. and Cohen, F. E. (1996) 'Structures of prion proteins and conformational models for prion diseases', *Curr Top Microbiol Immunol,* 207, pp. 49-67.

Hunter, N. (1997) 'PrP genetics in sheep and the applications for scrapie and BSE', *Trends Microbiol,* 5(8), pp. 331-4.

Hwang, D., Lee, I. Y., Yoo, H., Gehlenborg, N., Cho, J. H., Petritis, B., Baxter, D., Pitstick, R., Young, R., Spicer, D., Price, N. D., Hohmann, J. G., Dearmond, S. J., Carlson, G. A. and Hood, L. E. (2009) 'A systems approach to prion disease', *Mol Syst Biol,* 5, pp. 252.

Imran, M. and Mahmood, S. (2011a) 'An overview of animal prion diseases', *Virol J,* 8, pp. 493.

Imran, M. and Mahmood, S. (2011b) 'An overview of human prion diseases', *Virol J,* 8, pp. 559.

Jackson, G. R., Salecker, I., Dong, X., Yao, X., Arnheim, N., Faber, P. W., MacDonald, M. E. and Zipursky, S. L. (1998) 'Polyglutamine-expanded human huntingtin transgenes induce degeneration of *Drosophila* photoreceptor neurons', *Neuron,* 21(3), pp. 633-42.

Jackson, G. S., Murray, I., Hosszu, L. L., Gibbs, N., Waltho, J. P., Clarke, A. R. and Collinge, J. (2001) 'Location and properties of metal-binding sites on the human prion protein', *Proc Natl Acad Sci U S A,* 98(15), pp. 8531-5.

Jackson, W. S., Borkowski, A. W., Faas, H., Steele, A. D., King, O. D., Watson, N., Jasanoff, A. and Lindquist, S. (2009) 'Spontaneous generation of prion infectivity in fatal familial insomnia knockin mice', *Neuron,* 63(4), pp. 438-50.

Jackson, W. S., Borkowski, A. W., Watson, N. E., King, O. D., Faas, H., Jasanoff, A. and Lindquist, S. (2013) 'Profoundly different prion diseases in knock-in mice carrying single PrP codon substitutions associated with human diseases', *Proc Natl Acad Sci U S A,* 110(36), pp. 14759-64.

Jacobs, J. R. and Goodman, C. S. (1989) 'Embryonic development of axon pathways in the *Drosophila* CNS. II. Behavior of pioneer growth cones', *J Neurosci,* 9(7), pp. 2412-22.

Jan, L. Y. and Jan, Y. N. (1976) 'Properties of the larval neuromuscular junction in *Drosophila* melanogaster', *J Physiol,* 262(1), pp. 189-214.

Jang, B., Jin, J. K., Jeon, Y. C., Cho, H. J., Ishigami, A., Choi, K. C., Carp, R. I., Maruyama, N., Kim, Y. S. and Choi, E. K. (2010) 'Involvement of peptidylarginine deiminase-mediated post-translational citrullination in pathogenesis of sporadic Creutzfeldt-Jakob disease', *Acta Neuropathol,* 119(2), pp. 199-210.

Jansen, C., Parchi, P., Capellari, S., Vermeij, A. J., Corrado, P., Baas, F., Strammiello, R., van Gool, W. A., van Swieten, J. C. and Rozemuller, A. J. (2010) 'Prion protein amyloidosis with divergent phenotype associated with two novel nonsense mutations in PRNP', *Acta Neuropathol,* 119(2), pp. 189-97.

Jarrett, J. T. and Lansbury, P. T. (1993) 'Seeding "one-dimensional crystallization" of amyloid: a pathogenic mechanism in Alzheimer's disease and scrapie?', *Cell,* 73(6), pp. 1055-8.

Jayadev, S., Nochlin, D., Poorkaj, P., Steinbart, E. J., Mastrianni, J. A., Montine, T. J., Ghetti, B., Schellenberg, G. D., Bird, T. D. and Leverenz, J. B. (2011) 'Familial prion disease with Alzheimer disease-like tau pathology and clinical phenotype', *Ann Neurol,* 69(4), pp. 712-20.

Jeffrey, M. and González, L. (2007) 'Classical sheep transmissible spongiform encephalopathies: pathogenesis, pathological phenotypes and clinical disease', *Neuropathol Appl Neurobiol,* 33(4), pp. 373-94.

Jendroska, K., Heinzel, F. P., Torchia, M., Stowring, L., Kretzschmar, H. A., Kon, A., Stern, A., Prusiner, S. B. and DeArmond, S. J. (1991) 'Proteinase-resistant prion protein accumulation in Syrian hamster brain correlates with regional pathology and scrapie infectivity', *Neurology,* 41(9), pp. 1482-90.

Jenett, A., Rubin, G. M., Ngo, T. T., Shepherd, D., Murphy, C., Dionne, H., Pfeiffer, B. D., Cavallaro, A., Hall, D., Jeter, J., Iyer, N., Fetter, D., Hausenfluck, J. H., Peng, H., Trautman, E. T., Svirskas, R. R., Myers, E. W., Iwinski, Z. R., Aso, Y., DePasquale, G. M., Enos, A., Hulamm, P., Lam, S. C., Li, H. H., Laverty, T. R., Long, F., Qu, L., Murphy, S. D., Rokicki, K., Safford, T., Shaw, K., Simpson, J. H., Sowell, A., Tae, S., Yu, Y. and Zugates, C. T. (2012) 'A GAL4-driver line resource for *Drosophila* neurobiology', *Cell Rep,* 2(4), pp. 991-1001.

Johansen, J., Halpern, M. E., Johansen, K. M. and Keshishian, H. (1989) 'Stereotypic morphology of glutamatergic synapses on identified muscle cells of *Drosophila* larvae', *J Neurosci,* 9(2), pp. 710-25.

Kaatz, M., Fast, C., Ziegler, U., Balkema-Buschmann, A., Hammerschmidt, B., Keller, M., Oelschlegel, A., McIntyre, L. and Groschup, M. H. (2012) 'Spread of classic BSE prions from the gut via the peripheral nervous system to the brain', *Am J Pathol,* 181(2), pp. 515-24.

Kaczmarczyk, L. and Jackson, W. S. (2015) 'Astonishing advances in mouse genetic tools for biomedical research', *Swiss Med Wkly,* 145, pp. w14186.
Kanu, N., Imokawa, Y., Drechsel, D. N., Williamson, R. A., Birkett, C. R., Bostock, C. J. and Brockes, J. P. (2002) 'Transfer of scrapie prion infectivity by cell contact in culture', *Curr Biol,* 12(7), pp. 523-30.
Katz, P., Grillner, S., Wilson, R., Borst, A., Greenspan, R., Buzsáki, G., Martin, K., Marder, E., Kristan, W., Friedrich, R. and Chklovskii, D. (2013) 'Vertebrate versus invertebrate neural circuits', *Curr Biol,* 23(12), pp. R504-6.
Kaufman, S. K. and Diamond, M. I. (2013) 'Prion-like propagation of protein aggregation and related therapeutic strategies', *Neurotherapeutics,* 10(3), pp. 371-82.
Kavi, H. H., Fernandez, H. R., Xie, W. and Birchler, J. A. (2005) 'RNA silencing in *Drosophila*', *FEBS Lett,* 579(26), pp. 5940-9.
Keshishian, H., Broadie, K., Chiba, A. and Bate, M. (1996) 'The *Drosophila* neuromuscular junction: a model system for studying synaptic development and function', *Annu Rev Neurosci,* 19, pp. 545-75.
Khalifé, M., Young, R., Passet, B., Halliez, S., Vilotte, M., Jaffrezic, F., Marthey, S., Béringue, V., Vaiman, D., Le Provost, F., Laude, H. and Vilotte, J. L. (2011) 'Transcriptomic analysis brings new insight into the biological role of the prion protein during mouse embryogenesis', *PLoS One,* 6(8), pp. e23253.
Khanam, S., Naz, F., Ali, F., Jyoti, S., Fatima, A., Khan, W., Singh, B. R., Naqvi, A. H. and Siddique, Y. H. (2018) 'Effect of cabergoline alginate nanocomposite on the transgenic *Drosophila* melanogaster model of Parkinson's disease', *Toxicol Mech Methods,* pp. 1-31.
Kim, T. Y., Shon, H. J., Joo, Y. S., Mun, U. K., Kang, K. S. and Lee, Y. S. (2005) 'Additional cases of Chronic Wasting Disease in imported deer in Korea', *J Vet Med Sci,* 67(8), pp. 753-9.
Kimberlin, R. H. and Walker, C. (1977) 'Characteristics of a short incubation model of scrapie in the golden hamster', *J Gen Virol,* 34(2), pp. 295-304.
Kimberlin, R. H. and Walker, C. A. (1978) 'Evidence that the transmission of one source of scrapie agent to hamsters involves separation of agent strains from a mixture', *J Gen Virol,* 39(3), pp. 487-96.
Kimberlin, R. H. and Walker, C. A. (1989) 'Pathogenesis of scrapie in mice after intragastric infection', *Virus Res,* 12(3), pp. 213-20.
Kimberlin, R. H. and Wilesmith, J. W. (1994) 'Bovine spongiform encephalopathy. Epidemiology, low dose exposure and risks', *Ann N Y Acad Sci,* 724, pp. 210-20.
Kirschbaum, W. R. (1924) 'Zwei eigenartige Erkrankung des Zentralnervensystems nach Art der spatischen Pseudosklerose (Jakob)', *Z Neurol Psychiatry,* 92, pp. 175-220.
Klamt, F., Dal-Pizzol, F., Conte da Frota, M. L., Walz, R., Andrades, M. E., da Silva, E. G., Brentani, R. R., Izquierdo, I. and Fonseca Moreira, J. C. (2001) 'Imbalance of antioxidant defense in mice lacking cellular prion protein', *Free Radic Biol Med,* 30(10), pp. 1137-44.
Klueg, K. M., Alvarado, D., Muskavitch, M. A. and Duffy, J. B. (2002) 'Creation of a GAL4/UAS-coupled inducible gene expression system for use in *Drosophila* cultured cell lines', *Genesis,* 34(1-2), pp. 119-22.
Klöhn, P. C., Castro-Seoane, R. and Collinge, J. (2013) 'Exosome release from infected dendritic cells: a clue for a fast spread of prions in the periphery?', *J Infect,* 67(5), pp. 359-68.
Kocisko, D. A., Come, J. H., Priola, S. A., Chesebro, B., Raymond, G. J., Lansbury, P. T. and Caughey, B. (1994) 'Cell-free formation of protease-resistant prion protein', *Nature,* 370(6489), pp. 471-4.

Konold, T., Bone, G. E., Clifford, D., Chaplin, M. J., Cawthraw, S., Stack, M. J. and Simmons, M. M. (2012) 'Experimental H-type and L-type bovine spongiform encephalopathy in cattle: observation of two clinical syndromes and diagnostic challenges', *BMC Vet Res,* 8, pp. 22.

Kontopoulos, E., Parvin, J. D. and Feany, M. B. (2006) 'Alpha-synuclein acts in the nucleus to inhibit histone acetylation and promote neurotoxicity', *Hum Mol Genet,* 15(20), pp. 3012-23.

Kretzschmar, H. A. (1993) 'Human prion diseases (spongiform encephalopathies)', *Arch Virol Suppl,* 7, pp. 261-93.

Kretzschmar, H. A., Neumann, M. and Stavrou, D. (1995) 'Codon 178 mutation of the human prion protein gene in a German family (Backer family): sequencing data from 72-year-old celloidin-embedded brain tissue', *Acta Neuropathol,* 89(1), pp. 96-8.

Kurt, T. D. and Sigurdson, C. J. (2016) 'Cross-species transmission of CWD prions', *Prion,* 10(1), pp. 83-91.

Lacroux, C., Vilette, D., Fernández-Borges, N., Litaise, C., Lugan, S., Morel, N., Corbière, F., Simon, S., Simmons, H., Costes, P., Weisbecker, J. L., Lantier, I., Lantier, F., Schelcher, F., Grassi, J., Castilla, J. and Andréoletti, O. (2012) 'Prionemia and leukocyte-platelet-associated infectivity in sheep transmissible spongiform encephalopathy models', *J Virol,* 86(4), pp. 2056-66.

Lai, S. L. and Lee, T. (2006) 'Genetic mosaic with dual binary transcriptional systems in *Drosophila*', *Nat Neurosci,* 9(5), pp. 703-9.

Landgraf, M. and Thor, S. (2006) 'Development of *Drosophila* motoneurons: specification and morphology', *Semin Cell Dev Biol,* 17(1), pp. 3-11.

Lasmézas, C. I., Deslys, J. P., Demaimay, R., Adjou, K. T., Lamoury, F., Dormont, D., Robain, O., Ironside, J. and Hauw, J. J. (1996) 'BSE transmission to macaques', *Nature,* 381(6585), pp. 743-4.

Lasmézas, C. I., Deslys, J. P., Robain, O., Jaegly, A., Beringue, V., Peyrin, J. M., Fournier, J. G., Hauw, J. J., Rossier, J. and Dormont, D. (1997) 'Transmission of the BSE agent to mice in the absence of detectable abnormal prion protein', *Science,* 275(5298), pp. 402-5.

Lasmézas, C. I., Fournier, J. G., Nouvel, V., Boe, H., Marcé, D., Lamoury, F., Kopp, N., Hauw, J. J., Ironside, J., Bruce, M., Dormont, D. and Deslys, J. P. (2001) 'Adaptation of the bovine spongiform encephalopathy agent to primates and comparison with Creutzfeldt-- Jakob disease: implications for human health', *Proc Natl Acad Sci U S A,* 98(7), pp. 4142-7.

Lasmézas, C. I., Comoy, E., Hawkins, S., Herzog, C., Mouthon, F., Konold, T., Auvré, F., Correia, E., Lescoutra-Etchegaray, N., Salès, N., Wells, G., Brown, P. and Deslys, J. P. (2005) 'Risk of oral infection with bovine spongiform encephalopathy agent in primates', *Lancet,* 365(9461), pp. 781-3.

Latarjet, R., Muel, B., Haig, D. A., Clarke, M. C. and Alper, T. (1970) 'Inactivation of the scrapie agent by near monochromatic ultraviolet light', *Nature,* 227(5265), pp. 1341-3.

Lawson, V. A., Priola, S. A., Wehrly, K. and Chesebro, B. (2001) 'N-terminal truncation of prion protein affects both formation and conformation of abnormal protease-resistant prion protein generated in vitro', *J Biol Chem,* 276(38), pp. 35265-71.

Le Dur, A., Béringue, V., Andréoletti, O., Reine, F., Laï, T. L., Baron, T., Bratberg, B., Vilotte, J. L., Sarradin, P., Benestad, S. L. and Laude, H. (2005) 'A newly identified type of scrapie agent can naturally infect sheep with resistant PrP genotypes', *Proc Natl Acad Sci U S A,* 102(44), pp. 16031-6.

Le Pichon, C. E., Valley, M. T., Polymenidou, M., Chesler, A. T., Sagdullaev, B. T., Aguzzi, A. and Firestein, S. (2009) 'Olfactory behavior and physiology are disrupted in prion protein knockout mice', *Nat Neurosci,* 12(1), pp. 60-9.

Leblanc, P., Arellano-Anaya, Z. E., Bernard, E., Gallay, L., Provansal, M., Lehmann, S., Schaeffer, L., Raposo, G. and Vilette, D. (2017) 'Isolation of Exosomes and Microvesicles from Cell Culture Systems to Study Prion Transmission', *Methods Mol Biol,* 1545, pp. 153-176.

Lee, J., Ueda, A. and Wu, C. F. (2008) 'Pre- and post-synaptic mechanisms of synaptic strength homeostasis revealed by slowpoke and shaker K+ channel mutations in *Drosophila*', *Neuroscience,* 154(4), pp. 1283-96.

Legname, G. and Moda, F. (2017) 'The Prion Concept and Synthetic Prions', *Prog Mol Biol Transl Sci,* 150, pp. 147-156.

Lescoutra-Etchegaray, N., Jaffré, N., Sumian, C., Durand, V., Correia, E., Mikol, J., Luccantoni-Freire, S., Culeux, A., Deslys, J. P. and Comoy, E. E. (2015) 'Evaluation of the protection of primates transfused with variant Creutzfeldt-Jakob disease-infected blood products filtered with prion removal devices: a 5-year update', *Transfusion,* 55(6), pp. 1231-41.

Levin, E. C., Acharya, N. K., Sedeyn, J. C., Venkataraman, V., D'Andrea, M. R., Wang, H. Y. and Nagele, R. G. (2009) 'Neuronal expression of vimentin in the Alzheimer's disease brain may be part of a generalized dendritic damage-response mechanism', *Brain Res,* 1298, pp. 194-207.

Lewis, E. B. (1960) 'A new standard food medium', *Drosophila Information Service 34,* pp. 117-118.

Li, J., Browning, S., Mahal, S. P., Oelschlegel, A. M. and Weissmann, C. (2010) 'Darwinian evolution of prions in cell culture', *Science,* 327(5967), pp. 869-72.

Li, J. Y., Plomann, M. and Brundin, P. (2003) 'Huntington's disease: a synaptopathy?', *Trends Mol Med,* 9(10), pp. 414-20.

Li, X. L., Wang, G. R., Jing, Y. Y., Pan, M. M., Dong, C. F., Zhou, R. M., Wang, Z. Y., Shi, Q., Gao, C. and Dong, X. P. (2011) 'Cytosolic PrP induces apoptosis of cell by disrupting microtubule assembly', *J Mol Neurosci,* 43(3), pp. 316-25.

Liberski, P. P., Sikorska, B., Hauw, J. J., Kopp, N., Streichenberger, N., Giraud, P., Boellaard, J., Budka, H., Kovacs, G. G., Ironside, J. and Brown, P. (2010) 'Ultrastructural characteristics (or evaluation) of Creutzfeldt-Jakob disease and other human transmissible spongiform encephalopathies or prion diseases', *Ultrastruct Pathol,* 34(6), pp. 351-61.

Liemann, S. and Glockshuber, R. (1999) 'Influence of amino acid substitutions related to inherited human prion diseases on the thermodynamic stability of the cellular prion protein', *Biochemistry,* 38(11), pp. 3258-67.

Ligios, C., Sigurdson, C. J., Santucciu, C., Carcassola, G., Manco, G., Basagni, M., Maestrale, C., Cancedda, M. G., Madau, L. and Aguzzi, A. (2005) 'PrPSc in mammary glands of sheep affected by scrapie and mastitis', *Nat Med,* 11(11), pp. 1137-8.

Lima, F. R., Arantes, C. P., Muras, A. G., Nomizo, R., Brentani, R. R. and Martins, V. R. (2007) 'Cellular prion protein expression in astrocytes modulates neuronal survival and differentiation', *J Neurochem,* 103(6), pp. 2164-76.

Lin, D. M., Auld, V. J. and Goodman, C. S. (1995) 'Targeted neuronal cell ablation in the *Drosophila* embryo: pathfinding by follower growth cones in the absence of pioneers', *Neuron,* 14(4), pp. 707-15.

Lindholm, D., Wootz, H. and Korhonen, L. (2006) 'ER stress and neurodegenerative diseases', *Cell Death Differ,* 13(3), pp. 385-92.

Little, J. W. and Mount, D. W. (1982) 'The SOS regulatory system of Escherichia coli', *Cell,* 29(1), pp. 11-22.

Littleton, J. T. and Ganetzky, B. (2000) 'Ion channels and synaptic organization: analysis of the *Drosophila* genome', *Neuron,* 26(1), pp. 35-43.

Llewelyn, C. A., Hewitt, P. E., Knight, R. S., Amar, K., Cousens, S., Mackenzie, J. and Will, R. G. (2004) 'Possible transmission of variant Creutzfeldt-Jakob disease by blood transfusion', *Lancet,* 363(9407), pp. 417-21.

Lloyd, S. E., Mead, S. and Collinge, J. (2013) 'Genetics of prion diseases', *Curr Opin Genet Dev,* 23(3), pp. 345-51.

Lu, B. and Vogel, H. (2009) '*Drosophila* models of neurodegenerative diseases', *Annu Rev Pathol,* 4, pp. 315-42.

Lu, X., Wintrode, P. L. and Surewicz, W. K. (2007) 'Beta-sheet core of human prion protein amyloid fibrils as determined by hydrogen/deuterium exchange', *Proc Natl Acad Sci U S A,* 104(5), pp. 1510-5.

Lugaresi, E., Medori, R., Montagna, P., Baruzzi, A., Cortelli, P., Lugaresi, A., Tinuper, P., Zucconi, M. and Gambetti, P. (1986) 'Fatal familial insomnia and dysautonomia with selective degeneration of thalamic nuclei', *N Engl J Med,* 315(16), pp. 997-1003.

Lugaresi, E., Tobler, I., Gambetti, P. and Montagna, P. (1998) 'The pathophysiology of fatal familial insomnia', *Brain Pathol,* 8(3), pp. 521-6.

Luk, K. C., Kehm, V., Carroll, J., Zhang, B., O'Brien, P., Trojanowski, J. Q. and Lee, V. M. (2012) 'Pathological α-synuclein transmission initiates Parkinson-like neurodegeneration in nontransgenic mice', *Science,* 338(6109), pp. 949-53.

Luo, L., Tully, T. and White, K. (1992) 'Human amyloid precursor protein ameliorates behavioral deficit of flies deleted for Appl gene', *Neuron,* 9(4), pp. 595-605.

Ma, J. and Ptashne, M. (1987) 'The carboxy-terminal 30 amino acids of GAL4 are recognized by GAL80', *Cell,* 50(1), pp. 137-42.

Ma, J. and Lindquist, S. (2002) 'Conversion of PrP to a self-perpetuating PrPSc-like conformation in the cytosol', *Science,* 298(5599), pp. 1785-8.

Ma, J., Wollmann, R. and Lindquist, S. (2002) 'Neurotoxicity and neurodegeneration when PrP accumulates in the cytosol', *Science,* 298(5599), pp. 1781-5.

Ma, W. W., Tao, Y., Wang, Y. Y. and Peng, I. F. (2017) 'Effects of Gardenia jasminoides extracts on cognition and innate immune response in an adult *Drosophila* model of Alzheimer's disease', *Chin J Nat Med,* 15(12), pp. 899-904.

Maddison, B. C., Baker, C. A., Terry, L. A., Bellworthy, S. J., Thorne, L., Rees, H. C. and Gough, K. C. (2010a) 'Environmental sources of scrapie prions', *J Virol,* 84(21), pp. 11560-2.

Maddison, B. C., Rees, H. C., Baker, C. A., Taema, M., Bellworthy, S. J., Thorne, L., Terry, L. A. and Gough, K. C. (2010b) 'Prions are secreted into the oral cavity in sheep with preclinical scrapie', *J Infect Dis,* 201(11), pp. 1672-6.

Magalhães, A. C., Baron, G. S., Lee, K. S., Steele-Mortimer, O., Dorward, D., Prado, M. A. and Caughey, B. (2005) 'Uptake and neuritic transport of scrapie prion protein coincident with infection of neuronal cells', *J Neurosci,* 25(21), pp. 5207-16.

Makarava, N., Kovacs, G. G., Bocharova, O., Savtchenko, R., Alexeeva, I., Budka, H., Rohwer, R. G. and Baskakov, I. V. (2010) 'Recombinant prion protein induces a new transmissible prion disease in wild-type animals', *Acta Neuropathol,* 119(2), pp. 177-87.

Mallucci, G., Dickinson, A., Linehan, J., Klöhn, P. C., Brandner, S. and Collinge, J. (2003) 'Depleting neuronal PrP in prion infection prevents disease and reverses spongiosis', *Science,* 302(5646), pp. 871-4.

Mallucci, G. R., White, M. D., Farmer, M., Dickinson, A., Khatun, H., Powell, A. D., Brandner, S., Jefferys, J. G. and Collinge, J. (2007) 'Targeting cellular prion protein reverses early cognitive deficits and neurophysiological dysfunction in prion-infected mice', *Neuron,* 53(3), pp. 325-35.

Manson, J. C., Jamieson, E., Baybutt, H., Tuzi, N. L., Barron, R., McConnell, I., Somerville, R., Ironside, J., Will, R., Sy, M. S., Melton, D. W., Hope, J. and Bostock, C. (1999) 'A single amino acid alteration (101L) introduced into murine PrP dramatically alters incubation time of transmissible spongiform encephalopathy', *EMBO J,* 18(23), pp. 6855-64.

Markstein, M., Dettorre, S., Cho, J., Neumüller, R. A., Craig-Müller, S. and Perrimon, N. (2014) 'Systematic screen of chemotherapeutics in *Drosophila* stem cell tumors', *Proc Natl Acad Sci U S A,* 111(12), pp. 4530-5.

Marsh, R. F. and Hadlow, W. J. (1992) 'Transmissible mink encephalopathy', *Rev Sci Tech,* 11(2), pp. 539-50.

Martin, I., Abalde-Atristain, L., Kim, J. W., Dawson, T. M. and Dawson, V. L. (2014) 'Abberant protein synthesis in G2019S LRRK2 *Drosophila* Parkinson disease-related phenotypes', *Fly (Austin),* 8(3), pp. 165-9.

Martín-Peña, A., Rincón-Limas, D. E. and Fernandez-Fúnez, P. (2018) 'Engineered Hsp70 chaperones prevent Aβ42-induced memory impairments in a *Drosophila* model of Alzheimer's disease', *Sci Rep,* 8(1), pp. 9915.

Mastrianni, J. A. (2010) 'The genetics of prion diseases', *Genet Med,* 12(4), pp. 187-95.

Masuda-Suzukake, M., Nonaka, T., Hosokawa, M., Oikawa, T., Arai, T., Akiyama, H., Mann, D. M. and Hasegawa, M. (2013) 'Prion-like spreading of pathological α-synuclein in brain', *Brain,* 136(Pt 4), pp. 1128-38.

Mattei, V., Barenco, M. G., Tasciotti, V., Garofalo, T., Longo, A., Boller, K., Löwer, J., Misasi, R., Montrasio, F. and Sorice, M. (2009) 'Paracrine diffusion of PrP(C) and propagation of prion infectivity by plasma membrane-derived microvesicles', *PLoS One,* 4(4), pp. e5057.

McBride, P. A. and Beekes, M. (1999) 'Pathological PrP is abundant in sympathetic and sensory ganglia of hamsters fed with scrapie', *Neurosci Lett,* 265(2), pp. 135-8.

McGurk, L., Berson, A. and Bonini, N. M. (2015) '*Drosophila* as an In Vivo Model for Human Neurodegenerative Disease', *Genetics,* 201(2), pp. 377-402.

McKinley, M. P., Bolton, D. C. and Prusiner, S. B. (1983) 'A protease-resistant protein is a structural component of the scrapie prion', *Cell,* 35(1), pp. 57-62.

McKinley, M. P., Braunfeld, M. B., Bellinger, C. G. and Prusiner, S. B. (1986) 'Molecular characteristics of prion rods purified from scrapie-infected hamster brains', *J Infect Dis,* 154(1), pp. 110-20.

Mead, S., Stumpf, M. P., Whitfield, J., Beck, J. A., Poulter, M., Campbell, T., Uphill, J. B., Goldstein, D., Alpers, M., Fisher, E. M. and Collinge, J. (2003) 'Balancing selection at the prion protein gene consistent with prehistoric kurulike epidemics', *Science,* 300(5619), pp. 640-3.

Meade-White, K. D., Barbian, K. D., Race, B., Favara, C., Gardner, D., Taubner, L., Porcella, S. and Race, R. (2009) 'Characteristics of 263K scrapie agent in multiple hamster species', *Emerg Infect Dis,* 15(2), pp. 207-15.

Medori, R., Montagna, P., Tritschler, H. J., LeBlanc, A., Cortelli, P., Tinuper, P., Lugaresi, E. and Gambetti, P. (1992) 'Fatal familial insomnia: a second kindred with mutation of prion protein gene at codon 178', *Neurology,* 42(3 Pt 1), pp. 669-70.

Medori, R. and Tritschler, H. J. (1993) 'Prion protein gene analysis in three kindreds with fatal familial insomnia (FFI): codon 178 mutation and codon 129 polymorphism', *Am J Hum Genet,* 53(4), pp. 822-7.

Menon, K. P., Carrillo, R. A. and Zinn, K. (2013) 'Development and plasticity of the *Drosophila* larval neuromuscular junction', *Wiley Interdiscip Rev Dev Biol,* 2(5), pp. 647-70.

Meyer, R. K., McKinley, M. P., Bowman, K. A., Braunfeld, M. B., Barry, R. A. and Prusiner, S. B. (1986) 'Separation and properties of cellular and scrapie prion proteins', *Proc Natl Acad Sci U S A,* 83(8), pp. 2310-4.

Mhatre, S. D., Satyasi, V., Killen, M., Paddock, B. E., Moir, R. D., Saunders, A. J. and Marenda, D. R. (2014) 'Synaptic abnormalities in a *Drosophila* model of Alzheimer's disease', *Dis Model Mech,* 7(3), pp. 373-85.

Miele, G., Jeffrey, M., Turnbull, D., Manson, J. and Clinton, M. (2002) 'Ablation of cellular prion protein expression affects mitochondrial numbers and morphology', *Biochem Biophys Res Commun,* 291(2), pp. 372-7.

Miller, D. L., Ballard, S. L. and Ganetzky, B. (2012) 'Analysis of synaptic growth and function in *Drosophila* with an extended larval stage', *J Neurosci,* 32(40), pp. 13776-86.

Min, K. T. and Benzer, S. (1999) 'Preventing neurodegeneration in the *Drosophila* mutant bubblegum', *Science,* 284(5422), pp. 1985-8.

Mironov, A., Latawiec, D., Wille, H., Bouzamondo-Bernstein, E., Legname, G., Williamson, R. A., Burton, D., DeArmond, S. J., Prusiner, S. B. and Peters, P. J. (2003) 'Cytosolic prion protein in neurons', *J Neurosci,* 23(18), pp. 7183-93.

Mitchell, G. B., Sigurdson, C. J., O'Rourke, K. I., Algire, J., Harrington, N. P., Walther, I., Spraker, T. R. and Balachandran, A. (2012) 'Experimental oral transmission of chronic wasting disease to reindeer (Rangifer tarandus tarandus)', *PLoS One,* 7(6), pp. e39055.

Miyazaki, Y., Ishikawa, T., Kamatari, Y. O., Nakagaki, T., Takatsuki, H., Ishibashi, D., Kuwata, K., Nishida, N. and Atarashi, R. (2018) 'Identification of Alprenolol Hydrochloride as an Anti-prion Compound Using Surface Plasmon Resonance Imaging', *Mol Neurobiol.*

Moda, F., Le, T. N., Aulić, S., Bistaffa, E., Campagnani, I., Virgilio, T., Indaco, A., Palamara, L., Andréoletti, O., Tagliavini, F. and Legname, G. (2015) 'Synthetic prions with novel strain-specified properties', *PLoS Pathog,* 11(12), pp. e1005354.

Mohite, G. M., Dwivedi, S., Das, S., Kumar, R., Paluri, S., Mehra, S., Ruhela, N., S, A., Jha, N. N. and Maji, S. K. (2018) 'Parkinson's Disease Associated α-Synuclein Familial Mutants Promote Dopaminergic Neuronal Death in *Drosophila* melanogaster', *ACS Chem Neurosci.*

Moloney, E. B., de Winter, F. and Verhaagen, J. (2014) 'ALS as a distal axonopathy: molecular mechanisms affecting neuromuscular junction stability in the presymptomatic stages of the disease', *Front Neurosci,* 8, pp. 252.

Monari, L., Chen, S. G., Brown, P., Parchi, P., Petersen, R. B., Mikol, J., Gray, F., Cortelli, P., Montagna, P. and Ghetti, B. (1994) 'Fatal familial insomnia and familial Creutzfeldt-Jakob disease: different prion proteins determined by a DNA polymorphism', *Proc Natl Acad Sci U S A,* 91(7), pp. 2839-42.

Montagna, P., Gambetti, P., Cortelli, P. and Lugaresi, E. (2003) 'Familial and sporadic fatal insomnia', *Lancet Neurol,* 2(3), pp. 167-76.

Moore, R. A., Sturdevant, D. E., Chesebro, B. and Priola, S. A. (2014) 'Proteomics analysis of amyloid and nonamyloid prion disease phenotypes reveals both common and divergent mechanisms of neuropathogenesis', *J Proteome Res,* 13(11), pp. 4620-34.

Moore, R. A., Vorberg, I. and Priola, S. A. (2005) 'Species barriers in prion diseases--brief review', *Arch Virol Suppl,* (19), pp. 187-202.

Morales, R. (2017) 'Prion strains in mammals: Different conformations leading to disease', *PLoS Pathog,* 13(7), pp. e1006323.

Moreno, J. A., Radford, H., Peretti, D., Steinert, J. R., Verity, N., Martin, M. G., Halliday, M., Morgan, J., Dinsdale, D., Ortori, C. A., Barrett, D. A., Tsaytler, P., Bertolotti, A., Willis, A.

E., Bushell, M. and Mallucci, G. R. (2012) 'Sustained translational repression by eIF2α-P mediates prion neurodegeneration', *Nature,* 485(7399), pp. 507-11.
Mosher, K. I. and Wyss-Coray, T. (2014) 'Microglial dysfunction in brain aging and Alzheimer's disease', *Biochem Pharmacol,* 88(4), pp. 594-604.
Moum, T., Olsaker, I., Hopp, P., Moldal, T., Valheim, M. and Benestad, S. L. (2005) 'Polymorphisms at codons 141 and 154 in the ovine prion protein gene are associated with scrapie Nor98 cases', *J Gen Virol,* 86(Pt 1), pp. 231-5.
Moya, K. L., Salès, N., Hässig, R., Créminon, C., Grassi, J. and Di Giamberardino, L. (2000) 'Immunolocalization of the cellular prion protein in normal brain', *Microsc Res Tech,* 50(1), pp. 58-65.
Muhammad, F. (2012) *Use of Drosophila to model ovine prion disease.* PhD, University of Cambridge, Cambridge.
Murali, A., Maue, R. A. and Dolph, P. J. (2014) 'Reversible symptoms and clearance of mutant prion protein in an inducible model of a genetic prion disease in *Drosophila* melanogaster', *Neurobiol Dis,* 67, pp. 71-8.
Muramoto, T., Kitamoto, T., Hoque, M. Z., Tateishi, J. and Goto, I. (1993) 'Species barrier prevents an abnormal isoform of prion protein from accumulating in follicular dendritic cells of mice with Creutzfeldt-Jakob disease', *J Virol,* 67(11), pp. 6808-10.
Nathanson, N., Wilesmith, J. and Griot, C. (1997) 'Bovine spongiform encephalopathy (BSE): causes and consequences of a common source epidemic', *Am J Epidemiol,* 145(11), pp. 959-69.
Nishimune, H. (2012) 'Active zones of mammalian neuromuscular junctions: formation, density, and aging', *Ann N Y Acad Sci,* 1274, pp. 24-32.
Nonno, R., Di Bari, M. A., Cardone, F., Vaccari, G., Fazzi, P., Dell'Omo, G., Cartoni, C., Ingrosso, L., Boyle, A., Galeno, R., Sbriccoli, M., Lipp, H. P., Bruce, M., Pocchiari, M. and Agrimi, U. (2006) 'Efficient transmission and characterization of Creutzfeldt-Jakob disease strains in bank voles', *PLoS Pathog,* 2(2), pp. e12.
Nose, A. (2012) 'Generation of neuromuscular specificity in *Drosophila*: novel mechanisms revealed by new technologies', *Front Mol Neurosci,* 5, pp. 62.
Notari, S., Qing, L., Pocchiari, M., Dagdanova, A., Hatcher, K., Dogterom, A., Groisman, J. F., Lumholtz, I. B., Puopolo, M., Lasmezas, C., Chen, S. G., Kong, Q. and Gambetti, P. (2012) 'Assessing prion infectivity of human urine in sporadic Creutzfeldt-Jakob disease', *Emerg Infect Dis,* 18(1), pp. 21-8.
Novakofski, J., Brewer, M. S., Mateus-Pinilla, N., Killefer, J. and McCusker, R. H. (2005) 'Prion biology relevant to bovine spongiform encephalopathy', *J Anim Sci,* 83(6), pp. 1455-76.
Nozaki, I., Hamaguchi, T., Sanjo, N., Noguchi-Shinohara, M., Sakai, K., Nakamura, Y., Sato, T., Kitamoto, T., Mizusawa, H., Moriwaka, F., Shiga, Y., Kuroiwa, Y., Nishizawa, M., Kuzuhara, S., Inuzuka, T., Takeda, M., Kuroda, S., Abe, K., Murai, H., Murayama, S., Tateishi, J., Takumi, I., Shirabe, S., Harada, M., Sadakane, A. and Yamada, M. (2010) 'Prospective 10-year surveillance of human prion diseases in Japan', *Brain,* 133(10), pp. 3043-57.
Nuvolone, M., Hermann, M., Sorce, S., Russo, G., Tiberi, C., Schwarz, P., Minikel, E., Sanoudou, D., Pelczar, P. and Aguzzi, A. (2016) 'Strictly co-isogenic C57BL/6J-Prnp-/- mice: A rigorous resource for prion science', *J Exp Med,* 213(3), pp. 313-27.
Nuvolone, M., Schmid, N., Miele, G., Sorce, S., Moos, R., Schori, C., Beerli, R. R., Bauer, M., Saudan, P., Dietmeier, K., Lachmann, I., Linnebank, M., Martin, R., Kallweit, U., Kana, V., Rushing, E. J., Budka, H. and Aguzzi, A. (2017) 'Cystatin F is a biomarker of prion pathogenesis in mice', *PLoS One,* 12(2), pp. e0171923.

Obst, K., Yealland, G., Balzus, B., Miceli, E., Dimde, M., Weise, C., Eravci, M., Bodmeier, R., Haag, R., Calderón, M., Charbaji, N. and Hedtrich, S. (2017) 'Protein Corona Formation on Colloidal Polymeric Nanoparticles and Polymeric Nanogels: Impact on Cellular Uptake, Toxicity, Immunogenicity, and Drug Release Properties', *Biomacromolecules,* 18(6), pp. 1762-1771.

Oesch, B., Westaway, D., Wälchli, M., McKinley, M. P., Kent, S. B., Aebersold, R., Barry, R. A., Tempst, P., Teplow, D. B. and Hood, L. E. (1985) 'A cellular gene encodes scrapie PrP 27-30 protein', *Cell,* 40(4), pp. 735-46.

Olmos-Alonso, A., Schetters, S. T., Sri, S., Askew, K., Mancuso, R., Vargas-Caballero, M., Holscher, C., Perry, V. H. and Gomez-Nicola, D. (2016) 'Pharmacological targeting of CSF1R inhibits microglial proliferation and prevents the progression of Alzheimer's-like pathology', *Brain,* 139(Pt 3), pp. 891-907.

Orrú, C. D., Groveman, B. R., Hughson, A. G., Zanusso, G., Coulthart, M. B. and Caughey, B. (2015) 'Rapid and sensitive RT-QuIC detection of human Creutzfeldt-Jakob disease using cerebrospinal fluid', *MBio,* 6(1).

Ortiz-Pelaez, A., Thompson, C. E. and Dawson, M. (2014) 'The impact of the National Scrapie Plan on the PRNP genotype distribution of the British national flock, 2002-2012', *Vet Rec,* 174(21), pp. 530.

Packard, M., Mathew, D. and Budnik, V. (2003) 'FASt remodeling of synapses in *Drosophila*', *Curr Opin Neurobiol,* 13(5), pp. 527-34.

Palmer, M. S., Dryden, A. J., Hughes, J. T. and Collinge, J. (1991) 'Homozygous prion protein genotype predisposes to sporadic Creutzfeldt-Jakob disease', *Nature,* 352(6333), pp. 340-2.

Pan, K. M., Baldwin, M., Nguyen, J., Gasset, M., Serban, A., Groth, D., Mehlhorn, I., Huang, Z., Fletterick, R. J. and Cohen, F. E. (1993) 'Conversion of alpha-helices into beta-sheets features in the formation of the scrapie prion proteins', *Proc Natl Acad Sci U S A,* 90(23), pp. 10962-6.

Pan, T., Li, R., Wong, B. S., Liu, T., Gambetti, P. and Sy, M. S. (2002) 'Heterogeneity of normal prion protein in two- dimensional immunoblot: presence of various glycosylated and truncated forms', *J Neurochem,* 81(5), pp. 1092-101.

Pang, Y., Kurella, S., Voisset, C., Samanta, D., Banerjee, D., Schabe, A., Das Gupta, C., Galons, H., Blondel, M. and Sanyal, S. (2013) 'The antiprion compound 6-aminophenanthridine inhibits the protein folding activity of the ribosome by direct competition', *J Biol Chem,* 288(26), pp. 19081-9.

Paquet, S., Daude, N., Courageot, M. P., Chapuis, J., Laude, H. and Vilette, D. (2007a) 'PrPc does not mediate internalization of PrPSc but is required at an early stage for de novo prion infection of Rov cells', *J Virol,* 81(19), pp. 10786-91.

Paquet, S., Langevin, C., Chapuis, J., Jackson, G. S., Laude, H. and Vilette, D. (2007b) 'Efficient dissemination of prions through preferential transmission to nearby cells', *J Gen Virol,* 88(Pt 2), pp. 706-13.

Parchi, P. and Gambetti, P. (1995) 'Human prion diseases', *Curr Opin Neurol,* 8(4), pp. 286-93.

Parchi, P., Castellani, R., Capellari, S., Ghetti, B., Young, K., Chen, S. G., Farlow, M., Dickson, D. W., Sima, A. A., Trojanowski, J. Q., Petersen, R. B. and Gambetti, P. (1996) 'Molecular basis of phenotypic variability in sporadic Creutzfeldt-Jakob disease', *Ann Neurol,* 39(6), pp. 767-78.

Parchi, P., Giese, A., Capellari, S., Brown, P., Schulz-Schaeffer, W., Windl, O., Zerr, I., Budka, H., Kopp, N., Piccardo, P., Poser, S., Rojiani, A., Streichemberger, N., Julien, J., Vital, C., Ghetti, B., Gambetti, P. and Kretzschmar, H. (1999) 'Classification of sporadic

Creutzfeldt-Jakob disease based on molecular and phenotypic analysis of 300 subjects', *Ann Neurol,* 46(2), pp. 224-33.
Parchi, P., Cescatti, M., Notari, S., Schulz-Schaeffer, W. J., Capellari, S., Giese, A., Zou, W. Q., Kretzschmar, H., Ghetti, B. and Brown, P. (2010) 'Agent strain variation in human prion disease: insights from a molecular and pathological review of the National Institutes of Health series of experimentally transmitted disease', *Brain,* 133(10), pp. 3030-42.
Parizek, P., Roeckl, C., Weber, J., Flechsig, E., Aguzzi, A. and Raeber, A. J. (2001) 'Similar turnover and shedding of the cellular prion protein in primary lymphoid and neuronal cells', *J Biol Chem,* 276(48), pp. 44627-32.
Parkin, E. T., Watt, N. T., Turner, A. J. and Hooper, N. M. (2004) 'Dual mechanisms for shedding of the cellular prion protein', *J Biol Chem,* 279(12), pp. 11170-8.
Parry, H. B. (1960) 'Scrapie: a transmissible hereditary disease of sheep', *Nature,* 185(4711), pp. 441-3.
Paschen, W. and Frandsen, A. (2001) 'Endoplasmic reticulum dysfunction--a common denominator for cell injury in acute and degenerative diseases of the brain?', *J Neurochem,* 79(4), pp. 719-25.
Pattison, I. H. and Millson, G. C. (1961) 'Scrapie produced experimentally in goats with special reference to the clinical syndrome', *J Comp Pathol,* 71, pp. 101-9.
Pattison, I. H. (1965) 'Resistance of the scrapie agent to formalin', *J Comp Pathol,* 75, pp. 159-64.
Pattison, I. H. and Jones, K. M. (1968) 'Modification of a strain of mouse-adapted scrapie by passage through rats', *Res Vet Sci,* 9(5), pp. 408-10.
Pauly, P. C. and Harris, D. A. (1998) 'Copper stimulates endocytosis of the prion protein', *J Biol Chem,* 273(50), pp. 33107-10.
Pearce, M. M., Spartz, E. J., Hong, W., Luo, L. and Kopito, R. R. (2015) 'Prion-like transmission of neuronal huntingtin aggregates to phagocytic glia in the *Drosophila* brain', *Nat Commun,* 6, pp. 6768.
Peden, A. H., Head, M. W., Ritchie, D. L., Bell, J. E. and Ironside, J. W. (2004) 'Preclinical vCJD after blood transfusion in a PRNP codon 129 heterozygous patient', *Lancet,* 364(9433), pp. 527-9.
Peden, A. H., Sarode, D. P., Mulholland, C. R., Barria, M. A., Ritchie, D. L., Ironside, J. W. and Head, M. W. (2014) 'The prion protein protease sensitivity, stability and seeding activity in variably protease sensitive prionopathy brain tissue suggests molecular overlaps with sporadic Creutzfeldt-Jakob disease', *Acta Neuropathol Commun,* 2, pp. 152.
Perry, V. H., Cunningham, C. and Boche, D. (2002) 'Atypical inflammation in the central nervous system in prion disease', *Curr Opin Neurol,* 15(3), pp. 349-54.
Perry, V. H., Nicoll, J. A. and Holmes, C. (2010) 'Microglia in neurodegenerative disease', *Nat Rev Neurol,* 6(4), pp. 193-201.
Petersen, R. B., Parchi, P., Richardson, S. L., Urig, C. B. and Gambetti, P. (1996) 'Effect of the D178N mutation and the codon 129 polymorphism on the metabolism of the prion protein', *J Biol Chem,* 271(21), pp. 12661-8.
Pfeiffer, B. D., Ngo, T. T., Hibbard, K. L., Murphy, C., Jenett, A., Truman, J. W. and Rubin, G. M. (2010) 'Refinement of tools for targeted gene expression in *Drosophila*', *Genetics,* 186(2), pp. 735-55.
Piccardo, P., Liepnieks, J. J., William, A., Dlouhy, S. R., Farlow, M. R., Young, K., Nochlin, D., Bird, T. D., Nixon, R. R., Ball, M. J., DeCarli, C., Bugiani, O., Tagliavini, F., Benson, M. D. and Ghetti, B. (2001) 'Prion proteins with different conformations accumulate in Gerstmann-Sträussler-Scheinker disease caused by A117V and F198S mutations', *Am J Pathol,* 158(6), pp. 2201-7.

Piening, N., Weber, P., Giese, A. and Kretzschmar, H. (2005) 'Breakage of PrP aggregates is essential for efficient autocatalytic propagation of misfolded prion protein', *Biochem Biophys Res Commun,* 326(2), pp. 339-43.

Polymenidou, M., Stoeck, K., Glatzel, M., Vey, M., Bellon, A. and Aguzzi, A. (2005) 'Coexistence of multiple PrPSc types in individuals with Creutzfeldt-Jakob disease', *Lancet Neurol,* 4(12), pp. 805-14.

Poser, C. M. (2002) 'Notes on the history of the prion diseases. Part II', *Clin Neurol Neurosurg,* 104(2), pp. 77-86.

Potter, C. J., Tasic, B., Russler, E. V., Liang, L. and Luo, L. (2010) 'The Q system: a repressible binary system for transgene expression, lineage tracing, and mosaic analysis', *Cell,* 141(3), pp. 536-48.

Prince, M. J., Bailey, J. A., Barrowman, P. R., Bishop, K. J., Campbell, G. R. and Wood, J. M. (2003) 'Bovine spongiform encephalopathy', *Rev Sci Tech,* 22(1), pp. 37-60.

Provini, F., Vetrugno, R., Pierangeli, G., Cortelli, P., Rizzo, G., Filla, A., Strisciuglio, C., Gallassi, R. and Montagna, P. (2009) 'Sleep and temperature rhythms in two sisters with P102L Gerstmann-Sträussler-Scheinker (GSS) disease', *Sleep Med,* 10(3), pp. 374-7.

Prusiner, S. B., Cochran, S. P., Baringer, J. R., Groth, D., Masiarz, F., McKinley, M., Bildstein, C., Garfin, D., Hadlow, W. J., Race, R. E. and Eklund, C. M. (1980) 'Slow viruses: molecular properties of the agents causing scrapie in mice and hamsters', *Prog Clin Biol Res,* 39, pp. 73-89.

Prusiner, S. B. (1982) 'Novel proteinaceous infectious particles cause scrapie', *Science,* 216(4542), pp. 136-44.

Prusiner, S. B., Cochran, S. P. and Alpers, M. P. (1985) 'Transmission of scrapie in hamsters', *J Infect Dis,* 152(5), pp. 971-8.

Prusiner, S. B., Scott, M., Foster, D., Pan, K. M., Groth, D., Mirenda, C., Torchia, M., Yang, S. L., Serban, D. and Carlson, G. A. (1990) 'Transgenetic studies implicate interactions between homologous PrP isoforms in scrapie prion replication', *Cell,* 63(4), pp. 673-86.

Prusiner, S. B. (1991) 'Molecular biology of prion diseases', *Science,* 252(5012), pp. 1515-22.

Prusiner, S. B., Füzi, M., Scott, M., Serban, D., Serban, H., Taraboulos, A., Gabriel, J. M., Wells, G. A., Wilesmith, J. W. and Bradley, R. (1993) 'Immunologic and molecular biologic studies of prion proteins in bovine spongiform encephalopathy', *J Infect Dis,* 167(3), pp. 602-13.

Prusiner, S. B. and DeArmond, S. J. (1994) 'Prion diseases and neurodegeneration', *Annu Rev Neurosci,* 17, pp. 311-39.

Prusiner, S. B. (1998) 'Prions', *Proc Natl Acad Sci U S A,* 95(23), pp. 13363-83.

Ptashne, M. (1988) 'How eukaryotic transcriptional activators work', *Nature,* 335(6192), pp. 683-9.

Purro, S. A., Nicoll, A. J. and Collinge, J. (2018) 'Prion Protein as a Toxic Acceptor of Amyloid-β Oligomers', *Biol Psychiatry,* 83(4), pp. 358-368.

Qin, K., Yang, Y., Mastrangelo, P. and Westaway, D. (2002) 'Mapping Cu(II) binding sites in prion proteins by diethyl pyrocarbonate modification and matrix-assisted laser desorption ionization-time of flight (MALDI-TOF) mass spectrometric footprinting', *J Biol Chem,* 277(3), pp. 1981-90.

Race, B., Meade-White, K., Race, R. and Chesebro, B. (2009) 'Prion infectivity in fat of deer with chronic wasting disease', *J Virol,* 83(18), pp. 9608-10.

Race, B., Phillips, K., Meade-White, K., Striebel, J. and Chesebro, B. (2015) 'Increased infectivity of anchorless mouse scrapie prions in transgenic mice overexpressing human prion protein', *J Virol,* 89(11), pp. 6022-32.

Race, B., Williams, K., Orrú, C. D., Hughson, A. G., Lubke, L. and Chesebro, B. (2018) 'Lack of Transmission of Chronic Wasting Disease to Cynomolgus Macaques', *J Virol.*

Race, R. E. and Ernst, D. (1992) 'Detection of proteinase K-resistant prion protein and infectivity in mouse spleen by 2 weeks after scrapie agent inoculation', *J Gen Virol,* 73 (Pt 12), pp. 3319-23.

Radford, H., Moreno, J. A., Verity, N., Halliday, M. and Mallucci, G. R. (2015) 'PERK inhibition prevents tau-mediated neurodegeneration in a mouse model of frontotemporal dementia', *Acta Neuropathol,* 130(5), pp. 633-42.

Raeber, A. J., Muramoto, T., Kornberg, T. B. and Prusiner, S. B. (1995) 'Expression and targeting of Syrian hamster prion protein induced by heat shock in transgenic *Drosophila* melanogaster', *Mech Dev,* 51(2-3), pp. 317-27.

Raj, K. and Sarkar, S. (2017) 'Transactivation Domain of Human c-Myc Is Essential to Alleviate Poly(Q)-Mediated Neurotoxicity in *Drosophila* Disease Models', *J Mol Neurosci,* 62(1), pp. 55-66.

Rane, N. S., Chakrabarti, O., Feigenbaum, L. and Hegde, R. S. (2010) 'Signal sequence insufficiency contributes to neurodegeneration caused by transmembrane prion protein', *J Cell Biol,* 188(4), pp. 515-26.

Rane, N. S., Yonkovich, J. L. and Hegde, R. S. (2004) 'Protection from cytosolic prion protein toxicity by modulation of protein translocation', *EMBO J,* 23(23), pp. 4550-9.

Rao, R. V., Ellerby, H. M. and Bredesen, D. E. (2004) 'Coupling endoplasmic reticulum stress to the cell death program', *Cell Death Differ,* 11(4), pp. 372-80.

Rincon-Limas, D. E., Casas-Tinto, S. and Fernandez-Funez, P. (2010) 'Exploring prion protein biology in flies: genetics and beyond', *Prion,* 4(1), pp. 1-8.

Robinson, S. W., Nugent, M. L., Dinsdale, D. and Steinert, J. R. (2014) 'Prion protein facilitates synaptic vesicle release by enhancing release probability', *Hum Mol Genet,* 23(17), pp. 4581-96.

Rogers, M., Yehiely, F., Scott, M. and Prusiner, S. B. (1993) 'Conversion of truncated and elongated prion proteins into the scrapie isoform in cultured cells', *Proc Natl Acad Sci U S A,* 90(8), pp. 3182-6.

Rozas, J. L., Gómez-Sánchez, L., Tomás-Zapico, C., Lucas, J. J. and Fernández-Chacón, R. (2011) 'Increased neurotransmitter release at the neuromuscular junction in a mouse model of polyglutamine disease', *J Neurosci,* 31(3), pp. 1106-13.

Rubenstein, R., Kascsak, R. J., Merz, P. A., Papini, M. C., Carp, R. I., Robakis, N. K. and Wisniewski, H. M. (1986) 'Detection of scrapie-associated fibril (SAF) proteins using anti-SAF antibody in non-purified tissue preparations', *J Gen Virol,* 67 (Pt 4), pp. 671-81.

Rubin, G. M. and Lewis, E. B. (2000) 'A brief history of *Drosophila*'s contributions to genome research', *Science,* 287(5461), pp. 2216-8.

Rubin, G. M., Yandell, M. D., Wortman, J. R., Gabor Miklos, G. L., Nelson, C. R., Hariharan, I. K., Fortini, M. E., Li, P. W., Apweiler, R., Fleischmann, W., Cherry, J. M., Henikoff, S., Skupski, M. P., Misra, S., Ashburner, M., Birney, E., Boguski, M. S., Brody, T., Brokstein, P., Celniker, S. E., Chervitz, S. A., Coates, D., Cravchik, A., Gabrielian, A., Galle, R. F., Gelbart, W. M., George, R. A., Goldstein, L. S., Gong, F., Guan, P., Harris, N. L., Hay, B. A., Hoskins, R. A., Li, J., Li, Z., Hynes, R. O., Jones, S. J., Kuehl, P. M., Lemaitre, B., Littleton, J. T., Morrison, D. K., Mungall, C., O'Farrell, P. H., Pickeral, O. K., Shue, C., Vosshall, L. B., Zhang, J., Zhao, Q., Zheng, X. H. and Lewis, S. (2000) 'Comparative genomics of the eukaryotes', *Science,* 287(5461), pp. 2204-15.

Rudd, P. M., Endo, T., Colominas, C., Groth, D., Wheeler, S. F., Harvey, D. J., Wormald, M. R., Serban, H., Prusiner, S. B., Kobata, A. and Dwek, R. A. (1999) 'Glycosylation differences

between the normal and pathogenic prion protein isoforms', *Proc Natl Acad Sci U S A,* 96(23), pp. 13044-9.

Ruiz-Cañada, C. and Budnik, V. (2006) 'Introduction on the use of the *Drosophila* embryonic/larval neuromuscular junction as a model system to study synapse development and function, and a brief summary of pathfinding and target recognition', *Int Rev Neurobiol,* 75, pp. 1-31.

Rustom, A., Saffrich, R., Markovic, I., Walther, P. and Gerdes, H. H. (2004) 'Nanotubular highways for intercellular organelle transport', *Science,* 303(5660), pp. 1007-10.

Saborio, G. P., Permanne, B. and Soto, C. (2001) 'Sensitive detection of pathological prion protein by cyclic amplification of protein misfolding', *Nature,* 411(6839), pp. 810-3.

Sadowski, I., Ma, J., Triezenberg, S. and Ptashne, M. (1988) 'GAL4-VP16 is an unusually potent transcriptional activator', *Nature,* 335(6190), pp. 563-4.

Safar, J., Roller, P. P., Gajdusek, D. C. and Gibbs, C. J. (1993) 'Thermal stability and conformational transitions of scrapie amyloid (prion) protein correlate with infectivity', *Protein Sci,* 2(12), pp. 2206-16.

Sajnani, G., Silva, C. J., Ramos, A., Pastrana, M. A., Onisko, B. C., Erickson, M. L., Antaki, E. M., Dynin, I., Vázquez-Fernández, E., Sigurdson, C. J., Carter, J. M. and Requena, J. R. (2012) 'PK-sensitive PrP is infectious and shares basic structural features with PK-resistant PrP', *PLoS Pathog,* 8(3), pp. e1002547.

Salmona, M., Morbin, M., Massignan, T., Colombo, L., Mazzoleni, G., Capobianco, R., Diomede, L., Thaler, F., Mollica, L., Musco, G., Kourie, J. J., Bugiani, O., Sharma, D., Inouye, H., Kirschner, D. A., Forloni, G. and Tagliavini, F. (2003) 'Structural properties of Gerstmann-Straussler-Scheinker disease amyloid protein', *J Biol Chem,* 278(48), pp. 48146-53.

Sanghera, N. and Pinheiro, T. J. (2002) 'Binding of prion protein to lipid membranes and implications for prion conversion', *J Mol Biol,* 315(5), pp. 1241-56.

Saá, P., Castilla, J. and Soto, C. (2006) 'Ultra-efficient replication of infectious prions by automated protein misfolding cyclic amplification', *J Biol Chem,* 281(46), pp. 35245-52.

Scheff, S. W. and Price, D. A. (2006) 'Alzheimer's disease-related alterations in synaptic density: neocortex and hippocampus', *J Alzheimers Dis,* 9(3 Suppl), pp. 101-15.

Scherzer, C. R., Jensen, R. V., Gullans, S. R. and Feany, M. B. (2003) 'Gene expression changes presage neurodegeneration in a *Drosophila* model of Parkinson's disease', *Hum Mol Genet,* 12(19), pp. 2457-66.

Schmidt, C., Fizet, J., Properzi, F., Batchelor, M., Sandberg, M. K., Edgeworth, J. A., Afran, L., Ho, S., Badhan, A., Klier, S., Linehan, J. M., Brandner, S., Hosszu, L. L., Tattum, M. H., Jat, P., Clarke, A. R., Klöhn, P. C., Wadsworth, J. D., Jackson, G. S. and Collinge, J. (2015) 'A systematic investigation of production of synthetic prions from recombinant prion protein', *Open Biol,* 5(12), pp. 150165.

Schöndorf, D. C., Ivanyuk, D., Baden, P., Sanchez-Martinez, A., De Cicco, S., Yu, C., Giunta, I., Schwarz, L. K., Di Napoli, G., Panagiotakopoulou, V., Nestel, S., Keatinge, M., Pruszak, J., Bandmann, O., Heimrich, B., Gasser, T., Whitworth, A. J. and Deleidi, M. (2018) 'The NAD+ Precursor Nicotinamide Riboside Rescues Mitochondrial Defects and Neuronal Loss in iPSC and Fly Models of Parkinson's Disease', *Cell Rep,* 23(10), pp. 2976-2988.

Scott, M., Foster, D., Mirenda, C., Serban, D., Coufal, F., Wälchli, M., Torchia, M., Groth, D., Carlson, G., DeArmond, S. J., Westaway, D. and Prusiner, S. B. (1989) 'Transgenic mice expressing hamster prion protein produce species-specific scrapie infectivity and amyloid plaques', *Cell,* 59(5), pp. 847-57.

Scott, M. R., Groth, D., Tatzelt, J., Torchia, M., Tremblay, P., DeArmond, S. J. and Prusiner, S. B. (1997) 'Propagation of prion strains through specific conformers of the prion protein', *J Virol,* 71(12), pp. 9032-44.

Seed, C. R., Hewitt, P. E., Dodd, R. Y., Houston, F. and Cervenakova, L. (2018) 'Creutzfeldt-Jakob disease and blood transfusion safety', *Vox Sang,* 113(3), pp. 220-231.

Selariu, A., Powers, J. G., Nalls, A., Brandhuber, M., Mayfield, A., Fullaway, S., Wyckoff, C. A., Goldmann, W., Zabel, M. M., Wild, M. A., Hoover, E. A. and Mathiason, C. K. (2015) 'In utero transmission and tissue distribution of chronic wasting disease-associated prions in free-ranging Rocky Mountain elk', *J Gen Virol,* 96(11), pp. 3444-55.

Shaked, G. M., Fridlander, G., Meiner, Z., Taraboulos, A. and Gabizon, R. (1999) 'Protease-resistant and detergent-insoluble prion protein is not necessarily associated with prion infectivity', *J Biol Chem,* 274(25), pp. 17981-6.

Shang, Y., Griffith, L. C. and Rosbash, M. (2008) 'Light-arousal and circadian photoreception circuits intersect at the large PDF cells of the *Drosophila* brain', *Proc Natl Acad Sci U S A,* 105(50), pp. 19587-94.

Shi, S., Wagner, J., Mitteregger-Kretzschmar, G., Ryazanov, S., Leonov, A., Griesinger, C. and Giese, A. (2015) 'Quantitative Real-Time Quaking-Induced Conversion Allows Monitoring of Disease-Modifying Therapy in the Urine of Prion-Infected Mice', *J Neuropathol Exp Neurol,* 74(9), pp. 924-33.

Shibuya, S., Higuchi, J., Shin, R. W., Tateishi, J. and Kitamoto, T. (1998) 'Codon 219 Lys allele of PRNP is not found in sporadic Creutzfeldt-Jakob disease', *Ann Neurol,* 43(6), pp. 826-8.

Shmerling, D., Hegyi, I., Fischer, M., Blättler, T., Brandner, S., Götz, J., Rülicke, T., Flechsig, E., Cozzio, A., von Mering, C., Hangartner, C., Aguzzi, A. and Weissmann, C. (1998) 'Expression of amino-terminally truncated PrP in the mouse leading to ataxia and specific cerebellar lesions', *Cell,* 93(2), pp. 203-14.

Shyng, S. L., Huber, M. T. and Harris, D. A. (1993) 'A prion protein cycles between the cell surface and an endocytic compartment in cultured neuroblastoma cells', *J Biol Chem,* 268(21), pp. 15922-8.

Shyng, S. L., Heuser, J. E. and Harris, D. A. (1994) 'A glycolipid-anchored prion protein is endocytosed via clathrin-coated pits', *J Cell Biol,* 125(6), pp. 1239-50.

Shyng, S. L., Moulder, K. L., Lesko, A. and Harris, D. A. (1995) 'The N-terminal domain of a glycolipid-anchored prion protein is essential for its endocytosis via clathrin-coated pits', *J Biol Chem,* 270(24), pp. 14793-800.

Siddique, Y. H., Naz, F., Jyoti, S., Ali, F. and Rahul (2018) 'Effect of Genistein on the Transgenic *Drosophila* Model of Parkinson's Disease', *J Diet Suppl,* pp. 1-14.

Sigurdsson, B. (1954) 'Observations on three slow infections of sheep. Maedi, Paratubreculosis, Rida, a chronic encephalitis of sheep with general remarks on infections, which develop slowly, and some of their special characteristics.', *British Veterinary Journal,* 110, pp. 255-270, 307-322, 341-354.

Sigurdson, C. J., Williams, E. S., Miller, M. W., Spraker, T. R., O'Rourke, K. I. and Hoover, E. A. (1999) 'Oral transmission and early lymphoid tropism of chronic wasting disease PrPres in mule deer fawns (Odocoileus hemionus)', *J Gen Virol,* 80 (Pt 10), pp. 2757-64.

Sigurdson, C. J. and Miller, M. W. (2003) 'Other animal prion diseases', *Br Med Bull,* 66, pp. 199-212.

Sigurdson, C. J. and Aguzzi, A. (2007) 'Chronic wasting disease', *Biochim Biophys Acta,* 1772(6), pp. 610-8.

Sigurdson, C. J. (2008) 'A prion disease of cervids: chronic wasting disease', *Vet Res,* 39(4), pp. 41.

Sim, V. L. and Caughey, B. (2009) 'Ultrastructures and strain comparison of under-glycosylated scrapie prion fibrils', *Neurobiol Aging,* 30(12), pp. 2031-42.

Simmons, M. M., Konold, T., Simmons, H. A., Spencer, Y. I., Lockey, R., Spiropoulos, J., Everitt, S. and Clifford, D. (2007) 'Experimental transmission of atypical scrapie to sheep', *BMC Vet Res,* 3, pp. 20.

Simmons, M. M., Moore, S. J., Konold, T., Thurston, L., Terry, L. A., Thorne, L., Lockey, R., Vickery, C., Hawkins, S. A., Chaplin, M. J. and Spiropoulos, J. (2011) 'Experimental oral transmission of atypical scrapie to sheep', *Emerg Infect Dis,* 17(5), pp. 848-54.

Singh, A. P., Das, R. N., Rao, G., Aggarwal, A., Diegelmann, S., Evers, J. F., Karandikar, H., Landgraf, M., Rodrigues, V. and Vijayraghavan, K. (2013) 'Sensory neuron-derived eph regulates glomerular arbors and modulatory function of a central serotonergic neuron', *PLoS Genet,* 9(4), pp. e1003452.

Skinner, P. J., Abbassi, H., Chesebro, B., Race, R. E., Reilly, C. and Haase, A. T. (2006) 'Gene expression alterations in brains of mice infected with three strains of scrapie', *BMC Genomics,* 7, pp. 114.

Sleigh, J. N., Burgess, R. W., Gillingwater, T. H. and Cader, M. Z. (2014) 'Morphological analysis of neuromuscular junction development and degeneration in rodent lumbrical muscles', *J Neurosci Methods,* 227, pp. 159-65.

Solforosi, L., Milani, M., Mancini, N., Clementi, M. and Burioni, R. (2013) 'A closer look at prion strains: characterization and important implications', *Prion,* 7(2), pp. 99-108.

Sonati, T., Reimann, R. R., Falsig, J., Baral, P. K., O'Connor, T., Hornemann, S., Yaganoglu, S., Li, B., Herrmann, U. S., Wieland, B., Swayampakula, M., Rahman, M. H., Das, D., Kav, N., Riek, R., Liberski, P. P., James, M. N. and Aguzzi, A. (2013) 'The toxicity of antiprion antibodies is mediated by the flexible tail of the prion protein', *Nature,* 501(7465), pp. 102-6.

Sorensen, G., Medina, S., Parchaliuk, D., Phillipson, C., Robertson, C. and Booth, S. A. (2008) 'Comprehensive transcriptional profiling of prion infection in mouse models reveals networks of responsive genes', *BMC Genomics,* 9, pp. 114.

Soto, C., Saborio, G. P. and Anderes, L. (2002) 'Cyclic amplification of protein misfolding: application to prion-related disorders and beyond', *Trends Neurosci,* 25(8), pp. 390-4.

Southall, T. D. and Brand, A. H. (2008) 'Generation of Driver and Reporter Constructs for the GAL4 Expression System in *Drosophila*', *CSH Protoc,* 2008, pp. pdb.prot5029.

Sowade, R. F. and Jahn, T. R. (2017) 'Seed-induced acceleration of amyloid-β mediated neurotoxicity in vivo', *Nat Commun,* 8(1), pp. 512.

Spielhaupter, C. and Schätzl, H. M. (2001) 'PrPC directly interacts with proteins involved in signaling pathways', *J Biol Chem,* 276(48), pp. 44604-12.

Spraker, T. R., O'Rourke, K. I., Gidlewski, T., Powers, J. G., Greenlee, J. J. and Wild, M. A. (2010) 'Detection of the abnormal isoform of the prion protein associated with chronic wasting disease in the optic pathways of the brain and retina of Rocky Mountain elk (Cervus elaphus nelsoni)', *Vet Pathol,* 47(3), pp. 536-46.

St Johnston, D. (2002) 'The art and design of genetic screens: *Drosophila* melanogaster', *Nat Rev Genet,* 3(3), pp. 176-88.

Stahl, N., Borchelt, D. R. and Prusiner, S. B. (1990) 'Differential release of cellular and scrapie prion proteins from cellular membranes by phosphatidylinositol-specific phospholipase C', *Biochemistry,* 29(22), pp. 5405-12.

Stahl, N. and Prusiner, S. B. (1991) 'Prions and prion proteins', *FASEB J,* 5(13), pp. 2799-807.

Stahl, N., Baldwin, M. A., Hecker, R., Pan, K. M., Burlingame, A. L. and Prusiner, S. B. (1992) 'Glycosylinositol phospholipid anchors of the scrapie and cellular prion proteins contain sialic acid', *Biochemistry,* 31(21), pp. 5043-53.

Stahl, N., Baldwin, M. A., Teplow, D. B., Hood, L., Gibson, B. W., Burlingame, A. L. and Prusiner, S. B. (1993) 'Structural studies of the scrapie prion protein using mass spectrometry and amino acid sequencing', *Biochemistry,* 32(8), pp. 1991-2002.

Steffan, J. S., Agrawal, N., Pallos, J., Rockabrand, E., Trotman, L. C., Slepko, N., Illes, K., Lukacsovich, T., Zhu, Y. Z., Cattaneo, E., Pandolfi, P. P., Thompson, L. M. and Marsh, J. L. (2004) 'SUMO modification of Huntingtin and Huntington's disease pathology', *Science,* 304(5667), pp. 100-4.

Stephenson, J., Nutma, E., van der Valk, P. and Amor, S. (2018) 'Inflammation in CNS neurodegenerative diseases', *Immunology,* 154(2), pp. 204-219.

Stewart, R. S. and Harris, D. A. (2003) 'Mutational analysis of topological determinants in prion protein (PrP) and measurement of transmembrane and cytosolic PrP during prion infection', *J Biol Chem,* 278(46), pp. 45960-8.

Stöhr, J., Watts, J. C., Legname, G., Oehler, A., Lemus, A., Nguyen, H. O., Sussman, J., Wille, H., DeArmond, S. J., Prusiner, S. B. and Giles, K. (2011) 'Spontaneous generation of anchorless prions in transgenic mice', *Proc Natl Acad Sci U S A,* 108(52), pp. 21223-8.

Szüts, D. and Bienz, M. (2000) 'LexA chimeras reveal the function of *Drosophila* Fos as a context-dependent transcriptional activator', *Proc Natl Acad Sci U S A,* 97(10), pp. 5351-6.

Sánchez-Soriano, N. and Prokop, A. (2005) 'The influence of pioneer neurons on a growing motor nerve in *Drosophila* requires the neural cell adhesion molecule homolog FasciclinII', *J Neurosci,* 25(1), pp. 78-87.

Taguchi, Y., Mohri, S., Ironside, J. W., Muramoto, T. and Kitamoto, T. (2003) 'Humanized knock-in mice expressing chimeric prion protein showed varied susceptibility to different human prions', *Am J Pathol,* 163(6), pp. 2585-93.

Tateishi, J., Brown, P., Kitamoto, T., Hoque, Z. M., Roos, R., Wollman, R., Cervenáková, L. and Gajdusek, D. C. (1995) 'First experimental transmission of fatal familial insomnia', *Nature,* 376(6539), pp. 434-5.

Tatzelt, J. and Schätzl, H. M. (2007) 'Molecular basis of cerebral neurodegeneration in prion diseases', *FEBS J,* 274(3), pp. 606-11.

Taylor, D. M. and Woodgate, S. L. (1997) 'Bovine spongiform encephalopathy: the causal role of ruminant-derived protein in cattle diets', *Rev Sci Tech,* 16(1), pp. 187-98.

Telling, G. C., Parchi, P., DeArmond, S. J., Cortelli, P., Montagna, P., Gabizon, R., Mastrianni, J., Lugaresi, E., Gambetti, P. and Prusiner, S. B. (1996) 'Evidence for the conformation of the pathologic isoform of the prion protein enciphering and propagating prion diversity', *Science,* 274(5295), pp. 2079-82.

Telling, G. C., Scott, M., Mastrianni, J., Gabizon, R., Torchia, M., Cohen, F. E., DeArmond, S. J. and Prusiner, S. B. (1995) 'Prion propagation in mice expressing human and chimeric PrP transgenes implicates the interaction of cellular PrP with another protein', *Cell,* 83(1), pp. 79-90.

Thackray, A. M., Madec, J. Y., Wong, E., Morgan-Warren, R., Brown, D. R., Baron, T. and Bujdoso, R. (2003) 'Detection of bovine spongiform encephalopathy, ovine scrapie prion-related protein (PrPSc) and normal PrPc by monoclonal antibodies raised to copper-refolded prion protein', *Biochem J,* 370(Pt 1), pp. 81-90.

Thackray, A. M., Yang, S., Wong, E., Fitzmaurice, T. J., Morgan-Warren, R. J. and Bujdoso, R. (2004) 'Conformational variation between allelic variants of cell-surface ovine prion protein', *Biochem J,* 381(Pt 1), pp. 221-9.

Thackray, A. M., Hopkins, L. and Bujdoso, R. (2007) 'Proteinase K-sensitive disease-associated ovine prion protein revealed by conformation-dependent immunoassay', *Biochem J,* 401(2), pp. 475-83.

Thackray, A. M., Hopkins, L., Lockey, R., Spiropoulos, J. and Bujdoso, R. (2011) 'Emergence of multiple prion strains from single isolates of ovine scrapie', *J Gen Virol,* 92(Pt 6), pp. 1482-91.

Thackray, A. M., Muhammad, F., Zhang, C., Denyer, M., Spiropoulos, J., Crowther, D. C. and Bujdoso, R. (2012a) 'Prion-induced toxicity in PrP transgenic *Drosophila*', *Exp Mol Pathol,* 92(2), pp. 194-201.

Thackray, A. M., Muhammad, F., Zhang, C., Di, Y., Jahn, T. R., Landgraf, M., Crowther, D. C., Evers, J. F. and Bujdoso, R. (2012b) 'Ovine PrP transgenic *Drosophila* show reduced locomotor activity and decreased survival', *Biochem J,* 444(3), pp. 487-95.

Thackray, A. M., Di, Y., Zhang, C., Wolf, H., Pradl, L., Vorberg, I., Andréoletti, O. and Bujdoso, R. (2014a) 'Prion-induced and spontaneous formation of transmissible toxicity in PrP transgenic *Drosophila*', *Biochem J,* 463(1), pp. 31-40.

Thackray, A. M., Zhang, C., Arndt, T. and Bujdoso, R. (2014b) 'Cytosolic PrP can participate in prion-mediated toxicity', *J Virol,* 88(14), pp. 8129-38.

Thackray, A. M., Andreoletti, O. and Bujdoso, R. (2016) 'Bioassay of prion-infected blood plasma in PrP transgenic *Drosophila*', *Biochem J,* 473(23), pp. 4399-4412.

Thackray, A. M., Cardova, A., Wolf, H., Pradl, L., Vorberg, I., Jackson, W. S. and Bujdoso, R. (2017) 'Genetic human prion disease modelled in PrP transgenic *Drosophila*', *Biochem J,* 474(19), pp. 3253-3267.

Thackray, A. M., Andréoletti, O. and Bujdoso, R. (2018a) 'Mammalian prion propagation in PrP transgenic *Drosophila*', *Brain.*

Thackray, A. M., Andréoletti, O. and Bujdoso, R. (2018b) 'The use of PrP transgenic *Drosophila* to replace and reduce vertebrate hosts in the bioassay of mammalian prion infectivity', *F1000Res,* 7, pp. 595.

Thomas, J. B., Bastiani, M. J., Bate, M. and Goodman, C. S. (1984) 'From grasshopper to *Drosophila*: a common plan for neuronal development', *Nature,* 310(5974), pp. 203-7.

Thorpe, H. M. and Smith, M. C. (1998) 'In vitro site-specific integration of bacteriophage DNA catalyzed by a recombinase of the resolvase/invertase family', *Proc Natl Acad Sci U S A,* 95(10), pp. 5505-10.

Thorpe, H. M., Wilson, S. E. and Smith, M. C. (2000) 'Control of directionality in the site-specific recombination system of the Streptomyces phage phiC31', *Mol Microbiol,* 38(2), pp. 232-41.

Tobler, I., Deboer, T. and Fischer, M. (1997) 'Sleep and sleep regulation in normal and prion protein-deficient mice', *J Neurosci,* 17(5), pp. 1869-79.

Torres, J. M., Espinosa, J. C., Aguilar-Calvo, P., Herva, M. E., Relaño-Ginés, A., Villa-Diaz, A., Morales, M., Parra, B., Alamillo, E., Brun, A., Castilla, J., Molina, S., Hawkins, S. A. and Andreoletti, O. (2014) 'Elements modulating the prion species barrier and its passage consequences', *PLoS One,* 9(3), pp. e89722.

Tranulis, M. A., Benestad, S. L., Baron, T. and Kretzschmar, H. (2011) 'Atypical prion diseases in humans and animals', *Top Curr Chem,* 305, pp. 23-50.

Tribouillard-Tanvier, D., Béringue, V., Desban, N., Gug, F., Bach, S., Voisset, C., Galons, H., Laude, H., Vilette, D. and Blondel, M. (2008) 'Antihypertensive drug guanabenz is active in vivo against both yeast and mammalian prions', *PLoS One,* 3(4), pp. e1981.

Triezenberg, S. J., Kingsbury, R. C. and McKnight, S. L. (1988) 'Functional dissection of VP16, the trans-activator of herpes simplex virus immediate early gene expression', *Genes Dev,* 2(6), pp. 718-29.

Tripathi, A. K., Haldar, S., Qian, J., Beserra, A., Suda, S., Singh, A., Hopfer, U., Chen, S. G., Garrick, M. D., Turner, J. R., Knutson, M. D. and Singh, N. (2015) 'Prion protein functions as a ferrireductase partner for ZIP14 and DMT1', *Free Radic Biol Med,* 84, pp. 322-30.

Tsuda, H., Jafar-Nejad, H., Patel, A. J., Sun, Y., Chen, H. K., Rose, M. F., Venken, K. J., Botas, J., Orr, H. T., Bellen, H. J. and Zoghbi, H. Y. (2005) 'The AXH domain of Ataxin-1 mediates neurodegeneration through its interaction with Gfi-1/Senseless proteins', *Cell,* 122(4), pp. 633-44.

Tsuda, L. and Lim, Y. M. (2018) 'Alzheimer's Disease Model System Using *Drosophila*', *Adv Exp Med Biol,* 1076, pp. 25-40.

Turk, E., Teplow, D. B., Hood, L. E. and Prusiner, S. B. (1988) 'Purification and properties of the cellular and scrapie hamster prion proteins', *Eur J Biochem,* 176(1), pp. 21-30.

Um, J. W., Nygaard, H. B., Heiss, J. K., Kostylev, M. A., Stagi, M., Vortmeyer, A., Wisniewski, T., Gunther, E. C. and Strittmatter, S. M. (2012) 'Alzheimer amyloid-β oligomer bound to postsynaptic prion protein activates Fyn to impair neurons', *Nat Neurosci,* 15(9), pp. 1227-35.

Um, J. W., Kaufman, A. C., Kostylev, M., Heiss, J. K., Stagi, M., Takahashi, H., Kerrisk, M. E., Vortmeyer, A., Wisniewski, T., Koleske, A. J., Gunther, E. C., Nygaard, H. B. and Strittmatter, S. M. (2013) 'Metabotropic glutamate receptor 5 is a coreceptor for Alzheimer aβ oligomer bound to cellular prion protein', *Neuron,* 79(5), pp. 887-902.

Vaccari, G., Panagiotidis, C. H., Acin, C., Peletto, S., Barillet, F., Acutis, P., Bossers, A., Langeveld, J., van Keulen, L., Sklaviadis, T., Badiola, J. J., Andreéoletti, O., Groschup, M. H., Agrimi, U., Foster, J. and Goldmann, W. (2009) 'State-of-the-art review of goat TSE in the European Union, with special emphasis on PRNP genetics and epidemiology', *Vet Res,* 40(5), pp. 48.

Vactor, D. V., Sink, H., Fambrough, D., Tsoo, R. and Goodman, C. S. (1993) 'Genes that control neuromuscular specificity in *Drosophila*', *Cell,* 73(6), pp. 1137-53.

Van Gool, D., De Strooper, B., Van Leuven, F., Triau, E. and Dom, R. (1993) 'alpha 2-Macroglobulin expression in neuritic-type plaques in patients with Alzheimer's disease', *Neurobiol Aging,* 14(3), pp. 233-7.

Vascellari, S., Orrù, C. D., Hughson, A. G., King, D., Barron, R., Wilham, J. M., Baron, G. S., Race, B., Pani, A. and Caughey, B. (2012) 'Prion seeding activities of mouse scrapie strains with divergent PrPSc protease sensitivities and amyloid plaque content using RT-QuIC and eQuIC', *PLoS One,* 7(11), pp. e48969.

Victoria, G. S., Arkhipenko, A., Zhu, S., Syan, S. and Zurzolo, C. (2016) 'Astrocyte-to-neuron intercellular prion transfer is mediated by cell-cell contact', *Sci Rep,* 6, pp. 20762.

Wadsworth, J. D., Asante, E. A. and Collinge, J. (2010) 'Review: contribution of transgenic models to understanding human prion disease', *Neuropathol Appl Neurobiol,* 36(7), pp. 576-97.

Wagh, D. A., Rasse, T. M., Asan, E., Hofbauer, A., Schwenkert, I., Dürrbeck, H., Buchner, S., Dabauvalle, M. C., Schmidt, M., Qin, G., Wichmann, C., Kittel, R., Sigrist, S. J. and Buchner, E. (2006) 'Bruchpilot, a protein with homology to ELKS/CAST, is required for structural integrity and function of synaptic active zones in *Drosophila*', *Neuron,* 49(6), pp. 833-44.

Walker, G. C. (1984) 'Mutagenesis and inducible responses to deoxyribonucleic acid damage in Escherichia coli', *Microbiol Rev,* 48(1), pp. 60-93.

Wang, F., Wang, X., Yuan, C. G. and Ma, J. (2010) 'Generating a prion with bacterially expressed recombinant prion protein', *Science,* 327(5969), pp. 1132-5.
Wang, B., Su, C. J., Liu, T. T., Zhou, Y., Feng, Y., Huang, Y., Liu, X., Wang, Z. H., Chen, L. H., Luo, W. F. and Liu, T. (2018) 'The Neuroprotection of Low-Dose Morphine in Cellular and Animal Models of Parkinson's Disease Through Ameliorating Endoplasmic Reticulum (ER) Stress and Activating Autophagy', *Front Mol Neurosci,* 11, pp. 120.
Wang, F., Wang, X., Orrú, C. D., Groveman, B. R., Surewicz, K., Abskharon, R., Imamura, M., Yokoyama, T., Kim, Y. S., Vander Stel, K. J., Sinniah, K., Priola, S. A., Surewicz, W. K., Caughey, B. and Ma, J. (2017) 'Self-propagating, protease-resistant, recombinant prion protein conformers with or without in vivo pathogenicity', *PLoS Pathog,* 13(7), pp. e1006491.
Warrick, J. M., Paulson, H. L., Gray-Board, G. L., Bui, Q. T., Fischbeck, K. H., Pittman, R. N. and Bonini, N. M. (1998) 'Expanded polyglutamine protein forms nuclear inclusions and causes neural degeneration in *Drosophila*', *Cell,* 93(6), pp. 939-49.
Watts, J. C., Giles, K., Patel, S., Oehler, A., DeArmond, S. J. and Prusiner, S. B. (2014) 'Evidence that bank vole PrP is a universal acceptor for prions', *PLoS Pathog,* 10(4), pp. e1003990.
Watts, J. C. and Prusiner, S. B. (2014) 'Mouse models for studying the formation and propagation of prions', *J Biol Chem,* 289(29), pp. 19841-9.
Webster, N., Jin, J. R., Green, S., Hollis, M. and Chambon, P. (1988) 'The yeast UASG is a transcriptional enhancer in human HeLa cells in the presence of the GAL4 trans-activator', *Cell,* 52(2), pp. 169-78.
Wells, G. A., Scott, A. C., Johnson, C. T., Gunning, R. F., Hancock, R. D., Jeffrey, M., Dawson, M. and Bradley, R. (1987) 'A novel progressive spongiform encephalopathy in cattle', *Vet Rec,* 121(18), pp. 419-20.
Wells, G. A. and Wilesmith, J. W. (1995) 'The neuropathology and epidemiology of bovine spongiform encephalopathy', *Brain Pathol,* 5(1), pp. 91-103.
West, R. J., Furmston, R., Williams, C. A. and Elliott, C. J. (2015) 'Neurophysiology of *Drosophila* models of Parkinson's disease', *Parkinsons Dis,* 2015, pp. 381281.
White, M. D., Farmer, M., Mirabile, I., Brandner, S., Collinge, J. and Mallucci, G. R. (2008) 'Single treatment with RNAi against prion protein rescues early neuronal dysfunction and prolongs survival in mice with prion disease', *Proc Natl Acad Sci U S A,* 105(29), pp. 10238-43.
White, K. E., Humphrey, D. M. and Hirth, F. (2010) 'The dopaminergic system in the aging brain of *Drosophila*', *Front Neurosci,* 4, pp. 205.
WHO (2017) *Global action plan on public response to dementia 2017 - 2025.*
Wilesmith, J. W., Ryan, J. B. and Atkinson, M. J. (1991) 'Bovine spongiform encephalopathy: epidemiological studies on the origin', *Vet Rec,* 128(9), pp. 199-203.
Wilham, J. M., Orrú, C. D., Bessen, R. A., Atarashi, R., Sano, K., Race, B., Meade-White, K. D., Taubner, L. M., Timmes, A. and Caughey, B. (2010) 'Rapid end-point quantitation of prion seeding activity with sensitivity comparable to bioassays', *PLoS Pathog,* 6(12), pp. e1001217.
Will, R. G., Ironside, J. W., Zeidler, M., Cousens, S. N., Estibeiro, K., Alperovitch, A., Poser, S., Pocchiari, M., Hofman, A. and Smith, P. G. (1996) 'A new variant of Creutzfeldt-Jakob disease in the UK', *Lancet,* 347(9006), pp. 921-5.
Will, R. G. (2003a) 'Acquired prion disease: iatrogenic CJD, variant CJD, kuru', *Br Med Bull,* 66, pp. 255-65.
Will, R. G. (2003b) 'The biology and epidemiology of variant Creutzfeldt-Jakob disease', *Bull Mem Acad R Med Belg,* 158(5-6), pp. 250-6; discussion 256-7.

Wille, H., Zhang, G. F., Baldwin, M. A., Cohen, F. E. and Prusiner, S. B. (1996) 'Separation of scrapie prion infectivity from PrP amyloid polymers', *J Mol Biol,* 259(4), pp. 608-21.
Wille, H., Bian, W., McDonald, M., Kendall, A., Colby, D. W., Bloch, L., Ollesch, J., Borovinskiy, A. L., Cohen, F. E., Prusiner, S. B. and Stubbs, G. (2009) 'Natural and synthetic prion structure from X-ray fiber diffraction', *Proc Natl Acad Sci U S A,* 106(40), pp. 16990-5.
Williams, E. S. and Young, S. (1980) 'Chronic wasting disease of captive mule deer: a spongiform encephalopathy', *J Wildl Dis,* 16(1), pp. 89-98.
Williams, E. S. and Young, S. (1992) 'Spongiform encephalopathies in Cervidae', *Rev Sci Tech,* 11(2), pp. 551-67.
Williams, E. S. (2005) 'Chronic wasting disease', *Vet Pathol,* 42(5), pp. 530-49.
Willoughby, L. F., Schlosser, T., Manning, S. A., Parisot, J. P., Street, I. P., Richardson, H. E., Humbert, P. O. and Brumby, A. M. (2013) 'An in vivo large-scale chemical screening platform using *Drosophila* for anti-cancer drug discovery', *Dis Model Mech,* 6(2), pp. 521-9.
Wittmann, C. W., Wszolek, M. F., Shulman, J. M., Salvaterra, P. M., Lewis, J., Hutton, M. and Feany, M. B. (2001) 'Tauopathy in *Drosophila*: neurodegeneration without neurofibrillary tangles', *Science,* 293(5530), pp. 711-4.
Wolfram, V. and Baines, R. A. (2013) 'Blurring the boundaries: developmental and activity-dependent determinants of neural circuits', *Trends Neurosci,* 36(10), pp. 610-9.
Wong, B. S., Liu, T., Li, R., Pan, T., Petersen, R. B., Smith, M. A., Gambetti, P., Perry, G., Manson, J. C., Brown, D. R. and Sy, M. S. (2001) 'Increased levels of oxidative stress markers detected in the brains of mice devoid of prion protein', *J Neurochem,* 76(2), pp. 565-72.
Xiang, W., Windl, O., Wünsch, G., Dugas, M., Kohlmann, A., Dierkes, N., Westner, I. M. and Kretzschmar, H. A. (2004) 'Identification of differentially expressed genes in scrapie-infected mouse brains by using global gene expression technology', *J Virol,* 78(20), pp. 11051-60.
Yang, W., Cook, J., Rassbach, B., Lemus, A., DeArmond, S. J. and Mastrianni, J. A. (2009) 'A New Transgenic Mouse Model of Gerstmann-Straussler-Scheinker Syndrome Caused by the A117V Mutation of PRNP', *J Neurosci,* 29(32), pp. 10072-80.
Yoshihara, M., Ensminger, A. W. and Littleton, J. T. (2001) 'Neurobiology and the *Drosophila* genome', *Funct Integr Genomics,* 1(4), pp. 235-40.
Yost, C. S., Lopez, C. D., Prusiner, S. B., Myers, R. M. and Lingappa, V. R. (1990) 'Non-hydrophobic extracytoplasmic determinant of stop transfer in the prion protein', *Nature,* 343(6259), pp. 669-72.
Zahn, R., Liu, A., Lührs, T., Riek, R., von Schroetter, C., López García, F., Billeter, M., Calzolai, L., Wider, G. and Wüthrich, K. (2000) 'NMR solution structure of the human prion protein', *Proc Natl Acad Sci U S A,* 97(1), pp. 145-50.
Zanusso, G., Fiorini, M., Ferrari, S., Meade-White, K., Barbieri, I., Brocchi, E., Ghetti, B. and Monaco, S. (2014) 'Gerstmann-Sträussler-Scheinker disease and "anchorless prion protein" mice share prion conformational properties diverging from sporadic Creutzfeldt-Jakob disease', *J Biol Chem,* 289(8), pp. 4870-81.
Zhang, Y., Casas-Tinto, S., Rincon-Limas, D. E. and Fernandez-Funez, P. (2014) 'Combined pharmacological induction of Hsp70 suppresses prion protein neurotoxicity in *Drosophila*', *PLoS One,* 9(2), pp. e88522.

8 Appendix

8.1 Complete list of genotypes of PrP transgenic *Drosophila* and driver fly lines

Flies transgenic for ovine $V^{136}R^{154}Q^{171}$ (VRQ) PrP with insect signal peptide sequence

Chromosome 2

- w ; M{VRQ-PrP(GPI), 3xP3-RFP.attP}ZH-51D / CyO – ovine membrane bound PrP = VRQ(GPI) -chromosome 2
- w ; M{VRQ-PrP(ΔGPI), 3xP3-RFP.attP}ZH-51D / CyO – ovine secreted PrP lacking GPI-anchor = VRQ(ΔGPI) - chromosome 2
- w ; M{VRQ-PrP(cyt), 3xP3-RFP.attP}ZH-51D / CyO – ovine cytosolic PrP lacking signal peptide sequence and GPI-anchor = VRQ(cyt) – chromosome 2

Chromosome 3

- w- ; + / + ; 13xLexAop2-IVS-VRQ(GPI) / TM6C, Sb (attP2) – ovine membrane bound PrP – VRQ(GPI) – chromosome 3
- w- ; + / + ; 13xLexAop2-IVS-VRQ(ΔGPI) / TM6C, Sb (attP2) – ovine secreted PrP lacking GPI-anchor – VRQ(ΔGPI) – chromosome 3

Dual chromosome 2 + 3

- w ; M{VRQ-PrP(GPI), 3xP3-RFP.attP}ZH-51D / CyO ; 13xLexAop2-IVS-VRQ(GPI) / TM6C, Sb (attP2) – dual transgenic ovine membrane bound PrP VRQ(GPI) on chromosome 2 and ovine membrane bound PrP transgenic VRQ(GPI) on chromosome 3
- w ; M{VRQ-PrP(GPI), 3xP3-RFP.attP}ZH-51D / CyO ; 13xLexAop2-IVS-VRQ(ΔGPI) / TM6C, Sb (attP2) - dual transgenic ovine membrane bound PrP VRQ(GPI) on chromosome 2 and ovine secreted PrP lacking GPI-anchor VRQ(ΔGPI) on chromosome 3

Flies transgenic for ovine $A^{136}R^{154}Q^{171}$ (ARQ) PrP with insect signal peptide sequence – used as positive control in places

- w ; M{ARQ-PrP(GPI), 3xP3-RFP.attP}ZH-51D / CyO – ovine membrane bound PrP = ARQ(GPI) -chromosome 2

Flies transgenic for murine PrP with murine signal peptide sequence

- w ; M{Mo3F4WT, 3xP3-RFP.attP}ZH-51D / CyO – murine wild type PrP humanised by 3F4 epitope – chromosome 2
- w ; M{Mo3F4FFI, 3xP3-RFP.attP}ZH-51D / CyO – murine PrP humanised by 3F4 epitope and carrying FFI-associated mutation (D177N) – chromosome 2
- w ; M{Mo3F4CJD, 3xP3-RFP.attP}ZH-51D / CyO – murine PrP humanised by 3F4 epitope and carrying CJD-associated mutation (E199K) – chromosome 2

Flies transgenic for murine PrP with insect signal peptide sequence

- w ; M{VRQ-PrP(GPI), 3xP3-RFP.attP}ZH-51D / CyO – ovine membrane bound PrP = VRQ(GPI) -chromosome 2
- w ; M{Mo3F4WT, 3xP3-RFP.attP}ZH-51D / CyO – murine wild type PrP humanised by 3F4 epitope – chromosome 2 (transgenesis construct generated, not the flies yet)

Flies transgenic for hamster PrP with hamster signal peptide sequence

Chromosome 2

- w ; M{HaWT, 3xP3-RFP.attP}ZH-51D / CyO – hamster wild type PrP – chromosome 2
- w ; M{HaFFI, 3xP3-RFP.attP}ZH-51D / CyO – hamster PrP carrying FFI-associated mutation (D178N) – chromosome 2
- w ; M{HaCJD, 3xP3-RFP.attP}ZH-51D / CyO – hamster PrP carrying CJD-associated mutation (E200K) – chromosome 2

Chromosome 3

- w- ; + / + ; 13xLexAop2-IVS-HaCJD) / TM6C, Sb (attP2) – hamster PrP carrying CJD-associated mutation (E200K) – chromosome 3

Dual chromosome 2 + 3

- w ; M{HaWT, 3xP3-RFP.attP}ZH-51D / CyO ; 13xLexAop2-IVS-HaCJD) / TM6C, Sb (attP2) – dual transgenic hamster wild type PrP on chromosome 2 and hamster PrP carrying CJD-associated mutation (E200K) on chromosome 3

Flies transgenic for hamster PrP with insect signal peptide sequence

- w ; M{HaWT, 3xP3-RFP.attP}ZH-51D / CyO – hamster wild type PrP with insect signal peptide – chromosome 2
- w ; M{HaCJD, 3xP3-RFP.attP}ZH-51D / CyO – hamster PrP carrying CJD-associated mutation (E200K) with insect signal peptide – chromosome 2

Flies transgenic for human PrP with insect signal peptide sequence

Chromosome 2

- w ; M{Hu-M129, 3xP3-RFP.attP}ZH-51D / CyO – human PrP with M129 polymorphism with insect signal peptide – chromosome 2
- w ; M{Hu-V129, 3xP3-RFP.attP}ZH-51D / CyO – human PrP with V129 polymorphism with insect signal peptide – chromosome 2

Chromosome 3

- w ; + / + ; M{Hu-M129, 3xP3-RFP.attP}ZH-2A / TM6C, Sb – human PrP with M129 polymorphism with insect signal peptide – chromosome 3

- w ; + / + ; M{Hu-V129, 3xP3-RFP.attP}ZH-2A / TM6C, Sb – human PrP with V129 polymorphism with insect signal peptide – chromosome 3

Dual chromosome 2 + 3

- w ; M{Hu-M129, 3xP3-RFP.attP}ZH-51D / CyO ; w ; + / + ; M{Hu-M129, 3xP3-RFP.attP}ZH-2A / TM6C, Sb – dual transgenic human PrP with M129 polymorphism with insect signal peptide on chromosome 2 and human PrP with M129 polymorphism with insect signal peptide on chromosome 3
- w ; M{Hu-M129, 3xP3-RFP.attP}ZH-51D / CyO ; w ; + / + ; M{Hu-V129, 3xP3-RFP.attP}ZH-2A / TM6C, Sb – dual transgenic human PrP with M129 polymorphism with insect signal peptide on chromosome 2 and human PrP with V129 polymorphism with insect signal peptide on chromosome 3
- w ; M{Hu-V129, 3xP3-RFP.attP}ZH-51D / CyO ; w ; + / + ; M{Hu-M129, 3xP3-RFP.attP}ZH-AttP2 / TM6C, Sb – dual transgenic human PrP with V129 polymorphism with insect signal peptide on chromosome 2 and human PrP with M129 polymorphism with insect signal peptide on chromosome 3
- w ; M{Hu-V129, 3xP3-RFP.attP}ZH-51D / CyO ; w ; + / + ; M{Hu-V129, 3xP3-RFP.attP}ZH-AttP2 / TM6C, Sb – dual transgenic human PrP with V129 polymorphism with insect signal peptide on chromosome 2 and human PrP with V129 polymorphism with insect signal peptide on chromosome 3

Flies transgenic for cervid (white-tailed deer) PrP with insect signal peptide sequence

- w ; M{Cer-S138, 3xP3-RFP.attP}ZH-51D / CyO – cervid PrP with S138 polymorphism with insect signal peptide – chromosome 2
- w ; M{Cer-N138, 3xP3-RFP.attP}ZH-51D / CyO – cervid PrP with N138 polymorphism with insect signal peptide – chromosome 2

Negative control *Drosophila* genotypes – no PrP expression

- w ; M{3xP3-RFP.attP}ZH-51D – 51D fly, no PrP expression – 51D fly - chromosome 2
- y w ; M(eGFP, vas-int, dmRFP)ZH-2A;; M(attP)ZH-86Fb – attP2 fly - chromosome 3

Genotypes of *Drosophila* fluorescent reporter lines

- w ; +/+ ; 13xLexAop2-IVS-myr::tdTom (Su[Hw]attP5) – td Tomato red fluorescent reporter under the control of LexA (used for pan-neuronal expression under the 57C10-LexA control)
- w ; +/+ ; 13xLexAop2-IVS-myr::GFP (Su[Hw]attP5) – GFP fluorescent reporter under the control of LexA (used for pan-neuronal expression under the 57C10-LexA control)
- w ; +/+ ; 13xLexAop2-IVS-myr::GFP / CyO, DGY ; 10xUAS-IVS-myr::tdTom – dual reporter with GFP fluorescent reporter under the control of LexA and td Tomato red fluorescent reporter under the control of GAL4 (used for testing of dual expression of protein in fly larvae)

Genotypes of *Drosophila* driver fly lines

- P{w[+mW.hs]=GawB}elav[C155] – Elav-GAL4 pan-neuronal driver for chromosome 2 PrP flies
- w ; P{GAL4}repo / TM3, Sb - Repo-GAL4 glial cell driver for chromosome 2 PrP flies
- w- ; 57C10_n-Syb-LexAp65 (attP40) / CyO, Dfd-GMR-YFP – N-Syb-lexA pan-neuronal driver for chromosome 3 PrP flies
- w- ; If / [CyO, wg-Z] ; 57C10-Gal4 (attP2), Repo-LexAp65 (VK00027) / [TM6b] – Repo-LexA glial cell driver for chromosome 3 flies; 57C10-Gal4 pan-neuronal driver for chromosome 2 PrP flies
- w- ; 57C10-Gal4 (attP40) / CyO, Dfd-GMR-YFP ; iav-LexAp65 / TM6b, Dfd-GMR-YFP – iav-LexA sensory neurons specific driver for chromosome 3 PrP flies; 57C10-Gal4 pan-neuronal driver for chromosome 2 PrP flies
- w- ; 72F11-LexAp65 (JK22C), 13xLexAop2-IVS-myr::GFPp10 (Su[Hw]attP5) / CyO, Dfd-GMR-YFP ; 57C10-Gal4 (attP2) / TM6B, Sb, Dfd-GMR-YFP – 72F11-LexA driver for chromosome 3 PrP flies; 57C10-Gal4 pan-neuronal driver for chromosome 2 PrP flies
- w- ; 20B01-LexAp65 (JK22C), 13xLexAop2-IVS-myr::GFPp10 (su(Hw)attp5) / [CyO, Dfd-GMR-YFP] ; 57C10-Gal4 (attp2) / [TM6b, Sb, Dfd-GMR-YFP] – 20B01 LexA driver for chromosome 3 PrP flies; 57C10-Gal4 pan-neuronal driver for chromosome 2 PrP flies
- w- ; 71A10-LexAp65 (JK22C), 13xLexAop2-IVS-myr::GFPp10 (Su[Hw]attP5) / CyO, Dfd-GMR-YFP ; 57C10-Gal4 (attP2) / TM6B, Sb, Dfd-GMR-YFP – 71A10 LexA driver for chromosome 3 PrP flies; 57C10-Gal4 pan-neuronal driver for chromosome 2 PrP flies
- w- ; 57C10-Gal4 (attP40) / CyO, Dfd-GMR-YFP ; GMR-3-LexAp65 / TM6b, Dfd-GMR-YFP - GMR-LexA eye cell driver for chromosome 3 flies; 57C10-Gal4 pan-neuronal driver for chromosome 2 PrP flies

8.2 List of PrP transgene sequences

Mouse 3F4 WT with murine signal peptide

DNA sequence:

ATGGCGAACCTTGGCTACTGGCTGCTGGCCCTCTTTGTGACTATGTGGACTGATGTCGGCCTC
TGCAAAAAGCGGCCAAAGCCTGGAGGGTGGAACACCGGTGGAAGCCGGTATCCCGGGCAGGG
AAGCCCTGGAGGCAACCGTTACCCACCTCAGGGTGGCACCTGGGGGCAGCCCCACGGTGGTG
GCTGGGGACAACCCCATGGGGGCAGCTGGGGACAACCTCATGGTGGTAGTTGGGGTCAGCCC
CATGGCGGTGGATGGGGCCAAGGAGGGGGTACCCATAATCAGTGGAACAAGCCCAGCAAACC
AAAAACCAACATGAAGCATATGGCAGGGGCTGCGGCAGCTGGGGCAGTAGTGGGGGGCCTTG
GTGGCTACATGCTGGGGAGCGCCATGAGCAGGCCCATGATCCATTTTGGCAACGACTGGGAG
GACCGCTACTACCGTGAAAACATGTACCGCTACCCTAACCAAGTGTACTACAGGCCAGTGGAT
CAGTACAGCAACCAGAACAACTTCGTGCACGACTGCGTCAATATCACCATCAAGCAGCACACGG
TCACCACCACCACCAAGGGGGAGAACTTCACCGAGACCGATGTGAAGATGATGGAGCGCGTGG
TGGAGCAGATGTGCGTCACCCAGTACCAGAAGGAGTCCCAGGCCTATTACGACGGGAGAAGAT
CCAGCAGCACCGTGCTTTTCTCCTCCCCTCCTGTCATCCTCCTCATCTCCTTCCTCATCTTCCT
GATCGTGGGATGA

Protein sequence:

MANLGYWLLALFVTMWTDVGLCKKRPKPGGWNTGGSRYPGQGSPGGNRYPPQGGTWGQPHGG
GWGQPHGGSWGQPHGGSWGQPHGGGWGQGGGTHNQWNKPSKPKTNMKHMAGAAAAGAVVG
GLGGYMLGSAMSRPMIHFGNDWEDRYYRENMYRYPNQVYYRPVDQYSNQNNFVHDCVNITIKQH
TVTTTTKGENFTETDVKMMERVVEQMCVTQYQKESQAYYDGRRSSSTVLFSSPPVILLISFLIFLIVG-

Mouse 3F4 FFI with murine signal peptide

DNA sequence:

ATGGCGAACCTTGGCTACTGGCTGCTGGCCCTCTTTGTGACTATGTGGACTGATGTCGGCCTC
TGCAAAAAGCGGCCAAAGCCTGGAGGGTGGAACACCGGTGGAAGCCGGTATCCCGGGCAGGG
AAGCCCTGGAGGCAACCGTTACCCACCTCAGGGTGGCACCTGGGGGCAGCCCCACGGTGGTG
GCTGGGGACAACCCCATGGGGGCAGCTGGGGACAACCTCATGGTGGTAGTTGGGGTCAGCCC
CATGGCGGTGGATGGGGCCAAGGAGGGGGTACCCATAATCAGTGGAACAAGCCCAGCAAACC
AAAAACCAACATGAAGCATATGGCAGGGGCTGCGGCAGCTGGGGCAGTAGTGGGGGGCCTTG
GTGGCTACATGCTGGGGAGCGCCATGAGCAGGCCCATGATCCATTTTGGCAACGACTGGGAG
GACCGCTACTACCGTGAAAACATGTACCGCTACCCTAACCAAGTGTACTACAGGCCAGTGGAT
CAGTACAGCAACCAGAACAACTTCGTGCACAATTGCGTCAATATCACCATCAAGCAGCACACGG

TCACCACCACCACCAAGGGGGAGAACTTCACCGAGACCGATGTGAAGATGATGGAGCGCGTGG
TGGAGCAGATGTGCGTCACCCAGTACCAGAAGGAGTCCCAGGCCTATTACGACGGGAGAAGAT
CCAGCAGCACCGTGCTTTTCTCCTCCCCTCCTGTCATCCTCCTCATCTCCTTCCTCATCTTCCT
GATCGTGGGATGA

Protein sequence:

MANLGYWLLALFVTMWTDVGLCKKRPKPGGWNTGGSRYPGQGSPGGNRYPPQGGTWGQPHGG
GWGQPHGGSWGQPHGGSWGQPHGGGWGQGGGTHNQWNKPSKPKTNMKHMAGAAAAGAVVG
GLGGYMLGSAMSRPMIHFGNDWEDRYYRENMYRYPNQVYYRPVDQYSNQNNFVHNCVNITIKQH
TVTTTTKGENFTETDVKMMERVVEQMCVTQYQKESQAYYDGRRSSSTVLFSSPPVILLISFLIFLIVG-

Mouse 3F4 CJD with murine signal peptide

DNA sequence:

ATGGCGAACCTTGGCTACTGGCTGCTGGCCCTCTTTGTGACTATGTGGACTGATGTCGGCCTC
TGCAAAAAGCGGCCAAAGCCTGGAGGGTGGAACACCGGTGGAAGCCGGTATCCCGGGCAGGG
AAGCCCTGGAGGCAACCGTTACCCACCTCAGGGTGGCACNTGGGGGCAGCCCCACGGTGGTG
GCTGGGGACAACCCCATGGGGGCAGCTGGGGACAACCTCATGGTGGTAGTTGGGGTCAGCCC
CATGGCGGTGGATGGGGCCAAGGAGGGGGTACCCATAATCAGTGGAACAAGCCCAGCAAACC
AAAAACCAACATGAAGCATATGGCAGGGGCTGCGGCAGCTGGGGCAGTAGTGGGGGGCCTTG
GTGGCTACATGCTGGGGAGCGCCATGAGCAGGCCCATGATCCATTTTGGCAACGACTGGGAG
GACCGCTACTACCGTGAAAACATGTACCGCTACCCTAACCAAGTGTACTACAGGCCAGTGGAT
CAGTACAGCAACCAGAACAACTTCGTGCACGACTGCGTCAATATCACCATCAAGCAGCACACGG
TCACCACCACCACCAAGGGGGAGAACTTCACGAAGACCGATGTGAAGATGATGGAGCGCGTGG
TGGAGCAGATGTGCGTCACCCAGTACCAGAAGGAGTCCCAGGCCTATTACGACGGGAGAAGAT
CCAGCAGCACCGTGCTTTTCTCCTCCCCTCCTGTCATCCTCCTCATCTCCTTCCTCATCTTCCT
GATCGTGGGATGA

Protein sequence:

MANLGYWLLALFVTMWTDVGLCKKRPKPGGWNTGGSRYPGQGSPGGNRYPPQGGXWGQPHGG
GWGQPHGGSWGQPHGGSWGQPHGGGWGQGGGTHNQWNKPSKPKTNMKHMAGAAAAGAVVG
GLGGYMLGSAMSRPMIHFGNDWEDRYYRENMYRYPNQVYYRPVDQYSNQNNFVHDCVNITIKQH
TVTTTTKGENFTKTDVKMMERVVEQMCVTQYQKESQAYYDGRRSSSTVLFSSPPVILLISFLIFLIVG-

Hamster WT with hamster signal peptide

DNA sequence:

ATGGCGAACCTTAGCTACTGGCTGCTGGCACTCTTTGTGGCTATGTGGACTGATGTTGGCCTC
TGCAAGAAGCGGCCAAAGCCTGGAGGGTGGAACACTGGCGGAAGCCGATACCCTGGGCAGGG
CAGCCCTGGAGGCAACCGTTACCCACCTCAGGGTGGCGGCACATGGGGGCAACCCCATGGTG
GTGGCTGGGGACAGCCCCATGGTGGTGGCTGGGGACAGCCCCATGGTGGTGGCTGGGGTCA
GCCCCATGGTGGTGGCTGGGGTCAAGGAGGTGGCACCCACAATCAGTGGAACAAGCCCAGTA
AGCCAAAAACCAACATGAAGCACATGGCCGGCGCTGCTGCGGCAGGGGCCGTGGTGGGGGGC
CTTGGTGGCTACATGCTGGGGAGTGCCATGAGCAGGCCCATGATGCATTTTGGCAATGACTGG
GAGGACCGCTACTACCGTGAAAACATGAACCGCTACCCTAACCAAGTGTATTACCGGCCAGTG
GACCAGTACAACAACCAGAACAACTTTGTGCACGATTGTGTCAACATCACCATCAAGCAGCACA
CAGTCACCACCACCACCAAGGGGGAGAACTTCACGGAGACCGACATCAAGATAATGGAGCGCG
TGGTGGAGCAGATGTGTACCACCCAGTATCAGAAGGAGTCCCAGGCCTACTACGATGGAAGAA
GGTCCAGCGCGGTGCTGTTCTCCTCCCCTCCTGTGATCCTCCTCATTTCCTTTCTCATCTTCC
TGATGGTGGGATGA

Protein sequence:

MANLSYWLLALFVAMWTDVGLCKKRPKPGGWNTGGSRYPGQGSPGGNRYPPQGGGTWGQPHG
GGWGQPHGGGWGQPHGGGWGQPHGGGWGQGGGTHNQWNKPSKPKTNMKHMAGAAAAGAV
VGGLGGYMLGSAMSRPMMHFGNDWEDRYYRENMNRYPNQVYYRPVDQYNNQNNFVHDCVNIT
IKQHTVTTTTKGENFTETDIKIMERVVEQMCTTQYQKESQAYYDGRRSSAVLFSSPPVILLISFLIFLM
VG-

Hamster FFI with hamster signal peptide

DNA sequence:

ATGGCGAACCTTAGCTACTGGCTGCTGGNACTCTTTGTGGCTATGTGGACTGATGTTGGCCTC
TGCAAGAAGCGGCCAAAGCCTGGAGGGTGGAACACTGGCGGAAGCCGATACCCTGGGCAGGG
CAGCCCTGGAGGCAACCGTTACCCACCTCAGGGTGGCGGCACATGGGGGCAACCCCATGGTG
GTGGCTGGGGACAGCCCCATGGTGGTGGCTGGGGACAGCCCCATGGTGGTGGCTGGGGTCA
GCCCCATGGTGGTGGCTGGGGTCAAGGAGGTGGCACCCACAATCAGTGGAACAAGCCCAGTA
AGCCAAAAACCAACATGAAGCACATGGCCGGCGCTGCTGCGGCAGGGGCCGTGGTGGGGGGC
CTTGGTGGCTACATGCTGGGGAGTGCCATGAGCAGGCCCATGATGCATTTTGGCAATGACTGG
GAGGACCGCTACTACCGTGAAAACATGAACCGCTACCCTAACCAAGTGTATTACCGGCCAGTG
GACCAGTACAACAACCAGAACAACTTTGTGCACAATTGTGTCAACATCACCATCAAGCAGCACA
CAGTCACCACCACCACCAAGGGGGAGAACTTCACGGAGACCGACATCAAGATAATGGAGCGCG

TGGTGGAGCAGATGTGTACCACCCAGTATCAGAAGGAGTCCCAGGCCTACTACGATGGAAGAA
GGTCCAGCGCGGTGCTGTTCTCCTCCCCTCCTGTGATCCTCCTCATTTCCTTTCTCATCTTCC
TGATGGTGGGATGA

Protein sequence:

MANLSYWLLXLFVAMWTDVGLCKKRPKPGGWNTGGSRYPGQGSPGGNRYPPQGGGTWGQPHG
GGWGQPHGGGWGQPHGGGWGQPHGGGWGQGGGTHNQWNKPSKPKTNMKHMAGAAAAGAV
VGGLGGYMLGSAMSRPMMHFGNDWEDRYYRENMNRYPNQVYYRPVDQYNNQNNFVHNCVNIT
IKQHTVTTTTKGENFTETDIKIMERVVEQMCTTQYQKESQAYYDGRRSSAVLFSSPPVILLISFLIFLM
VG-

Hamster CJD with hamster signal peptide

DNA sequence:

ATGGCGAACCTTAGCTACTGGCTGCTGGCACTCTTTGTGGCTATGTGGACTGATGTTGGCCTC
TGCAAGAAGCGGCCAAAGCCTGGAGGGTGGAACACTGGCGGAAGCCGATACCCTGGGCAGGG
CAGCCCTGGAGGCAACCGTTACCCACCTCAGGGTGGCGGCACATGGGGGCAACCCCATGGTG
GTGGCTGGGGACAGCCCCATGGTGGTGGCTGGGGACAGCCCCATGGTGGTGGCTGGGGTCA
GCCCCATGGTGGTGGCTGGGGTCAAGGAGGTGGCACCCACAATCAGTGGAACAAGCCCAGTA
AGCCAAAAACCAACATGAAGCACATGGCCGGCGCTGCTGCGGCAGGGGCCGTGGTGGGGGGC
CTTGGTGGCTACATGCTGGGGAGTGCCATGAGCAGGCCCATGATGCATTTTGGCAATGACTGG
GAGGACCGCTACTACCGTGAAAACATGAACCGCTACCCTAACCAAGTGTATTACCGGCCAGTG
GACCAGTACAACAACCAGAACAACTTTGTGCACGATTGTGTCAACATCACCATCAAGCAGCACA
CAGTCACCACCACCACCAAGGGGGAGAACTTCACGAAGACCGACATCAAGATAATGGAGCGCG
TGGTGGAGCAGATGTGTACCACCCAGTATCAGAAGGAGTCCCAGGCCTACTACGATGGAAGAA
GGTCCAGCGCGGTGCTGTTCTCCTCCCCTCCTGTGATCCTCCTCATTTCCTTTCTCATCTTCC
TGATGGTGGGATGA

Protein sequence:

MANLSYWLLALFVAMWTDVGLCKKRPKPGGWNTGGSRYPGQGSPGGNRYPPQGGGTWGQPHG
GGWGQPHGGGWGQPHGGGWGQPHGGGWGQGGGTHNQWNKPSKPKTNMKHMAGAAAAGAV
VGGLGGYMLGSAMSRPMMHFGNDWEDRYYRENMNRYPNQVYYRPVDQYNNQNNFVHDCVNIT
IKQHTVTTTTKGENFTKTDIKIMERVVEQMCTTQYQKESQAYYDGRRSSAVLFSSPPVILLISFLIFLM
VG-

Mouse 3F4 WT with insect signal peptide

DNA sequence:

ATGGCGAGCAAAGTCTCGATCCTTCTCCTGCTAACCGTCCATCTTCTGGCTGCTCAGACCTTC
GCCCAGAAAAAGCGGCCAAAGCCTGGAGGGTGGAACACCGGTGGAAGCCGGTATCCCGGGCA
GGGAAGCCCTGGAGGCAACCGTTACCCACCTCAGGGTGGCACCTGGGGGCAGCCCCACGGTG
GTGGCTGGGGACAACCCCATGGGGGCAGCTGGGGACAACCTCATGGTGGTAGTTGGGGTCAG
CCCCATGGCGGTGGATGGGGCCAAGGAGGGGGTACCCATAATCAGTGGAACAAGCCCAGCAA
ACCAAAAACCAACATGAAGCATATGGCAGGGGCTGCGGCAGCTGGGGCAGTAGTGGGGGGCC
TTGGTGGCTACATGCTGGGGAGCGCCATGAGCAGGCCCATGATCCATTTTGGCAACGACTGG
GAGGACCGCTACTACCGTGAAAACATGTACCGCTACCCTAACCAAGTGTACTACAGGCCAGTG
GATCAGTACAGCAACCAGAACAACTTCGTGCACGACTGCGTCAATATCACCATCAAGCAGCACA
CGGTCACCACCACCACCAAGGGGGAGAACTTCACCGAGACCGATGTGAAGATGATGGAGCGCG
TGGTGGAGCAGATGTGCGTCACCCAGTACCAGAAGGAGTCCCAGGCCTATTACGACGGGAGAA
GATCCAGCAGCACCGTGCTTTTCTCCTCCCCTCCTGTCATCCTCCTCATCTCCTTCCTCATCTT
CCTGATCGTGGGATGA

Protein sequence:

MASKVSILLLLTVHLLAAQTFAQKKRPKPGGWNTGGSRYPGQGSPGGNRYPPQGGTWGQPHGGG
WGQPHGGSWGQPHGGSWGQPHGGGWGQGGGTHNQWNKPSKPKTNMKHMAGAAAAGAVVGG
LGGYMLGSAMSRPMIHFGNDWEDRYYRENMYRYPNQVYYRPVDQYSNQNNFVHDCVNITIKQHT
VTTTTKGENFTETDVKMMERVVEQMCVTQYQKESQAYYDGRRSSTVLFSSPPVILLISFLIFLIVG-

Hamster WT with insect signal peptide

DNA sequence:

ATGGCGAGCAAAGTCTCGATCCTTCTCCTGCTAACCGTCCATCTTCTGGCTGCTCAGACCTTC
GCCCAGAAGAAGCGGCCAAAGCCTGGAGGGTGGAACACTGGCGGAAGCCGATACCCTGGGCA
GGGCAGCCCTGGAGGCAACCGTTACCCACCTCAGGGTGGCGGCACATGGGGGCAACCCCATG
GTGGTGGCTGGGGACAGCCCCATGGTGGTGGCTGGGGACAGCCCCATGGTGGTGGCTGGGG
TCAGCCCCATGGTGGTGGCTGGGGTCAAGGAGGTGGCACCCACAATCAGTGGAACAAGCCCA
GTAAGCCAAAAACCAACATGAAGCACATGGCCGGCGCTGCTGCGGCAGGGGCCGTGGTGGGG
GGCCTTGGTGGCTACATGCTGGGGAGTGCCATGAGCAGGCCCATGATGCATTTTGGCAATGAC
TGGGAGGACCGCTACTACCGTGAAAACATGAACCGCTACCCTAACCAAGTGTATTACCGGCCA
GTGGACCAGTACAACAACCAGAACAACTTTGTGCACGATTGTGTCAACATCACCATCAAGCAGC

ACACAGTCACCACCACCACCAAGGGGGAGAACTTCACGGAGACCGACATCAAGATAATGGAGC
GCGTGGTGGAGCAGATGTGTACCACCCAGTATCAGAAGGAGTCCCAGGCCTACTACGATGGAA
GAAGGTCCAGCGCGGTGCTGTTCTCCTCCCCTCCTGTGATCCTCCTCATTTCCTTTCTCATCT
TCCTGATGGTGGGATGA

Protein sequence:

MASKVSILLLLTVHLLAAQTFAQKKRPKPGGWNTGGSRYPGQGSPGGNRYPPQGGGTWGQPHGG
GWGQPHGGGWGQPHGGGWGQPHGGGWGQGGGTHNQWNKPSKPKTNMKHMAGAAAAGAVV
GGLGGYMLGSAMSRPMMHFGNDWEDRYYRENMNRYPNQVYYRPVDQYNNQNNFVHDCVNITI
KQHTVTTTTKGENFTETDIKIMERVVEQMCTTQYQKESQAYYDGRRSSAVLFSSPPVILLISFLIFLMV
G-

Ovine VRQ(GPI)

DNA sequence:

ATGGCGAGCAAAGTCTCGATCCTTCTCCTGCTAACCGTCCATCTTCTGGCTGCTCAGACCTTC
GCCCAGAAGAAGCGACCAAAACCTGGCGGAGGATGGAACACTGGGGGGAGCCGATACCCGGG
ACAGGGCAGTCCTGGAGGCAACCGCTATCCACCTCAGGGAGGGGGTGGCTGGGGTCAGCCCC
ATGGAGGTGGCTGGGGCCAACCTCATGGAGGTGGCTGGGGTCAGCCCCATGGTGGTGGCTGG
GGACAGCCACATGGTGGTGGAGGCTGGGGTCAAGGTGGTAGCCACAGTCAGTGGAACAAGCC
CAGTAAGCCAAAAACCAACATGAAGCATGTGGCAGGAGCTGCTGCAGCTGGAGCAGTGGTAGG
GGGCCTTGGTGGCTACATGCTGGGAAGTGTCATGAGCAGGCCTCTTATACATTTTGGCAATGA
CTATGAGGACCGTTACTATCGTGAAAACATGTACCGTTACCCCAACCAAGTGTACTACAGACCA
GTGGATCAGTATAGTAACCAGAACAACTTTGTGCATGACTGTGTCAACATCACAGTCAAGCAAC
ACACAGTCACCACCACCACCAAGGGGGAGAACTTCACCGAAACTGACATCAAGATAATGGAGC
GAGTGGTGGAGCAAATGTGCATCACCCAGTACCAGAGAGAATCCCAGGCTTATTACCAAAGGG
GGGCAAGTGTGATCCTCTTTTCTTCCCCTCCTGTGATCCTCCTCATCTCTTTCCTCATTTTTCT
CATAGTAGGATAG

Protein sequence:

MASKVSILLLLTVHLLAAQTFAQKKRPKPGGGWNTGGSRYPGQGSPGGNRYPPQGGGGWGQPHG
GGWGQPHGGGWGQPHGGGWGQPHGGGGWGQGGSHSQWNKPSKPKTNMKHVAGAAAAGAVV
GGLGGYMLGSVMSRPLIHFGNDYEDRYYRENMYRYPNQVYYRPVDQYSNQNNFVHDCVNITVKQ
HTVTTTTKGENFTETDIKIMERVVEQMCITQYQRESQAYYQRGASVILFSSPPVILLISFLIFLIVG-

Ovine VRQ(ΔGPI)

DNA sequence:

ATGGCGAGCAAAGTCTCGATCCTTCTCCTGCTAACCGTCCATCTTCTGGCTGCTCAGACCTTC
GCCCAGAAGAAGCGACCAAAACCTGGCGGAGGATGGAACACTGGGGGGAGCCGATACCCGGG
ACAGGGCAGTCCTGGAGGCAACCGCTATCCACCTCAGGGAGGGGGTGGCTGGGGTCAGCCCC
ATGGAGGTGGCTGGGGCCAACCTCATGGAGGTGGCTGGGGTCAGCCCCATGGTGGTGGCTGG
GGACAGCCACATGGTGGTGGAGGCTGGGGTCAAGGTGGTAGCCACAGTCAGTGGAACAAGCC
CAGTAAGCCAAAAACCAACATGAAGCATGTGGCAGGAGCTGCTGCAGCTGGAGCAGTGGTAGG
GGGCCTTGGTGGCTACATGCTGGGAAGTGTCATGAGCAGGCCTCTTATACATTTTGGCAATGA
CTATGAGGACCGTTACTATCGTGAAAACATGTACCGTTACCCCAACCAAGTGTACTACAGACCA
GTGGATCAGTATAGTAACCAGAACAACTTTGTGCATGACTGTGTCAACATCACAGTCAAGCAAC
ACACAGTCACCACCACCACCAAGGGGGAGAACTTCACCGAAACTGACATCAAGATAATGGAGC
GAGTGGTGGAGCAAATGTGCATCACCCAGTACCAGAGAGAATCCCAGGCTTATTACCAAAGGG
GG

Protein sequence:

MASKVSILLLLTVHLLAAQTFAQKKRPKPGGGWNTGGSRYPGQGSPGGNRYPPQGGGGWGQPHG
GGWGQPHGGGWGQPHGGGWGQPHGGGGWGQGGSHSQWNKPSKPKTNMKHVAGAAAAGAVV
GGLGGYMLGSVMSRPLIHFGNDYEDRYYRENMYRYPNQVYYRPVDQYSNQNNFVHDCVNITVKQ
HTVTTTTKGENFTETDIKIMERVVEQMCITQYQRESQAYYQRG

Ovine VRQ(cyt)

DNA sequence:

AAGAAGCGACCAAAACCTGGCGGAGGATGGAACACTGGGGGGAGCCGATACCCGGGACAGGG
CAGTCCTGGAGGCAACCGCTATCCACCTCAGGGAGGGGGTGGCTGGGGTCAGCCCCATGGAG
GTGGCTGGGGCCAACCTCATGGAGGTGGCTGGGGTCAGCCCCATGGTGGTGGCTGGGGACAG
CCACATGGTGGTGGAGGCTGGGGTCAAGGTGGTAGCCACAGTCAGTGGAACAAGCCCAGTAA
GCCAAAAACCAACATGAAGCATGTGGCAGGAGCTGCTGCAGCTGGAGCAGTGGTAGGGGGCC
TTGGTGGCTACATGCTGGGAAGTGTCATGAGCAGGCCTCTTATACATTTTGGCAATGACTATG
AGGACCGTTACTATCGTGAAAACATGTACCGTTACCCCAACCAAGTGTACTACAGACCAGTGGA
TCAGTATAGTAACCAGAACAACTTTGTGCATGACTGTGTCAACATCACAGTCAAGCAACACACA
GTCACCACCACCACCAAGGGGGAGAACTTCACCGAAACTGACATCAAGATAATGGAGCGAGTG
GTGGAGCAAATGTGCATCACCCAGTACCAGAGAGAATCCCAGGCTTATTACCAAAGGGGG

Protein sequence:

KKRPKPGGGWNTGGSRYPGQGSPGGNRYPPQGGGGWGQPHGGGWGQPHGGGWGQPHGGGW
GQPHGGGGWGQGGSHSQWNKPSKPKTNMKHVAGAAAAGAVVGGLGGYMLGSVMSRPLIHFGN
DYEDRYYRENMYRYPNQVYYRPVDQYSNQNNFVHDCVNITVKQHTVTTTTKGENFTETDIKIMER
VVEQMCITQYQRESQAYYQRG

Ovine ARQ(GPI)

DNA sequence:

ATGGCGAGCAAAGTCTCGATCCTTCTCCTGCTAACCGTCCATCTTCTGGCTGCTCAGACCTTC
GCCCAGAAGAAGCGACCAAAACCTGGCGGAGGATGGAACACTGGGGGGAGCCGATACCCGGG
ACAGGGCAGTCCTGGAGGCAACCGCTATCCACCTCAGGGAGGGGGTGGCTGGGGTCAGCCCC
ATGGAGGTGGCTGGGGCCAACCTCATGGAGGTGGCTGGGGTCAGCCCCATGGTGGTGGCTGG
GGACAGCCACATGGTGGTGGAGGCTGGGGTCAAGGTGGTAGCCACAGTCAGTGGAACAAGCC
CAGTAAGCCAAAAACCAACATGAAGCATGTGGCAGGAGCTGCTGCAGCTGGAGCAGTGGTAGG
GGGCCTTGGTGGCTACATGCTGGGAAGTGCCATGAGCAGGCCTCTTATACATTTTGGCAATGA
CTATGAGGACCGTTACTATCGTGAAAACATGTACCGTTACCCCAACCAAGTGTACTACAGACCA
GTGGATCAGTATAGTAACCAGAACAACTTTGTGCATGACTGTGTCAACATCACAGTCAAGCAAC
ACACAGTCACCACCACCACCAAGGGGGAGAACTTCACCGAAACTGACATCAAGATAATGGAGC
GAGTGGTGGAGCAAATGTGCATCACCCAGTACCAGAGAGAATCCCAGGCTTATTACCAAAGGG
GGGCAAGTGTGATCCTCTTTTCTTCCCCTCCTGTGATCCTCCTCATCTCTTTCCTCATTTTTCT
CATAGTAGGATAG

Protein sequence:

MASKVSILLLLTVHLLAAQTFAQKKRPKPGGGWNTGGSRYPGQGSPGGNRYPPQGGGGWGQPHG
GGWGQPHGGGWGQPHGGGWGQPHGGGGWGQGGSHSQWNKPSKPKTNMKHVAGAAAAGAVV
GGLGGYMLGSAMSRPLIHFGNDYEDRYYRENMYRYPNQVYYRPVDQYSNQNNFVHDCVNITVKQ
HTVTTTTKGENFTETDIKIMERVVEQMCITQYQRESQAYYQRGASVILFSSPPVILLISFLIFLIVG-

Human M129 with insect signal peptide

DNA sequence:

ATGGCGAGCAAAGTCTCGATCCTTCTCCTGCTAACCGTCCATCTTCTGGCTGCTCAGACCTTC
GCCCAGAAGAAGCGCCCGAAGCCTGGAGGATGGAACACTGGGGGCAGCCGATACCCGGGGCA
GGGCAGCCCTGGAGGCAACCGCTACCCACCTCAGGGCGGTGGTGGCTGGGGGCAGCCTCATG

GTGGTGGCTGGGGGCAGCCTCATGGTGGTGGCTGGGGGCAGCCCCATGGTGGTGGCTGGGG
ACAGCCTCATGGTGGTGGCTGGGGTCAAGGAGGTGGCACCCACAGTCAGTGGAACAAGCCGA
GTAAGCCAAAAACCAACATGAAGCACATGGCTGGTGCTGCAGCAGCTGGGGCAGTGGTGGGG
GGCCTTGGCGGCTACATGCTGGGAAGTGCCATGAGCAGGCCCATCATACATTTCGGCAGTGAC
TATGAGGACCGCTACTATCGTGAAAACATGCACCGTTACCCCAACCAAGTGTACTACAGGCCCA
TGGATGAGTACAGCAACCAGAACAACTTTGTGCACGACTGCGTCAATATCACAATCAAGCAGCA
CACGGTCACCACAACCACCAAGGGGGAGAACTTCACCGAGACCGACGTTAAGATGATGGAGCG
CGTGGTTGAGCAGATGTGTATCACCCAGTACGAGAGGGAATCTCAGGCCTATTACCAGAGAGG
ATCGAGCATGGTCCTCTTCTCCTCTCCACCTGTGATCCTCCTGATCTCTTTCCTCATCTTCCTG
ATAGTGGGATGA

Protein sequence:

MASKVSILLLLTVHLLAAQTFAQKKRPKPGGWNTGGSRYPGQGSPGGNRYPPQGGGGWGQPHGG
GWGQPHGGGWGQPHGGGWGQPHGGGWGQGGGTHSQWNKPSKPKTNMKHMAGAAAAGAVV
GGLGGYMLGSAMSRPIIHFGSDYEDRYYRENMHRYPNQVYYRPMDEYSNQNNFVHDCVNITIKQH
TVTTTTKGENFTETDVKMMERVVEQMCITQYERESQAYYQRGSSMVLFSSPPVILLISFLIFLIVG-

Human V129 with insect signal peptide

DNA sequence:

ATGGCGAGCAAAGTCTCGATCCTTCTCCTGCTAACCGTCCATCTTCTGGCTGCTCAGACCTTC
GCCCAGAAGAAGCGCCCGAAGCCTGGAGGATGGAACACTGGGGGCAGCCGATACCCGGGGCA
GGGCAGCCCTGGAGGCAACCGCTACCCACCTCAGGGCGGTGGTGGCTGGGGGCAGCCTCATG
GTGGTGGCTGGGGGCAGCCTCATGGTGGTGGCTGGGGGCAGCCCCATGGTGGTGGCTGGGG
ACAGCCTCATGGTGGTGGCTGGGGTCAAGGAGGTGGCACCCACAGTCAGTGGAACAAGCCGA
GTAAGCCAAAAACCAACATGAAGCACATGGCTGGTGCTGCAGCAGCTGGGGCAGTGGTGGGG
GGCCTTGGCGGCTACGTGCTGGGAAGTGCCATGAGCAGGCCCATCATACATTTCGGCAGTGA
CTATGAGGACCGCTACTATCGTGAAAACATGCACCGTTACCCCAACCAAGTGTACTACAGGCCC
ATGGATGAGTACAGCAACCAGAACAACTTTGTGCACGACTGCGTCAATATCACAATCAAGCAGC
ACACGGTCACCACAACCACCAAGGGGGAGAACTTCACCGAGACCGACGTTAAGATGATGGAGC
GCGTGGTTGAGCAGATGTGTATCACCCAGTACGAGAGGGAATCTCAGGCCTATTACCAGAGAG
GATCGAGCATGGTCCTCTTCTCCTCTCCACCTGTGATCCTCCTGATCTCTTTCCTCATCTTCCT
GATAGTGGGATGA

Protein sequence:

MASKVSILLLLTVHLLAAQTFAQKKRPKPGGWNTGGSRYPGQGSPGGNRYPPQGGGGWGQPHGG
GWGQPHGGGWGQPHGGGWGQPHGGGWGQGGGTHSQWNKPSKPKTNMKHMAGAAAAGAVV
GGLGGYVLGSAMSRPIIHFGSDYEDRYYRENMHRYPNQVYYRPMDEYSNQNNFVHDCVNITIKQH
TVTTTTKGENFTETDVKMMERVVEQMCITQYERESQAYYQRGSSMVLFSSPPVILLISFLIFLIVG-

Cervid (white-tailed deer) S138 with insect signal peptide

DNA sequence:

ATGGCGAGCAAAGTCTCGATCCTTCTCCTGCTAACCGTCCATCTTCTGGCTGCTCAGACCTTC
GCCCAGAAGAAGCGACCAAAACCTGGAGGAGGATGGAACACTGGGGGGAGCCGATACCCGGG
ACAGGGAAGTCCTGGAGGCAACCGCTATCCACCTCAGGGAGGGGGTGGCTGGGGTCAGCCCC
ATGGAGGTGGCTGGGGCCAACCTCATGGAGGTGGCTGGGGTCAGCCCCATGGTGGTGGCTGG
GGGCAGCCACATGGTGGTGGAGGCTGGGGTCAAGGTGGTACCCACAGTCAGTGGAACAAGCC
CAGTAAACCAAAAACCAACATGAAGCATGTGGCAGGAGCTGCTGCCGCTGGAGCAGTGGTAGG
GGGCCTTGGTGGCTACATGCTGGGAAGTGCCATGAGCAGACCTCTTATACATTTTGGCAACGA
CTATGAGGACCGTTACTATCGTGAAAATATGTACCGTTACCCCAACCAAGTGTACTACAGGCCA
GTGGATCAGTATAATAACCAGAACACCTTTGTGCATGACTGTGTCAACATCACAGTCAAGCAAC
ACACAGTCACCACCACCACCAAGGGGGAGAACTTCACTGAAACTGACATTAAGATGATGGAGC
GAGTTGTGGAGCAAATGTGCATCACCCAGTACCAGAGAGAATCCCAGGCTTATTACCAAAGAG
GGGCAAGTGTGATCCTCTTCTCCTCCCCTCCTGTGATCCTCCTCATCTCTTTCCTCATTTTTCT
CATAGTAGGATAG

Protein sequence:

MASKVSILLLLTVHLLAAQTFAQKKRPKPGGGWNTGGSRYPGQGSPGGNRYPPQGGGGWGQPHG
GGWGQPHGGGWGQPHGGGWGQPHGGGGWGQGGTHSQWNKPSKPKTNMKHVAGAAAAGAVV
GGLGGYMLGSAMSRPLIHFGNDYEDRYYRENMYRYPNQVYYRPVDQYNNQNTFVHDCVNITVKQ
HTVTTTTKGENFTETDIKMMERVVEQMCITQYQRESQAYYQRGASVILFSSPPVILLISFLIFLIVG-

Cervid (white-tailed deer) N138 with insect signal peptide

DNA sequence:

ATGGCGAGCAAAGTCTCGATCCTTCTCCTGCTAACCGTCCATCTTCTGGCTGCTCAGACCTTC
GCCCAGAAGAAGCGACCAAAACCTGGAGGAGGATGGAACACTGGGGGGAGCCGATACCCGGG
ACAGGGAAGTCCTGGAGGCAACCGCTATCCACCTCAGGGAGGGGGTGGCTGGGGTCAGCCCC
ATGGAGGTGGCTGGGGCCAACCTCATGGAGGTGGCTGGGGTCAGCCCCATGGTGGTGGCTGG
GGGCAGCCACATGGTGGTGGAGGCTGGGGTCAAGGTGGTACCCACAGTCAGTGGAACAAGCC

CAGTAAACCAAAAACCAACATGAAGCATGTGGCAGGAGCTGCTGCCGCTGGAGCAGTGGTAGG
GGGCCTTGGTGGCTACATGCTGGGAAGTGCCATGAACAGACCTCTTATACATTTTGGCAACGA
CTATGAGGACCGTTACTATCGTGAAAATATGTACCGTTACCCCAACCAAGTGTACTACAGGCCA
GTGGATCAGTATAATAACCAGAACACCTTTGTGCATGACTGTGTCAACATCACAGTCAAGCAAC
ACACAGTCACCACCACCACCAAGGGGGAGAACTTCACTGAAACTGACATTAAGATGATGGAGC
GAGTTGTGGAGCAAATGTGCATCACCCAGTACCAGAGAGAATCCCAGGCTTATTACCAAAGAG
GGGCAAGTGTGATCCTCTTCTCCTCCCCTCCTGTGATCCTCCTCATCTCTTTCCTCATTTTTCT
CATAGTAGGATAG

Protein sequence:

MASKVSILLLLTVHLLAAQTFAQKKRPKPGGGWNTGGSRYPGQGSPGGNRYPPQGGGGWGQPHG
GGWGQPHGGGWGQPHGGGWGQPHGGGGWGQGGTHSQWNKPSKPKTNMKHVAGAAAAGAVV
GGLGGYMLGSAMNRPLIHFGNDYEDRYYRENMYRYPNQVYYRPVDQYNNQNTFVHDCVNITVKQ
HTVTTTTKGENFTETDIKMMERVVEQMCITQYQRESQAYYQRGASVILFSSPPVILLISFLIFLIVG-

8.3 List of primers used in the project

- MoFI (EcoRI) – forward mouse 3F4 transgene specific (murine signal peptide)

  5' GGC GAA TTC ATG GCG AAC CTT GGC TAC TGG 3'

- MoRI (XhoI) – reverse mouse 3F4 transgene specific (GPI anchor)

  5' GTC CGC TCG AGT CAT CCC ACG ATC AGG AAG ATG 3'

- HaFI (EcoRI) – forward hamster transgene specific (murine signal peptide)

  5' GGC GAA TTC ATG GCG AAC CTT AGC TAC TGG 3'

- HaRI (XhoI) – reverse hamster transgene specific (GPI anchor)

  5' GTC CGC TCG AGT CAT CCC ACC ATC AGG AAG ATG 3'

- pUAST-F (EcoRI) – forward pUAST plasmid specific (flanking the insert, used for sequencing)

  5' CTG CAA CTA CTG AAA TCT GCC 3'

- pUAST-R (XhoI) – reverse pUAST plasmid specific (flanking the insert, used for sequencing)

  5' GGC ATT CCA CCA CTG CTC 3'

- VRQs-F – forward ovine VRQ(ΔGPI) PrP insert specific (5' of mature form) for PCR verification of chromosome 3 VRQ(ΔGPI) transgenic flies

  5' TAT TCT CGA GAT GGC GAG CAA AG 3'

- VRQs-R – reverse ovine VRQ(ΔGPI) PrP insert specific (3' of mature form) for PCR verification of chromosome 3 VRQ(ΔGPI) transgenic flies

  5' TGA ATC TAG ACT ACC CCC TTT GG 3'

- VRQm-F – forward ovine VRQ(GPI) PrP insert specific (5' of mature form) for PCR verification of chromosome 3 VRQ(GPI) transgenic flies

  5' ATT TCT CGA GAG GGC GAG CAA AG 3'

- VRQm-R – reverse ovine VRQ(GPI) PrP insert specific (3' of mature form) for PCR verification of chromosome 3 VRQ(GPI) transgenic flies

  5' GCC CTC TAG ACT ATC CTA CTA TG 3'

- pJFRC19-F – forward pJFRC19-MUH plasmid specific (flanking the insert, used for sequencing)

  5' TAC AAG AAG AGA ACT CTG 3'

- pJFRC19-R – reverse pJFRC19-MUH plasmid specific (flanking the insert, used for sequencing)

  5' GTG TAT AAT GTG TTA AAC 3'

- MoPD1F – forward murine 3F4 PrP insert specific (5' of mature form) for synthesis of insect signal peptide (1st step)

  5' GTC CAT CTT CTG GCT GCT CAG ACC TTC GCC CAG AAA AAG CGG CCA AAG CCT GG 3'

- HaPD1F – forward hamster PrP insert specific (5' of mature form) for synthesis of insect signal peptide (1st step)

  5' GTC CAT CTT CTG GCT GCT CAG ACC TTC GCC CAG AAG AAG CGG CCA AAG CCT GG 3'

- PD2F (EcoRI) – forward primer that creates a template for insect signal peptide synthesis by binding to MoPD1F or HaPd1F primers (2nd step)

  5' GGC GAA TTC ATG GCG AGC AAA GTC TCG ATC CTT CTC CTG CTA ACC GTC CAT CTT CTG G 3'

- Chr3haFxho1 (XhoI) - forward primer for construction of hamster signal peptide hamster PrP transgenic flies on chromosome 3 (for insertion into pJFRC19-MUH plasmid)

  5' TAT TCT CGA GAT GGC GAA CCT TAG CTA CTG G 3'

- Chr3haRxba1 (XbaI) - reverse primer for construction of hamster signal peptide hamster PrP transgenic flies on chromosome 3 (for insertion into pJFRC19-MUH plasmid)

  5' GCC CTC TAG ATC ATC CCA CCA TCA GGA AGA TG 3'

- HuPrP-PDF1 – forward human PrP insert specific (5' of mature form) for synthesis of insect signal peptide (1st step)

  5' CCA TCT TCT GGC TGC TCA GAC CTT CGC CCA GAA GAA GCG CCC GAA GCC TGG AG 3'

- HuPrP-R (XbaI, XhoI) – reverse human transgene specific (GPI anchor)

  5' GTC CGC TCG AGT CTA GAT CAT CCC ACT ATC AGG AAG ATG 3'

- PD1FCerPrP – forward cervid PrP insert specific (5' of mature form) for synthesis of insect signal peptide (1st step)

  5' CCA TCT TCT GGC TGC TCA GAC CTT CGC CCA GAA GAA GCG ACC AAA ACC 3'

- CerPrPR1 (XbaI, XhoI) – reverse cervid transgene specific (GPI anchor)

  5' GTC CGC TCG AGT CTA GAC TAT CCT ACT ATG AGA AAA ATG 3'

8.4 Fly crosses for 57C10-n-Syb-LexA driven lethality tracing

Cross to add fluorescent tag to the LexA driver:

- w- ; 57C10_n-Syb-LexAp65 (attP40) / CyO, Dfd-GMR-YFP (♀) X w- ; 13xLexAOp2-IVS-myr::tdTom (in Su[Hw]attP5) / CyO, Dfd-GMR-YFP (♂) = w- ; 57C10-LexAp65 (attP40) / 13xLexAOp2-IVS-myr::tdTom (Su[Hw]attP5) (♀)

Cross to balance the fluorescent tag:

- w- ; 57C10-LexAp65 (attP40) / 13xLexAOp2-IVS-myr::tdTom (Su[Hw]attP5) (♀) X w- ; Sco /CyO, Dfd-GMR-YFP (♂) = w- ; 57C10-LexAp65 (attP40), 13xLexAOp2-IVS-myr::tdTom (Su[Hw]attP5) / CyO, Dfd-GMR-YFP (♀)

Cross to tag the VRQ(GPI) fly with a fluorescent marker:

- w- ; + / + ; 13xLexAop2-IVS-VRQ(GPI) / TM6C, Sb (attP2) (♀) X w[*] ; + / + ; Dr / TM3, Sb, Dfd-GMR-YFP (♂) = w- ; + / + ; 13xLexAop2-IVS-VRQ-m (attP2) / TM3, Sb, Dfd-GMR-YFP (♂)

Cross to select the progeny expressing PrP based on the fluorescent markers:

- w- ; + / + ; 13xLexAop2-IVS-VRQ(GPI) (attP2) / TM3, Sb, Dfd-GMR-YFP (♂) X w- ; 57C10-LexAp65 (attP40), 13xLexAOp2-IVS-myr::tdTom (Su[Hw]attP5) / CyO, Dfd-GMR-YFP (♀) =

PrP expressing fraction of progeny: w- ; 57C10-LexAp65 (attP40), 13xLexAOp2-IVS-myr::tdTom (Su[Hw]attP5) / + ; 13xLexAop2-IVS-VRQ(GPI) (attP2) / +

Fractions of progeny with no PrP expression: w- ; 57C10-LexAp65 (attP40), 13xLexAOp2-IVS-myr::tdTom (Su[Hw]attP5) / + ; TM3, Sb, Dfd-GMR-YFP / + and w- ; CyO, Dfd-GMR-YFP / + ; 13xLexAop2-IVS-VRQ(GPI) (attP2) / +

8.5 Methods performed in collaboration with other researchers

8.5.1 Locomotor ability assay

The locomotor ability assay was performed by Dr. Alana Thackray, Department of Veterinary Medicine, University of Cambridge, UK. The locomotor activity of PrP transgenic *Drosophila* was assessed by a negative geotaxis climbing assay (Thackray et al., 2012b). The fly crosses were set up either at 20 or 25°C and after hatching, age-matched, pre-mated female flies (3 x n=15 for each genotype, 45 flies in total) were placed in adapted plastic 25 ml pipettes that were used as vertical climbing columns. The flies were allowed to acclimatise for 30 minutes, tapped to the bottom of the climbing column and then allowed to climb for 45 seconds. At the end of the climbing period the number of flies above the 25 ml mark, below the 2 ml mark and between the 2 ml and 25 ml marks was recorded. This protocol was performed three times a week for 40 days and the mean ± SD performance index (PI) was calculated for each group of 45 flies (White et al., 2010, Thackray et al., 2012b).

8.5.2 Fly crosses for neuromuscular junction (NMJ) analysis

Subsequent fly crosses were performed by Dr. Alana Thackray, University of Cambridge, UK, prior to start of my PhD programme.

Paternal (ovine PrP transgenic) fly lines

Short name	Genotype	Description
51D	w ; 3xP3-RFP at attP ZH-51D	Control fly line containing common landing site only, but no transgenes mediating PrP expression
VRQ(GPI)	w ; UAS-VRQ-PrP(GPI), 3xP3-RFP at attP ZH-51D	Fly transgenic for Gal4 mediated expression of membrane bound (GPI-anchored) form of ovine VRQ cellular prion protein
VRQ(ΔGPI)	w ; UAS-VRQ-PrP(ΔGPI), 3xP3-RFP at attP ZH-51D	Fly transgenic for Gal4 mediated expression of secreted form (lacking GPI-anchor) of ovine VRQ cellular prion protein
VRQ(cyt)	w ; UAS-VRQ-PrP(cyt), 3xP3-RFP at attP ZH-51D	Fly transgenic for Gal4 mediated expression of cytosolic form (lacking GPI-anchor and signal peptide sequence) of ovine VRQ cellular prion protein

Males of the ovine VRQ PrP transgenic fly lines listed here were used for fly crosses to trigger GAL4/UAS-directed PrP expression in their progeny with the exception of non-PrP-transgenic 51D fly line that does not contain PrP transgene.

All *UAS-PrP* transgenic fly lines express ovine VRQ (valine at codon 136, arginine at codon 154 and glutamine at codon 171) PrP under the control of Gal4/UAS system (Fischer et al., 1988, Brand and Perrimon, 1993). Detailed information about the generation of ovine PrP transgenic fly lines can be found in Dr. Alana Thackray's publications (Thackray et al., 2012b, Thackray et al., 2012a, Thackray et al., 2014b, Thackray et al., 2014a).

Maternal Gal4 expression stock (driver line)

w- ; RN2-O-GAL4 ; Tub84B-FRT-CD2stop - FRT-GAL4, UAS-FLP, UAS – myr::mRFP(B2) ; RRFa-GAL4, 20xUAS-6xmCherry : : HA)

This driver fly line targets high levels of GAL4 expression specifically to aCC and RP2 motoneurons via the RN2-Gal4 and RRFa-Gal4 transgenes on chromosomes 2 and 3 (Fujioka et al., 1999); GAL4 levels are further boosted through a flippase and FLP-out based maintenance and amplification loop consisting of: UAS-FLP, tubulin FRT-CD2stop-FRT-Gal4 (Singh et al., 2013). This transgenic driver fly line was generated and kindly provided by Dr. Matthias Landgraf, Department of Zoology, University of Cambridge, UK.

The females of this fly line have been used to trigger targeted PrP expression in the progeny after crossing with males of PrP transgenic flies.

8.5.3 Prion-infection of *Drosophila* larvae for NMJ analysis

The scrapie infection and infected larvae collection were performed by Dr. Alana Thackray, Department of Veterinary Medicine, University of Cambridge, UK, prior to start of my PhD programme.

Ovine PrP transgenic and 51D control GAL4-driven *Drosophila* larvae were exposed to 250 µl of 1% w/v (in PBS pH 7.4) scrapie-infected inocula prepared from terminal scrapie-affected sheep identified by routine statutory surveillance (VRQ/VRQ isolate SE1848/0005) or negative control New Zealand-derived VRQ/VRQ scrapie-free sheep brain homogenate (Thackray et al., 2012a). The *Drosophila* larvae were exposed to the inoculum added to the top of the cornmeal after eclosion and the third instar late stage wandering larvae were harvested for neuronal synapse analysis.

8.5.4 Dissection of *Drosophila* larvae for NMJ analysis

The *Drosophila* larval dissection was performed by Dr. Matthias Landgraf and Dr. Matthew Oswald, Department of Zoology, University of Cambridge, UK.

Larvae were dissected and stretched maximally by conventional means to expose abdominal hemi segments of the body wall and allow access and visualisation of the NMJs associated with abdominal muscles 3, 4 and 5 (Brent et al., 2009). Dissected larvae were fixed in 3.5% formaldehyde in Sorenson's buffer (0.075M, pH 7.4) for 15 minutes at room temperature and washed twice in saline for 5 minutes.

8.5.5 Immunostaining of fly larvae for NMJ analysis

The *Drosophila* larval immunostaining was performed by Dr. Matthias Landgraf and Dr. Matthew Oswald, Department of Zoology, University of Cambridge, UK.

Immunostaining of NMJs was performed using anti-HRP antibody to label the presynaptic neuronal membrane of all bouton types (Menon et al., 2013). Bruchpilot (Brp) monoclonal antibody nc82 was used to label presynaptic active zones (Wagh et al., 2006) and Discs-large (Dlg) antibody to label type Ib and Is boutons in the subsynaptic reticulum (SSR) (Menon et al., 2013). Immunostained larvae were mounted on microscope slides, immersed in glycerol, cover slipped and stored at -20°C until visualisation.

8.5.6 Protein misfolding cyclic amplification (PMCA)

PMCA was kindly performed by Dr. Olivier Andreoletti (INRA, Toulouse, France).

The fly head homogenate samples were mixed with 10% (w/v) ovine VRQ PrP transgenic mouse brain homogenate of tg338 mouse (diluted in PBS, pH 7.4; 0.1% Triton X-100 and 150 mM NaCl buffer) in the ratio of 5 μl of the fly head homogenate to 45 μl of the PrP^{C} substrate of ovine VRQ PrP transgenic mouse brain homogenate. The solution was transferred into 0.2 ml sealed thin wall PCR tube. The tubes were then placed into the Misonix 4000 sonicator for 96 cycles of 10 seconds sonication step at 70% power combined with 14 minutes and 50 seconds incubation step. Each sample was then treated with 4 μg of PK per mg of protein at 37°C for 120 minutes. The reaction was then stopped by an addition of Pefabloc® (Sigma Aldrich) at 4 mM final concentration. The PK-resistant material was then visualised using SDS-PAGE and western blot with anti-PrP antibody Sha31 (Féraudet et al., 2005).

8.5.7 Real-time quaking-induced conversion (RT-QuIC)

The RT-QuIC was kindly performed by Dr. Marcelo A. Barria Matus, National CJD Research and Surveillance Unit, Edinburgh.

The RT-QuIC reactions were set up in a volume of 100 µl with the recombinant hamster PrP substrate concentration of 0.1 mg/ml and 2 µl of a diluted (PBS with 0.1% sodium dodecyl sulphate) seed. The samples were incubated at 42°C while intermittently shaken (87 seconds shaking at 900 rpm /33 minutes stationary) using the FLUOstar OMEGA double orbital microplate reader (BMG Labtech) for 100 h. The fluorescent readings were performed every 15 minutes after excitation by 20 flashes per well at 450 nm. The emission of Thioflavin-T was measured by emission counts of relative fluorescence units (rfu) with a maximum limit of 260,000 per well. The average fluorescence for each quadruplicate sample was plotted against time.

A positive reaction was defined as a fluorescence reading three times above the baseline for all repeats of the sample within a 100 hour run time. Typically, for sCJD control (10^{-3} dilution of 10% [w/v] brain homogenate) is positive within 6.5 hours (personal communication with Dr. Marcelo A. Barria Matus (National CJD Research and Surveillance Unit, Edinburgh).

8.5.8 Absence of PrP in the non-transgenic *Drosophila*

The absence of PrP and prion accumulation in 51D control flies were kindly investigated by Dr. Alana Thackray, Department of Veterinary Medicine, University of Cambridge, UK, prior to the start of my PhD programme.

The detectable PrP orthologue is absent from *Drosophila*, but the fly might still be able to act as a mechanical vector of prions after the oral inoculation with scrapie material. Prion accumulation and propagation in *Drosophila* was further tested by experimental inoculation of non-PrP transgenic *Drosophila* larvae of the 51D genotype with sheep scrapie prions (Thackray et al., 2012a, Thackray et al., 2014a). The disruption of the negative geotaxis climbing ability of a *Drosophila* fly is a known phenotypic marker of prion-related neurodegeneration (Thackray et al., 2012b, Thackray et al., 2012a). Onset of prion-associated behavioural changes was therefore assessed and quantified by the negative geotaxis climbing ability assay performed at various time points throughout the fly adult lives. The results of a locomotor ability climbing assay can be seen in **Figure A** (Thackray et al., 2014a). Control 51D flies were exposed to normal brain homogenate or scrapie positive ovine brain homogenate. However, no significant difference in climbing performance was found between the prion treated and control group of 51D flies. The slight decline in climbing ability towards the latter time points of the experiment was associated solely with the progressing age of flies and is the same in both control and prion-inoculated

group. This experiment verifies an absence of prion-associated neurodegeneration in wild type 51D *Drosophila* and therefore further confirms a lack of PrP orthologue in the fly.

To further investigate the presence of misfolded PrP in 51D *Drosophila*, the PMCA assay was performed. The result of PMCA in **Figure B** shows an absence of any amplifiable prion material in all cases. The assay is able to amplify mutant forms of PrP if just one molecule of misfolded PrP has been present in the tested sample. Therefore, it was concluded that there was no misfolded PrP material present at the start of an adult fly life (5 days old) as a carryover from a scrapie inoculum and not even later in the fly life as a result of misfolded PrP accumulation (Thackray et al., 2014a).

8.6 Fly crosses performed to obtain dual PrP transgenic flies

Pan-neuronal expression of VRQ(GPI) from chromosome 2 and glial cell expression of VRQ(ΔGPI) from chromosome 3

- w ; M{VRQ-PrP(GPI), 3xP3-RFP.attP}ZH-51D / + ; 13xLexAop2-IVS-VRQ(ΔGPI) / + - dual PrP transgenic fly crossed with w- ; If / [CyO, wg-Z] ; 57C10-Gal4 (attP2), Repo-LexAp65 (VK00027) / [TM6b] – Repo-LexA glial cell driver for chromosome 3 flies; 57C10-Gal4 pan-neuronal driver for chromosome 2 PrP flies

Pan-neuronal expression of VRQ(GPI) from chromosome 2 and neuronal subset expression (chordotonal organs) of VRQ(ΔGPI) from chromosome 3

- w ; M{VRQ-PrP(GPI), 3xP3-RFP.attP}ZH-51D / + ; 13xLexAop2-IVS-VRQ(ΔGPI) / + - dual PrP transgenic fly crossed with w- ; 57C10-Gal4 (attP40) / CyO, Dfd-GMR-YFP ; iav-LexAp65 / TM6b, Dfd-GMR-YFP – Iav-LexA sensory neurons specific driver for chromosome 3 PrP flies; 57C10-Gal4 pan-neuronal driver for chromosome 2 PrP flies

Pan-neuronal expression of VRQ(GPI) from chromosome 2 and eye expression of VRQ(ΔGPI) from chromosome 3

- w ; M{VRQ-PrP(GPI), 3xP3-RFP.attP}ZH-51D / + ; 13xLexAop2-IVS-VRQ(ΔGPI) / + - dual PrP transgenic fly crossed with w- ; 57C10-Gal4 (attP40) / CyO, Dfd-GMR-YFP ; GMR-3-LexAp65 / TM6b, Dfd-GMR-YFP – GMR-LexA eye specific driver for chromosome 3 PrP flies; 57C10-Gal4 pan-neuronal driver for chromosome 2 PrP flies

8.7 Multiple alignment of PrP amino acid sequences of different species

```
CLUSTAL O (1.2.4) multiple sequence alignment; all sequences compared have insect
signal peptide; human = M129, ovine = VRQ(GPI), mouse = mouse 3F4 WT, hamster =
hamster WT and cervid = N138

human         MASKVSILLLLTVHLLAAQTFAQKKRPKPG-GWNTGGSRYPGQGSPGGNRYPPQGGGGWG 59
mouse         MASKVSILLLLTVHLLAAQTFAQKKRPKPG-GWNTGGSRYPGQGSPGGNRYPPQG-GTWG 58
hamster       MASKVSILLLLTVHLLAAQTFAQKKRPKPG-GWNTGGSRYPGQGSPGGNRYPPQGGGTWG 59
ovine         MASKVSILLLLTVHLLAAQTFAQKKRPKPGGGWNTGGSRYPGQGSPGGNRYPPQGGGGWG 60
cervid        MASKVSILLLLTVHLLAAQTFAQKKRPKPGGGWNTGGSRYPGQGSPGGNRYPPQGGGGWG 60
              ****************************** ********************** * **

human         QPHGGGWGQPHGGGWGQPHGGGWGQPHGGGWGQGGGTHSQWNKPSKPKTNMKHMAGAAAA 119
mouse         QPHGGGWGQPHGGSWGQPHGGSWGQPHGGGWGQGGGTHNQWNKPSKPKTNMKHMAGAAAA 118
hamster       QPHGGGWGQPHGGGWGQPHGGGWGQPHGGGWGQGGGTHNQWNKPSKPKTNMKHMAGAAAA 119
ovine         QPHGGGWGQPHGGGWGQPHGGGWGQPHGGGGWGQGGSHSQWNKPSKPKTNMKHVAGAAAA 120
cervid        QPHGGGWGQPHGGGWGQPHGGGWGQPHGGGGWGQGGTHSQWNKPSKPKTNMKHVAGAAAA 120
              *************.*******.********    **:*.**************:****** 

human         GAVVGGLGGYMLGSAMSRPIIHFGSDYEDRYYRENMHRYPNQVYYRPMDEYSNQNNFVHD 179
mouse         GAVVGGLGGYMLGSAMSRPMIHFGNDWEDRYYRENMYRYPNQVYYRPVDQYSNQNNFVHD 178
hamster       GAVVGGLGGYMLGSAMSRPMMHFGNDWEDRYYRENMNRYPNQVYYRPVDQYNNQNNFVHD 179
ovine         GAVVGGLGGYMLGSVMSRPLIHFGNDYEDRYYRENMYRYPNQVYYRPVDQYSNQNNFVHD 180
cervid        GAVVGGLGGYMLGSAMNRPLIHFGNDYEDRYYRENMYRYPNQVYYRPVDQYNNQNTFVHD 180
              **************.*.**::***.*:********* **********:*:*.***.**** 

human         CVNITIKQHTVTTTTKGENFTETDVKMMERVVEQMCITQYERESQAYYQ--RGSSMVLFS 237
mouse         CVNITIKQHTVTTTTKGENFTETDVKMMERVVEQMCVTQYQKESQAYYDGRRSSSTVLFS 238
hamster       CVNITIKQHTVTTTTKGENFTETDIKIMERVVEQMCTTQYQKESQAYYDGRRSS-AVLFS 238
ovine         CVNITVKQHTVTTTTKGENFTETDIKIMERVVEQMCITQYQRESQAYYQ--RGASVILFS 238
cervid        CVNITVKQHTVTTTTKGENFTETDIKMMERVVEQMCITQYQRESQAYYQ--RGASVILFS 238
              *****:******************:*:********* ***::******:  *.:  :*** 

human         SPPVILLISFLIFLIVG   254
mouse         SPPVILLISFLIFLIVG   255
hamster       SPPVILLISFLIFLMVG   255
ovine         SPPVILLISFLIFLIVG   255
cervid        SPPVILLISFLIFLIVG   255
              **************:**
```

8.8 Multiple sequence alignment of mature PrP DNA from different species

CLUSTAL O(1.2.4) multiple sequence alignment; all sequences compared have insect signal peptide; human = M129, ovine = VRQ(GPI), mouse = mouse 3F4 WT, hamster = hamster WT and cervid = N138

```
ovine       ATGGCGAGCAAAGTCTCGATCCTTCTCCTGCTAACCGTCCATCTTCTGGCTGCTCAGACC   60
cervid      ATGGCGAGCAAAGTCTCGATCCTTCTCCTGCTAACCGTCCATCTTCTGGCTGCTCAGACC   60
human       ATGGCGAGCAAAGTCTCGATCCTTCTCCTGCTAACCGTCCATCTTCTGGCTGCTCAGACC   60
mouse       ATGGCGAGCAAAGTCTCGATCCTTCTCCTGCTAACCGTCCATCTTCTGGCTGCTCAGACC   60
hamster     ATGGCGAGCAAAGTCTCGATCCTTCTCCTGCTAACCGTCCATCTTCTGGCTGCTCAGACC   60
            ************************************************************

ovine       TTCGCCCAGAAGAAGCGACCAAAACCTGGCGGAGGATGGAACACTGGGGGGAGCCGATAC   120
cervid      TTCGCCCAGAAGAAGCGACCAAAACCTGGAGGAGGATGGAACACTGGGGGGAGCCGATAC   120
human       TTCGCCCAGAAGAAGCGCCCGAAGCCTGGA---GGATGGAACACTGGGGGCAGCCGATAC   117
mouse       TTCGCCCAGAAAAAGCGGCCAAAGCCTGGA---GGGTGGAACACCGGTGGAAGCCGGTAT   117
hamster     TTCGCCCAGAAGAAGCGGCCAAAGCCTGGA---GGGTGGAACACTGGCGGAAGCCGATAC   117
            *********** ***** ** ** *****    ** ******** ** ** ***** **

ovine       CCGGGACAGGGCAGTCCTGGAGGCAACCGCTATCCACCTCAGGGAGGGGGTGGCTGGGGT   180
cervid      CCGGGACAGGGAAGTCCTGGAGGCAACCGCTATCCACCTCAGGGAGGGGGTGGCTGGGGT   180
human       CCGGGGCAGGGCAGCCCTGGAGGCAACCGCTACCCACCTCAGGGCGGTGGTGGCTGGGGG   177
mouse       CCGGGGCAGGGAAGCCCTGGAGGCAACCGTTACCCACCTCAGGGTGGCA---CCTGGGGG   174
hamster     CCTGGGCAGGGCAGCCCTGGAGGCAACCGTTACCCACCTCAGGGTGGCGGCACATGGGGG   177
            ** ** ***** ** ************** ** *********** **       *****

ovine       CAGCCCCATGGAGGTGGCTGGGGCCAACCTCATGGAGGTGGCTGGGGTCAGCCCCATGGT   240
cervid      CAGCCCCATGGAGGTGGCTGGGGCCAACCTCATGGAGGTGGCTGGGGTCAGCCCCATGGT   240
human       CAGCCTCATGGTGGTGGCTGGGGGCAGCCTCATGGTGGTGGCTGGGGGCAGCCCCATGGT   237
mouse       CAGCCCCACGGTGGTGGCTGGGGACAACCCCATGGGGGCAGCTGGGGACAACCTCATGGT   234
hamster     CAACCCCATGGTGGTGGCTGGGGACAGCCCCATGGTGGTGGCTGGGGACAGCCCCATGGT   237
            ** ** ** ** *********** ** ** ***** **  ******* ** ** ******

ovine       GGTGGCTGGGGACAGCCACATGGTGGTGGAGGCTGGGGTCAAGGTGGTAGCCACAGTCAG   300
cervid      GGTGGCTGGGGGCAGCCACATGGTGGTGGAGGCTGGGGTCAAGGTGGTACCCACAGTCAG   300
human       GGTGGCTGGGGACAGCCTCATGGTGGTGGCTGGGGTCAAGGAGGTGGCACCCACAGTCAG   297
mouse       GGTAGTTGGGGTCAGCCCCATGGCGGTGGATGGGGCCAAGGAGGGGGTACCCATAATCAG   294
hamster     GGTGGCTGGGGTCAGCCCCATGGTGGTGGCTGGGGTCAAGGAGGTGGCACCCACAATCAG   297
            *** * ***** ***** ***** *****  *  *      *** ** * *** * ****

ovine       TGGAACAAGCCCAGTAAGCCAAAAACCAACATGAAGCATGTGGCAGGAGCTGCTGCAGCT   360
cervid      TGGAACAAGCCCAGTAAACCAAAAACCAACATGAAGCATGTGGCAGGAGCTGCTGCCGCT   360
human       TGGAACAAGCCGAGTAAGCCAAAAACCAACATGAAGCACATGGCTGGTGCTGCAGCAGCT   357
mouse       TGGAACAAGCCCAGCAAACCAAAAACCAACATGAAGCATATGGCAGGGGCTGCGGCAGCT   354
hamster     TGGAACAAGCCCAGTAAGCCAAAAACCAACATGAAGCACATGGCCGGCGCTGCTGCGGCA   357
            *********** ** ** ********************  **** ** ***** ** **

ovine       GGAGCAGTGGTAGGGGGCCTTGGTGGCTACATGCTGGGAAGTGTCATGAGCAGGCCTCTT   420
cervid      GGAGCAGTGGTAGGGGGCCTTGGTGGCTACATGCTGGGAAGTGCCATGAACAGACCTCTT   420
human       GGGGCAGTGGTGGGGGGCCTTGGCGGCTACATGCTGGGAAGTGCCATGAGCAGGCCCATC   417
mouse       GGGGCAGTAGTGGGGGGCCTTGGTGGCTACATGCTGGGGAGCGCCATGAGCAGGCCCATG   414
hamster     GGGGCCGTGGTGGGGGGCCTTGGTGGCTACATGCTGGGGAGTGCCATGAGCAGGCCCATG   417
            ** ** ** ** *********** ************** ** * ***** *** **  *

ovine       ATACATTTTGGCAATGACTATGAGGACCGTTACTATCGTGAAAACATGTACCGTTACCCC   480
cervid      ATACATTTTGGCAACGACTATGAGGACCGTTACTATCGTGAAAATATGTACCGTTACCCC   480
human       ATACATTTCGGCAGTGACTATGAGGACCGCTACTATCGTGAAAACATGCACCGTTACCCC   477
mouse       ATCCATTTTGGCAACGACTGGGAGGACCGCTACTACCGTGAAAACATGTACCGCTACCCT   474
hamster     ATGCATTTTGGCAATGACTGGGAGGACCGCTACTACCGTGAAAACATGAACCGCTACCCT   477
            ** ***** ****  ****  ******** ***** ******** *** **** *****

ovine       AACCAAGTGTACTACAGACCAGTGGATCAGTATAGTAACCAGAACAACTTTGTGCATGAC   540
cervid      AACCAAGTGTACTACAGGCCAGTGGATCAGTATAATAACCAGAACACCTTTGTGCATGAC   540
human       AACCAAGTGTACTACAGGCCCATGGATGAGTACAGCAACCAGAACAACTTTGTGCACGAC   537
```

```
mouse       AACCAAGTGTACTACAGGCCAGTGGATCAGTACAGCAACCAGAACAACTTCGTGCACGAC   534
hamster     AACCAAGTGTATTACCGGCCAGTGGACCAGTACAACAACCAGAACAACTTTGTGCACGAT   537
            ********** *** * **  ****  **** *  ********** *** ***** **

ovine       TGTGTCAACATCACAGTCAAGCAACACACAGTCACCACCACCACCAAGGGGGAGAACTTC   600
cervid      TGTGTCAACATCACAGTCAAGCAACACACAGTCACCACCACCACCAAGGGGGAGAACTTC   600
human       TGCGTCAATATCACAATCAAGCAGCACACGGTCACCACAACCACCAAGGGGGAGAACTTC   597
mouse       TGCGTCAATATCACCATCAAGCAGCACACGGTCACCACCACCACCAAGGGGGAGAACTTC   594
hamster     TGTGTCAACATCACCATCAAGCAGCACACAGTCACCACCACCACCAAGGGGGAGAACTTC   597
            ** ***** *****  ******* ***** ******** **********************

ovine       ACCGAAACTGACATCAAGATAATGGAGCGAGTGGTGGAGCAAATGTGCATCACCCAGTAC   660
cervid      ACTGAAACTGACATTAAGATGATGGAGCGAGTTGTGGAGCAAATGTGCATCACCCAGTAC   660
human       ACCGAGACCGACGTTAAGATGATGGAGCGCGTGGTTGAGCAGATGTGTATCACCCAGTAC   657
mouse       ACCGAGACCGATGTGAAGATGATGGAGCGCGTGGTGGAGCAGATGTGCGTCACCCAGTAC   654
hamster     ACGGAGACCGACATCAAGATAATGGAGCGCGTGGTGGAGCAGATGTGTACCACCCAGTAT   657
            ** ** ** **  * ***** ******** ** ** ***** *****   *********

ovine       CAGAGAGAATCCCAGGCTTATTACCAAAGGGGGGCA------AGTGTGATCCTCTTTTCT   714
cervid      CAGAGAGAATCCCAGGCTTATTACCAAAGAGGGGCA------AGTGTGATCCTCTTCTCC   714
human       GAGAGGGAATCTCAGGCCTATTACCAGAGAGGATCG------AGCATGGTCCTCTTCTCC   711
mouse       CAGAAGGAGTCCCAGGCCTATTACGACGGGAGAAGATCCAGCAGCACCGTGCTTTTCTCC   714
hamster     CAGAAGGAGTCCCAGGCCTACTACGATGGAAGAAGGTCCAG---CGCGGTGCTGTTCTCC   714
             ***  ** ** ***** ** *** *  *  *                 * ** ** **

ovine       TCCCCTCCTGTGATCCTCCTCATCTCTTTCCTCATTTTTCTCATAGTAGGATAG 768
cervid      TCCCCTCCTGTGATCCTCCTCATCTCTTTCCTCATTTTTCTCATAGTAGGATAG 768
human       TCTCCACCTGTGATCCTCCTGATCTCTTTCCTCATCTTCCTGATAGTGGGATGA 765
mouse       TCCCCTCCTGTCATCCTCCTCATCTCCTTCCTCATCTTCCTGATCGTGGGATGA 768
hamster     TCCCCTCCTGTGATCCTCCTCATTTCCTTTCTCATCTTCCTGATGGTGGGATGA 768
            ** ** ***** ******** ** ** ** ***** ** ** ** ** ****
```